

**ANALYZING TRENDS IN TEMPERATURE, PRECIPITATION AND  
STREAMFLOW DATA OVER SOUTHERN ONTARIO AND QUEBEC USING  
THE DISCRETE WAVELET TRANSFORM**

by

Deasy Nalley

Department of Bioresource Engineering

McGill University, Montreal

November 2012

A thesis submitted to McGill University

in partial fulfillment of the requirements of the degree of

Master of Science

Copyright © Deasy Nalley, 2012

## ABSTRACT

Analysis on hydroclimatic variables can provide information on how the climate has evolved over time. This can be accomplished through time series analysis. Trend analysis in hydroclimatic variables is challenging due to their non-stationary nature and the presence of noise and stochastic components in them. The principal objective of this study is to detect and analyze trends in mean surface air temperature, total precipitation and mean streamflow obtained from several stations in Ontario and Quebec, Canada. To accomplish this, we co-utilized the wavelet transform (WT) technique (more specifically, the discrete wavelet transform (DWT)) and the Mann-Kendall (MK) trend test. The time series used were decomposed via the DWT in order to separate their high-frequency and low-frequency components, prior to testing their statistical significance with the MK trend test. The trend (i.e. slowly changing processes) is assumed to be contained in the low-frequency component of the data. The trends in temperature, precipitation and flow are assessed on different bases: monthly, seasonal, and annual. Temperature trends for the different seasons (i.e. winter, spring, summer, and autumn) were also assessed.

In this study, we demonstrated the use of WT in extracting information contained in the time series that is not obvious in the raw data. The advantages of the WT technique are highlighted by its ability to extract time-frequency information contained in the analyzed time series manifested in the form of periodicities ranging from intra-annual to decadal events. A new criterion is also proposed in this study where the relative error of the MK Z-values between the approximation component of the last decomposition level and the original data was used to determine the number of decomposition levels of the analyzed time series, the type of Daubechies (db) mother wavelet, and the border condition to be used in the DWT procedure.

The procedures contained in the methodology for trend analysis outlined in this study have not been explored in the existing literature. First of all, we tested for the presence of a significant autocorrelation in a time series prior to applying the MK test, which is often ignored in many trend detection studies. The time series were then decomposed via the DWT; the MK trend test and sequential MK test were then applied in order to determine the most significant periodic mode affecting the observed trends. In

this study, three versions of MK test were used, depending on the characteristics of the analyzed data. The original MK test was used on data that exhibit neither seasonality patterns nor significant autocorrelations. Seasonal MK test by Hirsch and Slack (1984) was used on the time series exhibiting seasonality cycles (with or without significant autocorrelations). Modified MK test by Hamed and Rao (1998) was used on data with significant autocorrelations.

Finally, combining the application of the DWT and MK test in trend assessment in hydroclimatic time series (especially in the context of Canadian studies) has not been explored. Therefore, the results obtained in this study contribute to furthering the overall understanding of climatic change in Southern Ontario and Quebec. Although the trends in the different variables studied are affected by different time periodicities, the study found that generally positive trends are more dominant. Among the most important findings of this study are: (i) all temperature data show positive values, which implies warming trends (ii) precipitation and flow trends are affected by fluctuations of up to four years, and (iii) annual positive trends in temperature may be attributed mostly by winter and summer warming. This suggests that if the temperature trends remain in the positive direction, other hydroclimatic indices may also experience significant changes in the future.

## RÉSUMÉ

Quoique le système climatique soit très complexe, une analyse des variables hydroclimatiques peut indiquer l'évolution du climat avec le temps. Une analyse de séries temporelles peut servir à ces fins; plus spécifiquement, l'analyse des tendances des variables hydroclimatiques peut approfondir l'étude des retombées des changements climatiques.

L'analyse des tendances des variables hydroclimatiques est un défi en raison de leur caractère non stationnaire et la présence de bruit et d'autres éléments stochastiques. L'objectif principal de cette étude fut de détecter et d'analyser les tendances de différents types de données (débit, pluviométrie, température moyenne de l'air en surface), provenant de plusieurs stations en Ontario et au Québec (Canada). Ces stations sont concentrées dans le sud de ces provinces. Pour accomplir cette tâche, nous avons utilisé à la fois une technique de transformée par ondelettes (TO) [spécifiquement une transformée d'ondelette discrète (TOD)] et le test standard d'analyse des tendances Mann-Kendall (MK). Les séries temporelles furent décomposées par TOD afin de séparer à même les données les éléments à haute et basse fréquence, avant d'évaluer leur signification statistique avec le test MK. La tendance (*i.e.*, le procédé à changement lent) est censé appartenir à l'élément à basse fréquence de la série temporelle. Les tendances du débit, de la pluie et de la température furent évaluées sur différentes échelles temporelles : mensuelle, saisonnière et annuelle. Les tendances temporelles de température pour les différentes saisons (hiver, printemps, été, automne) furent également évaluées.

Cette étude montra comment l'utilisation du TO permet d'identifier et d'extraire des informations présentes dans une série temporelle qui ne sont pas évidentes à première vue dans les données brutes, ou suivant qu'on applique seulement le test des tendances MK. Les avantages de la méthode TO sont manifestes dans son habilité à extraire des informations temps-fréquence (*i.e.*, périodicité intra-annuelle à décennale selon le genre de données utilisées) de la série temporelle analysée. Nous proposons un nouveau critère, où l'erreur relative entre les valeurs-Z du test MK pour l'élément d'approximation du dernier niveau de décomposition et celui des données d'origine sert à déterminer le

nombre de niveaux de décomposition de la série temporelle analysée, le type d'ondelette mère de Daubechies (db), et les conditions de bordure devant servir à la TOD.

Particulièrement dans le contexte canadien, l'utilisation d'une combinaison de TOD et du test MK dans l'évaluation de tendances dans les séries temporelles de données hydroclimatiques demeure rare. Les résultats de cette étude contribueront donc à une compréhension globale grandissante des changements climatiques du sud de l'Ontario et du Québec. Quoique les tendances des différentes variables étudiées suivent différentes périodicités temporelles, l'étude montre que les tendances à la hausse dominent. Parmi les plus importantes conclusions de cette étude sont: (i) les tendances de débit et de précipitation suivent des fluctuations de jusqu'à quatre ans, (ii) toutes les catégories de données de température montrent des tendances à la hausse, laissant entendre une tendance au réchauffement, et (iii) les tendances annuelles à la hausse de la température peuvent être attribuées à un réchauffement des hivers et étés. Cela implique que si les tendances de température demeurent à la hausse, d'autres indices hydroclimatiques montreront des changements dans l'avenir.

## ACKNOWLEDGEMENTS

I would like to thank my supervisor, Dr. Jan Adamowski for his guidance, support, encouragement, enthusiasm, and understanding over these last two years. He has always provided me with useful advice and comments on how to best improve my work. Thank you for always being available for discussions whenever I needed!

I would like to express my gratitude to Dr. Bahaa Khalil, who has been very kind, helpful, and supportive during my research. He has shared his knowledge and experience toward my research project. Dr. Khalil has also provided me with many valuable feedback and suggestions. I am very grateful for the time you spent in helping me whenever I run into problems and always having your door open for discussions.

I would also like to extend my gratitude to a number of people who have assisted me during my research work. In particular, the assistance of Mr. Hiu Chan and Dr. Mukesh Tiwari with the MATLAB codes was much appreciated. In addition to this, I am also grateful for Dr. Éva Mekis from the Climate Research Division of Environment Canada for her assistance in obtaining some updated data used in this research.

I wish to express my most heartfelt thanks to my close friends, Anthony Lycett, Nelson Wedeingue, Prell Neri, Justina Amissah, Priyanka Pandey, Sourjya Bhattacharjee, and Bridget Robinson, for helping me to go through some very difficult times, and for the emotional support.

I wish to thank my sister, Nancy Nalley; my brother in law, Putra Tarigan; and my two brothers – Denny Nalley and Ricky Nalley, for caring and just being there when I needed to talk! I wish to thank my parents, Samuel Willem Nalley and Juniana Nalley for their constant support and prayers, and for their unconditional love. This thesis is for you!

Last but not least, I want to thank God for this opportunity in being able to study – what a privilege!

## CONTRIBUTIONS OF AUTHORS

Chapters 3 and 4 of this thesis have been prepared for submissions as manuscripts to peer-reviewed journals. Chapter 3 is being prepared for submission to the Journal of Hydrological Processes. Chapter 4 has been submitted to the Journal of Hydrology. Part of chapter 4 has been accepted to the Northeast Agricultural and Biological Engineering Conference - NABEC-CSBE/SCGAB Joint Meeting and Technical Conference on Ecological Engineering, which will be held in Orillia, Ontario from July 15 – 18, 2012.

The author of this thesis was responsible for gathering data, determining the step-by-step procedures involved in the methodology for data analysis, computing the data analysis, and preparing the manuscripts for journal submissions. Dr. Jan Adamowski is the supervisor of this thesis; he provided guidance and advice about the different technical aspects covered by this thesis. He also reviewed and edited this thesis. Dr. Bahaa Khalil of Bioresource Engineering at McGill University is also a co-author of the two manuscripts (chapters 3 and 4). He provided statistical and technical guidance during the data analysis. He also assisted in compiling the MATLAB codes used to analyze our data.

### **List of papers for journal submissions and conference associated with this thesis:**

- Nalley, D.**, Adamowski, J., Khalil, B., 2012. Trend detection in surface air temperature in Ontario and Quebec (1967 – 2006) using the discrete wavelet transform (DWT). Journal of Hydrology (submitted).
- Nalley, D.**, Adamowski, J., Khalil, B., 2012. Using discrete wavelet transforms to analyze trends in streamflow and precipitation in Ontario and Quebec (1954 – 2008). Journal of Hydrology (Accepted: DOI:10.1016/j.jhydrol.2012.09.049).
- Nalley, D.**, Adamowski, J., Khalil, B., 2012. The use of wavelet transform in trend analysis of streamflow in southern Quebec and Ontario during 1954 – 2008. NABEC-CSBE/SCGAB Joint Meeting and Technical Conference on Ecological Engineering.

## TABLE OF CONTENTS

<b><u>ABSTRACT</u></b>	<b><u>II</u></b>
<b><u>RÉSUMÉ</u></b>	<b><u>IV</u></b>
<b><u>ACKNOWLEDGEMENTS</u></b>	<b><u>VI</u></b>
<b><u>CONTRIBUTIONS OF AUTHORS</u></b>	<b><u>VII</u></b>
<b><u>TABLE OF CONTENTS</u></b>	<b><u>VIII</u></b>
<b><u>LIST OF TABLES</u></b>	<b><u>XIII</u></b>
<b><u>LIST OF FIGURES</u></b>	<b><u>XVI</u></b>
<b><u>LIST OF ABBREVIATIONS</u></b>	<b><u>XXII</u></b>
<b><u>CHAPTER 1 – GENERAL INTRODUCTION</u></b>	<b><u>1</u></b>
1.1. Climate Change and its General Impacts	1
1.2. Trends in Hydroclimatic Indices	3
1.3. Problems Faced in Time Series Analysis to Detect Trends	4
1.4. Time-Frequency Assessment of a Time Series	6
1.5. Research Objectives	7
1.6. Thesis Outline	9
1.7. References	10
<b><u>CHAPTER 2 – LITERATURE REVIEW</u></b>	<b><u>16</u></b>
2.1. General Implications of Changing Climate on Hydrology	16
2.2. Trend Detection and Analysis in Hydroclimatic Variables	17
2.3. Main Methods of Trend Analysis of Hydroclimatic Variables	20



2.3.1. Parametric and Non-Parametric Statistical Tests	21
2.3.2. The Bootstrap Method	22
2.3.3. Regression Analysis	23
2.3.4. The Mann-Kendall (MK) Trend Test	24
2.4. Addressing the Issue of Serial Correlation in Time Series Analysis	26
2.4.1. Prewhitening Method	26
2.4.2. Seasonal Kendall Test for Seasonal Data with or without Significant Autocorrelations	27
2.4.3. A Modified Mann-Kendall (MK) Trend Test for Data with Serial Correlation	28
2.5. Wavelet Transform in Hydroclimatic Studies and its Applications	29
2.5.1. Examples of Applications of the Wavelet Transform on Temperature Data	31
2.5.2. Examples of Applications of the Wavelet Transform on Precipitation and Streamflow Data	33
2.6. References	35

---

<b>CONNECTING STATEMENT TO CHAPTER 3</b>	<b>45</b>
--	-----------

---

<b>CHAPTER 3 – TREND DETECTION IN SURFACE AIR TEMPERATURE IN ONTARIO AND QUEBEC (1967 – 2006) USING THE DISCRETE WAVELET TRANSFORM</b>	<b>46</b>
--	-----------

---

3.1. Introduction	47
3.2. Theoretical Background	53
3.2.1. Time-Scale Representation of Signals by the Wavelet Transform	53
3.2.2. The Original Mann-Kendall (MK) Trend Test	55
3.2.3. Modified Mann-Kendall (MK) Trend Test	56
3.2.3.1. Modified Mann-Kendall (MK) Test for Data with Seasonality Patterns with or without Significant Autocorrelations	57
3.2.3.2. Modified Mann-Kendall (MK) Test for Significantly Autocorrelated Data	59

3.3. Data and Study Sites	61
3.4. Methodology	64
3.4.1. Serial Correlation and Seasonality Analyses	65
3.4.2. Discrete Wavelet Transform Applications on Different Temperature Time Series	66
3.4.3. The Mann-Kendall (MK) Trend Test	71
3.4.3.1. Applications of the Original and Modified Versions of the Mann-Kendall (MK) Trend Test	71
3.4.3.2. Sequential Mann-Kendall (MK) Analysis	72
3.4.4. Determining the Most Dominant Periodic Components that Affect Temperature Trends	73
3.5. Results and Discussions	74
3.5.1. Preliminary Data Analysis	74
3.5.1.1. Serial Correlation and Seasonality Factors	74
3.5.1.2. The Mann-Kendall (MK) Test on Original Data	75
3.5.1.3. The Number of Decomposition Levels for the Different Time Series	77
3.5.2. Monthly Temperature Data Analysis	77
3.5.3. Seasonally-based Temperature Data Analysis	78
3.5.4. Annual Temperature Data Analysis	82
3.5.5. Winter Temperature Data Analysis	84
3.5.6. Spring Temperature Data Analysis	87
3.5.7. Summer Temperature Data Analysis	90
3.5.8. Autumn Temperature Data Analysis	93
3.6. Conclusions and Recommendations	96
3.7. References	99
<b>CONNECTING STATEMENT TO CHAPTER 4</b>	<b>107</b>

**CHAPTER 4 – USING DISCRETE WAVELET TRANSFORMS TO ANALYZE  
TRENDS IN PRECIPITATION AND STREAMFLOW IN QUEBEC AND  
ONTARIO (1954 – 2008)** **108**

4.1. Introduction	109
4.2. Theoretical Background	114
4.2.1. Wavelet Transforms (WT)	114
4.2.1.1. Continuous Wavelet Transform (CWT)	116
4.2.1.2. Discrete Wavelet Transform (DWT)	117
4.2.2. The Mann-Kendall (MK) Trend Test	118
4.2.2.1. Modified Mann-Kendall (MK) Trend Tests that Account for Seasonality and Autocorrelation Structures in the Data	120
4.2.2.2. Modified Mann-Kendall (MK) Test to Account for Seasonality and Autocorrelation by Hirsch and Slack (1984)	121
4.2.2.3. Modified Mann-Kendall (MK) Test for Autocorrelated Data by Hamed and Rao (1998)	123
4.3. Study Sites and Datasets	124
4.3.1. Selection Criteria for the RHBN Flow Stations and Meteorological Stations	127
4.3.2. Flow Data	128
4.3.3. Precipitation Data	129
4.4. Methodology	130
4.4.1. Autocorrelation Analysis	131
4.4.2. Seasonality Factor	132
4.4.3. Time Series Decomposition via the Discrete Wavelet Transform (DWT)	132
4.4.4. Applying the Mann-Kendall (MK) Trend Tests	137
4.4.5. Sequential Mann-Kendall (MK) Analysis	137
4.4.6. Determining the Most Dominant Periodic Components for Trends	138
4.5. Results and Discussions	139
4.5.1. Preliminary Data Analysis	139
4.5.2. Monthly Data Analysis	142

4.5.2.1. Monthly Average Flow Data	143
4.5.2.2. Monthly Total Precipitation Data	148
4.5.3. Seasonally-based Data Analysis	149
4.5.3.1. Seasonally-based Average Flow Data	151
4.5.3.2. Seasonally-based Total Precipitation Data	154
4.5.4. Annual Data Analysis	157
4.6. Conclusions and Recommendations	164
4.7. Acknowledgement	166
4.8. References	166
<b><u>CHAPTER 5 – SUMMARY AND CONCLUSIONS</u></b>	<b>174</b>
5.1. General Summary	174
5.2. Trends in Temperature, Precipitation and Streamflow	175
5.3. References	177
<b><u>CHAPTER 6 – RECOMMENDATIONS FOR FUTURE STUDIES</u></b>	<b>179</b>
<b><u>CHAPTER 7 – CONTRIBUTIONS TO KNOWLEDGE</u></b>	<b>181</b>

## LIST OF TABLES

<b>Table 3.1.</b>	Key features of the meteorological stations used in this study.	<b>62</b>
<b>Table 3.2.</b>	Lag-1 autocorrelation functions (ACFs) of the different temperature data types.	<b>74</b>
<b>Table 3.3.</b>	Mann-Kendall $Z$ -values of the original time series for the different temperature data types.	<b>75</b>
<b>Table 3.4.</b>	Mann-Kendall $Z$ -values of the monthly temperature series: original data, details components, approximations, and a set of combinations of the details and their respective approximations. The most effective periodic components for trends are indicated in bold format.	<b>79</b>
<b>Table 3.5.</b>	Mann-Kendall $Z$ -values of the seasonally-based temperature series: original data, details components, approximations, and a set of combinations of the details and their respective approximations. The most effective periodic components for trends are indicated in bold format.	<b>82</b>
<b>Table 3.6.</b>	Mann-Kendall $Z$ -values of the annual temperature series: original data, details components, approximations, and a set of combinations of the details and their respective approximations. The most effective periodic components for trends are indicated in bold format.	<b>84</b>
<b>Table 3.7.</b>	Mann-Kendall $Z$ -values of the winter temperature series: original data, details components, approximations, and a set of combinations of the details and their respective approximations. The most effective periodic components for trends are indicated in bold format.	<b>88</b>
<b>Table 3.8.</b>	Mann-Kendall $Z$ -values of the spring temperature series: original data, details components, approximations, and a set of combinations of the details and their respective approximations. The most effective periodic components for trends are indicated in bold format.	<b>91</b>
<b>Table 3.9.</b>	Mann-Kendall $Z$ -values of the summer temperature series: original data, details components, approximations, and a set of combinations of	

	the details and their respective approximations. The most effective periodic components for trends are indicated in bold format.	<b>93</b>
<b>Table 3.10.</b>	Mann-Kendall Z-values of the autumn temperature series: original data, details components, approximations, and a set of combinations of the details and their respective approximations. The most effective periodic components for trends are indicated in bold format.	<b>95</b>
<b>Table 4.1.</b>	Unregulated RHBN gauging stations in Ontario and Quebec recording the streamflow data, which were used in this study.	<b>126</b>
<b>Table 4.2.</b>	Meteorological stations in Ontario and Quebec recording the precipitation data, which were used in this study.	<b>127</b>
<b>Table 4.3.</b>	Lag-1 Autocorrelation Functions (ACFs) of the original monthly, seasonally-based, and annual flow series.	<b>140</b>
<b>Table 4.4.</b>	Lag-1 Autocorrelation Functions (ACFs) of the original monthly, seasonally-based, and annual precipitation series.	<b>140</b>
<b>Table 4.5.</b>	Mann-Kendall values of the monthly flow series: original data, details components (D1-D6), approximations (A6), and a set of combination of the details and their respective approximations. The most effective periodic components for trends are indicated in bold format.	<b>144</b>
<b>Table 4.6.</b>	Mann-Kendall values of the monthly precipitation series: original data, details components (D1-D6), approximations (A6), and a set of combination of the details and their respective approximation. The most effective periodic components for trend are indicated in bold format.	<b>148</b>
<b>Table 4.7.</b>	Mann-Kendall values of the seasonally-based flow series: original data, details components (D1-D4), approximations (A4), and a set of combination of the details and their respective approximations. The most dominant periodic components for trend are indicated in bold format.	<b>155</b>
<b>Table 4.8.</b>	Mann Mann-Kendall values of the seasonally-based precipitation series: original data, details components (D1-D4), approximations (A4), and a set of combination of the details and their respective approximation.	

The most dominant periodic components for trends are indicated in bold format. **156**

**Table 4.9.** Mann-Kendall values of the annual flow series: original data, details components (D1-D4), approximations (A4), and a set of combination of the details and their respective approximation. The most influential periodic components for trends are indicated in bold format. **159**

**Table 4.10.** Mann-Kendall values of the annual precipitation series: original data, details components (D1-D4), approximations (A4), and a set of combination of the details and their respective approximation. The most influential periodic components for trends are indicated in bold format. **160**

## LIST OF FIGURES

- Figure 3.1.** A map of the weather stations used in this study. **61**
- Figure 3.2.** Examples of the monthly data correlograms: stations Harrow (left) and Vineland (right). High coefficient values at every sixth lag indicate the presence of semiannual and annual seasonality patterns. The upper and lower confidence limits are shown by the straight lines. **76**
- Figure 3.3.** Examples of the seasonally-based data correlograms: stations Harrow (left) and Vineland (right). High coefficient values at every second lag indicate the presence of semiannual and annual seasonality patterns. The upper and lower confidence limits are shown by the straight lines. **76**
- Figure 3.4.** Station Harrow's original monthly temperature series and its decomposition via the DWT using db3 wavelet, into six levels (D1-D6 and A6). **80**
- Figure 3.5.** Sequential Mann-Kendall graphs of station Harrow's monthly temperature data. The progressive trend lines of the original data are represented by the solid lines and the trend lines of the detail components (with their approximation added) are represented by the dashed line. The upper and lower dashed lines represent the confidence limits ( $\alpha = 5\%$ ). **81**
- Figure 3.6.** Sequential Mann-Kendall graphs of station Harrow's seasonally-based temperature data. The progressive trend lines of the original data are represented by the solid lines and the trend lines of the detail components (with their approximation added) are represented by the dashed lines. The upper and lower dashed lines represent the confidence limits ( $\alpha = 5\%$ ). **83**
- Figure 3.7.** Sequential Mann-Kendall graphs of station Harrow's annual temperature data. The progressive trend lines of the original data are represented by the solid lines and the trend lines of the detail components (with their approximation added) are represented by the



dashed lines. The upper and lower dashed lines represent the confidence limits ( $\alpha = 5\%$ ). **85**

**Figure 3.8.** Sequential Mann-Kendall graphs of station Harrow's winter temperature data. The progressive trend lines of the original data are represented by the solid lines and the trend lines of the detail components (with their approximation added) are represented by the dashed lines. The upper and lower dashed lines represent the confidence limits ( $\alpha = 5\%$ ). **89**

**Figure 3.9.** A comparison of the sequential Mann-Kendall graphs among D3, D4, and D5 (all with approximation added) of station Vineland's winter temperature data. The progressive trend lines of the original data are represented by the solid lines and the trend lines of the detail components are represented by the dashed lines. The upper and lower dashed lines represent the confidence limits ( $\alpha = 5\%$ ). **90**

**Figure 3.10.** Sequential Mann-Kendall graphs of station Harrow's spring temperature data. The progressive trend lines of the original data are represented by the solid line and the trend lines of the detail components (with their approximation added) are represented by the dashed lines. The upper and lower dashed lines represent the confidence limits ( $\alpha = 5\%$ ). **92**

**Figure 3.11.** Sequential Mann-Kendall graphs of station Harrow's summer temperature data. The progressive trend lines of the original data are represented by the solid lines and the trend lines of the detail components (with their approximation added) are represented by the dashed lines. The upper and lower dashed lines represent the confidence limits ( $\alpha = 5\%$ ). **94**

**Figure 3.12.** Sequential Mann-Kendall graphs of station Harrow's autumn temperature data. The progressive trend lines of the original data are represented by the solid lines and the trend lines of the detail components (with their approximation added) are represented by the

	dashed lines. The upper and lower dashed lines represent the confidence limits ( $\alpha = 5\%$ ).	96
<b>Figure 4.1.</b>	A map of the flow and precipitation stations used in this study.	125
<b>Figure 4.2.</b>	Examples of annual cycles in the monthly series (left: Richelieu River; right: Montreal/Pierre Elliot Trudeau) are seen in these correlograms as there are higher ACF values at every 12 <sup>th</sup> lag. The upper and lower solid lines represent the confidence intervals.	141
<b>Figure 4.3.</b>	Annual cycles are also seen in the seasonally-based series (left: Richelieu River; right: Montreal/Pierre Elliot Trudeau), where the values of ACFs at every 4 <sup>th</sup> lag are higher compared to the other lags. The upper and lower solid lines represent the confidence intervals.	142
<b>Figure 4.4.</b>	Sydenham River's original monthly flow series and its transforms via the DWT using db9 wavelet, into six decomposition levels (D1-D6) and one approximation (A6).	145
<b>Figure 4.5.</b>	Montreal/Pierre Elliot Trudeau's original monthly flow series and its transforms via the DWT using db9 wavelet, into six decomposition levels (D6-D6) and one approximation (A6).	146
<b>Figure 4.6.</b>	Sequential Mann-Kendall graphs of station Sydenham River monthly data displaying the progressive trend lines of each detail (with the approximation added). The upper and lower dashed lines represent the confidence limits ( $\alpha = 5\%$ ); the solid and dashed progressive lines are the original and detail sequential MK lines, respectively.	147
<b>Figure 4.7.</b>	Examples of correlograms of the D1 periodic components (left: Neebing River; right: Missinaibi River) of the seasonally-based data, which display strong annual cycles as seen in their repeated high values at every 4 <sup>th</sup> lag. Note that the cycles do not dampen over time.	150
<b>Figure 4.8.</b>	The correlograms of the D1-D4 components of Nagagami River's seasonally-based data. The D1 and D2 components have high ACF values at every 4 <sup>th</sup> lag, which indicates the presence of 12-month cycles. D3 and D4 show some patterns of oscillations that may dampen over time, which are not considered annual cycles.	152

- Figure 4.9.** The correlograms of several approximation components (A4) of the seasonally-based data showing a lack of constant oscillations. **153**
- Figure 4.10.** Illustration of the sequential Mann-Kendall graphs of the D1 – D4 components (with approximation) of the seasonally-based data in order to determine the most dominant periodic component for trend (Sydenham River’s data were used in this example). The upper and lower dashed lines represent the confidence limits ( $\alpha = 5\%$ ); the solid and dashed progressive lines are the original and detail component sequential MK lines, respectively. **154**
- Figure 4.11.** Sequential Mann-Kendall graphs of the D2 components, which represent the 12-month periodic components from several seasonally-based flow data. These trend lines show good matches with respect their original trend lines. The upper and lower dashed lines represent the confidence limits ( $\alpha = 5\%$ ); the solid and dashed progressive lines are the original and detail component sequential MK lines, respectively. **156**
- Figure 4.12.** Progressive Mann-Kendall graphs of the components of the seasonally-based precipitation data from Ottawa CDA station. The upper and lower dashed lines represent the confidence limits ( $\alpha = 5\%$ ); the solid and dashed progressive lines are the original and detail sequential MK lines, respectively. Based on the MK values and the sequential MK graphs, D3 and D4 (with approximations) were determined to be the most effective periodic components contributing to the trend production. **157**
- Figure 4.13.** Examples of sequential Mann-Kendall graphs of the detail components of the annual flow data in order to determine the most dominant periodicity for trends (Sydenham River’s data were used in this example). The upper and lower dashed lines represent the confidence limits ( $\alpha = 5\%$ ); the solid and dashed progressive lines are the original and detail sequential MK lines, respectively. **161**

**Figure 4.14.** Examples of sequential Mann-Kendall graphs of the detail components of the annual precipitation data in order to determine the most dominant periodicity for trends (Ottawa CDA's data were used in this example). The upper and lower dashed lines represent the confidence limits ( $\alpha = 5\%$ ); the solid and dashed progressive lines are the original and detail sequential MK lines, respectively. **162**

**Figure 4.15.** Progressive Mann-Kendall graphs of all the original annual flow data used in the study. The upper and lower dashed lines represent the confidence limits ( $\alpha = 5\%$ ). These graphs were used to determine the possible starting time of the observed trends for the different stations. **163**

**Figure 4.16.** Progressive Mann-Kendall graphs of all the original precipitation data used in the study. The upper and lower dashed lines represent the confidence limits ( $\alpha = 5\%$ ). These graphs were used to determine the possible starting time of the observed trends for the different stations. **163**

## LIST OF ABBREVIATIONS

A	Approximation
ACF	Autocorrelation Function
AR	Autoregressive
ARIMA	Autoregressive Integrated Moving Average
BS-MK	Bootstrap-Based Mann-Kendall
BS-Slope	Bootstrap-Based Slope
D	Detail
ENSO	El Niño–Southern Oscillation
CGCM	Canadian General Circulation Model
CO <sub>2</sub>	Carbon dioxide
CWT	Continuous Wavelet Transform
db	Daubechies
DWT	Discrete Wavelet Transform
FT	Fourier Transform
GCM	General Circulation Model
GHG	Green House Gas
GTA	Greater Toronto Area
IDWT	Inverse Discrete Wavelet Transform
IPCC	Intergovernmental Panel on Climate Change
LA	Least Asymmetric
MK	Mann-Kendall
MRE	Mean Relative Error
NAO	North Atlantic Oscillation
OLS	Ordinary Least Squares
PDO	Pacific Decadal Oscillation
PNA	Pacific-North America
RE	Relative Error
RHBN	Reference Hydrometric Basin Network
SPRC	Spearman Partial Rank Correlation
TFPW	Trend-Free Pre-whitening

UNFCCC	United Nation Framework Convention on Climate Change
WA	Wavelet Analysis
WFT	Windowed Fourier Transform
WT	Wavelet Transform

## **CHAPTER 1 – GENERAL INTRODUCTION**

### **1.1. Climate Change and its General Impacts**

Changes in climate are a result of both natural and human activities, particularly those that alter the chemistry of the atmosphere. Climate change itself is represented by a complex mixture of stressors involving elevated atmospheric greenhouse gas (GHG) concentrations, increased frequencies and intensities of extreme weather events, and alterations in temperature, precipitation, and hydrologic cycles (Durdu, 2010).

Examples of human anthropogenic activities that have contributed to the elevated GHG include deforestation, industrial activities, agriculture-related processes, and most importantly the burning of fossil fuels (UNFCCC, 2007). Increased atmospheric carbon-dioxide concentrations have especially been documented since the start of the Industrial Revolution. From this time, major changes in sectors such as agriculture, manufacturing, mining, transportations, and technology have taken place, resulting in the increased burning of fossil fuels (UNFCCC, 2007). It has generally been perceived that such conditions cause temperatures to increase (Scavia et al., 2002).

The most recent assessment conducted by the Intergovernmental Panel on Climate Change (IPCC) reported an increase in the mean surface temperature of between 0.56°C and 0.92°C from 1906 to 2005 (IPCC, 2007). This increase is larger than what had been mentioned by the previous IPCC report, which mentioned that the global mean surface temperature has increased by approximately 0.3 °C to 0.6 °C from 1901-2000 (IPCC, 2001).

While the temperature is expected to increase practically everywhere over land, precipitation is expected to increase globally (IPCC, 2007). In many river basins precipitation is expected to increase, but in many others a decrease is expected instead (IPCC, 2007). In addition, precipitation intensities are expected to increase in some seasons or areas but decrease in others (IPCC, 2007). All these changes in the climate may threaten the global freshwater system and increase the uncertainty associated with hydrological processes (IPCC, 2007; Koutsouris et al., 2010). The IPCC (2007) documented with strong confidence that the impacts of climate change on freshwater

systems and their management are mostly caused by increases in temperature, sea level and precipitation variability that have been observed.

Numerous studies all over the world have been conducted to analyze and forecast the impacts of climate change on hydrological variables, such as precipitation and streamflow. For example, Beyene et al. (2010) simulated the impacts of climate change on the hydrology of the Nile River basin and found that the basin is likely to have higher streamflow up to 2039 as a result of increased precipitation; however, from 2040 to 2099, streamflow is expected to decrease. Austin et al. (2010) used the Biophysical Capacity to Change and Cubic Conformal models together with different climate change scenarios in order to predict the impacts of climate change on Murray-Darling Basin in Australia. Their projections revealed that by the year 2070, the mean annual rainfall could decline and the potential evapotranspiration could go up – both by up to 25% (Austin et al., 2010). Shepherd et al. (2010) forecasted river flows in the Oldman River Basin draining the North American Rocky Mountains using projection analyses and hydroclimatic modelling. Using six different GCMs, both methods showed similar results: increased flow in spring and winter, and reduced flow in the summer. The latest report by the IPCC (2007) (Fourth assessment) presents a thorough assessment on the potential impacts of climate change on many aspects of fresh water systems.

In Canada, many areas are also known to be sensitive to changes in precipitation that are associated with climate change (Environment Canada, 2004). For example, a reduction in the mean annual flow for the Great-Lakes-St. Lawrence watershed in the USA and Canada is projected to be between 4% and 24% over the next 90 years, due to increased evaporation (Croley, 2003). When analyzed using the Canadian General Circulation Model (CGCM I) where the concentration of CO<sub>2</sub> is doubled, the sea ice in Hudson Bay practically vanished (Gough and Wolfe, 2001). Roy et al. (2001) also looked at the seasonal flooding associated with climate change in the Chateauguay River Basin, which is situated in southern Quebec. Using the outcome from the CGCM I and a coupled hydrology-hydraulics model, they forecasted that there would be dramatic increase in the amount of runoff, maximum discharge (up to 250%), and water level by 2080-2100 (Roy et al., 2001). For drainage into high-latitude oceans (Arctic and North Atlantic), Dery and Wood (2005) examined the total annual discharge in 64 Canadian



rivers for the period of 1964-2003. They found that the discharge was reduced by about 10% from 1964 to 2003, which is in agreement with the decrease in the amount of precipitation for the period of 1964 to 2000 over areas in northern Canada (Dery and Wood, 2005).

## **1.2. Trends in Hydroclimatic Indices**

As can be seen, the effects of changes in climate have attracted widespread interest in the fields of hydrology, meteorology and climatology. Most studies conducted to investigate the impacts of climate change on water resources concluded that climate change will have an adverse impact (or at least pose significant challenges) on water resources, both on quality and quantity. As such, it is crucial to understand how the effects of climate change on water resources are extended to nature and society. Canada holds a special role because it has approximately one tenth of the world's renewable water; therefore, changes in its quantity and/or quality will have consequences beyond Canada's border (Environment Canada, 2004).

Since the climate is continuously changing, the investigation of climate change is linked directly with trends in different climatic indices. Many studies have been conducted in the fields of hydro-climatology and hydro-meteorology in order to detect and quantify the existence of trends. Some of the most common parameters included in these studies are temperature (Pişoft et al, 2004; Prokoph and Patterson, 2004; Mohsin and Gough, 2010), streamflow (Zhang et al., 2001; Burn and Hag Elnur, 2002; Anctil and Coulibaly, 2004; Zume and Tarhule, 2006, Partal, 2010), precipitation (Kim, 2004; Mishra and Singh, 2010), surface runoff (Labat et al., 2004; Liu, et al., 2010), and snowpack (Hamlet et al., 2005), among others. Most of the studies observed that trends – positive or negative – have been variously attributed to climate change and climate variability.

It is important to differentiate between climatic change and climate variability. Climate variability is the natural process of climate variation occurring within a period of time, whereas climate change refers to a long-term alteration in the climate itself (Kundzewicz and Robson, 2004). Changes can occur as a trend gradually, abruptly, or in

a more complex form (Xiong and Guo, 2004; Zhang et al., 2010). Climate variability may produce highly noticeable effects on hydrological records, which result in: (i) evidence of trends existing when the length of data used is short, but these trends may disappear if longer data are used, (ii) large climatic variation can effectively hide changes that are caused by climate change (Kundzewicz and Robson, 2004). As climatic changes continue to occur, we should expect to see more statistically significant trends in hydro-climatic data. This would provide evidence that the hydrologic regime will continue to change in the future – it is not a stationary system.

### **1.3. Problems Faced in Time Series Analysis to Detect Trends**

Data are a central part of studies that attempt to detect trends and changes in hydro-meteorological processes. Hydro-meteorological data are usually characterized by non-stationary properties, and are composed of trend, periodic, autoregressive, and random residual factors (Kite, 1993). The trend is usually a result of changes in the structure, which are caused by natural or anthropogenic activities (e.g., climatic variability, land-use changes, etc). Periodicities are mainly associated with astronomical phenomena such as the earth's rotation around the sun. Autoregressive components show that the information in the time series may be dependent on the magnitude of the preceding events. Since hydrological processes may be affected by factors such as weather, vegetation cover, infiltration and evapotranspiration, they contain stochastic constituents, and multi-time scale and nonlinear properties (Wang and Ding, 2003). Trend detection and estimation in the presence of all these stochastic components is an essential part of hydrological studies.

Some other issues that may be faced in trend detection studies are caused by the existence of data gaps in the records, and the presence of outliers and autocorrelation (Lattenmaier, 1988). To deal with this, many authors have employed the use of both parametric and non-parametric statistical tests. Shao et al. (2010) pointed out that most of the methods used in the literature are unable to detect both long-term trends and abrupt changes simultaneously. Common non-parametric approaches, such as the Mann-Kendall, the Wilcoxon–Mann–Whitney, t-test, and Pettitt's, can only detect a monotonic trend or a

single abrupt change (Shao et al., 2010). Thus, the use of any one of these tests alone cannot efficiently detect trends in hydrological time series. This is because hydrological time series are known to often exhibit multiple abrupt changes and different trends, occurring in different periods, which are caused by inter-annual and decadal variability associated with the climate system (Peel and McMahon, 2006). Additionally, classical trend tests do not deal well with the effects of persistence and seasonality (Cluis et al., 1989).

Some authors have also attempted to detect the trend and abrupt change components in a time series separately (e.g., Zhao et al., 2008), but this approach is not statistically satisfactory because the conclusions obtained from the different tests may not be compatible (Shao et al., 2010). Though a single trend test is considered appropriate for trend testing and detection with specified start and end times, it does not illustrate whether any changes are due to gradual or abrupt occurrences (Zhang et al., 2010).

Yue et al. (2002) and Mohsin and Gough (2010) recognized that a number of trend-related studies contained some flaws because when using trend detection tests, such as the Mann-Kendall test, the studies did not include testing for autocorrelation. They simply assumed that the observations contained in the time series being analyzed are serially independent. The effect of one data point on the next one (serial correlation) in a sequential times series can lead to a misleading interpretation (type I error) – the rejection of the null hypothesis will be more likely to occur when in fact it should be accepted (Kulkarni and von Storch, 1995; Hamed and Rao, 1998; Partal, 2010). Positive serial correlation can lead to an increase in type I error (Douglas et al., 2000), whereas the presence of negative serial correlation can lead to an increase in type II error (i.e., falsely accepting the null hypothesis) (Yue and Wang, 2002). As such, it is important to address the issue of serial correlation in a time series prior to applying a trend test. Since the MK test was used in this present study, the extended versions of the original MK test were applied in case of the existence of significant autocorrelations in the time series.

#### **1.4. Time-Frequency Assessment of a Time Series**

When analyzing trends in hydroclimatic time series, not only is it important to check for whether the direction of trends is positive or negative, but also how these changes fluctuate within different time scales (e.g. intra-annual, inter-annual, decadal events). A traditional tool that has been frequently used to detect oscillatory signals is the Fourier Transform (FT), which uses sine and cosine basis functions. The FT has some major drawbacks. Since this method uses single-window analysis, it is unable to detect the properties of signals that are much shorter or longer than the size of the window (Torrence and Compo, 1998). Furthermore, the sinusoids used in FT are only localized in the frequency domain and not in time domain. Therefore, FT only provides time-averaged results and extracts details from the signal frequency, but loses its temporal information (Drago and Boxall, 2002). As a result, the location of the frequency within the signal cannot be identified (Oh et al., 2003). Fourier analysis is more suited for fields that involve stationary processes, such as in electronics; but when the focus is shifted to hydrological processes, FT is not an ideal approach because earth-science processes involve signals that tend to have high fluctuations and are often not stationary (Labat, 2005).

The wavelet transform (WT) approach is a relatively recent advancement in the field of signal processing (Santos et al., 2001). Wavelet transforms analyze the non-stationary variance at differing frequency levels of a time series by employing mathematical transformations. A signal to be localized is broken up into functions, known as wavelets. Unlike the FT that uses a single-window analysis, WT uses both narrow and wide windows at high frequencies and at low frequencies, respectively (Drago and Boxall, 2002). For the lower scale, this means the window size of the wavelet is compressed, which allows the tracking of abrupt changes or high frequency components in the signal. In contrast, the window size is stretched at higher scales, which allows for tracking slowly progressing events, or low frequency components in the signal. This demonstrates one of the biggest advantages of WT over FT, which is its ability to scale the wavelet according to its width (Santos et al., 2001). In addition to this, WT also deals well with jumps, shifts, and even discontinuous patterns in the data, which are

indeed often observed in hydro-meteorological data (Prokoph and Patterson, 2004; Adamowski et al., 2009).

WT produces the time-frequency representation of the signals (or time series) being analyzed. In other words, wavelet transforms allow the one-dimensional time series to be decomposed into different levels of time-frequency space (i.e. two-dimensional information) (Zume and Tarhule, 2006; Kim, 2004). Thus, the major variability components or dominant modes can be identified, and their variation with time can be investigated (these features are not readily apparent in the raw signal) (Oh et al., 2003). In this study, WT was used to decompose the time series into their calculated number of decomposition levels and into their details (scales) and approximation components. The different detail components represent higher-frequency components (at lower detail levels) and lower-frequency components (at higher detail levels). Additionally, we assumed that the approximation component contains the trend element of the analyzed time series. The wavelet transform is discussed in more detail in sections 2.5, 3.2, and 4.2.

## **1.5. Research Objectives**

A number of studies have recommended studying the trends for different hydroclimatic variables, so as to understand the relationship between hydrology and climate. In light of this, the main objective of this research is to analyze the trends that may exist in the time series of three hydroclimatic variables, namely precipitation, streamflow, and temperature. These parameters serve as good indicators of how the climate has evolved because: (1) studies on climate change indicate an increase in temperature, and patterns of precipitation have experienced changes in different parts of the world (Burn and Hag Elnur, 2002); (2) Streamflow tends to reflect how a catchment area as a whole has been responding to the variability in climate (Gaucherel, 2002). Zhang et al. (2009) also indicated that in order to understand the effects of climate change on global and regional water resources, information about the impacts of climate change on the spatiotemporal characteristics of precipitation is required.

To accomplish the main goal of this study, the specific objectives are as follows:

1. To couple the WT technique and the MK trend test in analyzing trends in flow, precipitation, and temperature data from several flow and meteorological stations located in southern parts of Ontario and Quebec.
2. To decompose the data of the variables used into their lower resolution components via the discrete wavelet transform (DWT) approach.
3. To assess the significance of trends in the original data and in the time series resulting from the wavelet decomposition using the MK trend test.
4. To determine the most influential periodicity that affect trends by examining each periodic mode's sequential MK trend line and how close its MK Z-value is compared to the original MK Z-value.

One of the reasons that the DWT method is chosen is because many real-life occurrences in hydrology such as rainstorms, flood events, and streamflow are recorded in discrete manner (Wang and Ding, 2003). Since the procedure of applying the MK test on the decomposed hydroclimatic time series via the WT is considered very new, this application in a North American context (and more specifically, in Ontario and Quebec) is original.

The evaluation of hydroclimatic trends on a smaller spatial scale (e.g. watershed scale) provides information on catchment dynamics (Gautam et al., 2010). The findings and results obtained from this study will be useful for many aspects of infrastructure design, modelling, and management of water resources (such as in planning and monitoring of integrated and adaptive water management programs). Trend detection and analysis in hydroclimatic variables can also bring out issues which need to be considered as part of adaptation and mitigation efforts associated with climate change. This implies that public policies created to address the impacts of climate change for a specific region should be done based on the knowledge for that particular region, rather than on the global climate change information (Clark et al., 2000). The results of trend analysis in these hydroclimatic variables can also be incorporated into prediction models of future scenarios applied to many different fields, such as in agriculture (e.g. growing seasons, irrigation schemes, crop productions) and food security, water supplies, extreme weather forecast, etc.

Although many trend detection studies have been conducted in Canada, using the DWT in conjunction with the MK test as part of the methodology has not been explored. As will be seen, the DWT provides very detailed information of the analyzed time series by extracting its different periodicities. Furthermore, applying the MK test and the sequential MK analysis enabled us to determine the periodic modes that are more influential for trends. Some potential drivers behind these dominant modes are also discussed.

The results of this research should be useful for current and future water resources planning efforts in Ontario and Quebec, as it involves making reasonable predictions or assumptions about future hydro-climatic conditions. This study will also significantly contribute to current research in the field of trend detection in Canada, particularly in Ontario and Quebec.

## **1.6. Thesis Outline**

This thesis is submitted in the format of papers suitable for journal publications. Chapter 1 of this thesis briefly discusses climate change and its general projected impacts on hydrological variables. It then links climate change with detecting trends in different hydroclimatic indices. Chapter 1 also presents the problem statement of this thesis, which contains some reviews about issues that arise when attempting to detect trends in hydroclimatic data, which have a nonstationary nature. The chapter then mentions the importance of investigating the variability of the different time-scale events (e.g. inter-annual, decadal, etc.) that may be present in the data being analyzed. Finally, this chapter discusses how the WT approach can be used to efficiently extract information (including trends) from a time series; and then test the significance of the different detail and approximation components with the MK test.

Chapter 2 presents a literature review related to the effects of climate change on hydrology, followed by detecting trends in hydroclimatic indices. Several common methods used to estimate and detect trends in hydroclimatic studies are also discussed, along with their strengths and weaknesses. In this chapter, the justifications for choosing

the methods employed in this study (i.e., coupling of the WT approach and the MK trend test) are also presented.

Chapter 3 describes the application of the DWT and the MK test in assessing trends in surface air temperature series from a total of five stations in Ontario and Quebec during the period 1967 – 2006. The detailed procedures of data transformation using the DWT and how the MK test is used to assess the statistical significance of the different time series at different scales are described in this chapter. In chapter 3, we proposed a method where the relative error criterion is used to determine the type of Daubechies (db) mother wavelet, the boundary condition, and the number of decomposition levels in decomposing the data used via the DWT. The relative error used was of the MK Z-values of the approximation component and the original data. This chapter is being prepared for submission as a manuscript for a journal publication (and will be submitted to the *Journal of Hydrological Processes*).

Chapter 4 presents the application of the DWT and the MK test in analyzing trends in streamflow and precipitation in Ontario and Quebec during the period 1954 – 2008. This chapter discusses the different types of data used, which were obtained from a total of 13 flow and meteorological stations. The methodology follows what has been outlined in chapter 3. This chapter has been submitted as a manuscript to the *Journal of Hydrology*.

Chapter 5 summarizes the main findings of this study and presents the general conclusions obtained from this work. Chapter 6 presents several recommendations that future studies can consider. Finally, chapter 7 explicitly lists the contributions to knowledge made by this present study.

## **1.7. References**

- Adamowski, K., Prokoph, A., Adamowski, J., 2009. Development of a new method of wavelet aided trend detection and estimation. *Hydrological Processes*, 23(18): 2686-2696.
- Anctil, F., Coulibaly, P., 2004. Wavelet analysis of the interannual variability in southern Québec streamflow. *Journal of Climate*, 17(1): 163-173.



- Austin, J., Zhang, L., Jones, R., Durack, P., Dawes, W., Hairsine, P., 2010. Climate change impact on water and salt balances: An assessment of the impact of climate change on catchment salt and water balances in the Murray-Darling Basin, Australia. *Climatic Change*, 100(3): 607-631.
- Beyene, T., Lettenmaier, D., Kabat, P., 2010. Hydrologic impacts of climate change on the Nile River Basin: Implications of the 2007 IPCC scenarios. *Climatic Change*, 100(3): 433-461.
- Burn, D.H., Hag Elnur, M.A., 2002. Detection of hydrologic trends and variability. *Journal of Hydrology*, 255(1-4): 107-122.
- Clark, J.S., Yiridoe, E.K., Burns, N.D., Astatkie, T., 2000. Regional climate change: Trend analysis of temperature and precipitation series at selected canadian sites. *Canadian Journal of Agricultural Economics*, 48(1): 27-38.
- Cluis, D., Langlois, C., Coillie, R., Laberge, C., 1989. Development of a software package for trend detection in temporal series: Application to water and industrial effluent quality data for the St. Lawrence River. *Environmental Monitoring and Assessment*, 13(2): 429-441.
- Croley, T.E. (2003). Great Lakes climate change hydrological impact assessment, IJC Lake Ontario—St. Lawrence River regulation study. (NOAA Tech. Memo. GLERL-126). Ann Arbor, Michigan: Great Lakes Environmental Research Laboratory.
- Déry, S.J., Wood, E.F., 2005. Decreasing river discharge in northern Canada. *Geophys. Res. Lett.*, 32(10): L10401.
- Douglas, E.M., Vogel, R.M., Kroll, C.N., 2000. Trends in floods and low flows in the United States: Impact of spatial correlation. *Journal of Hydrology*, 240(1-2): 90-105.
- Drago, A.F., Boxall, S.R., 2002. Use of the wavelet transform on hydro-meteorological data. *Physics and Chemistry of the Earth*, 27(32-34): 1387-1399.
- Durdu, Ö.F., 2010. Effects of climate change on water resources of the Büyük Menderes River Basin, western Turkey. *Turk. J. Agric. For.*, 34(4): 319-332.
- Gaucherel, C., 2002. Use of wavelet transform for temporal characterisation of remote watersheds. *Journal of Hydrology*, 269(3): 101-121.

- Gautam, M.R., Acharya, K., Tuladhar, M.K., 2010. Upward trend of streamflow and precipitation in a small, non-snow-fed, mountainous watershed in Nepal. *Journal of Hydrology*, 387(3–4): 304-311.
- Gough, W.A., Wolfe, E., 2001. Climate change scenarios for Hudson Bay, Canada, from General Circulation Models. *Arctic*, 54(2): 142-148.
- Hamed, K.H., Rao, A.R., 1998. A modified Mann-Kendall trend test for autocorrelated data. *Journal of Hydrology*, 204(1–4): 182-196.
- Hamlet, A.F., Mote, P.W., Clark, M.P., Lettenmaier, D.P., 2005. Effects of temperature and precipitation variability on snowpack trends in the western United States. *Journal of Climate*, 18: 4546-4561.
- IPCC, 2001. Climate change 2001: the third IPCC scientific assessment. In: J.J. McCarthy, O.F. Canziani, N.A. Leary, D.J. Dokken and K.S. White (eds). Intergovernmental Panel on Climate change. Cambridge University Press, Cambridge, United Kingdom and New York, NY, USA.
- IPCC, 2007. Climate change 2007: the fourth IPCC scientific assessment. In: M.L. Parry, O.F. Canziani, J.P. Palutikof, P.J. van der Linden and C.E. Hanson (eds). Intergovernmental Panel on Climate Change. Cambridge University Press, Cambridge, United Kingdom and New York, NY, USA.
- Kim, S., 2004. Wavelet analysis of precipitation variability in northern California, U.S.A. *KSCE Journal of Civil Engineering*, 8(4): 471-477.
- Kite, G., 1993. Analysing hydrometeorological time series for evidence of climatic change. *Nordic Hydrology*, 24: 135-150.
- Koutsouris, A.J., Destouni, G., Lyon, S.W., 2010. Hydro-climatic trends and water resource management implications based on multi-scale data for the Lake Victoria region, Kenya. *Environmental Research Letters*, 5(3): 034005.
- Kulkarni, A., von Storch, H., 1995. Monte carlo experiments on the effect of serial correlation on the Mann-Kendall test of trend. *Meteorol. Z.*, 4(2): 82-85.
- Kundzewicz, Z.W., Robson, A.J., 2004. Change detection in hydrological records—A review of the methodology. *Hydrological Sciences Journal*, 49(1): 7-19.
- Labat, D., 2005. Recent advances in wavelet analyses: Part 1. A review of concepts. *Journal of Hydrology*, 314(1–4): 275-288.

- Labat, D., Godd  ris, Y., Probst, J.L., Guyot, J.L., 2004. Evidence for global runoff increase related to climate warming. *Advances in Water Resources*, 27(6): 631-642.
- Lettenmaier, D.P., 1988. Multivariate nonparametric tests for trend in water quality. *JAWRA Journal of the American Water Resources Association*, 24(3): 505-512.
- Liu, D., Chen, X., Lian, Y., Lou, Z., 2010. Impacts of climate change and human activities on surface runoff in the Dongjiang River Basin of China. *Hydrological Processes*, 24(11): 1487-1495.
- Mishra, A.K., Singh, V.P., 2010. Changes in extreme precipitation in Texas. *Journal of Geophysical Research*, 115(D14): D14106.
- Mohsin, T., Gough, W., 2010. Trend analysis of long-term temperature time series in the Greater Toronto Area (GTA). *Theoretical and Applied Climatology*, 101(3): 311-327.
- Oh, H.-S., Ammann, C.M., Naveau, P., Nychka, D., Otto-Bliesner, B.L., 2003. Multi-resolution time series analysis applied to solar irradiance and climate reconstructions. *Journal of Atmospheric and Solar-Terrestrial Physics*, 65(2): 191-201.
- Partal, T., 2010. Wavelet transform-based analysis of periodicities and trends of Sakarya Basin (Turkey) streamflow data. *River Research and Applications*, 26(6): 695-711.
- Peel, M.C., McMahon, T.A., 2006. Recent frequency component changes in interannual climate variability. *Geophys. Res. Lett.*, 33(16): L16810.
- Pi  soft, P., Kalvov  , J., Br  zdil, R., 2004. Cycles and trends in the Czech temperature series using wavelet transforms. *International Journal of Climatology*, 24(13): 1661-1670.
- Prokoph, A., Patterson, R.T., 2004. Application of wavelet and regression analysis in assessing temporal and geographic climate variability: Eastern Ontario, Canada as a case study. *Atmosphere Ocean*, 43(2): 201-212.
- Roy, L., Leconte, R., Brissette, F.P., Marche, C., 2001. The impact of climate change on seasonal floods of a southern Quebec River basin. *Hydrological Processes*, 15(16): 3167-3179.

- Santos, C.A.G., Galvão, C.d.O., Suzuki, K., Trigo, R.M., 2001. Matsuyama city rainfall data analysis using wavelet transform. *Annual Journal of Hydraulic Engineering, JSCE*, 45: 6.
- Scavia, D. et al., 2002. Climate change impacts on U. S. coastal and marine ecosystems. *Estuaries*, 25(2): 149-164.
- Shao, Q., Li, Z., Xu, Z., 2010. Trend detection in hydrological time series by segment regression with application to Shiyang River Basin. *Stochastic Environmental Research and Risk Assessment*, 24(2): 221-233.
- Shepherd, A., Gill, K.M., Rood, S.B., 2010. Climate change and future flows of Rocky Mountain rivers: Converging forecasts from empirical trend projection and down-scaled global circulation modelling. *Hydrological Processes*, 24(26): 3864-3877.
- Torrence, C., Compo, G.P., 1998. A practical guide to wavelet analysis. *Bulletin of the American Meteorological Society*, 79(1): 61-78.
- UNFCCC, 2007. Climate change: Impacts, vulnerabilities and adaptation in developing countries. UNFCCC Secretariat. Bonn, Germany. <http://unfccc.int/resource/docs/publications/impacts.pdf>.
- Wang, W., Ding, J., 2003. Wavelet network model and its application to the prediction of hydrology. *Nature and Science*, 1(1): 67-71.
- Xiong, L., Guo, S., 2004. Trend test and change-point detection for the annual discharge series of the Yangtze River at the Yichang hydrological station. *Hydrological Sciences Journal*, 49(1): 99-112.
- Yue, S., Pilon, P., Phinney, B., Cavadias, G., 2002. The influence of autocorrelation on the ability to detect trend in hydrological series. *Hydrological Processes*, 16(9): 1807-1829.
- Yue, S., Wang, C.Y., 2002. Assessment of the significance of sample serial correlation by the bootstrap test. *Water Resources Management*, 16(1): 23-35.
- Zhang, Q., Xu, C.Y., Zhang, Z., Chen, Y.D., Liu, C.L., 2009. Spatial and temporal variability of precipitation over China, 1951-2005. *Theoretical and Applied Climatology*, 95(1-2): 53-68.
- Zhang, X., Harvey, K.D., Hogg, W.D., Yuzyk, T.R., 2001. Trends in Canadian streamflow. *Water Resources Research*, 37(4): 987-998.

- Zhang, Z., Dehoff, A., Pody, R., Balay, J., 2010. Detection of streamflow change in the Susquehanna River Basin. *Water Resources Management*, 24(10): 1947-1964.
- Zhao, F.F., Xu, Z.X., Huang, J.X., Li, J.Y., 2008. Monotonic trend and abrupt changes for major climate variables in the headwater catchment of the Yellow River Basin. *Hydrological Processes*, 22(23): 4587-4599.
- Zume, J., Tarhule, A., 2006. Precipitation and streamflow variability in Northwestern Oklahoma, 1894-2003. *Physical Geography*, 27(3): 189-205.

## **CHAPTER 2 – LITERATURE REVIEW**

In this chapter, relevant methods used in trend detection in hydroclimatic studies are reviewed and discussed. In particular, the applications of the wavelet transform (WT) on streamflow, precipitation and temperature data are given to emphasize its applications and usefulness.

### **2.1. General Implications of Changing Climate on Hydrology**

Changes in the earth's climate can have multiple significant implications for hydrologic regimes. Increased concentrations of greenhouse gas (GHG) will cause much of the solar radiation to be trapped inside the earth, hence elevating its temperature (Trenberth, 1998). Rising global temperatures will lead to changes in the characteristics of the hydrologic cycle – influencing the spatiotemporal characteristics of precipitation and rainfall, runoff, and potential evapotranspiration (IPCC, 2007). For example, the intensification of the hydrologic cycle that has been observed can lead to a decrease in precipitation in subtropical areas, which then increases the probability of drought (Dai et al., 1998; Huntington, 2006). On the other hand, increased annual precipitation in the tropics and at high latitudes will lead to an increasing probability of floods (Huntington, 2006). The melting of glaciers and rising sea levels as a result of climate change can threaten fresh water supplies (Jackson et al., 2001). These overall changes are likely to have a strong influence on the environment, including water resources availability and accessibility, and therefore pose challenges in water resources planning and management.

On the global scale, the general pattern of climate change has been studied quite extensively and is no longer very controversial argument in the scientific world (Oreskes, 2004). However, climate change has varying impacts in different geographical regions (i.e., it is not spatially uniform) (Clark et al., 2000; Burn and Hag Elnur, 2002), and the nature of these variations has a high degree of uncertainty. Having said this, hydro-climatological parameters can serve as indicators in detecting and monitoring climate change as these variables have the tendency to reflect climatic changes (Burn and Hag

Elnur, 2002). Therefore, studying them is very useful in understanding the relationships between hydrology and climate.

Recent studies have demonstrated the vulnerability of water resources to changes in temperature and precipitation characteristics (Lahmer et al., 2001; Ampitiyawatta and Guo, 2009). The environment, economy and society are largely dependent on water resources; thus, changes in the processes involved in the hydrological cycle will undoubtedly have significant implications on the environment and socio-economic profile (Arnell, 1999). Studies have also shown that since hydrologic conditions are different for different regions, the effects of climate change on local hydrological processes will differ within localities, even under the same climate setting (Zhang et al., 2001). Therefore, it is important for policy and decision makers to carefully address changes caused by climate change when managing water resources. The consequences and risks associated with climate change should be properly managed not only at the local and regional level, but also at a smaller and more localized scale (Durdu, 2010).

## **2.2. Trend Detection and Analysis in Hydroclimatic Variables**

Trend analysis in hydroclimatic variables is one way to assess how the climate has evolved over time. Trend detection refers to methods used to extract an underlying behavioral pattern in a time series that would otherwise be partly or fully hidden by noise. The detection of abrupt and gradual changes in hydrological and meteorological records has been explored in considerable detail by researchers. Information about spatiotemporal variability in hydroclimatic time series is of great importance from both scientific and practical viewpoints. For example, the interpretation of the significance of trends existing in the annual maximum (flood), mean, and low flows in rivers is very valuable for flow regulation (Tharme, 2003). This is because they are considered when designing flood mitigation structures, flood-protection systems, and water storage reservoirs. Trend detection and forecasting of low flow is of importance due to the quantity of water to be released downstream of a dam, in order to protect ecological integrity and sustainability (Smakhtin, 2001).

The detection and estimation of past trend changes and variability in hydroclimatic variables is also important for the understanding of potential future changes caused by factors that affect climate change. This applies especially to high-latitude regions such as Canada, where climate change signals are anticipated to be stronger, and where the impacts of climate change may be more severe (Nicholls et al., 1996). Boyer et al. (2010) noted that the hydrological regime of rivers at higher latitudes in the northern hemisphere (including Canada) could be dramatically modified as a result of the changes in temperature and precipitation during the current century, especially during winter and spring seasons. These modifications may include a reduction in mean annual discharge (Arora and Boer, 2001), increased evaporation (Croley, 2003), increased winter runoff (Payne et al., 2004), and less snowpack accumulation (Whitfield et al., 2003; Hamlet et al., 2005).

Research undertaken in hydroclimatic fields provides a systematic framework for the study of how local and global space / time variations in the hydrologic cycle are affected by the climate system (IPCC, 2007). If it is indeed the case that trends exist in a hydroclimatic time series, it is then essential to analyze their significance and to confirm whether these trends occurred as a result of stochastic or more deterministic processes.

In general, data used in planning and designing water resources and engineering projects imply an assumption of stationarity (Partal and Küçük, 2006; Burn et al., 2010). For example, for a long period of time, hydrologists considered floods to be events that resulted from stationary, independent and random processes. Such assumptions can probably no longer be integrated into the planning and design procedures of water resources works if the discussed global climate change (more specifically, due to anthropogenic-induced factors) is indeed occurring (Beyene et al., 2010).

One of the goals of trend detection is to determine the main causes affecting these trends (Yu et al., 1993). With growing demand for water and problems related to water resources, it is essential to understand the effects of climatic variability/change on hydrological processes, as they are indicators of how the climate has changed over time (Burn, 1994). Additionally, analyzing and predicting the likely impacts of climatic change on water resources availability is very important to support sustainable water management and its future planning (Durdu, 2010). For example, in order to manage and



understand the causes of water shortages, it is important to investigate in detail the hydrological process of the area (Durdu, 2010). Furthermore, a thorough understanding of how changes in climate affect the hydrological processes in a watershed is needed in order to carry out work such as stormwater planning, water quality management, river restoration projects, etc. (Coats, 2010). One way to understand the changes in the hydrological processes in a watershed is by analyzing the trends involved in these processes (e.g. precipitation and streamflow). Trends in climate are partly caused by the increase in the concentration of GHGs in the atmosphere. Having said this, natural cycles of climate indices such the North Atlantic Oscillation (NAO), El Niño Southern Oscillation (ENSO), Pacific North American (PNA) – which are prominent in the Northern hemisphere – have been found to also affect the trends in temperature, precipitation, and streamflow (Wettstein and Mearns, 2002; Coulibaly and Burn, 2004; Anctil and Coulibaly, 2004; Bonsal et al., 2006; Damyanov et al., 2012; Fu et al., 2012).

When attempting to detect trends in a natural series, it is important to be aware of the inherent variability of hydrologic time series. Differentiating between natural variability and distinct trends is not straightforward (Askew, 1987; Burn, 1994). Furthermore, analyzing hydroclimatic time series data is challenging since it can: be non-normally shaped in distribution; have serial dependency, uneven spacing and timescale uncertainties (Koutsoyiannis and Montanari, 2007); and can also be subject to shifts and abrupt changes. The focus of trend analysis in hydrology is on determining the exact evolution of these hydroclimatic conditions and variables over time. However, problems can arise because the available data are usually: (i) limited in length, (ii) influenced by background noise (errors), and (iii) can consist of multiple signals, sections of increasing and decreasing trends, and sometimes discontinuities (Adamowski et al, 2009).

In order to be able to draw useful and accurate conclusions about these changes, the acquisition of long-term data is a useful approach to adopt (De Jongh et al., 2006; Pekarova and Pekar, 2007). Studies conducted by different authors in analyzing hydroclimatic trends have used different lengths of data. Kahya and Kalayci (2004) and Burn and Hag Elnur (2002) consider a minimum of 31 and 25 years worth of data, respectively, are needed to acquire a valid mean statistic in analyzing trends in their flow data. However, Kundzewicz and Robson (2004) argue that due to the variation in climate,

data consisting of 30 years or less of records are considered insufficient for trend detection associated with climate change. Approximately four decades worth of data would be sufficient to determine the existence of possible trends in annual streamflow series and their dominant periodicities ( Ampitiyawatta and Guo, 2009; Partal, 2010). In light of this information, in this study, we used 55 years worth of data (for flow and precipitation) and 40 years worth of data (for temperature) in order to analyze their trends.

### **2.3. Main Methods of Trend Analysis of Hydroclimatic Variables**

Trends in hydroclimatic variables can be examined in many different ways. Land-based data, satellite data, statistical tests, computer-intensive approaches and models play significant roles in enhancing the understanding of the complex time and space variations in hydro-climatic systems. Prior to choosing the methods that will be used to study trends, it is important to take into account the characteristics of the data, such as data length and distribution, the structure of the sample, the possible types of existing trends (monotonic or stepwise), and the presence of persistence and seasonal fluctuations (Cluis et al., 1989).

Some of the more commonly used methods for trend investigation in hydroclimatic research involve the use of the bootstrap method (e.g. Douglas et al., 2000; Di Stefano et al., 2000; Chingombe et al., 2005), Monte Carlo simulation (e.g. Yue et al., 2002b), the Spearman's rho (SR) test (e.g. McLeod et al., 1991; Yue et al., 2002a), regression models (e.g. Svensson et al., 2005; Shao et al., 2010; Timofeev and Sterin, 2010), the Mann-Kendall (MK) trend test (e.g. Burn and Hag Elnur, 2002; Yue et al., 2003; Partal and Küçük, 2006; Partal, 2010), and non-parametric statistical tests (e.g. Birsan et al., 2005; Zhang et al., 2009; Durdu, 2010; Zhang et al., 2010; Liu et al., 2010), among others. Some of these commonly used methods are discussed in the following sections, along with their strength and weaknesses.

Recently, a number of studies have also employed the use of wavelet analysis (WA) approaches in detecting and estimating trends in hydroclimatic time series (e.g. Kirkup et al., 2001; Anctil and Coulibaly, 2004; Kim, 2004; Prokoph and Patterson, 2004; Partal and Küçük, 2006; Adamowski et al., 2009; Partal, 2010). The use of wavelet transforms in detecting trends is usually combined with statistical tests such as regression

models or the MK test in order study these trends (e.g., Partal and Küçük, 2006; Zume and Tarhule, 2006; Xu et al., 2009; Adamowski et al., 2009; Partal, 2010).

### **2.3.1. Parametric and Non-parametric Statistical Tests**

Both parametric and non-parametric statistical tests are used in trend detection in order to quantify the significance of trends in a time series (Durdu, 2010). These may include tests such as linear regression, ordinary least squares (OLS), regression autoregressive integrated moving average (ARIMA) models, the Spearman partial rank correlation test (SPRC), and the MK trend test, among others.

The use of statistical tests involves testing of the null hypothesis – which assumes that the data are random and are not correlated (i.e., no trend will be observed) – against the alternative hypothesis (there will be a significant trend detected, either positive or negative). Although parametric tests are more powerful in nature, they have to satisfy the assumption of normal distribution, homoscedasticity, and independent observation (Önöz and Bayazit, 2003). If the assumptions made are not met, then the tests will yield unreliable results and interpretations, because the estimates of the significance level will not be correct (Kundzewicz and Robson, 2004).

Non-parametric tests are used when the assumptions of the parametric tests cannot be fully met. Non-parametric tests have less strict assumptions and have a higher tolerance with respect to missing values and non-normal distribution (Cunderlik and Burn, 2004). Since earth-based scientific phenomena (including hydrological processes) tend to have non-stationary characteristics and non-normal distributions, non-parametric tests are usually preferred over parametric tests in conducting a trend analysis (Hirsch and Slack, 1984; Lattenmaier, 1988). Furthermore, hydrological data normally exhibit autocorrelation; therefore, data values are not independent. They may also show seasonality, which violates the assumption of constant distribution (Kundzewicz and Robson, 2004).

It is important to note that both parametric and non-parametric tests still require that the observations be independent, since the existence of serial correlation can significantly impact trend determination leading to inaccurate conclusions (Adamowski

and Bougadis, 2003). Having said that, the strength of non-parametric tests is found in their exact level of significance (even if the data exhibit non-normal distributions) (Johnson, 2000). Helsel (1987) concluded that the advantages of non-parametric tests are as follows:

1. Transformation of data is not required.
2. The results produced should still be reliable even if data exhibit non-normal distribution.
3. The tests are still powerful even though the distribution of samples is not symmetrical (skewed).
4. The results of non-parametric tests should still be reliable even if there are outliers present in the data.

### **2.3.2. The Bootstrap Method**

Kundzewicz and Robson (2004) recommended the bootstrap method for evaluating the significance level of a test statistic (when detecting change in a time series that occurs either gradually or abruptly). The bootstrap method is also known as a resampling method. The bootstrap approach does not require many assumptions about the available data and does not depend on the type of distribution of the sample (Yue and Wang, 2002). It has been found to be flexible, robust and powerful, and easy to implement (Simon and Bruce, 1991; Kundzewicz and Robson, 2004). In addition to this, it is suited to the characteristics of hydrological data, which are often strongly skewed, exhibiting seasonal and serial correlation, and having data gaps.

Kundzewicz and Robson (2004) explained the basic principle of the bootstrap method in a very straightforward manner. If a trend does not exist in a time series, then the order of observations should not matter much; therefore, by resampling or shuffling these values of the time series, the gradients should not change by much either (Kundzewicz or Robson, 2004). The higher the number of bootstrapped samples created, the better the accuracy of the statistical estimates will be (Yue and Pilon, 2004). The process of shuffling is repeated many times and for each repetition the test statistic is calculated. If the test statistic of the original data is very different from the ones produced

by the shuffling procedures, the presence of a trend is very likely (Kundzewicz and Robson, 2004). If the test statistic of the original data is found to be among the values produced by the shuffling procedures, then it implies that the order of the observations in the data is not important; thus, the null hypothesis of no trend should be accepted (Kundzewicz and Robson, 2004). Several trend-detection studies have utilized the bootstrap method as part of their methodology. Examples of this can be found in studies conducted by Adamowski and Bougadis (2003), Yue and Pilon (2004), Burn et al. (2010), among others.

In practice, it is usually impractical to actually draw all possible resamples. The bootstrap method also involves an intensive computation for measuring the accuracy of statistical estimates by creating bootstrapped samples from the original records (Yue and Pilon, 2004). In this study, we do not require a resampling method to analyze trends in the time series we explore because first of all, we aim to extract the different frequency components contained in our datasets – this cannot be accomplished using the bootstrap method. Furthermore, since one of the objectives of this study is to determine the most harmonious periodic component with regards to the original data (over the study period), we need a method that can provide sequential or progressive information on how the trend of a periodic component behaves in comparison to the trend of original data. As such, the bootstrap method is not employed in our study.

### **2.3.3. Regression Analysis**

Regression analysis has been used in almost every field for data analysis, including in many trend assessments for hydrological related studies (e.g., Prokoph and Patterson, 2004; Caloiero et al., 2011; Timofeev and Sterin, 2010; Shao et al., 2010). Regression models are considered flexible and can be used with records which are not evenly spaced; therefore, many types of regression models have been used to trace trends (Hipel and McLeod, 1994). Since linear regression is fitted directly on to the data, it is very helpful for visual presentation (Svennson, et al., 2005).

Linear regression is the simplest form of regression model and has been frequently used to indicate the presence of trends (e.g., McBean and Motiee, 2006). If the

calculated regression gradient is close to zero, the null hypothesis of no trend should be accepted. In contrast, if the gradient is very different from zero, then the null hypothesis should not be accepted.

Some of the limitations of linear regression include its dependency on the normal distribution of the data and its high sensitivity to the presence of outliers (Svennson et al., 2005). It may also cause non-homogeneous residuals (Jones, 2008). This implies that if the size of trends changes over a period of time, the residuals cannot be considered as being independent and having the same distribution (Shao et al., 2010). Another reason why classical regression would not be suitable to be used in our study is because this study aims to analyze the low- and high-frequency events and how they vary in time – classical regression does not explore the differing frequency characteristics of a time series (Goodwin, 2008) – the wavelet transform is therefore considered more suitable (see subsequent sections on wavelet transform for details).

Andreas and Treviño (1997) compared wavelet-based method and the least squared regression in detecting linear and quadratic trends in a time series. They found that the wavelet-based method is more efficient because of the computational operations (Andreas and Treviño, 1997). Kim (2004) also noticed that trend values produced using the ordinary least squares is systematically larger compared to the values obtained from using wavelet analysis. This is because the wavelet transform method segregates the different periodic components from the trends, whereas the linear least square method incorporates the components into one total trend.

#### **2.3.4. The Mann-Kendall (MK) Trend Test**

The MK (Mann, 1945; Kendall, 1975) trend test is a rank-based test of randomness against monotonic trends (Zhang et al., 2001; Déry and Wood, 2005; Kallache et al., 2005; Zume and Tarhule, 2006, Burn et al., 2010). Numerous studies have employed the MK trend test in their data analysis in order to assess and identify trends in a time series. It is possibly the most widely used non-parametric test for trend detection in hydrological studies (Yue and Pilon, 2004; Hamed, 2008). This is because not only is it simple to use, but it is also resilient to skewed distribution, missing values

and values that fall outside the detection limit, and to the non-stationary nature of data (Lins and Slack, 1999; Partal and Küçük, 2006). Since it is rank-based, it placed emphasis on the order of the rank, and not on the actual value of the records themselves. Thus, if some values are missing or if an outlier is present, the results would not be affected much because the ranks would not significantly change. The hypothesis of the MK test is based on the occurrence of monotonic change, not a break change (Chaouche et al., 2010). The MK test, however, still performs well even if a break is present in the time series (Lemaitre, 2002; Chaouche et al., 2010). Chaouche (2010) also emphasized that changes in a time series that is affected by climate change, should occur in a more gradual manner. As such, the MK test was deemed to be suitable to be used in our study.

Önöz and Bayazit (2003) compared the power of the *t*-test and the MK test in analyzing the annual streamflow series at 107 sites across Turkey by Monte Carlo Simulation. They found that the *t*-test had slightly more power than the MK test when the distribution is normal; however, for skewed distribution, the MK test was more powerful, particularly when the coefficient of skewness is high (Önöz and Bayazit, 2003). Similarly, when Yue and Pilon (2004) compared the power of the parametric *t*-test, the M-K test, the bootstrap-based slope test (BS-slope), and the bootstrap-based MK test (BS-MK), they found that the *t*-test and BS-slope test were more powerful than the rank-based tests for data having a normal distribution, regardless of the linearity of the trend. For data that are not normally distributed, the rank-based tests were much more powerful in detecting trends, regardless of their linearity (Yue and Pilon, 2004).

Although the MK test is robust and very useful in many hydrological studies, using the MK test on its own for detecting trends may not always be ideal. That is because the MK test does not account for the serial correlation that very often exists in a hydrological time series (Hamed and Rao, 1998; Yue et al., 2002b; Partal and Küçük, 2006). The presence of serial correlation in a dataset may lead to a misleading result interpretation because it enhances the probability of finding a significant trend, when actually there is an absence of a significant trend. As such, in our study, each time series was first checked for whether a significant autocorrelation (more specifically, lag-1 autocorrelation coefficient) exists. If a time series did not exhibit a significant autocorrelation, the original MK test was used to analyze the data. In the event that a

significant autocorrelation was present in a time series, we adopted the modified versions of the original MK test because these modified MK tests have shown that they are more powerful and thus, more suitable for data with significant autocorrelation (see the following sections for details on the modified MK tests by Hirsch and Slack, 1984; and Hamed and Rao, 1998).

## **2.4. Addressing the Issue of Serial Correlation in Time Series Analysis**

Several proposals that attempt to deal with the presence of serial correlation in a time series have been made: (1) Prewhitening method by Kulkarni and von Storch (1995); (2) modified MK test by Hirsch and Slack (1984); (3) and modified MK test by Hamed and Rao (1998). These are discussed in the following sections.

### **2.4.1. Prewhitening Method**

Kulkarni and von Storch (1995) proposed the prewhitening method to remove the autocorrelation from a dataset. A commonly used correlation coefficient (i.e., correlation coefficient between the value of the time series at time  $t$  and its value at time  $t-1$ ) in determining whether an autocorrelation is present in a dataset is the lag-1 autocorrelation coefficient. If the calculated lag-1 autocorrelation coefficients of a time series is significant at a pre-specified significance level (e.g. the 5% level), the autocorrelation is eliminated through prewhitening procedures (before applying the MK trend) by assuming that the time series' autocorrelation is an AR(1)-process. An autoregressive process of first order or an AR(1)-process is removed or reduced by subtracting the observation at time  $t-1$  (that has been multiplied with its estimated autocorrelation at lag-1) from the observation at time  $t$  (Kulkarni and von Storch, 1995). This is done in order to create a time series that is independently sampled and identically distributed (iid). Kulkarni and von Storch (1995) used Monte Carlo simulations on 1000 prewhitened time series (with an AR (1) process originally) and with  $\alpha = 5\%$ , the prewhitening procedures produced rejection rates of the correct null hypothesis that are very close to the  $\alpha$  value. Kulkarni and von Storch (1995) noted that the prewhitening method is not powerful for data with



large autoregressive coefficient ( $\alpha$ ) values or when the length of the time series is short. The prewhitening method has been used in Zhang et al. (2001); Burn and Hag Elnur (2002); and Mohsin and Gough (2010), among others.

Yue and Wang (2002) evaluated the effectiveness of the pre-whitening procedure through a simulation process using the estimation of the first order autocorrelation coefficient produced by a Markov process that was coupled with trends. They found that the pre-whitening procedure is not fully effective in removing the effect of autocorrelation in the data when later detecting trends via the M-K test (commonly used on pre-whitened data), when the sequence of records do in fact show trending observations (Yue and Wang, 2002). Additionally, Yue et al. (2002b) also noted that by removing the positive serial correlation from the time series through the pre-whitening method, the magnitude of the trends that may be present in the series is reduced, and some of the trend components are also removed. On the other hand, removing the negative serial correlation using the same procedure may enhance the magnitude of the existing trends (Yue et al., 2002b). Therefore, the use of the pre-whitening procedure may lead to incorrect interpretations (Yue et al., 2002b), and was therefore not used in this study.

#### **2.4.2. Seasonal Kendall Test for Seasonal Data with or without Significant Autocorrelations**

The initial modification to the original MK test to remove the effect of seasonality in a time series was proposed by Hirsch et al. (1982). The effect of seasonality was removed by dividing the data into separate categories, and the MK trend test is then performed on the sum of the statistics from each season (Hirsch et al., 1982). This test however, does not solve the autocorrelation issue because the effect of serial dependence within the same season still exists (Yue et al., 2002b).

Hirsch and Slack (1984) then proposed an extension to this seasonal MK test, which would be robust against autocorrelation in a time series. The ranks of the data values are ordered for each season and the MK test statistic for each season is calculated. In order to calculate the variance of the seasonal Kendall statistics, the value of the

covariance is not taken to be zero. Instead, the covariance is estimated using a consistent estimator defined by Dietz and Killen (1981) (Dietz and Killeen, 1981; Hirsch and Slack, 1984) – sections 3.2.2.2 and 4.2.3.1 provide the equation for this estimator. However, in the event that there are neither missing values nor tied values, the Spearman’s correlation coefficients can be used to calculate the covariance (Lehman 1975; Conover, 1980; Hirsch and Slack, 1984). Although this modified version of the MK test is more powerful than the original MK for use with data exhibiting serial correlation, Hirsch and Slack (1984) noted that this test is not powerful when there is a strong long-term persistence in the dataset or when the length of records is very short (five years worth of data). Since the datasets used in this study are at least 40 years in length and many of them show patterns of semi-annual and/or annual cycles, this test is adopted when the analyzed time series show patterns of seasonality with or without the existence of a significant autocorrelation.

#### **2.4.3. A Modified Mann-Kendall (MK) Test for Data with Serial Correlation**

Hamed and Rao (1998) proposed a modified MK test that modifies the variance of the MK test statistics for datasets exhibiting autocorrelation. They first demonstrated how the original MK test found a significant trend on a time series with an AR(1) process ( $\phi = 0.4$ ), when in fact the trend is only due to the effects between observations in that dataset. This is because the presence of significant positive autocorrelation underestimates the variance used to calculate the original MK test statistic. Hamed and Rao (1998) established a theoretical relationship that is used to calculate the variance of the MK test statistics when a significant autocorrelation is present in a dataset. The autocorrelation between the ranks of the data values is calculated first and then it is transformed to normalized data autocorrelation. From this, the variance of the MK test statistic is then calculated, which will not depend on the distribution of data. However, if there are a large number of observations in the dataset, the computational time may become an issue. To deal with this, an approximation formula to calculate the variance of  $S$  was developed by considering a correction factor for the autocorrelation found in the data. This correction factor is the autocorrelation function between the ranks of

observations. The empirical approximation formula was verified using numerical simulation. Empirically, Hamed and Rao (1998) found that this modified test is more powerful compared to the original MK test when an autocorrelation is present in the data. Since some of the datasets used in this study exhibit significant lag-1 autocorrelation, this modified version of the MK test is used in the data analysis of such data.

## **2.5. Wavelet Transform in Hydroclimatic Studies and its Applications**

The use of WT acts as an effective method for analyzing and synthesizing the variable structure of a signal in time. WT is used in order to isolate different periodicities embedded in a time series and closely examine the composition of a signal (Pişoft et al., 2004; Prokoph and Patterson, 2004; Zume and Tarhule, 2006). It can identify components that may be considered important in a signal, at their exact temporal location, which otherwise may not be clearly detected by the use of regular statistical tests alone (Drago and Boxall, 2002). This is one of the most obvious strengths of the WT because it gives a more complete picture of the dynamics contained in the signal being analyzed.

The use of wavelets has been applied in fields such as astronomy, geophysics, medical research, signal and image processing, image compressing, and tongue encoding (Santos et al., 2001; Wang et al., 2011). However, the use of WT in hydrology and climatology is still relatively rare even though it clearly has advantages over the classical Fourier analysis (Lau and Weng, 1995; Kim, 2004; Labat, 2005). Studies that have applied the WT approach in analyzing hydroclimatic time series have found it to be effective because it uncovers otherwise hidden phenomena in the time series (e.g. Partal and Küçük, 2006; Adamowski et al., 2009).

The fundamental wavelet functions used in WT can localize time and frequency components of a signal simultaneously and also conserve the temporal features and periodic cycle patterns of a series without assuming stationarity, which makes WT an ideal tool for hydrologic related time-series analyses because climate and hydrology generally have a non-stationary nature. Wavelets can be stretched and translated into different resolutions in both frequency and time (Kim, 2004). The advantage of this is that it allows the observed time series to be transformed into wavelet coefficients

according to time and scale simultaneously. The wavelet coefficients can then be utilized in analyzing the long-term fluctuations (i.e. trends), or in the reconstruction of signals that are of interest (Adamowski et al., 2009). Not only are the dominant modes or periodicities revealed, but also how they have fluctuated in time (Torrence and Compo, 1998).

The application of the wavelet transform can be achieved in two ways: the continuous wavelet transform (CWT) and the discrete wavelet transform (DWT). In CWT, the analysis can be accomplished at all scales, and thus, all frequencies are detected (Adamowski et al., 2009). With DWT, the analysis is carried out in the dyadic scales (i.e. integer powers of two) (Chou, 2007). As such, the advantage of DWT lies in its ability to conserve the amount of information in the signal that is needed (Kulkarni, 2000) by removing some redundancy of information in the wavelet coefficients; hence, it can more precisely distinguish the signal processes (Daubechies, 1992). In the DWT, signals are passed through high-pass and low-pass filters – this process produces detail and approximation coefficients. This process is repeated until the pre-determined number of decomposition levels has been reached (at each successive level of decomposition, the signal is down-sampled by a factor of 2) (Chaovalit et al., 2011). The approximation component of the last decomposition level resulting from the DWT application carries the most important information – which is referred to as data reduction (Chaovalit et al., 2011). This is also an advantage of using the DWT instead of the CWT. Furthermore, signal reconstructions in DWT can be accomplished in a straightforward manner and usually the reconstruction is perfect (by up-sampling procedures), whereas signal reconstructions in CWT are complicated due to edge effects (Adamowski et al., 2009). Even so, both CWT and DWT have been employed in a variety of hydroclimatic studies. The use of CWT to study the variability of hydroclimatic data was explored by a number of authors such as: Gaucherel, 2002; Anctil and Coulibaly, 2004; Coulibaly and Burn, 2004; Kim, 2004; Pişoft et al., 2004; Zume and Tarhule, 2006; Adamowski et al., 2009; Kravchenko et al., 2011; Subash et al., 2011, etc. The use of DWT in examining the variability of several different hydroclimatic data has been performed in studies by Kulkarni, 2000; Drago and Boxall, 2002; Xu et al., 2009; Partal, 2010, among others.

### **2.5.1. Examples of Applications of Wavelet Transform on Temperature Data**

The WT technique has been applied to different temperature indices in order to detect trends and analyze the variability of different time scales contained in a time series. In this section, several examples are detailed in order to highlight the advantages of employing the WT technique as a part of a time series analysis.

Pišoft et al. (2004) analyzed trends and oscillations in the mean monthly temperature time series in the Czech Republic on four data sets: Prague-Klementinum (1775-2001), Brno (1848-2001), Mt Milešovka (1905-2001) and the gridded temperature (1901-2001) for the entire country. After taking the difference between the original series and the inverse of the WT, a positive trend in temperature was very obvious for every time series set. It also provided an idea of when specific events occur. For the Prague and Brno series, it was shown that temperatures started to increase around 1850 and 1890, respectively. For the gridded Czech series, temperatures started to rise in the 1970s. The wavelet power spectra (between 1930 and 2001) showed very noticeable oscillations centered around 8 and 12-14 years for all series. Apart from the relation of the temperature increase with anthropogenic-related factors, the increase has also been associated with atmospheric variability such as NAO cycles (Pišoft and Kalvova, 2003).

Oh et al. (2003) also argued that the increasing trend observed in northern hemisphere temperature has not only been caused by anthropogenic influences and natural variations in the climate as generally recognized, but could result partly from contributions of external forcing mechanisms such as volcanism and solar radiation activities. The application of the WT on solar activity data revealed strong oscillation around 85.3 and 10.9 years, which are very close to two classical solar modes: 85-year Gleissberg and 11-year sunspot cycle. The WA also revealed that during 1610-1960, there was a strong correlation between the solar forcing and the temperature at the low-frequency scale (i.e. 85.3 years), but not so much at the high-frequency scale (i.e. 11 years). This suggests that the temperature data used may not be very sensitive to the high frequency variations of solar activity. Although the climate system is undoubtedly a complex system, it can be seen that WT can be used as a tool to reveal hidden phenomena

in climate variability at different temporal scales that otherwise would be hidden by the strong background noise in the climate system (Pišoft et al., 2004).

WT has also been used in studies to detect the effects of anthropogenic-related activities. Prokoph and Patterson (2004) assessed temperature trends by comparing Ottawa (urban location) and two rural areas: Maniwaki, Quebec and Morrisburg, Ontario. The WT was used to describe the path of the trends over time because the time series may have abrupt jumps, temporal discontinuities, long wavelengths, and non-stationary high amplitude signals. This resulted in the recognition of four different temperature regimes, divided by abrupt changes: (i) 1890-1937 was characterized by non-periodic patterns of cycles with fluctuating wavelengths (e.g. 5.5 and 8 years), and short-term influences on temperature; (ii) 1937-1971 was characterized by 2-year cycles and low variation in temperatures; (iii) 1971-1989 was characterized by low temperature variability with high frequency cycles of about 2 years; (iv) Post 1989 was characterized by high temperature variations, as well as high cycle variations (e.g. 1.8, 3.7, 12 years wavelength). This clearly demonstrates how the WT was able to detect changes in trends including their periodic cycles, and the non-stationarities at different temporal scales in the time series data. Using regression, Prokoph and Patterson (2004) found that the temperature increase in Ottawa was 0.0138°C per year, in comparison to the rural stations, which had relatively unchanged temperature profiles. Finally, the results of the wavelet analysis revealed that the warming trend in Ottawa occurred mainly in multidecadal and interseasonal cycles, which are thought to be related with the heat island effects.

Similarly, urbanization in the Greater Toronto Area (GTA) over the last several decades was thought to be one of the contributing factors that produced increasing trends in the annual mean temperature series (Mohsin and Gough, 2010). Using WA and the sequential M-K test, Mohsin and Gough (2010) were able to reveal that increasing temperature trends in urban and suburban stations began around the 1920s and continued until the 1960s.

There have not been any studies that exclusively explored the use of the DWT technique and combined it with the Mann-Kendall trend test (especially using its modified version to account for seasonality and/or autocorrelation factors in a time series). Therefore, the application of these two approaches is very new.

### **2.5.2. Examples of Applications of Wavelet Transform on Precipitation and Streamflow Data**

The applications of the WT on different types of streamflow and precipitation data have been accomplished in a number of studies. Here we present examples aiming primarily to illustrate the usefulness of the WT technique.

Santos et al. (2001) successfully applied the CWT to analyze the monthly total precipitation in Matsuyama city in Japan. They found strong peaks centered around 8-16 months, which can also indicate periods of dry and wet years. An interesting point of the study was to show that results from previous studies using classical statistical analysis that concluded low-frequency periodicities (at 32 and 128 months) were important, are in fact misleading. Xu et al. (2009) analyzed trends in precipitation by focusing on the temporal variability of the 4-, 8-, and 16-year periodicities. This enabled them to see that generally the trends were positive and other important features of each periodic mode such as some turning points and amplitude of the fluctuations over time were also able to be observed.

Long-term trend extraction in streamflow was studied by Adamowski et al., (2009) by means of CWT. Using CWT, Adamowski et al. (2009) developed a new technique for long-term trend detection and estimation that can be used for hydroclimatic variables, which may contain discontinuities, multiple signals, and a mix of positive and negative trends. This method aimed to reconstruct signals of just a few periodic wavebands that are deemed important for trend reconstructions, and to correct the edge effect (associated with using CWT). The reconstruction technique for long-term trend determination of just the important periodicities was applied to several streamflow datasets in Canada. For example, for the Belly River station near Mountain View, Alberta, semiannual (at 4-6 months) and annual (at 10-13 months) periodic wavebands were strongly dominating the data. With the edge effect correction, it was found that the annual and semiannual periodic components are much stronger compared to the low-frequency periodic wavebands. This illustrates how the use of CWT is able to identify and remove high-frequency variability in order to extract the trend. When the multi-decadal variability (55-year periodicity) was reconstructed, it was seen that it correlated with the Pacific Decadal

Oscillation (PDO) and North Atlantic Oscillation (NAO) cycles (Adamowski et al., 2009). Anctil and Coulibaly (2004) also used wavelet analysis to study the interannual variability of streamflow in southern Quebec and found a correlation in the waveband of 2-3 years with the Pacific-North America (PNA) index since 1970. In contrast, Kim (2004) discounted the effects of large teleconnection patterns in precipitation variability over northern California. Using wavelet analysis, Kim (2004) separated the short, medium, and long periodic components of total precipitation in northern California (1905-2001). They found that after 1945, the behavior of these different components is different, and a new local maximum was identified. Kim (2004) believed that the positive trends in precipitation in northern California is caused by the effect of very low-frequency and multi-decadal periodicities.

Partal and Küçük (2006) used the WT technique to analyze the non-stationary characteristics and trends in Turkish precipitation data from Çanakkale, Balıkesir, and Siirt stations. The CWT was applied to the original data to obtain general information about the periodic structure of the data. Using the DWT, the data were then decomposed into dyadic scales (from 2 – 32 years). With such a multi-resolution analysis, properties of the sub-series, such as its monthly and annual periods can be seen more clearly than in the original signal especially for trends. Common decadal events of 18 – 28 years were found to be important for producing trends for both Çanakkale and Balıkesir stations, which are situated within the same region. An application of the WT on datasets from a different region (Siirt station) revealed that the DW2 component, which represents the 4-year periodic mode, was responsible in producing the real trend (Partal and Küçük, 2006).

Partal (2010) also employed the DWT to study trends in Turkish streamflow series from four stations: three stations in Sakarya Basin and one station in Seyhan Basin. All time series were decomposed into four decomposition levels (2 – 16 years). For all stations in the Sakarya Basin, the 16-year periodicity was found to be most important component that affects streamflow trends in the basin. The 16-year component had the highest correlation coefficient and the nearest trend value to the original data. When the method was applied to the Seyhan basin, it showed that the dominant periodic component was different – the 8-year periodicity was found to be the dominant mode. This suggests that dominant periodic components, responsible for producing a real trend, are different



for different climatic regions in Turkey. The findings of Partal and Küçük (2006) and Partal (2010), which found that the use of WT is able to consistently identify the periodic mode that affects trends within the same region or basin, affirms how WT can extract information in a time series that is not obvious in the raw data.

Zume and Tarhule (2006) used the CWT and the Mann-Kendall trend test to analyze precipitation and streamflow trends in northwestern Oklahoma, USA over the period 1894-2003. They were able to illustrate how the use of CWT enables the analysis of data where anthropogenic impacts (in this case: ground water extraction) were superimposed on the variability of natural phenomenon (such as El Niño–Southern Oscillation (ENSO) and the Pacific Decadal Oscillation (PDO)). This is done by analyzing the temporal distribution of peaks of the power spectrum produced by the CWT and correlating the data used with the large teleconnection patterns.

To date, only Partal and Küçük (2006) and Partal (2010) have exclusively employed the DWT and the original MK test in order to detect trends in precipitation and streamflow. In this present study, we will extend this new approach to include testing for serial correlation and the use of different types of the MK test depending on the characteristics of the analyzed data – this approach is new, especially in the context of Canadian studies.

## **2.6. References**

- Adamowski, K., Bougadis, J., 2003. Detection of trends in annual extreme rainfall. *Hydrological Processes*, 17(18): 3547-3560.
- Adamowski, K., Prokoph, A., Adamowski, J., 2009. Development of a new method of wavelet aided trend detection and estimation. *Hydrological Processes*, 23(18): 2686-2696.
- Ampitiyawatta, A.D., Guo, S., 2009. Precipitation trends in the Kalu Ganga Basin in Sri Lanka. *The Journal of Agricultural Science*, 4(1): 10-18.
- Anctil, F., Coulibaly, P., 2004. Wavelet analysis of the interannual variability in southern Québec streamflow. *Journal of Climate*, 17(1): 163-173.

- Andreas, E.L., Treviño, G., 1997. Using wavelets to detect trends. *Journal of Atmospheric and Oceanic Technology*, 14(3): 554-564.
- Arnell, N.W., 1999. Climate change and global water resources. *Global Environmental Change*, 9(1): 31-49.
- Arora, V.K., Boer, G.J., 2001. Effects of simulated climate change on the hydrology of major river basins. *Journal of Geophysical Research*, 106(D4): 3335-3348.
- Askew, A.J., 1987. Climate change and water resources. *IAHS Publication*, 168: 421-430.
- Beyene, T., Lettenmaier, D., Kabat, P., 2010. Hydrologic impacts of climate change on the Nile River Basin: Implications of the 2007 IPCC scenarios. *Climatic Change*, 100(3): 433-461.
- Birsan, M.-V., Molnar, P., Burlando, P., Pfaundler, M., 2005. Streamflow trends in Switzerland. *Journal of Hydrology*, 314(1-4): 312-329.
- Bonsal, B.R., Prowse, T.D., Duguay, C.R., Lacroix, M.P., 2006. Impacts of large-scale teleconnections on freshwater-ice break/freeze-up dates over Canada. *Journal of Hydrology*, 330 (1-2): 340-353.
- Boyer, C., Chaumont, D., Chartier, I., Roy, A.G., 2010. Impact of climate change on the hydrology of St. Lawrence tributaries. *Journal of Hydrology*, 384(1-2): 65-83.
- Burn, D.H., 1994. Hydrologic effects of climatic change in west-central Canada. *Journal of Hydrology*, 160(1-4): 53-70.
- Burn, D.H., Hag Elnur, M.A., 2002. Detection of hydrologic trends and variability. *Journal of Hydrology*, 255(1-4): 107-122.
- Burn, D.H., Sharif, M., Zhang, K., 2010. Detection of trends in hydrological extremes for Canadian watersheds. *Hydrological Processes*, 24(13): 1781-1790.
- Caloiero, T., Coscarelli, R., Ferrari, E., Mancini, M., 2011. Trend detection of annual and seasonal rainfall in Calabria (Southern Italy). *International Journal of Climatology*, 31(1): 44-56.
- Chaouche, K., Neppel, L., Dieulin, C., Pujol, N., Ladouche, B., Martin, E., Salas, D., Caballero, Y., 2010. Analyses of precipitation, temperature and evapotranspiration in a French Mediterranean region in the context of climate change. *Comptes Rendus Geoscience*, 342(3): 234-243.

- Chaovalit, P., Gangopadhyay, A., Karabatis, G., Chen, Z., 2011. Discrete wavelet transform-based time series analysis and mining. *ACM Comput. Surv.*, 43(2): 1-37.
- Chingombe, W., Gutierrez, J.E., Pedzisai, E., Siziba, E., 2005. A study of hydrological trends and variability of Upper Mazowe Catchment-Zimbabwe. *Journal of Sustainable Development in Africa*, 7(1): ISSN:1520-550 Fayetteville State University, Fayetteville, North Carolina.
- Chou, C.-m., 2007. Applying multi-resolution analysis to differential hydrological grey models with dual series. *Journal of Hydrology*, 332(1–2): 174-186.
- Clark, J.S., Yiridoe, E.K., Burns, N.D., Astatkie, T., 2000. Regional climate change: Trend analysis of temperature and precipitation series at selected canadian sites. *Canadian Journal of Agricultural Economics*, 48(1): 27-38.
- Cluis, D., Langlois, C., Coillie, R., Laberge, C., 1989. Development of a software package for trend detection in temporal series: Application to water and industrial effluent quality data for the St. Lawrence River. *Environmental Monitoring and Assessment*, 13(2): 429-441.
- Coats, R., 2010. Climate change in the Tahoe basin: Regional trends, impacts and drivers. *Climatic Change*, 102(3): 435-466.
- Conover, W.J., 1980. *Practical nonparametric statistics*, 2nd ed., John Wiley, New York, 1980.
- Coulibaly, P., Burn, D.H., 2004. Wavelet analysis of variability in annual Canadian streamflows. *Water Resources Research*, 40(3): W03105.
- Croley, T.E. (2003). Great Lakes climate change hydrological impact assessment, IJC Lake Ontario—St. Lawrence River regulation study. (NOAA Tech. Memo. GLERL-126). Ann Arbor, Michigan: Great Lakes Environmental Research Laboratory.
- Cunderlik, J.M., Burn, D.H., 2004. Linkages between regional trends in monthly maximum flows and selected climatic variables. *J. Hydrol. Eng.*, 9(4): 246-256.
- Dai, A., Trenberth, K.E., Karl, T.R., 1998. Global variations in droughts and wet spells: 1900-1995. *Geophys. Res. Lett.*, 25(17): 3367-3370.

- Damyanov, N.N., Matthews, H.D., Mysak, L.A., 2012. Observed decreases in the Canadian outdoor skating season due to recent winter warming *Environmental Research Letters*, 7(1): 014028.
- Daubechies, I., 1992. Ten lectures on wavelets. Philadelphia: SIAM.
- De Jongh, I.L.M., Verhoest, N.E.C., De Troch, F.P., 2006. Analysis Of A 105-year time series of precipitation observed at Uccle, Belgium. *International Journal of Climatology*, 26(14): 2023-2039.
- Déry, S.J., Wood, E.F., 2005. Decreasing river discharge in northern Canada. *Geophys. Res. Lett.*, 32(10): L10401.
- Di Stefano, C., Ferro, V., Porto, P., 2000. Applying the bootstrap technique for studying soil redistribution by caesium-137 measurements at basin scale. *Hydrological Sciences Journal*, 45(2): 171-183.
- Dietz, E.J., Killeen, T.J., 1981. A nonparametric multivariate test for monotone trend with pharamaceutical applications. *Journal of the American Statistical Association*, 76(373): 169-174.
- Douglas, E.M., Vogel, R.M., Kroll, C.N., 2000. Trends in floods and low flows in the United States: Impact of spatial correlation. *Journal of Hydrology*, 240(1–2): 90-105.
- Drago, A.F., Boxall, S.R., 2002. Use of the wavelet transform on hydro-meteorological data. *Physics and Chemistry of the Earth*, 27(32–34): 1387-1399.
- Durdu, Ö.F., 2010. Effects of climate change on water resources of the Büyük Menderes River Basin, western Turkey. *Turk. J. Agric. For.*, 34(4): 319-332.
- Fu, C., James, A.L., Wachowiak, M.P., 2012. Analyzing the combined influence of solar activity and El Niño on streamflow across southern Canada. *Water Resour. Res.*, 48(5): W05507.
- Gaucherel, C., 2002. Use of wavelet transform for temporal characterisation of remote watersheds. *Journal of Hydrology*, 269(3): 101-121.
- Goodwin, D.A., 2008. Wavelet analysis of temporal data. Dissertation, Department of Statistics, The University of Leeds, Leeds, UK.
- Hamed, K.H., 2008. Trend detection in hydrologic data: The Mann–Kendall trend test under the scaling hypothesis. *Journal of Hydrology*, 349(3–4): 350-363.

- Hamed, K.H., Rao, A.R., 1998. A modified Mann-Kendall trend test for autocorrelated data. *Journal of Hydrology*, 204(1–4): 182-196.
- Hamlet, A.F., Mote, P.W., Clark, M.P., Lettenmaier, D.P., 2005. Effects of temperature and precipitation variability on snowpack trends in the western United States. *Journal of Climate*, 18: 4546-4561.
- Helsel, D.R., 1987. Advantages of nonparametric procedures for analysis of water quality data. *Hydrological Sciences Journal*, 32(2): 179-190.
- Hipel, K.W., McLeod, A.I., 1994. Time series modelling of water resources and environmental systems. Elsevier, Amsterdam. ISBN 0-444-89270-2, 1013 pp.
- Hirsch, R.M., Slack, J.R., 1984. A nonparametric trend test for seasonal data with serial dependence. *Water Resources Research*, 20(6): 727-732.
- Hirsch, R.M., Slack, J.R., Smith, R.A., 1982. Techniques of trend analysis for monthly water quality data. *Water Resources Research*, 18(1): 107-121.
- Huntington, T.G., 2006. Evidence for intensification of the global water cycle: Review and synthesis. *Journal of Hydrology*, 319(1–4): 83-95.
- IPCC. 2007. Climate change 2007: the fourth IPCC scientific assessment. In: M.L. Parry, O.F. Canziani, J.P. Palutikof, P.J. van der Linden and C.E. Hanson (eds). Intergovernmental Panel on Climate Change. Cambridge University Press, Cambridge, United Kingdom and New York, NY, USA.
- Jackson, R. B., Carpenter, S. R., Dahm, C. N., McKnight, D. M., Naiman, R. J., Postel, S. L., Running, S. W., 2001. Issues in ecology: Water in a changing world. *Ecological Applications*, 11(4): 1027-1045.
- Johnson, R.A. (2000). *Miller & Freund's probability and statistics for engineers*, Prentice Hall, Upper Saddle River, New Jersey.
- Jones, N.K., 2008. On the impact of recent climate change on seasonal floods—A case study from a river basin in southern Quebec. *Canadian Water Resources Journal*, 33(1): 55-72.
- Kahya, E., Kalaycı, S., 2004. Trend analysis of streamflow in Turkey. *Journal of Hydrology*, 289(1–4): 128-144.
- Kallache, M., Rust, H.W., Kropp, J., 2005. Trend assessment: applications for hydrology and climate research. *Nonlinear Processes in Geophysics*, 12(2): 201-210.

- Kendall, M.G., 1975. Rank Correlation Methods. Charles Griffin, London.
- Kim, S., 2004. Wavelet analysis of precipitation variability in northern California, U.S.A. KSCE Journal of Civil Engineering, 8(4): 471-477.
- Kirkup, H., Pitman, A.J., Hogan, J., Brierley, G., 2001. An initial analysis of river discharge and rainfall in coastal New South Wales, Australia using wavelet transforms. Australian Geographical Studies, 39(3): 313-334.
- Koutsoyiannis, D., Montanari, A., 2007. Statistical analysis of hydroclimatic time series: Uncertainty and insights. Water Resour. Res., 43(5): W05429.
- Kravchenko, V.O., Evtushevsky, O.M., Grytsai, A.V., Milinevsky, G.P., 2011. Decadal variability of winter temperatures in the Antarctic Peninsula region. Antarctic Science, 23(6): 614-622.
- Kulkarni, A., von Storch, H., 1995. Monte Carlo experiments on the effect of serial correlation on the Mann-Kendall test of trend. Meteorol. Z., 4(2): 82-85.
- Kulkarni, J.R., 2000. Wavelet analysis of the association between the Southern Oscillation and the Indian summer monsoon. International Journal of Climatology, 20(1): 89-104.
- Kundzewicz, Z.W., Robson, A.J., 2004. Change detection in hydrological records—A review of the methodology. Hydrological Sciences Journal, 49(1): 7-19.
- Labat, D., 2005. Recent advances in wavelet analyses: Part 1. A review of concepts. Journal of Hydrology, 314(1–4): 275-288.
- Lahmer, W., Pfützner, B., Becker, A., 2001. Assessment of land use and climate change impacts on the mesoscale. Physics and Chemistry of the Earth, Part B: Hydrology, Oceans and Atmosphere, 26(7–8): 565-575.
- Lau, K.M., Weng, H., 1995. Climate signal detection using wavelet transform: How to make a time series sing. Bulletin of the American Meteorological Society, 76(12): 2391-2402.
- Lehman, E.L., 1975. Nonparametrics: Statistical methods based on ranks, Holden-Day, San Francisco.
- Lemaitre, F., 2002. Recensement des tests de de' tecton de tendances ou de ruptures adapte's a' l'analyse de stationnarite' des re'gimes de crues en France. Travail de fin d'e' tude. ENTPE, Cemagref Lyon, 94 p.

- Lettenmaier, D.P., 1988. Multivariate nonparametric tests for trend in water quality. JAWRA Journal of the American Water Resources Association, 24(3): 505-512.
- Lins, H.F., Slack, J.R., 1999. Streamflow trends in the United States. Geophys. Res. Lett., 26(2): 227-230.
- Liu, D., Chen, X., Lian, Y., Lou, Z., 2010. Impacts of climate change and human activities on surface runoff in the Dongjiang River Basin of China. Hydrological Processes, 24(11): 1487-1495.
- Mann, H.B., 1945. Nonparametric tests against trend. Econometrica, 13(3): 245-259.
- McBean, E., Motiee, H., 2006. Assessment of impacts of climate change on water resources – A case study of the Great Lakes of North America. Hydrology and Earth System Sciences Discussions, 3(5): 3183-3209.
- McLeod, A.I., Hipel, K.W., Bodo, B.A., 1991. Trend analysis methodology for water quality time series. Environmetrics, 2(2): 169-200.
- Mohsin, T., Gough, W., 2010. Trend analysis of long-term temperature time series in the Greater Toronto Area (GTA). Theoretical and Applied Climatology, 101(3): 311-327.
- Nicholls, N. et al., 1996. Observed climate variability and change. In Climate Change 1995: The Science of Climate Change, 132-192, (Eds J. T. Houghton, L. G. M. Filho, B. A. Callander, N. Harris, A. Kattenberg, and K. Maskell), Cambridge University Press, Cambridge, UK.
- Oh, H.-S., Ammann, C.M., Naveau, P., Nychka, D., Otto-Bliesner, B.L., 2003. Multi-resolution time series analysis applied to solar irradiance and climate reconstructions. Journal of Atmospheric and Solar-Terrestrial Physics, 65(2): 191-201.
- Önöz, B., Bayazit, M., 2003. The power of statistical tests for trend detection. Turkish Journal of Engineering & Environmental Sciences, 27(4): 247.
- Oreskes, N., 2004. The scientific consensus on climate change. Science, 306(5702): 1686.
- Partal, T., 2010. Wavelet transform-based analysis of periodicities and trends of Sakarya basin (Turkey) streamflow data. River Research and Applications, 26(6): 695-711.

- Partal, T., Küçük, M., 2006. Long-term trend analysis using discrete wavelet components of annual precipitations measurements in Marmara region (Turkey). *Physics and Chemistry of the Earth*, 31(18): 1189-1200.
- Payne, J.T., Wood, A.W., Hamlet, A.F., Palmer, R.N., Lettenmaier, D.P., 2004. Mitigating the effects of climate change on the water resources of the Columbia River Basin. *Climatic Change*, 62: 233-256.
- Pekarova, P., Pekar, J., 2007. Teleconnections of inter-annual streamflow fluctuation in Slovakia with Arctic Oscillation, North Atlantic Oscillation, Southern Oscillation, and Quasi-Biennial Oscillation phenomena. *Advances in Atmospheric Sciences*, 24(4): 655-663.
- Percival, D.B., Walden, A.T., 2000. *Wavelet methods for time series analysis*. Cambridge University Press, Cambridge, UK.
- Pišoft, P., Kalvová, J., 2003. Climate quantities interconnections and the wavelet transform of secular meteorological time series. . In *WDS'03 Proceedings of Contributed Papers: Part III - Physics*, Safrankova J (ed.). Matfyzpress: Prague: 556-561.
- Pišoft, P., Kalvová, J., Brázdil, R., 2004. Cycles and trends in the Czech temperature series using wavelet transforms. *International Journal of Climatology*, 24(13): 1661-1670.
- Prokoph, A., Patterson, R.T., 2004. Application of wavelet and regression analysis in assessing temporal and geographic climate variability: Eastern Ontario, Canada as a case study. *Atmosphere Ocean*, 43(2): 201-212.
- Santos, C.A.G., Galvão, C.d.O., Suzuki, K., Trigo, R.M., 2001. Matsuyama city rainfall data analysis using wavelet transform. *Annual Journal of Hydraulic Engineering, JSCE*, 45: 6.
- Shao, Q., Li, Z., Xu, Z., 2010. Trend detection in hydrological time series by segment regression with application to Shiyang River Basin. *Stochastic Environmental Research and Risk Assessment*, 24(2): 221-233.
- Simon, J.L., Bruce, P., 1991. Resampling: A tool for everyday statistical work. *Chance*, 4(1): 22-32.



- Smakhtin, V.U., 2001. Low flow hydrology: A review. *Journal of Hydrology*, 240(3–4): 147-186.
- Subash, N., Sikka, A., Ram Mohan, H., 2011. An investigation into observational characteristics of rainfall and temperature in Central Northeast India—A historical perspective 1889–2008. *Theoretical and Applied Climatology*, 103(3): 305-319.
- Svensson, C., Kundzewicz, W.Z., Maurer, T., 2005. Trend detection in river flow series: 2. Flood and low-flow index series. *Hydrological Sciences Journal*, 50(5): 824.
- Tharme, R.E., 2003. A global perspective on environmental flow assessment: Emerging trends in the development and application of environmental flow methodologies for rivers. *River Research and Applications*, 19(5-6): 397-441.
- Timofeev, A., Sterin, A., 2010. Using the quantile regression method to analyze changes in climate characteristics. *Russian Meteorology and Hydrology*, 35(5): 310-319.
- Torrence, C., Compo, G.P., 1998. A practical guide to wavelet analysis. *Bulletin of the American Meteorological Society*, 79(1): 61-78.
- Trenberth, K.E., 1998. Atmospheric moisture residence times and cycling: Implications for rainfall rates and climate change. *Climatic Change*, 39: 667-694.
- Wang, W., Hu, S., Li, Y., 2011. Wavelet transform method for synthetic generation of daily streamflow. *Water Resources Management*, 25(1): 41-57.
- Wettstein, J.J., Mearns, L.O., 2002. The influence of the North Atlantic–Arctic Oscillation on mean, variance, and extremes of temperature in the northeastern United States and Canada. *Journal of Climate*, 15(24): 3586-3600.
- Whitfield, P.H., Wang, J.Y., Cannon, A.J., 2003. Modelling future streamflow extremes—Floods and low flows in Georgia Basin, British Columbia. *Canadian Water Resources Journal*, 28(4): 633-656.
- Xu, J., Chen, Y., Li, W., Ji, M., Dong, S., Hong, Y., 2009. Wavelet analysis and nonparametric test for climate change in Tarim River Basin of Xinjiang during 1959-2006. *Chinese Geographical Science*, 19(4): 306-313.
- Yu, Y.-S., Zou, S., Whittemore, D., 1993. Non-parametric trend analysis of water quality data of rivers in Kansas. *Journal of Hydrology*, 150(1): 61-80.

- Yue, S., Pilon, P., 2004. A comparison of the power of the  $t$  test, Mann-Kendall and bootstrap tests for trend detection. *Hydrological Sciences Journal*, 49(1): 21-37.
- Yue, S., Pilon, P., Cavadias, G., 2002a. Power of the Mann-Kendall and Spearman's rho tests for detecting monotonic trends in hydrological series. *Journal of Hydrology*, 259(1-4): 254-271.
- Yue, S., Pilon, P., Phinney, B., Cavadias, G., 2002b. The influence of autocorrelation on the ability to detect trend in hydrological series. *Hydrological Processes*, 16(9): 1807-1829.
- Yue, S., Pilon, P., Phinney, B.O.B., 2003. Canadian streamflow trend detection: Impacts of serial and cross-correlation. *Hydrological Sciences Journal*, 48(1): 51-63.
- Yue, S., Wang, C.Y., 2002. Assessment of the significance of sample serial correlation by the bootstrap test. *Water Resources Management*, 16(1): 23-35.
- Zhang, Q., Xu, C.Y., Zhang, Z., Chen, Y.D., Liu, C.L., 2009. Spatial and temporal variability of precipitation over China, 1951-2005. *Theoretical and Applied Climatology*, 95(1-2): 53-68.
- Zhang, X., Harvey, K.D., Hogg, W.D., Yuzyk, T.R., 2001. Trends in Canadian streamflow. *Water Resources Research*, 37(4): 987-998.
- Zhang, Z., Dehoff, A., Pody, R., Balay, J., 2010. Detection of streamflow change in the Susquehanna River Basin. *Water Resources Management*, 24(10): 1947-1964.
- Zume, J., Tarhule, A., 2006. Precipitation and streamflow variability in Northwestern Oklahoma, 1894-2003. *Physical Geography*, 27(3): 189-205.

### CONNECTING STATEMENT TO CHAPTER 3

Chapters 1 and 2 revealed that a substantial body of evidence suggests that surface air temperature has been increasing in many parts of the world. The prevailing view is that the measurement of air temperature can be directly related to climate change; therefore, its trend assessment is of great importance. Useful methods used to extract trend information and its fluctuations from these climatic time series in the presence of noise and other stochastic elements are therefore, important to explore. In light of this, chapter 3 focuses on trend detection in surface air temperature time series obtained from a total of five stations located in Ontario and Quebec, Canada by applying the discrete wavelet transform (DWT) and the Mann-Kendall (MK) trend test. In this chapter, a new criterion was proposed and used in the DWT procedure to determine: the number of decomposition levels, the type of Daubechies (db) mother wavelet, and the type of periodic extension. This new criterion is based on the relative error of the MK Z-values between the approximation component of the last decomposition level and the original data – it performs better compared to when the mean relative error criterion was used. The results of this Chapter have been submitted as a manuscript to the Journal of Hydrology. The manuscript has been co-authored by Deasy Nalley, Jan Adamowski, and Bahaa Khalil.

### **CHAPTER 3 – TREND DETECTION IN SURFACE AIR TEMPERATURE IN ONTARIO AND QUEBEC (1967 – 2006) USING THE DISCRETE WAVELET TRANSFORM**

Deasy Nalley, Jan Adamowski, Bahaa Khalil

#### **Abstract:**

This main purpose of this paper is to detect trends in surface air temperature over southern parts of Ontario and Quebec, Canada, for the period 1967-2006. More specifically, this paper aims to determine the most dominant periodic components that affect trends in different categories of temperature data: monthly, seasonally-based, seasonal (winter, spring, summer, and autumn), and annual time series, obtained from a total of five stations. In this study, the trend detection procedures involve the use of the discrete wavelet transform (DWT) technique, the Mann-Kendall (MK) trend test, and the sequential Mann-Kendall analysis – the combination of these procedures are considered new in climatic studies and have not been explored extensively. The number of decomposition levels, mother wavelet, and boundary condition were determined using the newly proposed criterion based on the relative error of the MK Z-values between the original data and the approximation component of the last decomposition level. The most dominant periodic components that are considered important for trends were determined using the sequential MK analysis and the difference in the MK Z-values between the detail components and the original data. In this study, it was found that for the higher resolution data (i.e. monthly and seasonally-based), high-frequency fluctuations from two to twelve months were more prominent for trends. The positive trends observed for the annual data are thought to be mostly attributed to warming during winter and summer seasons, which are manifested in the form of multiyear to decadal events (mostly between 8 and 16 years). The use of the DWT is clearly highlighted by its ability to reveal the different characteristics in terms of time scale fluctuations of the different types of data used.

**Keywords:** temperature series, trend detection, discrete wavelet transform, Mann-Kendall trend test

### 3.1. Introduction

According to the latest assessment report by the Intergovernmental Panel on Climate Change (IPCC), mean surface air temperature has experienced an increase between 0.56°C and 0.92°C from 1996 to 2005 (IPCC, 2007). The amount of carbon dioxide in the atmosphere has also increased by approximately 35% since the industrial revolution; most of this increase can be attributed to a variety of anthropogenic activities, especially deforestation and the combustion of fossil fuel (IPCC, 2007).

Many studies that analyze the impacts of climate variability and climate change focus on the trends in surface air temperature. The United Nations Framework Convention on Climate Change (UNFCCC) and the IPCC consider air temperature an important index when evaluating how the climate has evolved over a long period of time. Changes in surface air temperature as a result of changing climate are very important as it may have serious ramifications on the hydrological cycle (and therefore, on water resources) and the surface energy budget (Vincent et al., 2007). Examples of these consequences resulting for temperature rise are: intensification of the hydrological cycle (Mishra and Singh, 2010), modification of hydrological indicators such as seasonal runoff, precipitation and streamflow, and potential evapotranspiration (Mimikou et al., 2000; Labat et al., 2004), more severe flood discharges (Ludwig et al., 2004), sea-level rise (which has serious implications on the economy and societies in general) (Nicholls and Tol, 2006), and increased risks of health-related problems (Karaburun et al., 2011.), etc.

Since global warming is directly linked to temperature, a large number of studies examining a variety of temporal and spatial coverage in temperature have been undertaken in many different parts of the world to assess its trends and to quantify the impacts of increasing temperature. Since climate variability differs from one climatic region to another, different findings associated with temperature changes and trends have been reported. Even so, most studies conducted in different parts of the world have emphasized trends in temperature indices are on the rise. For instance, Shrestha et al. (1999) found that the temperature patterns were increasing in Nepal after 1977, with a rate of increase ranging from 0.03 to 0.12°C per year. Domroes and El-Tantawi (2005)

reported upward mean temperature trends in northern Egypt over the period 1941-2000. Fan and Wang (2011) studied climate change by looking at the monotonic trends in annual and seasonal air temperature indices across Shanxi province in China. They found that there has been warming trends both in the mean annual temperature and seasonally, over the period 1959-2008. Karaburun et al. (2011) also analyzed the spatiotemporal patterns of temperature change in Istanbul, Turkey for the period of 1975 to 2006. In general, warmer temperatures were observed for seasonal and annual temperature indices. Although many studies found that all seasons showed positive trends, winter usually experiences the greatest warming (e.g. Lund et al., 2001; Rebetez and Reinhard, 2007; Fan and Wang, 2011). Fan and Wang (2011) observed that winter warming in Shanxi province of China was statistically significant at less than 0.1% significance level. Rebetez and Reinhard (2007) also found that the greatest warming occurred during winter (1975-2004) in Switzerland.

It has been mentioned that the even though increases in temperature has been occurring in both the northern and southern hemispheres, the northern hemisphere has been experiencing more warming since the 1950s (Jones and Moberg, 2003; Chaouche et al., 2010; Karaburun, 2011). More specifically, North America is expected to experience warmer climate, in which the increase in the mean annual temperature could be more than the global mean warming in many parts of the world (IPCC, 2007). Moberg et al. (2005) analyzed the variation in temperature in the northern hemisphere by reconstructing long-term proxy data from tree-ring and sediments in lakes and oceans. They found that there has never been any period within the past 2000 years that is as warm as post 1990 (Moberg et al., 2005). Lund et al. (2001), who analyzed temperature trends during 1922-1996 in 359 stations located across the United States concluded that in general, the East and West Coasts, as well as the northern Midwest of the country, experienced increasing temperature trends. Lu et al. (2005) completed an extension of this study to cover 969 stations. The findings showed that the areas of warming were in accordance with those from Lund et al. (2001), but the magnitude of warming was slightly higher; all seasons experienced increasing temperature with winter having the most warming.

Zhang et al. (2000) mentioned that it may be easier to assess climate change in countries such as Canada because according to Nicholls et al. (1996), climate change that is due to anthropogenic impacts is foreseen to be more severe in high-latitude areas. As such, numerous authors have conducted studies on Canadian temperature trends, nationally and regionally, because climate change is a cause for concern in Canada. These studies include variables such as the mean annual temperature, seasonal temperatures, extreme temperatures, and diurnal temperature ranges, among others. At the national level it was found that the annual mean temperature has experienced an increase of approximately 1°C during the last half of the 20th century (Zhang et al., 2000). Zhang et al. (2000) provided comprehensive information on Canada's temperature and precipitation trends. Their analysis on the gridded annual mean temperature datasets for areas below 60°N (for the period 1900-1998) revealed that although trends are not monotonic and there are differences regionally, there is a statistically significant increase in the mean annual temperature that was caused by the increases before the 1940s and after the 1970s. With respect to the different seasons, although all seasons experienced significant changes for different temperature parameters, it was noted that spring showed the greatest magnitude of temperature rise. Mohsin and Gough (2010) analyzed the temperature trends in a smaller spatial scale covering Toronto and the Greater Toronto area for the period 1970-2000. Based on linear trend analysis on the annual indices, it was concluded that Toronto Pearson exhibited the highest warming trend, which could partly be caused by anthropogenic activities (in this case, construction and urbanization). Similarly, Prokoph and Patterson (2004) found that the temperature increase in urban Ottawa was going up by more than 0.01°C per year compared to the nearby rural areas over the past 100 years; this warming trend was associated with the growth in population, and urban heat island effects.

Many studies conducted in analyzing trends in temperature involve the use of the Mann-Kendall (MK) trend test. This trend test is usually preferred over other statistical tests because of its robustness and power. The MK test may be used even if the analyzed data does not follow a Gaussian normal frequency distribution (Kadioğlu, 1997). Chaouche et al. (2010) chose to employ the MK test in studying climatic indices (including temperature) in the context of climate change because they assumed that

trends are supposed to be slowly changing phenomena; but even if a break change occurs, the MK test is still found to be powerful. Having said this, the results obtained from using the original MK test are only accurate when the data being analyzed are free from serial correlation (Mohsin and Gough, 2010). Hirsch and Slack (1984) and Hamed and Rao (1998) proposed modifications to the original MK test in order to account for seasonality and serial correlation factors that may be present in a time series.

As can be seen, studying trends in temperature associated with global warming is of great interest because of its wide range of impacts. When analyzing changes and trends in temperature, it is also crucial that information be obtained on how these changes fluctuate within different low- and high-frequency time scales, such as interannual, decadal, etc. (Baliunas et al. 1997). A spectral analysis method that has been found very useful for analyzing geophysical time series (which are often characterized by nonstationarity) is the wavelet transform (WT) (Lau and Weng, 1995; Lindsay et al., 1996).

Since temperature time series are normally of non-stationary nature, the WT is suitable for decomposing such one-dimensional time series into its two-dimensional (time-frequency) information (Lau and Weng, 1995; Torrence and Compo, 1998; Pišoft et al., 2004). More specifically, it enables the quantification of how different scales in a time series fluctuate over some time intervals – it produces a time-frequency representation of a signal in the time domain (Percival and Walden, 2000; Pišoft et al., 2004). It has been acknowledged in many studies, that the WT is superior for use in analyzing non-stationary data compared to conventional spectral analysis methods, such as the Fourier transform (FT). The Fourier transform decomposes signals into sine wave functions, which have unlimited duration, whereas the wavelet transform, having irregular and non-symmetrical function shape, decomposes signals into wavelet functions having limited duration and zero mean (Drago and Boxall, 2002).

Wavelet transform can be performed using the continuous or discrete modes, both of which have been applied in several climatological studies, including studying spatiotemporal patterns of temperature changes. Baliunas et al. (1997), for instance, employed the WT in order to analyze temperature trends and their time-scale information in central England. The results of their WA revealed the dominant periodic modes within



the range of 2 to 105, and how their amplitudes have varied over time. WA also allows for the determination of whether specific spectra are continuous with respect to time. For example, the 7.5-year scale is the most stable peak within the range and the other apparent strong time peaks were only dominant during certain time periods (Baliunas et al. 1997). Pišoft et al. (2004) was able to demonstrate that the global wavelet spectrum of the continuous wavelet transform (CWT) had better accuracy in determining the years of local maxima for the longest time periods of the studied Czech temperature series compared to the Fourier transform. The wavelet power was able to reveal different features and activities of each periodic component. Similarly, Jung et al. (2002) and Prokoph and Patterson (2004) utilized the CWT to analyze the warming trends in the winter temperature data in South Korea and Ottawa, respectively. The results of the wavelet analysis (WA) for the winter temperature over South Korea revealed that the decadal-interdecadal events of 16 and 33 years were strongly persistent during 1954-1999 (Jung et al., 2002). A slightly weaker inter-annual event of 4.9 years was found to be associated with the El Niño cycle (Jung et al., 2002). The results of WA in studying urban warming trends in Ottawa, Ontario as compared to the nearby rural areas, revealed that multidecadal and interseasonal fluctuations are thought to be the cause of winter heating in Ottawa, which is related to the urban heat island (Prokoph and Patterson, 2004).

The majority of studies that employed WT in investigating trends in temperature used the CWT (e.g. Baliunas et al., 1997; Jung et al., 2002; Polyakov et al., 2003; Pišoft et al., 2004; Prokoph and Patterson, 2004; Kravchenko et al., 2011, etc.). This is due to the fact that the CWT allows the analysis of data at all locations of time and space (Wang and Lu, 2009). However, this causes redundancy in the information produced by the CWT because a two-dimensional scalogram is produced rather than a one-dimensional time series (Percival, 2008). Furthermore, edge effects associated with the application of the CWT complicates signal reconstruction (Adamowski et al., 2009). If the DWT approach is chosen the work is simplified and efficient, through a decomposition process that is normally computed based on a dyadic discretization (Chou, 2007). This generates a compact representation of the analyzed signal (Wang and Lu, 2009) and thus, the redundancy of the information is reduced. When using the DWT, achieving perfect signal reconstruction is also relatively simple.

The main purpose of this study is to analyze trends in four temperature categories – monthly, seasonally-based, seasonal, and annual – by combining the use of the DWT approach with the MK trend test. The DWT is used to decompose the time series into their different lower-resolution components. The MK trend test was then applied to each time series resulting from the decomposition in order to check for their statistical significance. Sequential MK analysis was also used in determining the most dominant periodic modes that affect the trends in the different data types used in this study.

The use of monthly data in this study allows for the investigation of short-term (high-frequency) variations in temperature over the study area. Seasonally-based data were used in order to address the seasonality factor encountered in the temperature time series – in this study it is seen that the 6-month and 12-month cycles are strongly apparent in the monthly time series (see section 3.5). Seasonal and annual data were used to investigate the low-frequency events in temperature changes. Additionally, as mentioned previously, temperature changes are not only observed in annual datasets, but also in different seasons. Karaburun et al. (2011) indicated that positive trends in annual data may not show that in some seasons the temperature trends are actually negative. Therefore, it is also important to analyze individual seasons separately. Karaburun et al. (2011) further emphasized that assessment on global warming should not only involve global and regional information, but also information from more localized.

Although there are numerous trend detection studies in temperature that have been conducted in Canada, they have not given much focus in analyzing the high- and low-frequency components of the time series and how they vary over time, by using signal analysis techniques such as the WT. It is important to examine these variations on short- and long-term scales, such as inter-annual, annual, decadal, multi-decadal, etc. Additionally, temperature trend studies that focus on localized areas in Canada are still rare. Furthermore, to the best of our knowledge, using the DWT in combination with the Mann-Kendall trend test to analyze temperature trends in Canada has not been explored in any Canadian studies.

## **3.2. Theoretical Background**

### **3.2.1. Time-Scale Representation of Signals by the Wavelet Transform (WT)**

Wavelet transform is a mathematical tool that uses wave functions similar to sine and cosine functions, known as wavelets. A wavelet must satisfy the admissibility condition of having a zero mean (Farge, 1992; Torrence and Compo, 1998). These wavelets can be stretched and shifted and have flexible resolution in frequency and time domains (Lau and Weng, 1995). WT has been found to be very suitable for studying climate signals that possess characteristics such as nonstationarity, time-dependence, and having a wide range of variability localized in the time domain (Lau and Weng, 1995). The property of the WT in which it is localized in time and frequency domains is very useful because it allows for the extraction of the different modes of variability that vary in time (Lim and Lye, 2004). The window used in the WT can be adjusted to the whole time-frequency domain – it can be dilated and shifted with a resolution that is adjustable in both time and frequency domains (Lau and Weng, 1995). The narrow and wide windows are used to capture the high-frequency and low-frequency components of the signal, respectively (Lau and Weng, 1995). Therefore, WT is able to separate the short and long-period components of a signal (Drago and Boxall, 2002). This is the reason why the wavelet transform is more advantageous when used for decomposing signals with non-stationary characteristics, compared to the more conventional spectral analysis, such as the Fourier transform (FT) or windowed Fourier transform (WFT). FT employs the use of sine and cosine functions, which do not involve or produce any time information of the signals being analyzed; therefore, it cannot provide how information has changed from one time interval to the next (Lau and Weng, 1995). With the WFT, the window used to analyze a time series is fixed, so when there are many different frequencies involved in the time series, the fixed window picks up more of the high-frequency information and just a few low-frequency fluctuations (Lau and Weng, 1995).

Decomposing a time series using the WT technique involves translating the mother wavelet (using high-pass and low-pass filters) along the signal in a number of steps, which then produce wavelet coefficients. These wavelet coefficients measure the

correlation of the wavelet to the original signal at a specific scale as a function of time – this is the time-scale representation of the signal, which holds information about the magnitude and location of different events at difference scales (Lindsay et al., 1996; Drago and Boxall, 2002). Different scales use different stretched versions of the mother wavelet; hence, different wavelet coefficients are produced (Drago and Boxall, 2002).

The WT can be performed via the continuous or the discrete approaches. Signal reconstructions from the wavelet coefficients are relatively simple to compute when using the DWT approach – this is done by using the inverse filter function of the wavelet transform (Torrence and Compo, 1998). Signal reconstructions for the CWT are somewhat problematic because of the redundancy in the time-scale information (Torrence and Compo, 1998). The DWT normally operates on dyadic scales, which are integer powers of two (Lindsay et al., 1996; Chou, 2007). This is one of the advantages of using the DWT as it is able to separate the signal being analyzed scale by scale (Lindsay et al., 1996). For the discrete scale operation in the DWT, the signal decomposition starts out with the smallest scales and continues to larger scales, doubling in size for each round of operation.

The decomposition of a time series  $x_t$ , via the wavelet transform is accomplished using the following function (Lau and Weng, 1995):

$$\psi_{a,s}(t) = \frac{1}{\sqrt{s}} \psi\left(\frac{t-a}{s}\right) \quad (3.1)$$

where  $s$  (which is greater than zero) represents the scaling factor,  $a$  is the translation factor, and  $\psi(t)$  is the analyzing wavelet. The wavelet coefficients ( $C$ ) via the continuous wavelet approach for the time series  $x_t$  (with equal time interval,  $dt$ ), is calculated as follows (Lau and Weng, 1995):

$$C(a,s) = \frac{1}{\sqrt{s}} \int \psi^*\left(\frac{t-a}{s}\right) x(t) dt \quad (3.2)$$

where  $\Psi^*$  is the complex conjugate number based on the scaling ( $s$ ) and translation ( $a$ ) factors. The wavelet coefficients ( $w$ ) via the discrete wavelet approach for the time series (with dyadic grid arrangement) is calculated as follows (Partal and Küçük, 2006):

$$C(a, s) = \frac{1}{(2)^{\frac{s}{2}}} \sum_{t=0}^{N-1} x_t \Psi\left(\frac{t}{2^s} - a\right) \quad (3.3)$$

### 3.2.2. The Original Mann-Kendall (MK) Trend Test

The original MK test is based on Mann (1945) and Kendall (1975). It is a rank correlation test for two sets of observations between the rank of the values and the ordered values in the dataset. The null hypothesis of the MK test for a dataset ( $X_h$ ,  $h = 1, 2, 3, \dots, n$ ) is that the dataset is independent and identically distributed (Yue et al., 2002). The alternative hypothesis would state that a monotonic trend is contained in the dataset. The calculation of the MK test statistic, which is also known as the Kendall's tau, is as follows (Yue et al., 2002):

$$S_k = \sum_{h=1}^{n-1} \sum_{i=h+1}^n \text{sign}(X_i - X_h) \quad (3.4)$$

$X_i$  denotes the ordered data values, and  $n$  is the length of observations; the sign test is (Yue et al., 2002):

$$\text{Sign}(X_i - X_h) = \begin{cases} +1 & \text{if } X_i > X_h \\ 0 & \text{if } X_i = X_h \\ -1 & \text{if } X_i < X_h \end{cases} \quad (3.5)$$

When the number of observations is greater than 10, the Kendall's tau  $S_k$  has a distribution that is approximately normal with zero mean (Hamed and Rao, 1998; Adamowski and Bougadis, 2003). The variance of the statistic  $S_k$  can then be calculated using the following equation (Kendall, 1975; Yue et al., 2002):

$$V(S_k) = \left\{ n(n-1)(2n+5) - \sum_{h=1}^n t_h(h)(h-1)(2h+5) \right\} / 18 \quad (3.6)$$

$t_h$  represents the number of ties to the extent  $h$ . The standardized test statistic for the Mann-Kendall test, which is approximately normally distributed and having a zero mean and variance of one, can then be calculated using (Yue et al., 2002):

$$Z = \begin{cases} \frac{S_k - 1}{\sqrt{V(S_k)}}, & (if S_k > 0) \\ 0, & (if S_k = 0) \\ \frac{S_k + 1}{\sqrt{V(S_k)}}, & (if S_k < 0) \end{cases} \quad (3.7)$$

Positive and negative  $Z$  values indicate that the direction of the trend is upward and downward, respectively. The calculated  $Z$  value is then compared to the standard normal variate at some level of statistical significance ( $\alpha$ ) (Hamed and Rao, 1998). In a two-sided test, if the calculated  $|Z|$  is greater than  $Z_{\alpha/2}$ , it implies that there is a significant trend (i.e. the null hypothesis should not be accepted).

### 3.2.3. Modified Mann-Kendall (MK) Trend Test

One issue that is very important to investigate prior to applying the MK test is the possible existence of serial correlation in the time series being analyzed. It has been widely recognized that the original Mann-Kendall trend test should only be applied to test for a trend in a dataset that does not exhibit serial dependency (Hamed and Rao, 1998; Adamowski and Bougadis, 2003; Mohsin and Gough, 2010). If the original Mann-Kendall test is used on a time series that exhibits positive serial correlation, the likelihood of finding trends is enhanced, when in fact, there is no trend; and vice versa (Hirsh and Slack, 1984; Hamed and Rao, 1998). Hamed and Rao (1998) tested a time series with an AR(1) of 0.4 using the original MK test and they were able to demonstrate that the

significant positive trend found (at the 5% significance level) was merely due to the effect of autocorrelation in the data.

Modifications to the original MK test to account for autocorrelation issues have been proposed. The seasonal Kendall test proposed by Hirsch and Slack (1984) is suitable for use with data that exhibit seasonality pattern and autocorrelation (Kundzewicz and Robson, 2004). Using a Monte Carlo experiment, Hirsch and Slack (1984) were able to show that the seasonal Kendall test can be used with data exhibiting serial correlation; however, this modified MK test is not powerful when there is a very strong long-term persistence or when the record length is very short (less than five years worth of monthly data).

Another modification to the original Mann-Kendall test was developed by Hamed and Rao (1998) for autocorrelated data. Hamed and Rao (1998) developed a formula based on an empirical approximation/experiment, which modifies the variance of the original MK test statistic. This is because if a significant autocorrelation is present in a time series, the variance of the original MK test is underestimated, and vice versa.

### 3.2.3.1. Modified Mann-Kendall (MK) Test for Data with Seasonality Patterns with or without Significant Autocorrelations

This modified version of the Mann-Kendall test was developed by Hirsch and Slack (1984) in order to deal with the seasonality and serial correlation in a time series. Let the matrix:

$$x = \begin{pmatrix} x_{11} & x_{12} & x_{13} & \dots & x_{1v} \\ x_{21} & x_{22} & x_{23} & \dots & x_{2v} \\ x_{31} & x_{32} & x_{33} & \dots & x_{3v} \\ \cdot & \cdot & \cdot & \cdot & \cdot \\ \cdot & \cdot & \cdot & \cdot & \cdot \\ \cdot & \cdot & \cdot & \cdot & \cdot \\ x_{u1} & x_{u2} & x_{u3} & \dots & x_{uv} \end{pmatrix} \quad (3.8)$$

The matrix  $x$  is a dataset containing observations recorded over  $v$  seasons for  $u$  years (without any missing or tied values) (Hirsch and Slack, 1984). The ranks of the data in matrix  $x$  are represented by matrix  $r$  (Hirsch and Slack, 1984):

$$r = \begin{pmatrix} r_{11} & r_{12} & r_{13} & \dots & r_{1v} \\ r_{21} & r_{22} & r_{23} & \dots & r_{2v} \\ r_{31} & r_{32} & r_{33} & \dots & r_{3v} \\ \vdots & \vdots & \vdots & \ddots & \vdots \\ r_{u1} & r_{u2} & r_{u3} & \dots & r_{uv} \end{pmatrix} \quad (3.9)$$

Since the values within each season are ranked among themselves, the ranks ( $r_{iz}$ ) are computed using the following equation, and where each column in matrix  $r$  is a permutation of  $(1, 2, \dots, n)$  (Hirsch and Slack, 1984):

$$r_{iz} = \frac{[u + 1 + \sum_{h=1}^u \text{sgn}(x_{iz} - x_{hz})]}{2} \quad (3.10)$$

The test statistics  $S_z$  is calculated using (for each season):

$$S_z = \sum_{h < i} \text{sgn}(x_{iz} - x_{hz}); \text{ where } z = 1, 2, 3, \dots, v \quad (3.11)$$

The test statistics for the seasonal Kendall is the calculated using:

$$S_s = \sum_{z=1}^v S_z \quad (3.12)$$

with variance of:

$$V(S_s) = \sum_z (\sigma_z)^2 + \sum_{z, w; z \neq w} \sigma_{zw} \quad (3.13)$$



$\sigma_z^2$  is the variance of  $(S_z)$ ,  $\sigma_{zw}$  and denotes the covariance of  $(S_z, S_w)$ . The estimator of the covariance is  $\hat{\sigma}_{zw}$  and was explained by Dietz and Killeen (1981):

$$\hat{\sigma}_{zw} = \frac{K_{zw}}{3} + (u^3 - u) \frac{r_{zw}}{9} \quad (3.14)$$

where  $K_{zw}$  is represented by:

$$K_{zw} = \sum_{h < i} \text{Sign} \{ (X_{hz} - X_{iz})(X_{hw} - X_{iw}) \} \quad (3.15)$$

and  $r_{zw}$  is calculated using:

$$r_{zw} = (3/(u^3 - u)) \sum_{h,i,j} \text{sign} (X_{hz} - X_{iz})(X_{hw} - X_{jw}) \quad (3.16)$$

In the case where there are no tied values and no missing values,  $r_{zw}$  is simply the Spearman's correlation coefficient for  $z$  and  $w$  seasons. When there are no missing values, the estimator of the covariance becomes (Hirsch and Slack, 1984):

$$\hat{\sigma}_{zw} = \frac{(K_{zw} + 4 \sum_{h=1}^u r_{hz} r_{hw} - u(u+1)^2)}{3} \quad (3.17)$$

Hirsch and Slack (1984) demonstrated that by using these consistent estimators for the covariance in order to calculate the variance of the seasonal Kendall test statistic, the assumption of independence in a time series is no longer required.

### 3.2.3.2. Modified Mann-Kendall (MK) Test for Significantly Autocorrelated Data

Hamed and Rao (1998) developed another modified version of the MK test, which is intended to address the issue of serial correlation structures in a dataset when detecting its trend. Hamed and Rao (1998) investigated the effect of serial correlation on

the mean and variance of the original Mann-Kendall test; they came up with an empirical approximation for the variance for the MK test, which is considered suitable for autocorrelated data. This is because the existence of serial correlation in a dataset can change the variance of the original MK test (the existence of positive autocorrelation will cause the variance of  $S$  to be underestimated and the existence of negative autocorrelation will cause the opposite effect). Hamed and Rao (1998) used their proposed modified version of the MK test and precipitation and streamflow series exhibiting autocorrelation and found that the power of the test is the same as that of the original MK test with better accuracy when data exhibit autocorrelation.

In this version of the modified MK test, Hamed and Rao (1998) altered the calculation of the variance of the test statistic  $S$ :

$$Var(S') = \left( n(n-1)(2n+5)/18 \right) \cdot \left( \frac{n}{n_e^*} \right) \quad (3.18)$$

$n_e^*$  denotes the effective number of samples required to account for the autocorrelation in the dataset (autocorrelation between ranks is used instead of between the actual data values to evaluate  $n_e^*$ ). The notation  $n/n_e^*$  is the correction factor associated with the autocorrelation of the data. Empirically,  $n/n_e^*$  is expressed by (Hamed and Rao, 1998):

$$\frac{n}{n_e^*} = 1 + \left( \frac{2}{n^3 - 3n^2 + 2n} \right) \cdot \sum_{f=1}^{n-1} (n-f)(n-f-1)(n-f-2)\rho_e(f) \quad (3.19)$$

$\rho_e(f)$  symbolizes the autocorrelation function between the ranks of the observations, computed using the inverse of equation (3.20) (Kendall, 1975; Hamed and Rao, 1998). This transforms the rank autocorrelation into the normalized data autocorrelation, as the estimate of the normalized autocorrelation structure is needed to evaluate the variance of  $S$  for data  $X$  whose distribution may not be normal or rather arbitrary (Hamed and Rao, 1998):

$$\rho(f) = 2 \sin\left(\frac{\pi}{6}\rho_e(f)\right) \quad (3.20)$$

### 3.3. Data and Study Sites

Data from a total of five meteorological stations located in southern Ontario and Quebec were used in this study. The Harrow, Vineland, Belleville and Peterborough stations are located in Ontario and the Val d'Or station is located in Quebec. These are the only stations in Ontario and Quebec that satisfy the requirement of having 40 years worth of data without any missing values, and as such only these data sets were used in this study. The locations of the stations used in the study are shown in figure 3.1; and the key features of the stations are given in table 3.1 – joint stations indicate that records from nearby stations were combined in order to produce longer time series. The detail of how data from nearby stations were combined can be found in Mekis and Vincent, 2011.

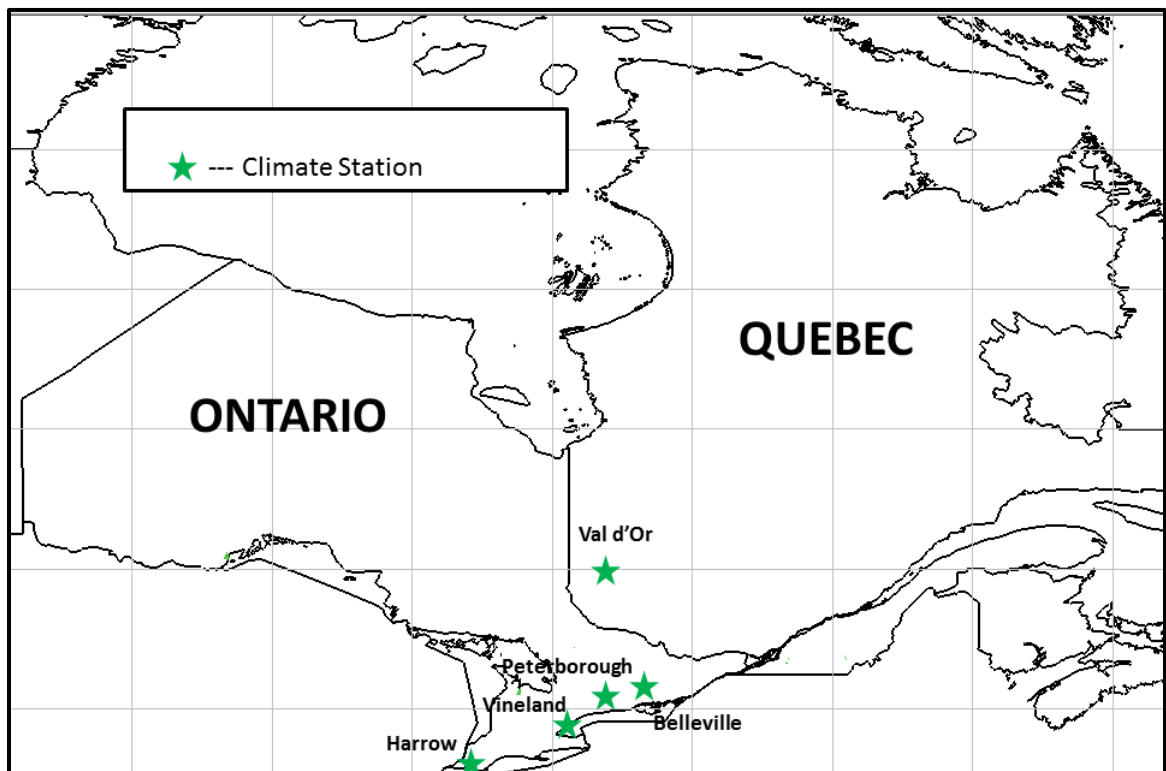


Figure 3.1. A map of the weather stations used in this study.

Table 3.1. Key features of the meteorological stations used in this study.

Station Name	Province	Station Location		Elevation (m)	Joint Station
		Latitude (°)	Longitude (°)		
Harrow	ON	42.0	-82.9	182	Yes
Vineland	ON	43.2	-79.4	79	Yes
Belleville	ON	44.2	-77.4	76	No
Peterborough	ON	44.2	-78.4	191	Yes
Val d'Or	QC	48.1	-77.8	337	No

The data used in this study came from the second generation homogenized temperature data of Environment Canada. These homogenized temperature data are specially developed for trend studies in climatic indices. Adjustment procedures on monthly and daily maximum and daily minimum temperature indices were implemented to create the first generation homogenized temperature data. The adjustments were applied in order to account for non-climatic shifts such as station relocations, changes in recording procedures and automation (Vincent and Gullet, 1999). These non-climatic shifts may cause inhomogeneities in the temperature data, which in turn leads to inaccurate trend estimates if the data were to be used for trend analysis (Zhang et al., 2000). In the second generation homogenized sets, the spatial and temporal coverage of temperature data have been improved. Furthermore, additional adjustment procedures were implemented in order to solve the bias caused by the redefinition of the end time of the climatological day, which occurred as of July 1, 1961 (refer to Vincent et al., 2009 for the details of the adjustments). The adjustment procedures in the second generation homogenized datasets involved adjusting the daily minimum temperatures, which are based on hourly data for the period 1961-2007 – the adjustment in any one day was between 0.58-12.58°C (Vincent et al., 2009). We believe that by using the homogenized temperature data in this study, the results of our trend analysis are more reliable.

There are four categories of temperature data analyzed in this study: (i) monthly, (ii) seasonally-based, (iii) seasonal (i.e. winter, spring, summer, and autumn), and (iv) annual. The data spanned from 1967 to 2006, with the exception of station Harrow, whose annual and autumn data end in 2005 due to missing observations at the end of 2006. Forty years worth of data is considered sufficient to conduct a trend analysis study (Partial, 2010). A number of authors have also used forty years worth of data or less, for

their trend analysis studies in hydroclimatic indices (e.g. Domroes and El-Tantawi, 2005; Chaouche et al., 2010; Makokha and Shisanya, 2010; Karaburun et al., 2011).

The monthly data contain observations starting from January 1967 to December 2006 (with the exception of station Harrow whose monthly time series ends in August 2006). Seasonally-based data use information from each season in a year continuously from winter 1967 to autumn 2006 (with the exception of station Harrow whose seasonally-based data ends in summer 2006). The standard climatological season was used. Each winter data record was obtained by averaging the December to February values; each spring data record was obtained by averaging the March to May values; each summer data record was obtained by averaging the June to August values. Finally, each autumn data record was obtained by averaging the September to November values. For seasonal data, each season (winter, spring, summer, and autumn) was analyzed separately (there was one value every year for each season).

Monthly data were analyzed in order to investigate the short-term fluctuations that could affect the temperature trends. These fluctuations could include cycles such as intra-annual and inter-annual cycles (as will be seen in section 3.4 the decompositions of monthly data represent fluctuations ranging from two to 64 months). Seasonally-based time series were analyzed in order to investigate whether the strong semiannual and annual seasonal patterns that are apparent in temperature time series play a role in affecting the temperature trends (it will be seen in section 3.5 that the temperature time series used in this study exhibit strong cycles at six and 12 months).. Annual time series were included in the study in order to investigate events that are fluctuating in long terms, such as multi-year and decadal events. Similarly, analyzing each season separately allowed us to study the long-term event fluctuations. Additionally, seasonal data were included because it has been shown in several Canadian studies that changes in temperature do not only occur in annual data but also within the different seasons (e.g. Zhang et al., 2000; Vincent et al., 2007).

### 3.4. Methodology

This study employed the DWT approach to decompose the surface air temperature time series obtained from a total of five stations located in southern Ontario and Quebec. The wavelet decomposition was applied to the different data types used in order to analyze the high- and low-frequency events that affect the temperature fluctuations over the study area. The data used were: monthly, seasonally-based, seasonal, and annual. The trend component is assumed to be contained in the low-frequency part of the time series. The MK trend test was then applied to the different detail and approximation components (and also to the detail plus approximation series) resulting from the time series decomposition. This was done to determine their statistical significance, as well as to identify the periodic modes that affect the trends in each data type.

The data analysis in this study was carried out using procedures summarized as follows:

1. The presence (or lack thereof) of serial correlation was checked for each dataset.
2. The presence (or lack thereof) of seasonality patterns in each dataset was determined using their correlograms.
3. Using the DWT approach, each dataset was decomposed into its detail and approximation components.
4. The MK trend test and the sequential MK analysis were applied to the original datasets and to the different detail and approximation series produced by the wavelet decomposition.
5. The most common periodicities that are responsible for the observed trends were determined by examining the sequential MK graphs and the MK Z-values of the detail (plus approximation) components, and then comparing them to that of the original data.

### 3.4.1. Serial Correlation and Seasonality Analyses

In order to identify if the time series exhibited non-random characteristics, the serial correlation test was applied. The issue of serial correlation was first investigated prior to applying the trend test on a time series. This is because the original Mann-Kendall test should only be used when the data points in a time series are not serially correlated with each other (Mohsin and Gough, 2010). If serial correlation exists in a time series, it increases the likelihood to reject the null hypothesis of no trend, when in fact the null hypothesis should be accepted (Yue et al., 2002). This is because the variance of the Mann-Kendall test statistics is underestimated (Hamed and Rao, 1998).

In this study, the autocorrelation in each time series was examined and correlograms were produced. Autocorrelation coefficients at lag-1 are commonly used to examine whether a time series exhibit non-random characteristics (e.g. Partal and Kahya, 2006; Mohsin and Gough, 2010). Lag-1 autocorrelation coefficients were computed using the following equations (Yue et al., 2002; Mohsin and Gough, 2010):

$$R = \frac{(1/n - 1) \sum_{t=1}^{n-1} [x_t - \bar{x}_t] [x_{t+1} - \bar{x}_t]}{(1/n) \sum_{t=1}^n [x_t - \bar{x}_t]^2} \quad (3.21)$$

$$\frac{\{-1 - 1.645 \sqrt{n} - 2\}}{n - 1} \leq R \leq \frac{\{-1 + 1.645 \sqrt{n} - 2\}}{n - 1} \quad (3.22)$$

$R$  represents the first autocorrelation coefficient (i.e. lag-1) of the time series  $x_t$ ,  $\bar{x}_t$  represents the mean of the data, and  $n$  is the number of data points in the time series. If the lag-1 autocorrelation coefficient is found to be within the interval defined by equation (3.22), it can be concluded that the time series does not exhibit a significant autocorrelation. On the contrary, if the calculated lag-1 autocorrelation coefficient is found to be outside of the interval, it can be said that the time series exhibits a significant autocorrelation at the 5% significance level.

The correlograms or autocorrelation plots depicting the autocorrelation functions of the time series being analyzed in this study were obtained using IBM SPSS Statistics 19. If an autocorrelation coefficient value crosses the upper or lower confidence limits, then that autocorrelation is significant (see an example in figure 3.2: the lag-1 autocorrelation coefficient is the first one on the plot). The correlograms were also used to identify whether cycles of seasonality were present in a particular time series. If there were repeated oscillating patterns that continued for many lags, it was concluded that the analyzed time series exhibited seasonality patterns (as shown in figures 3.2 and 3.3).

### **3.4.2. Discrete Wavelet Transform (DWT) Applications on Different Temperature Time Series**

Time series decomposition via the DWT was computed using the *multilevel one-dimensional wavelet analysis* function and performed in MATLAB. The signal (i.e. time series) is convolved (processed) with low-pass and high-pass filters, followed by a dyadic discretization or downsampling procedure, in order to produce the approximation and detail coefficients. These coefficients are re-adjusted to the entire signal to determine their contribution to the original signal (Dong et al., 2008). The signal is then reconstructed by using the *multilevel one-dimensional wavelet reconstruction* function using the same low-pass and high-pass filters.

Daubechies (db) wavelets were used as the mother wavelet in the time series decomposition. The Daubechies wavelets were used in this study because of their ease of use, compact support, and orthogonality (Ma et al., 2003; Vonesch et al., 2007), which implies that the wavelets have non-zero basis functions over a finite interval, and also full scaling and translational orthonormality properties (Popivanov and Miller, 2002; de Artigas et al., 2006). These properties are very important for localizing events when analyzing signals that are characterized by time dependency – this localizing property also implies that wavelets can be adjusted to accommodate both high and low frequencies of the analyzed signals (Wang et al., 1998; Popivanov and Miller, 2002). Changing the scale in order to improve the accuracy of data analysis (during the DWT procedure) is relatively straightforward with the Daubechies wavelet due to its compact support and



orthogonality (Ma et al., 2003). Furthermore, the compact support provided by the Daubechies wavelet has fewer degrees of freedom (associated with the wavelet coefficients), which is ideal for analyzing signals with complex structures (Ma et al., 2003). The scaling function of a Daubechies wavelet also represents polynomials with order up to  $N/2-1$  very well. In order to determine the db type to be used in the data analysis of a particular time series, the Daubechies wavelets, db1 to db 10 were tried out.

Border extensions were also considered important because when performing the DWT decomposition on signals with finite length, the issue of border distortion effects is introduced. This happens because convolution processes cannot occur outside the ends of signals that have limited length due to information being unavailable outside the borders (Su et al., 2011). Extending the ends of the signal produces several extra coefficients during the decomposition process, which are needed in order to ensure a perfect signal reconstruction. There are three border extensions that are normally used in the DWT: zero padding, periodic extension, and boundary value replication (symmetrization). Zero-padding uses zeros outside of the original support of the mother wavelet, to pad the signal being analyzed; periodic padding recovers the signal beyond the original support by periodic extension; and symmetrization – which is the default mode in MATLAB – assumes that signals outside the original support can be recovered by symmetric boundary replication (de Artigas et al., 2006). The inverse discrete wavelet transform (IDWT) was then run in MATLAB to ensure perfect signal reconstruction.

Both the mean relative error (*MRE*) and the relative error (*RE*) were tried out as criteria in order to calculate the number of decomposition levels, and determine the border extension type and the type of mother wavelet used. The lowest *MRE* and *RE* values were sought. The mean relative error (*MRE*) was calculated using the following equation (Popivanov and Miller, 2002; de Artigas et al., 2006):

$$MRE = 1/n \sum_{j=1}^n \frac{|a_j - x_j|}{|x_j|} \quad (3.23)$$

where  $x_j$  is the original data value of a signal whose number of records is  $n$ , and  $a_j$  is the approximation value of  $x_j$ . The relative error criterion is a new criterion proposed in this

study and is based on the error of the MK Z-values between the last decomposition level and the original data. The relative error was calculated using the following proposed formula:

$$RE = \frac{|Z_{ap} - Z_{or}|}{|Z_{or}|} \quad (3.24)$$

$Z_{or}$  represents the MK Z-value of the original time series; and  $Z_{ap}$  is the MK Z-value of the approximation component of the last decomposition level of the DWT.

In the monthly time series used in this study, there were 480 data points in each dataset, with an exception of station Harrow having only 476. The following equation was proposed by de Artigas et al. (2006), who conducted a study on monthly geomagnetic activity indices, to calculate the number of decomposition levels:

$$L = \frac{\text{Log} \left( \frac{n}{2^v - 1} \right)}{\text{Log} (2)} \quad (3.25)$$

where  $v$  represents the number of vanishing moments of a db wavelet,  $n$  is the number of records in a monthly-based time series, and  $L$  is the maximum decomposition levels. In MATLAB, the number of vanishing moments for a db wavelet should be only half of the length of its starting filter. For example, if using the db3 mother wavelet in MATLAB, it implies that the wavelet is Daubechies3, which has a 6-point filter length. It should also be noted that if the number of data points in a time series is not exactly in a dyadic format (as is the case in this study), the DWT computation in MATLAB would be performed using the next dyadic arrangement. Therefore, with either 476 or 480 data points (in the monthly time series), the value of  $n$  in equation (3.25) would be represented by  $2^9 = 512$  (which is the next dyadic format from 476 or 480). So, for example, if db3 wavelet is used on the monthly data, the number of decomposition level,  $L$ , would be 6.68 (seven levels would then be used).

Similarly, for the seasonally-based time series, there were either 159 (for station Harrow) or 160 data points. In MATLAB, the DWT computation would use 256 ( $2^8$ ) as the number of data points. If db3 was used in equation (3.24) for the seasonally-based data, the calculated  $L$  would be 5.68 (six levels would then be used).

When the MRE criterion was used to determine the number of decomposition levels (using different db types and extension border conditions), the differences in the MRE between different decomposition levels were not noticeable. For example, for station Vineland's annual data, the MRE for four decomposition levels using different db wavelets were: 0.06-0.07, 0.055-0.059, and 0.11-0.22 using periodic extension, symmetrization, and zero-padding border, respectively. The MRE for five decomposition levels for the same station were: 0.06-0.08, 0.06-0.07, and 0.19-0.24 using periodic extension, symmetrization, and zero-padding border, respectively. When the relative error criterion was used on this station, noticeable differences were observed. For Vineland's annual data, the relative errors obtained from using four decomposition levels were: 0.01-1.58, 1.00-3.40, and 0.03-1.84 using periodic extension, symmetrization, and zero-padding borders, respectively. For the same data, the relative errors obtained from using five decomposition levels were: 0.02-2.16, 0.58-7.66, and 0.04-2.60 using periodic extension, symmetrization, and zero-padding extension, respectively. Therefore, for Vineland's annual data, four decomposition levels were used (the lowest relative error of 0.01 was obtained from using db6 wavelet). The latter is an example of how the number of decomposition levels was determined on a case by case basis in this study.

As can be seen, using the relative error criterion was more precise for the temperature data used in this study. The noticeable differences in the relative error were not only seen for Vineland station, but for all other stations as well. In light of this, the relative error criterion (of the MK Z-values between the approximation component of the last decomposition level and the original time series) was used instead of the MRE to determine: (i) the mother wavelet to be used in the DWT procedures; (ii) the extension-border method to be used in the DWT procedures; and (iii) the number of decomposition levels up to which the analyzed time series should be decomposed. This was done by seeking the lowest MK Z-value relative error produced. Another example is for Vineland's monthly data ( $Z = +3.39$ ), where the lowest MK Z-value relative error of

0.046 was obtained by employing the periodic extension condition and db3 mother wavelet (at six decomposition levels). Therefore, six decomposition levels were used to analyze the monthly time series of the Vineland station. Similarly, for station Peterborough's seasonally-based data (whose MK Z-value is +2.48), the lowest MK Z-value relative error of 0.057 was produced by using the periodic extension condition and db7 mother wavelet (at four decomposition levels). Therefore, four decomposition levels were used to analyze the seasonally-based time series of the Peterborough station.

For the annual and seasonal data, there was 40 years worth of annual data, except for station Harrow annual and autumn data, which have only 39 years worth of annual data. With the dyadic scale arrangement (integer powers of two) in the DWT procedure, the annual and seasonal data could be decomposed up to five decomposition levels, in which the last decomposition level is represented by the 32-year periodic mode. However, we did not always need to decompose the annual and seasonal time series into five levels because even three or four levels may be sufficient. Again, the lowest MK Z-value relative error was sought in order to determine the appropriate number of time series decomposition levels. In addition, the lowest MK Z-value relative error was also used to determine the type of db wavelet (db1-db10) and the type of border extension (zero-padding, periodic extension, or symmetrization), to be used during the DWT procedure. Generally, the lowest MK Z-value relative errors were obtained when the periodic extension border was used. For example, for station Harrow's winter data ( $Z = +1.97$ ), the MK Z-value relative errors for the periodic extension, symmetrization, and zero-padding extension ranged from 0.06-2.26, 0.11-3.61, and 0.24-2.26, respectively. The lowest MK Z-value relative error of 0.06 was produced using db7 wavelet at three decomposition levels – therefore, station Harrow's winter time series was decomposed into three levels, using the db7 wavelet and the periodic extension mode. For other data sets, the number of decomposition levels and the mother wavelet may vary. For example, the lowest MK Z-value relative error of 0.05 for Harrow's summer data ( $Z = +2.87$ ) was observed when the periodic extension was used (with db5 at five levels of decomposition). Thus, Harrow's summer time series was decomposed into five decomposition levels using the db5 wavelet and the periodic extension border.

### **3.4.3. The Mann-Kendall (MK) Trend Test**

The Mann-Kendall trend test is a rank-based test that has been very commonly used to test for randomness against trends in the field of climatological studies. The MK test statistic  $S$  and the variance were calculated (see equations 3.4 and 3.6, respectively) for each dataset in order to obtain the standard normal value,  $Z$  score (see equation 3.7). In the data analysis of this study, the significant level used was  $\alpha = 5\%$  (or 95% confidence intervals) for a two-sided probability. The absolute value of this  $Z$  score was then compared to the critical two-tailed  $Z$ -value (area under the normal curve) of  $\alpha/2$ . The  $Z$  values in a two-tailed test for  $\alpha = 5\%$  are  $\pm 1.96$ . If the calculated MK  $Z$ -score is outside the range of -1.96 and +1.96, the trends are statistically significant. The MK test tests the null hypothesis of no trend (independent observations and they are ordered randomly) against the alternative hypothesis of positive or negative monotonic trends over time that is present in the dataset being analyzed (Hirsch and Slack, 1984; Mohsin and Gough 2010; Karaburun et al., 2011).

#### **3.4.3.1. Applications of the Original and Modified Versions of the Mann-Kendall (MK) Trend Test**

Since the monthly and seasonally-based time series in this study exhibited seasonality patterns (some with significant autocorrelations at lag-1), the modified Mann-Kendall test by Hirsch and Slack (1984) was used. For the annual and seasonal datasets, the original Mann-Kendall test and the modified Mann-Kendall test by Hamed and Rao (1998) were employed, depending on whether the dataset being analyzed was free from a significant autocorrelation or not. If the correlogram of a time series did not portray significant autocorrelation functions (at  $\alpha = 5\%$ ), then the original Mann-Kendall test was applied to the original data and to the detail, approximation and detail (plus approximation) components resulting from the time series decomposition. If, on the other hand, the correlogram of a time series showed a significant autocorrelation function (at lag-1), then the modified Mann-Kendall test by Hamed and Rao (1998) was used.

### 3.4.3.2. Sequential Mann-Kendall (MK) Analysis

The Mann-Kendall test was employed sequentially in order to analyze how the trends in each time series used in this study have fluctuated over the study period. This is useful because positive and negative trends, which may or may not be significant, can be observed in the sequential MK graphs (Makokha and Shisanya, 2010). Additionally, with sequential MK analysis, we could also observe if a series of significant positive and negative trends may cancel each other out and thus, produce an MK Z-value that is not significant at the end of the study period. Some authors have used the sequential MK analysis to identify the start of significant trends (e.g. Esteban-Parra et al., 1995; Makokha and Shisanya, 2010). The sequential Mann-Kendall analysis in this study was also used to determine the time periodicities that are considered the most influential in affecting the temperature trends over the study area (see the following section: 3.4.4).

The progressive MK values were calculated using the appropriate MK test (i.e. original or the modified version) for each dataset, from the start to the end of the study period. The progressive MK values were then graphed. In the sequential MK graph, the upper and lower lines correspond to the confidence limits of the standard normal Z values at  $\alpha = 5\%$ . The upper and lower confidence limits therefore correspond to +1.96 and -1.96, respectively. When the progressive MK value crosses either of the confidence limit lines, it indicates a significant trend at the 5%-significance level – crossing the upper line implies a significant positive trend, whereas crossing the lower line implies a significant negative trend.

It is important to recall that the standard normal Z-score can be used in the MK test only when the number of observation in a dataset is more than 10. With this in mind, the accuracy of the first 10 MK values (up to year 1976) in the sequential MK graphs may be overlooked.

#### **3.4.4. Determining the Most Dominant Periodic Components that Affect Temperature Trends**

The most dominant periodic components that affect the temperature trends over the study area were determined in two steps. First, the MK Z-values of each of the detail components with its approximation added were compared to the MK Z-value of their respective original data. Secondly, the sequential Mann-Kendall values of each of the detail components (with its approximation added) were graphed along with the sequential Mann-Kendall values of the original data. The periodic components that are considered the most dominant in affecting the trends in temperature over the study area are the ones whose MK Z-values were close to that of the original data and whose sequential MK graphs were observed to be harmonious with the sequential MK of the original series.

We also tested a number of combinations of detail components with approximation series (e.g. D1 + D2 + Approximation) in order to see if two or more periodic modes are influencing trends observed for a specific time series, but the results produced were not conclusive (based on the observations of the MK Z-values and the sequential MK graphs). For example, Harrow's spring temperature data has an MK Z-value of +1.67; based on the nearest MK Z-value and the sequential MK graphs (see figure 4.10), D3 (plus A5) component is considered the most influential periodicity for trends (see section 3.5.6 for more detail). When we combine different detail components (with approximation), even when D3 is present, it does not always produce MK Z-values that are close to the MK Z-value of the original data and/or good sequential MK graphs. For example, D1 + D3 + A5 only gives an MK Z-value of +0.62; D2 + D3 + A5 had an MK Z-value of only +0.57. However, D2 + D5 + A5 produced a relatively close MK Z-value of +1.48, which is close to the MK Z-value of the original data (+1.67); although neither D2 nor D5 was considered important periodicities for trends. Therefore, in this study we only chose to include analysis on individual detail components (with their respective approximation components added).

### 3.5. Results and Discussions

#### 3.5.1. Preliminary Data Analysis

##### 3.5.1.1. Serial Correlation and Seasonality Factors

The trends of temperature time series from a total of five meteorological stations in southern Quebec and Ontario were analyzed in order to determine the periodic modes that affect the observed trends. The data used are: monthly, seasonally-based, seasonal (winter, spring, summer, and autumn), and annual. All the monthly data experienced significant lag-1 autocorrelation coefficients, which indicate that the observations within the datasets are not independent. When the autocorrelation analysis was run on the seasonally-based, seasonal, and annual data, the lag-1 autocorrelation coefficients were not significant; with the exception of the annual data from station Vineland ( $R = 0.35$ ). It is commonly expected that a monthly time series would have a stronger autocorrelation compared to its annual time series (Hirsch and Slack, 1984). The lag-1 autocorrelation coefficients for the data used in this study are summarized in table 3.2.

Table 3.2. Lag-1 autocorrelation functions (ACFs) of the different temperature data types.

	Harrow	Vineland	Belleville	Peterborough	Val d'Or
Monthly Data	0.84* (S)	0.84* (S)	0.84* (S)	0.84* (S)	0.84* (S)
Seasonally-based Data	0.004 (S)	0.008 (S)	0.006 (S)	0.003 (S)	0.001 (S)
Winter Data	0.14	0.12	0.19	0.05	-0.10
Spring Data	0.05	0.14	0.07	-0.01	-0.02
Summer Data	0.03	0.03	-0.06	0.01	-0.10
Autumn Data	-0.05	0.12	0.09	0.02	-0.04
Annual Data	0.29	0.35*	0.28	0.12	-0.004

\* indicates a significant trend value at  $\alpha = 5\%$

(S) indicates the presence of seasonality

The correlograms of all the monthly data showed strong seasonality patterns as there are repeated cyclical fluctuations. Semiannual and annual seasonality patterns are very strongly apparent in all the monthly data as there are high coefficients at every sixth



lag (figure 3.2). This is again confirmed by the correlograms of the seasonally-based data, where the autocorrelation functions are much higher at every second lag (figure 3.3). The second and fourth lags in the seasonally-based data correspond to six and 12 months cycles, respectively.

### 3.5.1.2. The Mann-Kendall (MK) Test on Original Data

Due to the presence of a seasonality pattern in the monthly and seasonally-based data, the modified version of the Mann-Kendall test by Hirsch and Slack (1984) was used to test for trend significance in these data sets. As for the seasonal and annual data sets, which exhibited an absence of serial correlation, the original Mann-Kendall test was used (except for the Vineland station's annual data). The modified Mann-Kendall version by Hamed and Rao (1998) was used on the annual data for Vineland station.

As shown in table 3.3, all of the trend values show positive signs, which indicate that all temperature indices analyzed in this study have positive trends. For the monthly, seasonally-based, and annual data analysis, all stations are experiencing statistically significant positive trends (at the 5%-level). For the seasonal data, most stations are experiencing significant positive trends for the winter season (except for station Val d'Or) and for the summer season (except for station Peterborough); although the MK Z-value of Val d'Or winter and Peterborough summer are +1.80 +1.87, respectively, which are just slightly below +1.96. Only station Vineland showed a significant trend value for the spring season; and there was no station with significant trend values for autumn.

Table 3.3. Mann-Kendall Z-values of the original time series for the different temperature data types.

	Harrow	Vineland	Belleville	Peterborough	Val d'Or
Monthly Data	3.25*	3.39*	3.33*	2.45*	2.80*
Seasonally-based Data	3.09*	3.25*	3.26*	2.48*	2.57*
Annual Data	2.88*	3.15*	3.58*	2.49*	2.18*
Winter Data	1.97*	1.97*	2.60*	2.37*	1.80
Spring Data	1.67	2.15*	1.59	1.09	1.03
Summer Data	2.87*	2.81*	2.59*	1.87	1.98*
Autumn Data	1.21	1.73	1.69	0.91	1.38

\* indicates a significant trend value at  $\alpha = 5\%$

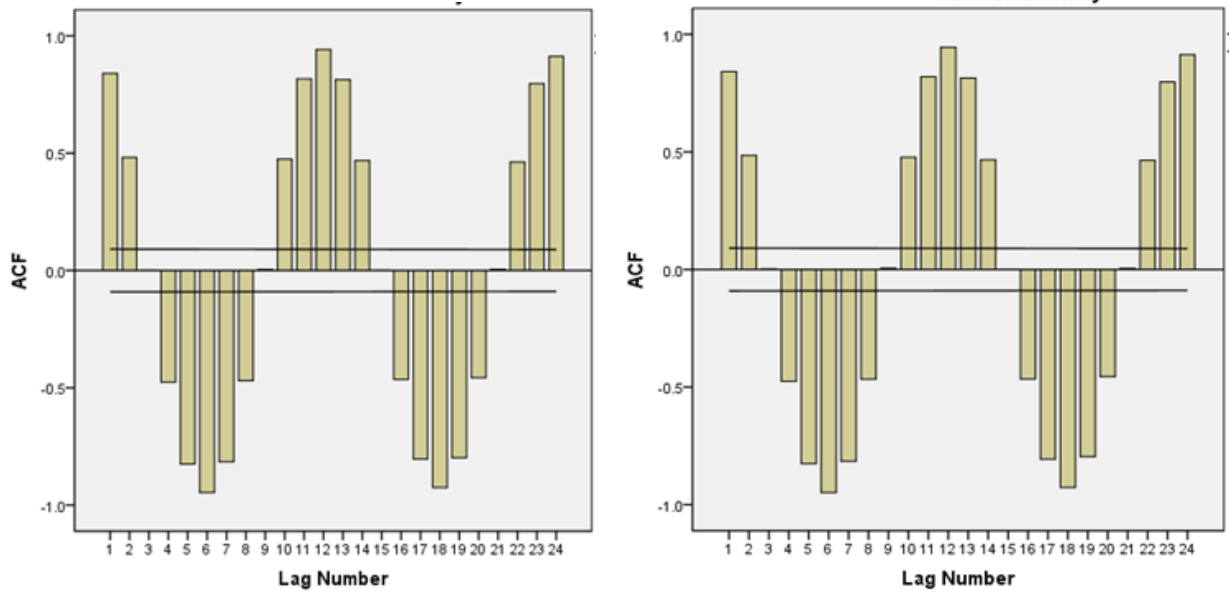


Figure 3.2. Examples of the monthly data correlograms: stations Harrow (left) and Vineland (right). High coefficient values at every sixth lag indicate the presence of semiannual and annual seasonality patterns. The upper and lower confidence limits are shown by the straight lines.

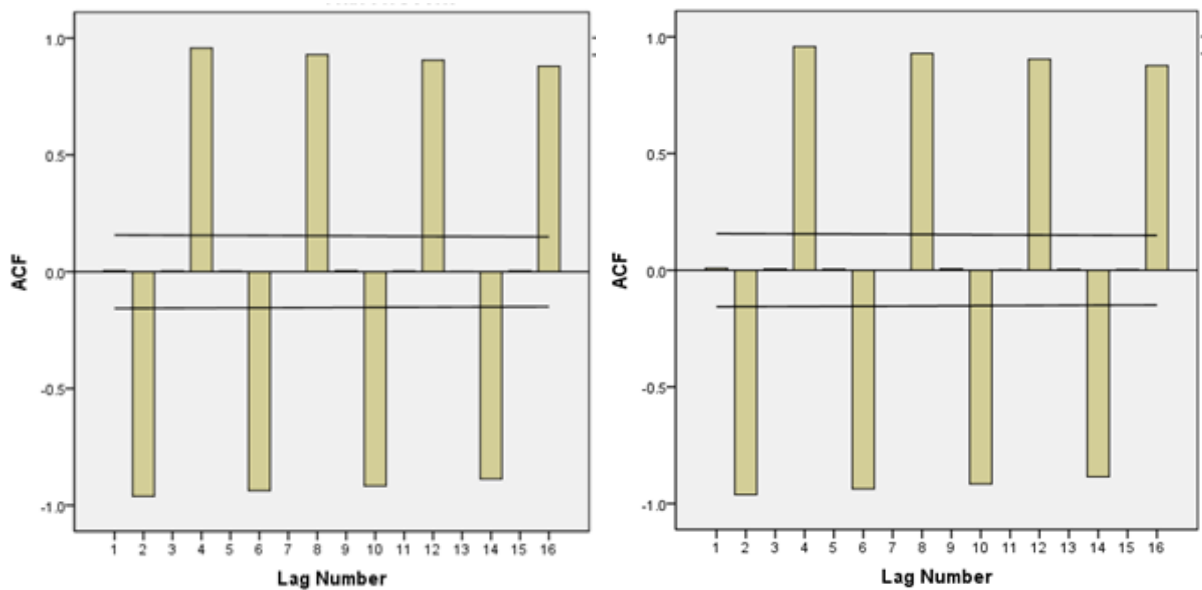


Figure 3.3. Examples of the seasonally-based data correlograms: stations Harrow (left) and Vineland (right). High coefficient values at every second lag indicate the presence of semiannual and annual seasonality patterns. The upper and lower confidence limits are shown by the straight lines.

### **3.5.1.3. The Number of Decomposition Levels for the Different Time Series**

The number of decomposition levels for each time series was determined using the MK Z-value relative error criterion. As seen in tables 3.4-3.10, the numbers of decomposition levels may not all be the same for the same temperature index. For example, for the annual data, the number of decomposition levels for station Vineland is four, but for all the other stations the number of levels is five. Similarly, for the winter data analysis, station Harrow only has three levels of decomposition while the other stations have five. These differences were caused by the differences in the mother wavelet used giving the lowest relative error.

Since only the DWT approach was used, the scales are arranged in a dyadic format (integer powers of two) from the lowest scale. Therefore, D1 represents the 2-unit periodic components, D2 represents the 4-unit periodic components, D3 represents the 8-unit periodic components, and so on. An example of time series decomposition used in this study via the DWT is given in figure 3.4, representing monthly data analysis for station Harrow. In this result section, station Harrow will be presented in detail for the different data analysis. It should be noted that the MK Z-values discussed in the results section are of the detail components with its approximation added. We found that after the addition of the approximation components to their details, the interpretation of the MK Z-values become more sensible. Furthermore, since the approximation components are representative of the large-scale variability (i.e. trends) (Craigmile et al., 2004; Kallache et al., 2005), it makes sense to add them to the detail prior to applying the appropriate Mann-Kendall test.

### **3.5.2. Monthly Temperature Data Analysis**

As shown in table 3.4, all stations are experiencing significant positive trends. Based on the lowest relative error of the MK Z-values, all monthly time series were decomposed into six decomposition levels (D1 – D6), except for station Val d’Or whose data were decomposed into five levels (D1 – D5). The results of the Mann-Kendall test showed that none of the individual detail components showed significant MK Z-values,

except for the D6 component of station Vineland ( $Z = +2.03$ ) (table 3.4). After the addition of the approximation components to their respective detail components, it is observed that most of the trend values became significant ( $\alpha = 5\%$ ). By examining the sequential Mann-Kendall graphs, and by comparing the MK Z-values of the detail components and the original data (an example is given in figure 3.5), it is found that the periodic modes responsible for trends are relatively similar for all stations. Figure 3.5 illustrates how the most dominant periodic component(s) are chosen – although graphically, all detail components show harmonious trend lines, details that have the closest MK Z-values to that of the original data are D1 and D2. Therefore, for station Harrow’s monthly temperature data, 2-month and 4-month periodicities are the most dominant ones for trends. Similarly, for stations Belleville, Peterborough, and Val d’Or, the most dominant periodic modes for trends were also observed to be the D1 and D2 components. Station Vineland’s most dominant detail component for trends is observed to be the D1 component (i.e. the 2-month periodicity). The trends for the monthly data in all stations seem to be affected by high-frequency fluctuations ranging from two to four months. The D6 component – representing the 64-month periodicity – of station Vineland is not seen as the most influential periodic component for trend. Although none of the most dominant periodic components for any of the stations are between six and 12 months, it is still worthwhile to investigate their seasonally-based data, in order to investigate whether the semiannual and annual seasonal cycles may be contributing to the observed warming trends in temperature over the study area.

### **3.5.3. Seasonally-based Temperature Data Analysis**

The appropriate number of decomposition levels for the seasonally-based time series was determined to be four (for stations Peterborough and Val d’Or) and six (for stations Harrow, Vineland, and Belleville). Again, this difference in the number of decomposition level was due to the lowest relative error of the MK Z-value – whichever level produced the lowest relative error for a particular time series, that number of decomposition levels was used. Particular attention is given to the D1 and D2 components because they represent the 6-month and 12-month periodicities. These time

modes are important in this study because of the seasonality factor observed in the monthly and seasonally-based time series. As can be seen in table 3.5, the D2 component seems to be the most frequently observed as the most dominant periodic mode affecting trends – all stations have D2 as one of the most dominant components (except for Val d’Or). The D3 and D4 components were also seen as being important in some stations. An example of the sequential MK analysis to see the most harmonious detail component (with the approximation added) for the seasonally-based data is shown in figure 3.6. As can be seen, the yearly fluctuations, which are represented by the D2 component, are also contributing in affecting the warming trends in temperature over the study area.

Table 3.4. Mann-Kendall Z-values of the monthly temperature series: original data, details components, approximations, and a set of combinations of the details and their respective approximations. The most effective periodic components for trends are indicated in bold format.

	Harrow	Vineleand	Belleville	Peterborough	Val d'Or
Original	3.25*	3.39*	3.33*	2.45*	Original: 2.80*
D1	-0.37	-0.36	0.31	0.00	D1: 0.75
D2	1.49	0.90	0.53	0.71	D2: -0.02
D3	-0.35	-0.67	-0.48	-0.50	D3: 0.41
D4	0.03	0.43	0.46	0.52	D4: 0.04
D5	-0.38	0.59	0.63	0.68	D5: 0.16
D6	1.06	2.03*	1.45	1.63	A5: 2.83*
A6	3.32*	3.55*	3.24*	2.43*	D1 + A5: <b>3.20*</b>
D1 + A6	<b>3.30*</b>	<b>3.53*</b>	<b>3.63*</b>	<b>2.56*</b>	D2 + A5: <b>3.27*</b>
D2 + A6	<b>3.15*</b>	3.91*	<b>3.62*</b>	<b>2.55*</b>	D3 + A5: 2.18*
D3 + A6	1.30	1.68	1.69	0.73	D4 + A5: 1.43
D4 + A6	1.17	1.74	1.57	1.15	D5 + A5: 2.10*
D5 + A6	1.56	2.59*	2.40*	1.65	
D6 + A6	3.63*	4.19*	4.19*	3.71*	

\* indicates a significant trend value at  $\alpha = 5\%$

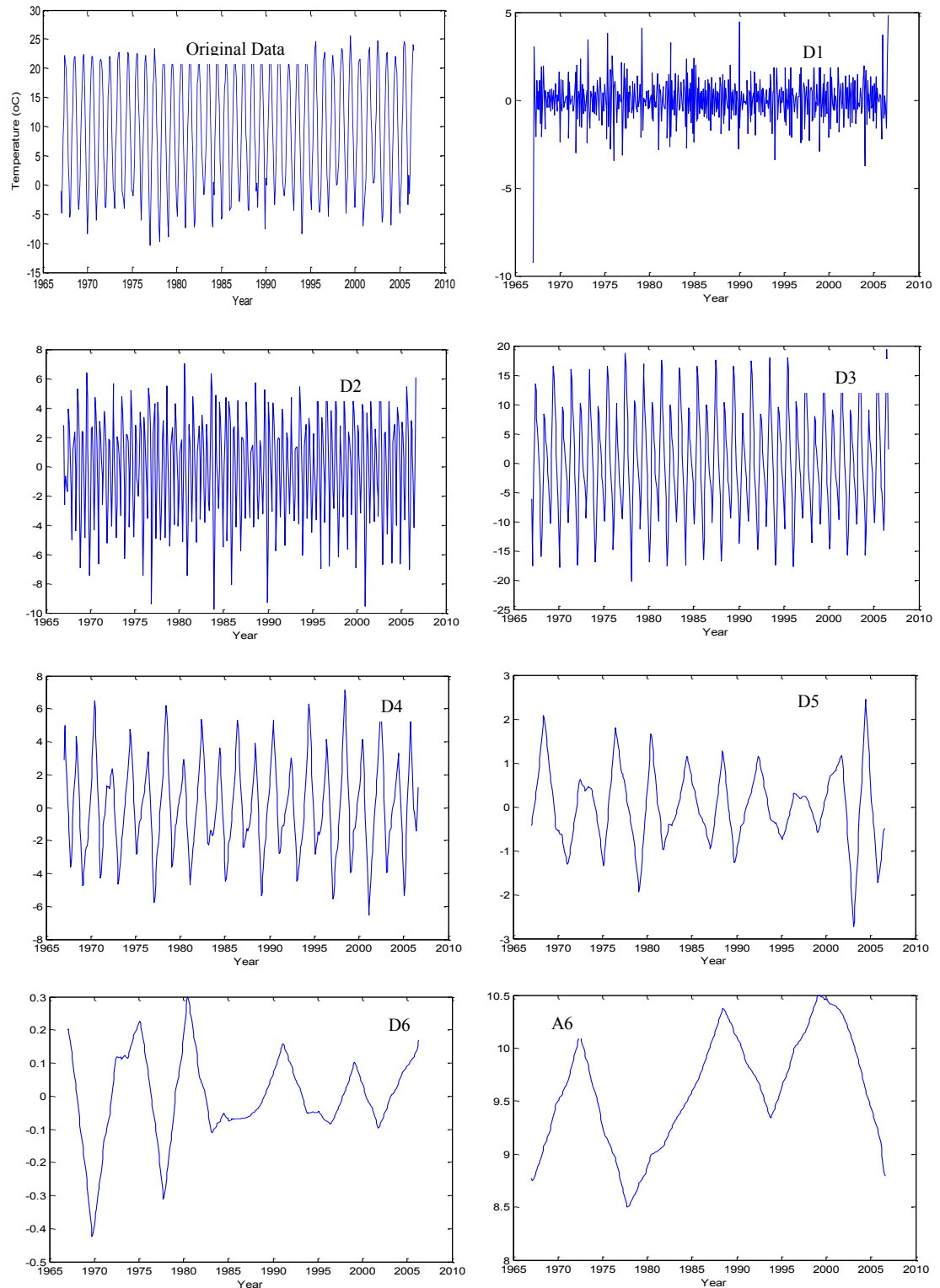


Figure 3.4. Station Harrow's original monthly temperature series and its decomposition via the DWT using db3 wavelet, into six levels (D1-D6 and A6).

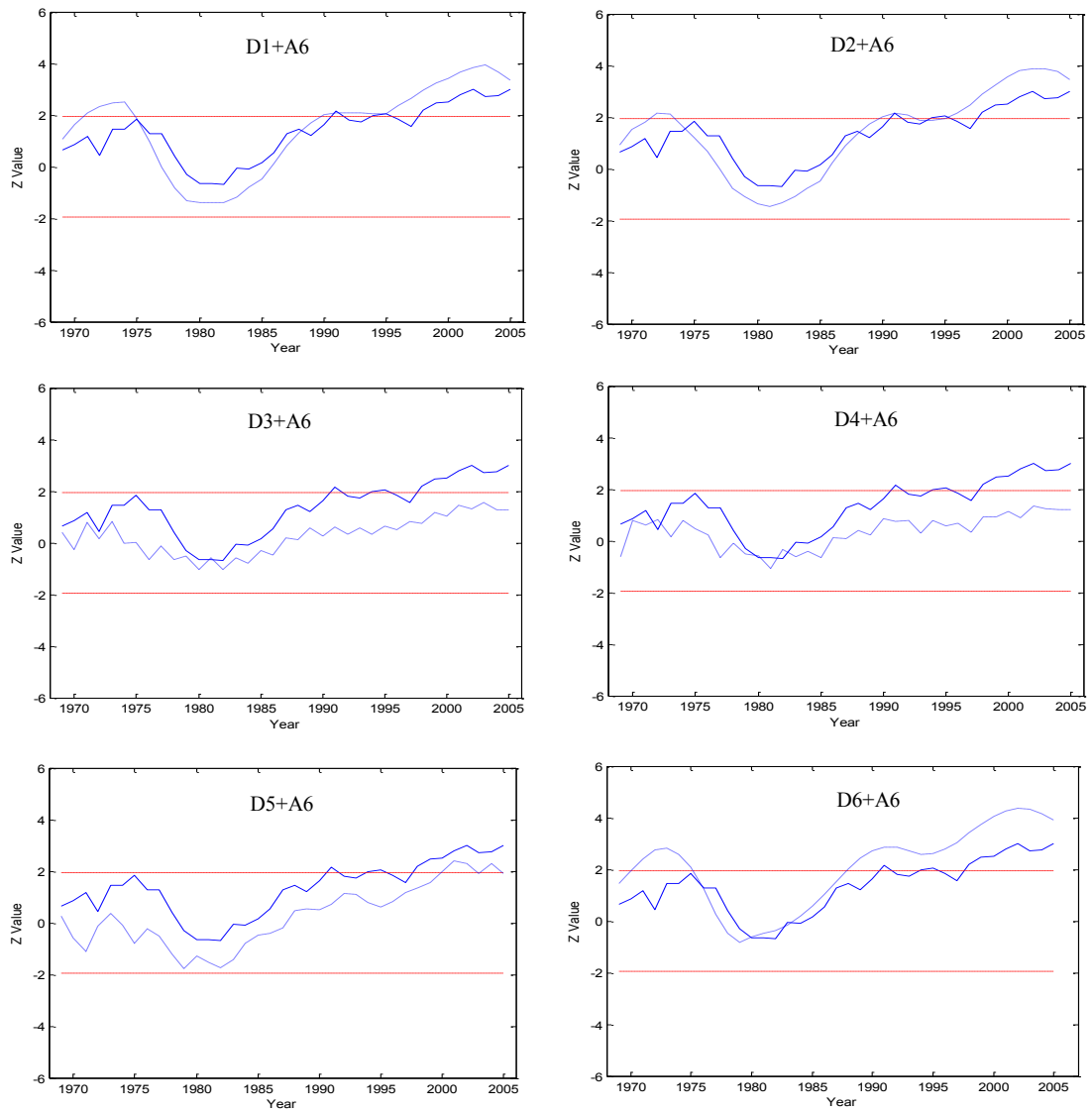


Figure 3.5. Sequential Mann-Kendall graphs of station Harrow's monthly temperature data. The progressive trend lines of the original data are represented by the solid lines and the trend lines of the detail components (with their approximation added) are represented by the dashed line. The upper and lower dashed lines represent the confidence limits ( $\alpha = 5\%$ ).

Table 3.5. Mann-Kendall Z-values of the seasonally-based temperature series: original data, details components, approximations, and a set of combinations of the details and their respective approximations. The most effective periodic components for trends are indicated in bold format.

Harrow		Vineland		Belleville		Peterborough		Val d'or	
Original	3.09*	Original	3.25*	Original	3.26*	Original	2.48*	Original	2.57*
D1	0.50	D1	-0.26	D1	0.31	D1	0.43	D1	0.17
D2	0.19	D2	0.31	D2	0.53	D2	-0.13	D2	0.10
D3	-0.29	D3	0.25	D3	-0.48	D3	0.15	D3	0.50
D4	0.08	D4	0.51	D4	0.46	D4	0.50	D4	0.53
D5	0.40	D5	-0.27	D5	0.63	A4	2.62*	A4	2.58*
D6	1.95	D6	2.01*	D6	1.45	D1 + A4	2.84*	D1+A4	2.97*
A6	2.69*	A6	3.11*	A6	3.24*	D2 + A4	<b>2.36*</b>	D2+A4	2.96*
D1 + A6	4.14*	D1 + A6	4.06*	D1 + A6	<b>3.63*</b>	D3 + A4	<b>2.13*</b>	D3+A4	<b>2.46*</b>
D2 + A6	<b>2.99*</b>	D2 + A6	<b>3.16*</b>	D2 + A6	<b>3.62*</b>	D4 + A4	3.15*	D4+A4	<b>2.55*</b>
D3 + A6	2.90*	D3 + A6	<b>3.36*</b>	D3 + A6	1.69				
D4 + A6	<b>3.14*</b>	D4 + A6	3.70*	D4 + A6	1.57				
D5 + A6	3.88*	D5 + A6	3.02*	D5 + A6	2.40*				
D6 + A6	4.39*	D6 + A6	4.97*	D6 + A6	4.19*				

\* indicates a significant trend value at  $\alpha = 5\%$

### 3.5.4. Annual Temperature Data Analysis

For station Vineland's annual temperature time series the lowest MK Z-value relative error was observed at four decomposition levels; the rest of the annual data had their lowest MK Z-value relative error when five decomposition levels were used. All the MK Z-values showed significant positive trends. For stations Harrow and Vineland, the D3 components (with approximations) were considered to be the most dominant periodicity affecting the temperature trends in the annual data (table 3.6). The MK Z-values of the D3 components for these stations showed the closest MK Z-values to the values of the original data; the sequential Mann-Kendall graphs are also harmonious with those of the original data (an example is given in figure 3.7). This implies that the observed trends in the annual data of stations Harrows and Vineland are affected by 8-year periodicity. For station Belleville, the 32-year periodicity is the most dominant one; and for stations Peterborough and Val d'Or, the 16-year mode is considered the most influential for trends.



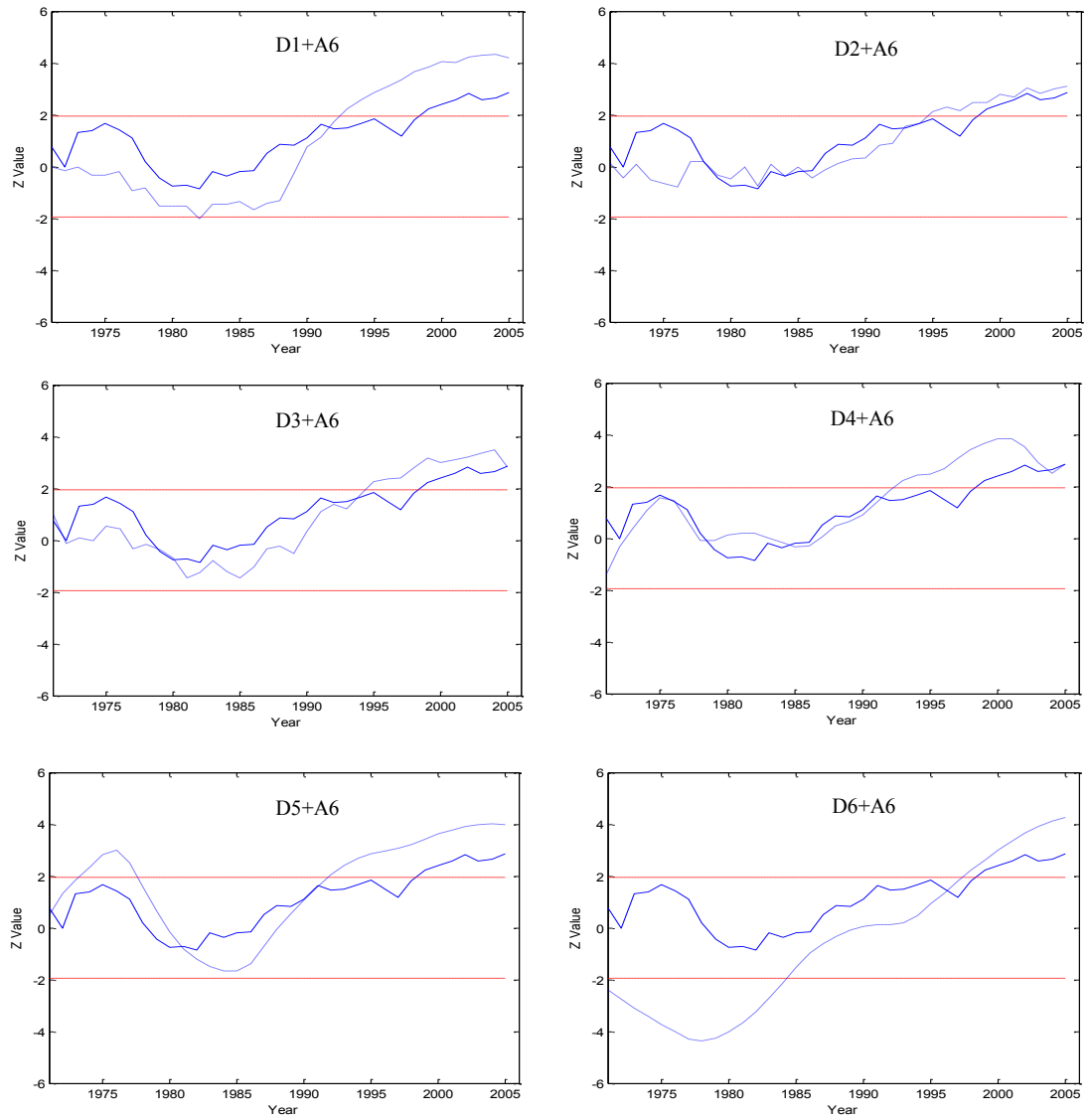


Figure 3.6. Sequential Mann-Kendall graphs of station Harrow's seasonally-based temperature data. The progressive trend lines of the original data are represented by the solid lines and the trend lines of the detail components (with their approximation added) are represented by the dashed lines. The upper and lower dashed lines represent the confidence limits ( $\alpha = 5\%$ ).

Table 3.6. Mann-Kendall Z-values of the annual temperature series: original data, details components, approximations, and a set of combinations of the details and their respective approximations. The most effective periodic components for trends are indicated in bold format.

Harrow		Vineland		Belleville		Peterborough		Val d'Or	
Original	2.88*	Original	3.15*	Original	3.58*	Original	2.49*	Original	2.18*
D1	-0.15	D1	0.55	D1	0.36	D1	0.22	D1	-0.01
D2	0.31	D2	0.59	D2	0.48	D2	0.80	D2	1.04
D3	0.51	D3	1.25	D3	0.69	D3	0.52	D3	-0.13
D4	0.68	D4	2.92*	D4	3.23*	D4	0.85	D4	1.78
D5	3.70*	A4	3.11*	D5	3.32*	D5	2.37*	D5	2.50*
A5	2.85*	D1 + A4	2.37*	A5	3.72*	A5	2.37*	A5	2.37*
D1 + A5	1.62	D2 + A4	2.27*	D1 + A5	1.29	D1 + A5	0.66	D1 + A5	0.17
D2 + A5	1.98*	D3 + A4	<b>2.90*</b>	D2 + A5	2.02*	D2 + A5	2.78*	D2 + A5	1.32
D3 + A5	<b>2.71*</b>	D4 + A4	4.93*	D3 + A5	1.92	D3 + A5	1.41	D3 + A5	0.41
D4 + A5	3.80*			D4 + A5	4.42*	D4 + A5	<b>2.16*</b>	D4 + A5	<b>2.25*</b>
D5 + A5	4.94*			D5 + A5	<b>3.23*</b>	D5 + A5	5.28*	D5 + A5	3.88*

\* indicates a significant trend value at  $\alpha = 5\%$

### 3.5.5. Winter Temperature Data Analysis

Analyzing temperature trends in winter is important because several studies have mentioned that winter experiences very important warming trends in the northern hemisphere and countries such as Canada and the USA (e.g. Jones and Briffa, 1992, Lu et al., 2005, Vincent et al., 2007, Mohsin and Gough, 2010). In this study, it is also confirmed that winter warming is very apparent because except for station Val d'Or, all stations have significant positive trends with MK Z-values that are relatively high. Even for Val d'Or, the winter MK Z-value (+1.80) is also just slightly below +1.96.

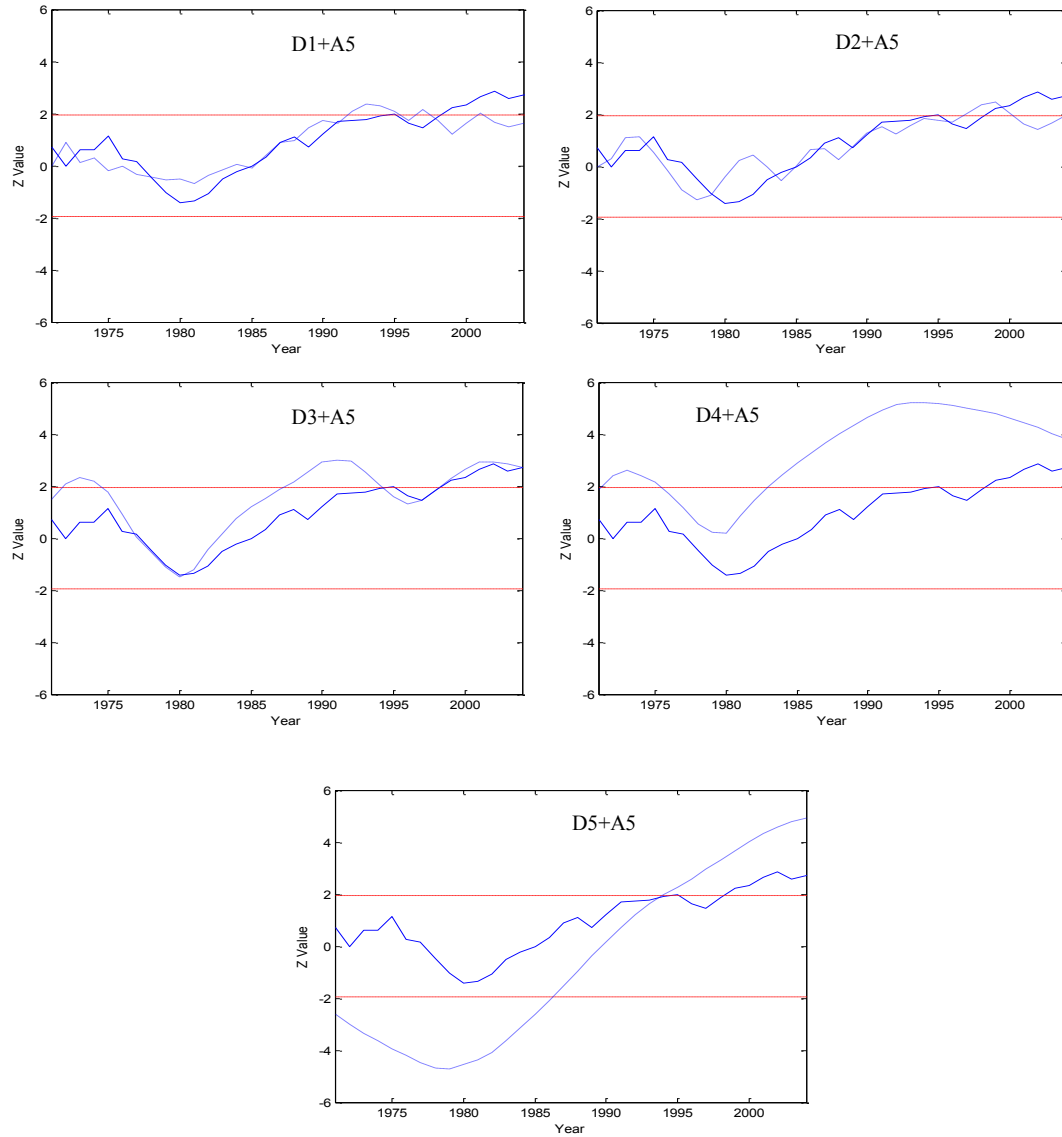


Figure 3.7. Sequential Mann-Kendall graphs of station Harrow's annual temperature data. The progressive trend lines of the original data are represented by the solid lines and the trend lines of the detail components (with their approximation added) are represented by the dashed lines. The upper and lower dashed lines represent the confidence limits ( $\alpha = 5\%$ ).

The winter time series for station Harrow was decomposed into three levels, and the remaining time series were decomposed into five levels (table 3.7). The winter temperature trends for station Harrow are mostly affected by the 2-year and 8-year periodicities (i.e. D1 and D3 components) (figure 3.8). Peterborough station's most dominant periodicity is the D4 component, which represents the 16-yearly cycle. For

station Vineland, although only D5 (with approximation component) was found to be statistically significant ( $Z = +5.28$ ), the MK Z-value is not the closest one to the original data Z value (+1.97). Although D3 and D4 (both with approximation) are not statistically significant, their MK Z-values are closest to that of the original data. Graphically, D3 and D4 have good sequential harmony with the original data compared to D5 (figure 3.9). Therefore, it may be said that for station Vineland, D3 and D4, which represent 8-year and 16-year fluctuations, are the ones affecting the trend. Similarly, for station Belleville, D4 and D5 have MK Z-values that are statistically significant; however, the D3 component has the closest MK Z-value ( $Z = +1.64$ ) to that of the original data ( $Z = +2.60$ ) with better sequential MK compared to D4 and D5. Table 3.7 summarizes the MK Z-values for the winter temperature data decompositions, as well as the periodic modes that are considered most influential in affecting winter temperature trends. Similar to the results of the annual data analysis, the winter warming trends are also mostly affected by periodic events of eight years or greater (in the case of winter temperature trends, the dominant periodicities are mostly between eight and 16 years). These important periodicities may perhaps be related to the variability of natural climatic phenomena such as the large-scale atmospheric circulations; some of the major oscillations affecting eastern Canada are discussed in this section. For example, the dominant periodicities of 8-16 years found in this study may be associated with the North Atlantic Oscillation (NAO), which are known to strongly exhibit inter-annual to decadal variability with some of the major peaks being centered around 2.1, 8 and 24 years (Cook et al., 1998; Anctil and Coulibaly, 2004). The NAO is a very important large-scale climatic phenomenon in the northern hemisphere (Anctil and Coulibaly, 2004), especially in central and eastern Canada (Damyanov et al., 2012). Many studies have found that the NAO is strongly associated with temperature trends over the northern hemisphere (e.g. for Canada: Wettstein and Mearns, 2002; Bonsal et al., 2006; Damyanov et al., 2012). Positive phases of the NAO cycles tend to cause above-normal temperature; it has been mentioned that the NAO has been in its positive phase since 1970 (Anctil and Coulibaly, 2004). As observed in this study, all of the temperature data categories are showing positive trends. Hasanean (2001) also mentioned that the NAO variability is strongest in winter and the winter NAO cycle is very effective in affecting temperature variability in mid-latitude

areas. In addition to this, El Niño and the Pacific North American (PNA) cycles have also been considered important natural cycles in central and eastern Canada. Most likely they are also contributing to the important periodicities of trends observed in this study (or the combination of these natural factors). For example, Bonsal and Shabbar (2011) found that between 1950 and 2008, half of the occurrences of PNA in Canada coincided with the El Niño. It is important to also note that the variability in these large-scale teleconnection patterns is related to factors such as solar activities or radiative forcing (mostly observed at the 11-year solar cycle period). Several studies have found that there are similar cyclical behavior between surface temperatures and the 11-year solar cycle, which may contribute to the observed global warming to some extent (e.g. Lassen, 1991; Erlykin et al., 2009; de Jager et al., 2010; Solheim et al., 2011). Although solar activities and its effects on the atmospheric circulation are not likely to be exclusive factors in affecting the apparent temperature rise over southern Ontario and Quebec (as there are various anthropogenic-related factors), they should also be considered when investigating the current state (and future predictions) of climate change over the study area. As can be seen, the complexity of the climate system (in addition to anthropogenic activities) makes it very challenging to determine the exact cause of the periodicities of the trends observed in this study (or in any climatic trend studies).

### **3.5.6. Spring Temperature Data Analysis**

Most stations did not experience a significant temperature increase for the spring season, except for Vineland. This is somewhat inconsistent with the findings from several studies that analyzed seasonal temperatures in mid-latitude areas (including Canada). Zhang et al (2001) found that spring experienced the greatest warming in southern Canada. Vincent et al., 2007 also emphasized that there is a significant warming for spring season in southern Canada during the period 1953-2005. This disagreement could be caused by the differences in the geographical locations of the stations used and the time period chosen. The stations are only concentrated around the most south-westerly parts of Ontario and Quebec. Even so, these differences suggest that it is also important to conduct a more localized assessment of trends in temperature.

Table 3.7. Mann-Kendall Z-values of the winter temperature series: original data, details components, approximations, and a set of combinations of the details and their respective approximations. The most effective periodic components for trends are indicated in bold format.

Harrow		Vineland		Belleville		Peterborough		Val d'Or	
Original	1.97*	Original	1.97*	Original	2.60*	Original	2.37*	Original	1.80
D1	-0.10	D1	0.06	D1	0.24	D1	0.01	D1	0.22
D2	0.29	D2	-0.13	D2	0.41	D2	0.15	D2	-0.06
D3	-0.20	D3	0.90	D3	0.06	D3	0.38	D3	-0.38
A3	2.09*	D4	0.41	D4	2.69*	D4	0.83	D4	0.85
D1 + A3	<b>1.88*</b>	D5	2.37*	D5	3.95*	D5	2.34*	D5	2.39*
D2 + A3	2.69*	A5	2.37*	A5	2.74*	A5	2.37*	A5	2.37*
D3 + A3	<b>2.23*</b>	D1 + A5	1.08	D1 + A5	1.08	D1 + A5	1.13	D1 + A5	0.52
		D2 + A5	1.11	D2 + A5	1.55	D2 + A5	1.34	D2 + A5	0.80
		D3 + A5	<b>1.41</b>	D3 + A5	<b>1.64</b>	D3 + A5	1.60	D3 + A5	0.71
		D4 + A5	<b>1.76</b>	D4 + A5	5.04*	D4 + A5	<b>2.39*</b>	D4 + A5	<b>2.27*</b>
		D5 + A5	5.28	D5 + A5	4.91*	D5 + A5	5.21*	D5 + A5	5.28*

\* indicates a significant trend value at  $\alpha = 5\%$

Even though significant spring warming is experienced only by one station, all of the spring temperature time series were still decomposed and analyzed. The data from stations Harrow and Belleville were decomposed into five levels; stations Vineland's and Peterborough's data were decomposed into three levels; and station Val d'Or spring time series was decomposed into four levels. As revealed in table 3.8, the D3 (8-year periodicity) component is the one considered most influential for the spring temperature trend in stations Harrow and Peterborough. For stations Vineland, it is the D2 (4-year periodicity) that is responsible for trends; and for stations Belleville and Val d'Or, D1 (2-year periodicity) is the most dominant for trend. An example of spring temperature analysis using the DWT and sequential MK analysis is shown in figure 3.10 (station Harrow is used). It should be noted that for station Harrow, the dominant 8-year periodicity is consistent with the observations in the winter and annual data. Even though spring temperature trends over the study area are mostly not significant, the trend values are all positive. It is also possible that positive and negative trends may cancel each other out over the study period. Therefore, it is important to determine the most dominant periodic modes for trends as it helps to understand the fluctuations that affect the spring temperature.

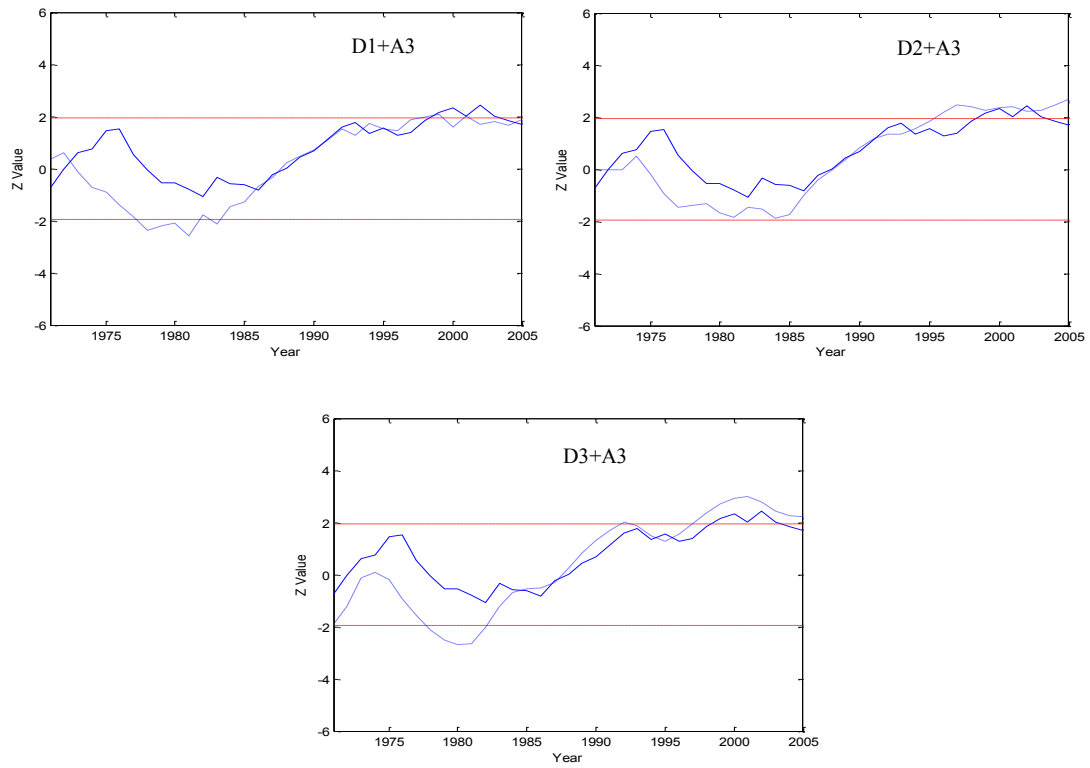


Figure 3.8. Sequential Mann-Kendall graphs of station Harrow's winter temperature data. The progressive trend lines of the original data are represented by the solid lines and the trend lines of the detail components (with their approximation added) are represented by the dashed lines. The upper and lower dashed lines represent the confidence limits ( $\alpha = 5\%$ ).

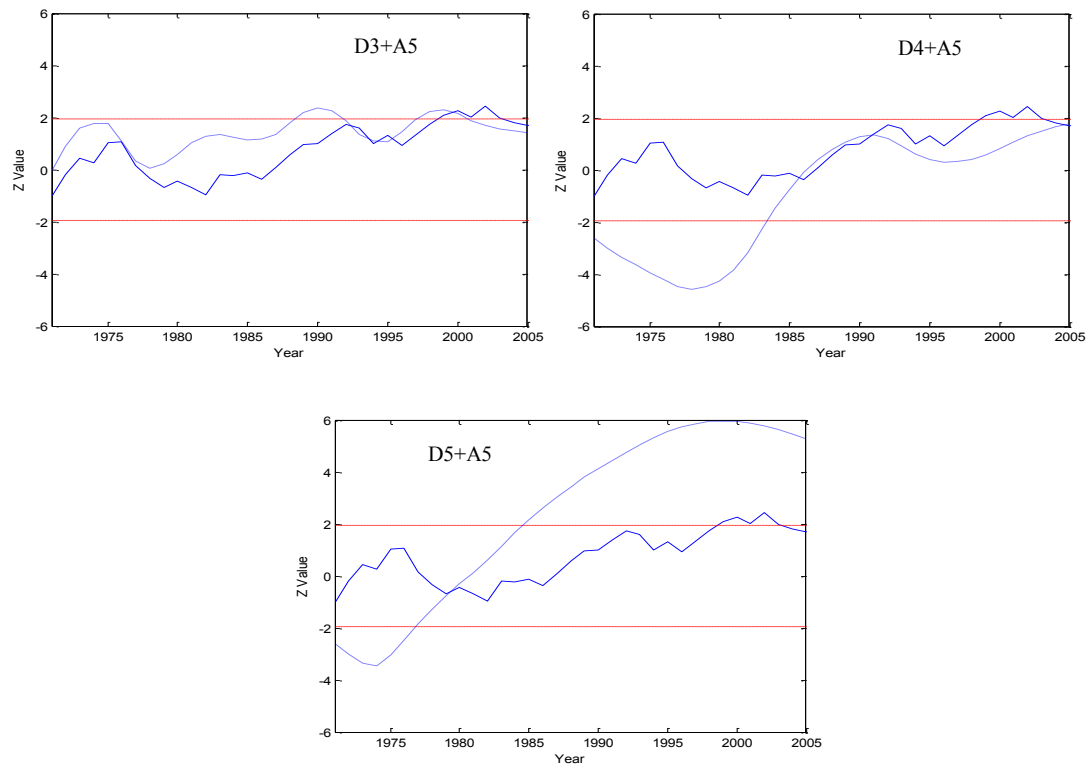


Figure 3.9. A comparison of the sequential Mann-Kendall graphs among D3, D4, and D5 (all with approximation added) of station Vineland's winter temperature data. The progressive trend lines of the original data are represented by the solid lines and the trend lines of the detail components are represented by the dashed lines. The upper and lower dashed lines represent the confidence limits ( $\alpha = 5\%$ ).

### 3.5.7. Summer Temperature Data Analysis

In addition to the winter season, it has also been pointed out by other Canadian studies that the summer season also experiences significant important warming although sometimes to a lesser extent compared to winter warming (e.g. Vincent et al., 2007; Mohsin and Gough, 2010). In this study, all stations are experiencing significant positive summer temperature trends, except for Peterborough. The summer temperature time series were decomposed into four levels (for stations Belleville, Peterborough and Val d'Or) and five levels (for stations Harrow and Vineland). Table 3.9 summarizes the decomposition of the summer temperature time series and the MK Z-values of the different detail components, and the details plus their respective approximations.



Table 3.8. Mann-Kendall Z-values of the spring temperature series: original data, details components, approximations, and a set of combinations of the details and their respective approximations. The most effective periodic components for trends are indicated in bold format.

Harrow		Vineland		Belleville		Peterborough		Val d'Or	
Original	1.67	Original	2.15*	Original	1.59	Original	1.09	Original	1.03
D1	0.69	D1	0.22	D1	0.83	D1	0.10	D1	0.48
D2	-0.08	D2	0.43	D2	-0.10	D2	0.08	D2	1.11
D3	0.78	D3	1.13	D3	-0.15	D3	0.41	D3	-0.85
D4	7.38*	A3	2.19*	D4	3.58*	A3	1.25	D4	1.97
D5	6.47*	D1+A3	2.53*	D5	0.24	D1+A3	0.55	A4	0.92
A5	1.67	D2+A3	<b>1.99*</b>	A5	1.67	D2+A3	0.31	D1+A4	<b>0.52</b>
D1 + A5	0.73	D3+A3	3.25*	D1 + A5	<b>0.92</b>	D3+A3	<b>0.71</b>	D2+A4	1.88
D2 + A5	0.15			D2 + A5	0.36			D3+A4	0.00
D3 + A5	<b>0.87</b>			D3 + A5	0.08			D4+A4	2.69
D4 + A5	7.10*			D4 + A5	3.97*				
D5 + A5	6.05*			D5 + A5	0.80				

\* indicates a significant trend value at  $\alpha = 5\%$

Looking at table 3.9 it is clear that the detail components (with approximation) whose MK Z-values are closest to those of their respective original data, consist of D3 and D4 components, which represent the 8-year and 16-year time periodicities. Figure 3.11 shows an example of the sequential MK analysis on Harrow's summer temperature series, and how the D2 and D3 components (with approximation) show that their trend lines behave similarly with respect to the original trend line. It is interesting to note that the most dominant periodicities in stations Harrows and Peterborough are again consistent with their results from the annual and winter data analysis: D3 for Harrow and D4 for Peterborough. In addition, it is verified that in the summer data analysis, the most influential periodocities that affect the trends are made up of multiyear and decadal events (between eight and 16 years). The agreement found in annual, winter, and summer temperature trends could suggest that the upward trends in the annual temperature over the study area may be contributed mostly by the increase in winter and summer temperatures.

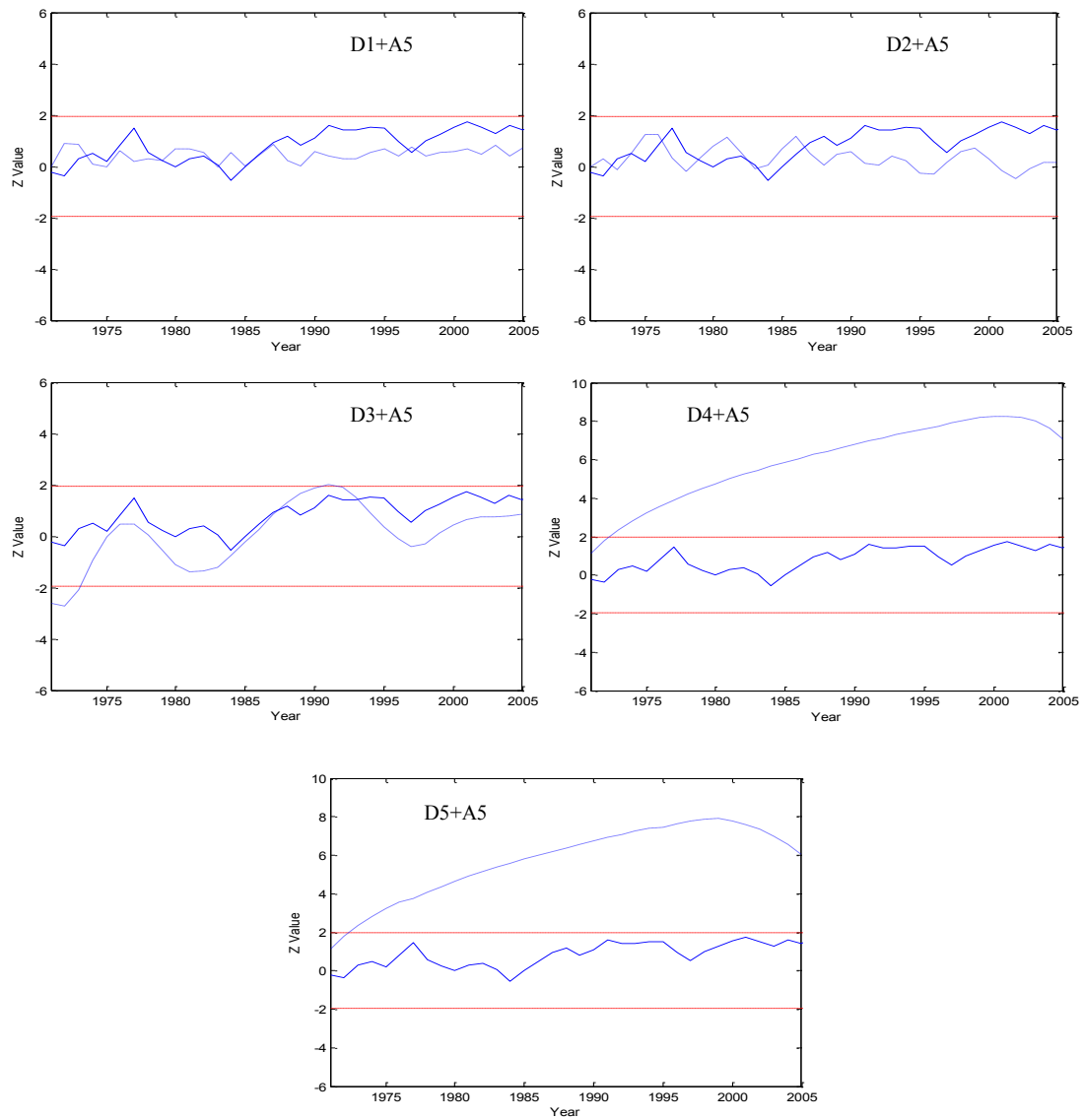


Figure 3.10. Sequential Mann-Kendall graphs of station Harrow's spring temperature data. The progressive trend lines of the original data are represented by the solid line and the trend lines of the detail components (with their approximation added) are represented by the dashed lines. The upper and lower dashed lines represent the confidence limits ( $\alpha = 5\%$ ).

Table 3.9. Mann-Kendall Z-values of the summer temperature series: original data, details components, approximations, and a set of combinations of the details and their respective approximations. The most effective periodic components for trends are indicated in bold format.

Harrow		Vineland		Belleville		Peterborough		Val d'or	
Original	2.87*	Original	2.81*	Original	2.59*	Original	1.87	Original	1.98*
D1	0.66	D1	0.85	D1	-0.29	D1	0.78	D1	-0.50
D2	0.55	D2	0.45	D2	0.59	D2	-0.24	D2	0.38
D3	2.23*	D3	2.53*	D3	1.39	D3	1.69	D3	1.15
D4	2.25*	D4	-0.38	D4	5.35*	D4	-0.78	D4	4.53*
D5	3.62*	D5	3.32*	A4	2.35*	A4	1.90	A4	1.85
A5	2.74*	A5	2.74*	D1 + A4	0.48	D1 + A4	1.39	D1+A4	-0.08
D1 + A5	1.50	D1 + A5	1.53	D2 + A4	1.67	D2 + A4	0.57	D2+A4	0.92
D2 + A5	<b>1.92</b>	D2 + A5	1.62	D3 + A4	<b>2.25*</b>	D3 + A4	2.57*	D3+A4	<b>2.09*</b>
D3 + A5	<b>3.97*</b>	D3 + A5	4.09*	D4 + A4	5.23*	D4 + A4	<b>1.74</b>	D4+A4	2.88*
D4 + A5	4.70*	D4 + A5	<b>3.41*</b>						
D5 + A5	5.00*	D5 + A5	4.58*						

\* indicates a significant trend value at  $\alpha = 5\%$

### 3.5.8. Autumn Temperature Data Analysis

Although it is noted that all the MK Z-values for autumn temperature from different stations are positive, autumn is the only season in which none of the stations explored in this study experience significant trends (table 3.10). This observation is not surprising as it is in agreement with several studies where autumn has the least number of stations with significant warming (see for example: Vincent et al., 2007). The autumn temperature series were decomposed into four levels (for stations Harrow, Belleville, and Peterborough) and three levels (for stations Vineland and Val d'Or). Table 3.10 shows that the most influential periodic components to affect the trends in spring temperature are slightly different from station to station. For station Harrow and Peterborough, it is the D2 (4-year mode); for station Vineland, it is the D3 (8-year mode); and for stations Belleville and Val d'Or, it is the D1 (2-year mode) – again, these important periodic modes coincide with some of the major peaks of the NAO cycle (i.e. 2 and 8 years).

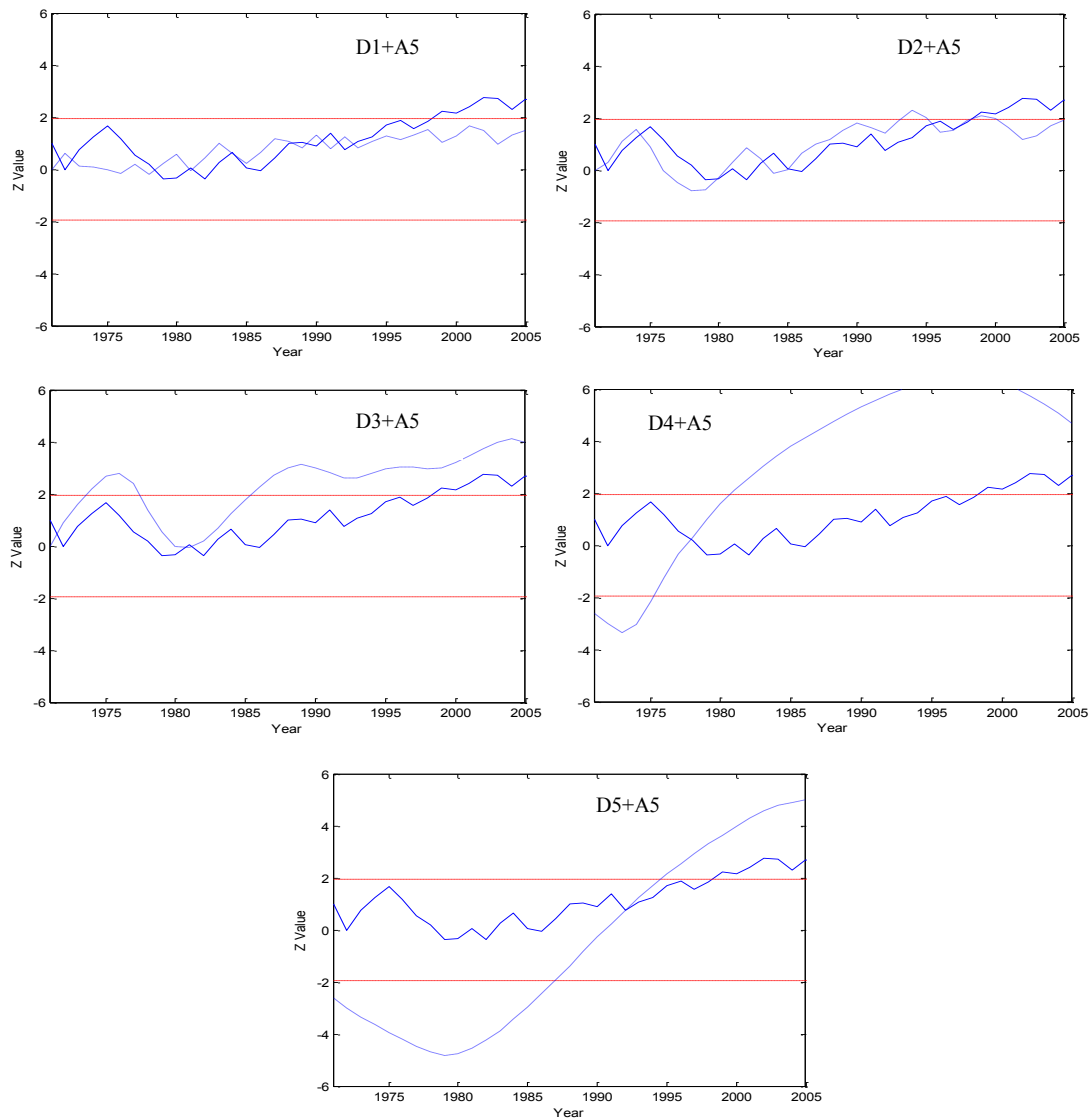


Figure 3.11. Sequential Mann-Kendall graphs of station Harrow's summer temperature data. The progressive trend lines of the original data are represented by the solid lines and the trend lines of the detail components (with their approximation added) are represented by the dashed lines. The upper and lower dashed lines represent the confidence limits ( $\alpha = 5\%$ ).

Table 3.10. Mann-Kendall Z-values of the autumn temperature series: original data, details components, approximations, and a set of combinations of the details and their respective approximations. The most effective periodic components for trends are indicated in bold format.

Harrow		Vineland		Belleville		Peterborough		Val d'Or	
Original	1.21	Original	1.73	Original	1.69	Original	0.91	Original	1.38
D1	0.15	D1	0.43	D1	0.03	D1	-0.03	D1	-0.03
D2	-0.05	D2	0.76	D2	0.01	D2	0.27	D2	-0.08
D3	-0.07	D3	-1.50	D3	0.48	D3	-0.15	D3	0.18
D4	0.8	A3	1.88	D4	0.66	D4	-0.27	A3	1.51
A4	1.16	D1+A3	2.16*	A4	1.88	A4	0.85	D1+A3	<b>1.53</b>
D1 + A4	1.81	D2+A3	2.06*	D1 + A4	<b>1.48</b>	D1 + A4	1.11	D2+A3	1.72
D2 + A4	<b>1.31</b>	D3+A3	<b>1.76</b>	D2 + A4	1.90	D2 + A4	<b>1.01</b>	D3+A3	1.68
D3 + A4	2.69*			D3 + A4	1.90	D3 + A4	0.76		
D4 + A4	1.86			D4 + A4	2.46*	D4 + A4	-0.48		

\* indicates a significant trend value at  $\alpha = 5\%$

Although the NAO may not be the only factor that influences the temperature variability over the study area, it can potentially be considered an important factor. An example of autumn temperature decomposition and sequential MK analysis is given in figure 3.12. As can be seen, generally the trends in autumn temperatures are characterized by events between two- and eight-year fluctuations. This is inconsistent with the annual, winter, and summer trends where most of the trends are dominated by fluctuations that are greater than eight years. This could suggest that autumn has minimal contribution towards the warming trends observed in the annual temperature series over the study area.

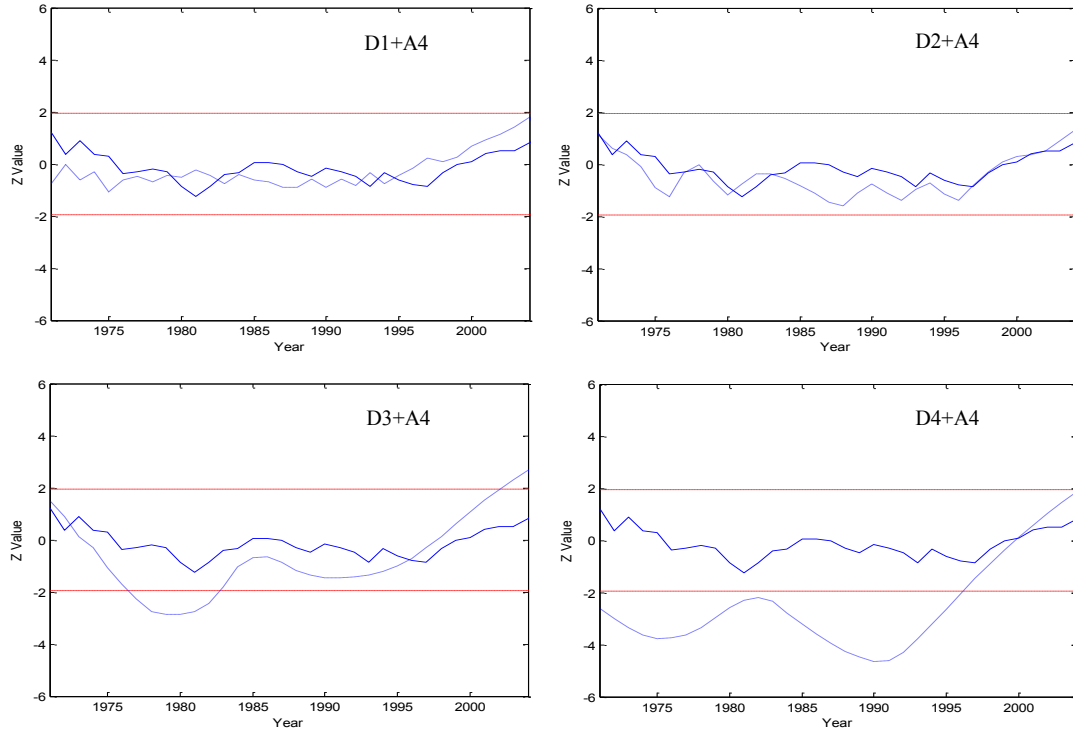


Figure 3.12. Sequential Mann-Kendall graphs of station Harrow's autumn temperature data. The progressive trend lines of the original data are represented by the solid lines and the trend lines of the detail components (with their approximation added) are represented by the dashed lines. The upper and lower dashed lines represent the confidence limits ( $\alpha = 5\%$ ).

### 3.6. Conclusions and Recommendations

Surface air temperature trends from a total of five stations located in Ontario and Quebec were analyzed using the wavelet transform and the Mann-Kendall trend test. The spatial coverage may not be very representative of the entire two provinces due to the low number of stations used in this study. The reason for this is because of the length of data chosen for this study, which requires 40 years worth of data with no missing values. Even so, there are some findings observed in this study which are in agreement with previously conducted trend studies in Canadian temperature.

The use of the DWT prior to applying the Mann-Kendall test on the time series that results from the decomposition is found to be very useful in this study. By

decomposing the original time series into its detail and approximation components and testing them with the Mann-Kendall test, we were able to obtain information about the most dominant periodic modes that affect trends in the different datasets from the stations explored in this study.

The southern parts of Ontario and Quebec are experiencing warming temperature trends. This is observed in all of the data types used in this study. For the monthly data analysis, it was found that high-frequency periodicities ranging from two to four months are responsible for the trends. Annual cycles are also found to be very influential in affecting the trends in seasonally-based data. The use of monthly and seasonally-based data is seen to be useful in determining the influence of higher-frequency events (short-term fluctuations) on the observed trends. Since the data are based on daily measurements, there could be many daily (high-frequency) variations that may be contributing to the trends in the higher resolution data used in this study (i.e. the monthly data). Examples of these daily variations are: variation in solar radiation (which can be associated with seasonality), cloud cover, albedo, air moisture content, soil heat capacity, and atmospheric wind movements that can have significant effects on the diurnal temperature (Gough, 2008). Gough (2008) also emphasized that in mid-latitude regions, mid-latitude cyclones may produce temperature clusters whose effects may last for a month. These daily variations may be very strong, and thus, conceal the effects of low-frequency periodicities (i.e. higher detail component levels of the DWT).

The analysis of the lower-resolution data (i.e. annual, winter, spring, summer, and autumn) revealed that low-frequency periodicities were found to be important in affecting the trends in temperature over the study area. For the annual time series, the most important periodic modes that affect the trends are made up of multiyear and decadal events, mostly between eight and 16 years. From the seasonal point of analysis, winter and summer are experiencing the most uniform trends in temperature, where all the sites are experiencing significant positive trends (except for Val d'Or winter). The results of the winter and summer analysis are also the most consistent with those of the annual data, in which most of the influential periodic components affecting the trends are between eight and 16 years. More specifically, station Harrow's most dominant periodic modes for the annual and seasonal data are all made up of multiyear events fluctuating around

eight years. These findings may be associated not only with anthropogenic activities such as the effect of the urban heat island, but also with the variability of climate indices such as the NAO (which has some major peaks at eight and 24 years).

Based on the findings of this study, it can be suggested that the long-term trends in temperature over the study area may be associated with the winter and summer warming. Apart from the possible relation of the temperature trends with the large teleconnection pattern (in this study, we suggest the effect of the NAO cycle – see the discussions in the results section), there are other possible causes of winter and summer warming, which have been investigated in several past Canadian studies. Vincent et al. (2007) concluded that winter warming in Canada is due to an increase in dewpoint and specific humidity. Additionally, Prokoph and Patterson (2004) associated winter warming in urban settings in eastern Ontario with the heat island effect. Summer warming is associated with the increase in air moisture, especially around the Great Lakes and St. Lawrence areas (Vincent et al., 2007).

We recommend that future studies should consider more climatic indices in order to investigate the possible causes of summer and winter warming in southern Ontario and Quebec. More specifically, correlation analysis can be explored between the different important periodic components, which are responsible for trends and the different teleconnection patterns, such as the NAO and possibly other major large scale climatic indices in Canada (e.g. the El Niño Southern Oscillation (ENSO) and Pacific-North American (PNA)). This way, more quantitative assessments on the possible drivers behind the observed variability in temperature trends can be obtained. Other local factors such as the effect of urban heat island, specific humidity, and dew point may also be included in a more quantitative analysis in order to determine how they have contributed to the temperature warming over the study area. In this way, we can potentially obtain information on how the temperature trends over the study area are attributed to anthropogenic impacts (e.g. urbanization, urban heat island effect, etc.) and to natural variability such as the large-scale climatic teleconnection patterns (e.g. NAO, ENSO, PNA, etc.). Future studies can look into developing methods that aim to differentiate the impacts between natural climatic variability and human-caused climate change. In this present study, we have established the baseline information about the important



periodicities that affect the temperature trends over southern Ontario and Quebec. This then can be incorporated into the methods/model aiming to investigate how natural fluctuations and anthropogenic activities can affect the temperature trends over southern Ontario and Quebec – i.e. climate change associated with cycles of natural processes (e.g. effect of radiative forcing) or with human activities (e.g. measured in levels of greenhouse gas).

The impacts that warming temperatures may have on precipitation, and therefore streamflow, over the study area should also be investigated (e.g. winter warming may be associated with higher winter precipitation, snowfall-total precipitation relationship, etc.). Since changes in temperature will affect the processes involved in the hydrological cycles, analyzing the linkages between temperatures (or the potential large-scale teleconnection patterns that potentially drive the changes in temperature) and the hydrological processes is crucial for understanding the long-term fluctuations involved in the hydrological processes and to better manage water resources. The results obtained in this study in terms of discovering the main periodicities that affect the temperature trends (long-term component of the temperature data sets used) over southern Ontario and Quebec, can be incorporated when correlation analyses are made among temperatures and the different climatic phenomena and hydrological processes.

Finally, it will also be very useful to include more stations (perhaps with longer data records) in future studies to get more representative results for the whole province. However, suitable interpolation methods to fill the missing records found in many stations have to be carefully researched in order to minimize the errors associated with interpolations. In this study, only five stations were included because they are the only ones that have complete records (with no missing values) for forty years.

### **3.7. References**

Adamowski, K., Bougadis, J., 2003. Detection of trends in annual extreme rainfall. *Hydrological Processes*, 17(18): 3547-3560.

- Adamowski, K., Prokoph, A., Adamowski, J., 2009. Development of a new method of wavelet aided trend detection and estimation. *Hydrological Processes*, 23(18): 2686-2696.
- Anctil, F., Coulibaly, P., 2004. Wavelet analysis of the interannual variability in southern Québec streamflow. *Journal of Climate*, 17(1): 163-173.
- Baliunas, S., Frick, P., Sokoloff, D., Soon, W., 1997. Time scales and trends in the central England temperature data (1659-1990): A wavelet analysis. *Geophys. Res. Lett.*, 24(11): 1351-1354.
- Bonsal, B.R., Prowse, T.D., Duguay, C.R., Lacroix, M.P., 2006. Impacts of large-scale teleconnections on freshwater-ice break/freeze-up dates over Canada. *Journal of Hydrology*, 330 (1–2): 340-353.
- Bonsal, B. and Shabbar, A. 2011. Large-scale climate oscillations influencing Canada, 1900-2008. *Canadian Biodiversity: Ecosystem Status and Trends 2010*, Technical Thematic Report No. 4. Canadian Councils of Resource Ministers. Ottawa, ON. iii + 15 p. <http://www.biodivcanada.ca/default.asp?lang=En&n=137E1147-0>
- Chaouche, K., Neppel, L., Dieulin, C., Pujol, N., Ladouche, B., Martin, E., Salas, D., Caballero, Y., 2010. Analyses of precipitation, temperature and evapotranspiration in a French Mediterranean region in the context of climate change. *Comptes Rendus Geoscience*, 342(3): 234-243.
- Chou, C.-M., 2007. Applying multi-resolution analysis to differential hydrological grey models with dual series. *Journal of Hydrology*, 332(1–2): 174-186.
- Cook, E.R., D'Arrigo, R.D., Briffa, K.R., 1998. A reconstruction of the North Atlantic Oscillation using tree-ring chronologies from North America and Europe. *The Holocene*, 8(1): 9-17.
- Craigmile, P.F., Guttorp, P., Percival, D.B., 2004. Trend assessment in a long memory dependence model using the discrete wavelet transform. *Environmetrics*, 15(4): 313-335.
- Damyanov, N.N., Matthews, H.D., Mysak, L.A., 2012. Observed decreases in the Canadian outdoor skating season due to recent winter warming *Environmental Research Letters*, 7(1): 014028.

- de Artigas, M.Z., Elias, A.G., de Campra, P.F., 2006. Discrete wavelet analysis to assess long-term trends in geomagnetic activity. *Physics and Chemistry of the Earth*, 31(1–3): 77-80.
- de Jager, C., Duhau, S., van Geel, B., 2010. Quantifying and specifying the solar influence on terrestrial surface temperature. *Journal of Atmospheric and Solar-Terrestrial Physics* 72: 926-937.
- Dietz, E.J., Killeen, T.J., 1981. A nonparametric multivariate test for monotone trend with pharmaceutical applications. *Journal of the American Statistical Association*, 76(373): 169-174.
- Domroes, M., El-Tantawi, A., 2005. Recent temporal and spatial temperature changes in Egypt. *International Journal of Climatology*, 25(1): 51-63.
- Dong, X., Nyren, P., Patton, B., Nyren, A., Richardson, J., Maresca, T., 2008. Wavelets for agriculture and biology: A tutorial with applications and outlook. *BioScience*, 58(5): 445-453.
- Drago, A.F., Boxall, S.R., 2002. Use of the wavelet transform on hydro-meteorological data. *Physics and Chemistry of the Earth*, 27(32–34): 1387-1399.
- Erlykin, A.D., Sloan, T., Wolfendale, A.W., 2009. Solar activity and the mean global temperature. *Environmental Research Letters*, 4(2009) 014006.
- Esteban-Parra, M.J., Rodrigo, F.S., Castro-Díez, Y., 1995. Temperature trends and change points in the northern Spanish Plateau during the last 100 years. *International Journal of Climatology*, 15(9): 1031-1042.
- Fan, X.-H., Wang, M.-B., 2011. Change trends of air temperature and precipitation over Shanxi Province, China. *Theoretical and Applied Climatology*, 103(3-4): 519-531.
- Farge, M., 1992. Wavelet transforms and their applications to turbulence. *Annual Reviews Fluid Mechanics*, 24: 395-457.
- Gough, W.A., 2008. Theoretical considerations of day-to-day temperature variability applied to Toronto and Calgary, Canada data. *Theoretical and Applied Climatology*, 94(1-2): 97-105.
- Hamed, K.H., Rao, A.R., 1998. A modified Mann-Kendall trend test for autocorrelated data. *Journal of Hydrology*, 204(1–4): 182-196.

- Hasanean, H.M., 2001. Fluctuations of surface air temperature in the Eastern Mediterranean. *Theoretical and Applied Climatology*, 68(1-2): 75-87.
- Hirsch, R.M., Slack, J.R., 1984. A nonparametric trend test for seasonal data with serial dependence. *Water Resources Research*, 20(6): 727-732.
- IPCC. 2007. Climate change 2007: the fourth IPCC scientific assessment. In: M.L. Parry, O.F. Canziani, J.P. Palutikof, P.J. van der Linden and C.E. Hanson (eds). Intergovernmental Panel on Climate Change. Cambridge University Press, Cambridge, United Kingdom and New York, NY, USA.
- Jones, P.D., Briffa, K.R., 1992. Global surface air temperature variations during the twentieth century: Part 1, spatial, temporal and seasonal details. *The Holocene*, 2(2): 165-179.
- Jones, P.D., Moberg, A., 2003. Hemispheric and large-scale surface air temperature variations: An extensive revision and an update to 2001. *Journal of Climate*, 16: 206-223.
- Jung, H.-S., Choi, Y., Oh, J.-H., Lim, G.-H., 2002. Recent trends in temperature and precipitation over South Korea. *International Journal of Climatology*, 22(11): 1327-1337.
- Kadioğlu, M., 1997. Trends in surface air temperature data over Turkey. *International Journal of Climatology*, 17(5): 511-520.
- Kallache, M., Rust, H.W., Kropp, J., 2005. Trend assessment: applications for hydrology and climate research. *Nonlinear Processes in Geophysics*, 12(2): 201-210.
- Karaburun, A., Demirci, A., Kara, F., 2011. Analysis of spatially distributed annual, seasonal and monthly temperatures in Istanbul from 1975 to 2006. *World Applied Sciences Journal* 12(10): 1662-1675.
- Kendall, M.G., 1975. *Rank Correlation Methods*. Charles Griffin, London.
- Kravchenko, V.O., Evtushevsky, O.M., Grytsai, A.V., Milinevsky, G.P., 2011. Decadal variability of winter temperatures in the Antarctic Peninsula region. *Antarctic Science*, 23(6): 614-622.
- Kundzewicz, Z.W., Robson, A.J., 2004. Change detection in hydrological records—A review of the methodology. *Hydrological Sciences Journal*, 49(1): 7-19.

- Labat, D., Godd  ris, Y., Probst, J.L., Guyot, J.L., 2004. Evidence for global runoff increase related to climate warming. *Advances in Water Resources*, 27(6): 631-642.
- Lassen, K., 1991. Long-term variations in solar activity and their apparent effect on the earth's climate. <http://www.tmgnow.com/repository/solar/lassen1.html>.
- Lau, K.M., Weng, H., 1995. Climate signal detection using wavelet transform: How to make a time series sing. *Bulletin of the American Meteorological Society*, 76(12): 2391-2402.
- Lim, Y.-H., Lye, L.M., 2004. Wavelet analysis of tide-affected low streamflows series. *Journal of Data Science*, 2: 149-163.
- Lindsay, R.W., Percival, D.B., Rothrock, D.A., 1996. The discrete wavelet transform and the scale analysis of the surface properties of sea ice. *Geoscience and Remote Sensing, IEEE Transactions on*, 34(3): 771-787.
- Lu, Q., Lund, R., Seymour, L., 2005. An update of U.S. temperature trends. *Journal of Climate*, 18: 4906-4914.
- Ludwig, W., Serrat, P., Cesmat, L., Garcia-Esteves, J., 2004. Evaluating the impact of the recent temperature increase on the hydrology of the T  t River (Southern France). *Journal of Hydrology*, 289(1-4): 204-221.
- Lund, R., Seymour, L., Kafadar, K., 2001. Temperature trends in the United States. *Environmetrics*, 12(7): 673-690.
- Ma, J., Xue, J., Yang, S., He, Z., 2003. A study of the construction and application of a Daubechies wavelet-based beam element. *Finite Elements in Analysis and Design*, 39: 965-975.
- Makokha, G.L., Shisanya, C.A., 2010. Trends in mean annual minimum and maximum near surface temperature in Nairobi City, Kenya. *Advances in Meteorology*, 2010.
- Mann, H.B., 1945. Nonparametric tests against trend. *Econometrica*, 13(3): 245-259.
- Mekis,   ., Vincent, L.A., 2011. An overview of the second generation adjusted daily precipitation dataset for trend analysis in Canada. *Atmosphere-Ocean*, 49(2): 163-177.

- Mimikou, M.A., Baltas, E., Varanou, E., Pantazis, K., 2000. Regional impacts of climate change on water resources quantity and quality indicators. *Journal of Hydrology*, 234(1–2): 95-109.
- Mishra, A.K., Singh, V.P., 2010. Changes in extreme precipitation in Texas. *Journal of Geophysical Research*, 115(D14): D14106.
- Moberg, A., Sonechkin, D.M., Holmgren, K., Datsenko, N.M., Karlen, W., 2005. Highly variable Northern Hemisphere temperatures reconstructed from low- and high-resolution proxy data. *Nature*, 433(7026): 613-617.
- Mohsin, T., Gough, W., 2010. Trend analysis of long-term temperature time series in the Greater Toronto Area (GTA). *Theoretical and Applied Climatology*, 101(3): 311-327.
- Nicholls, N., Gruza, G. V., Jouzel, J., Karl, T. R., Ogallo, L. A., Parker, D. E., 1996. Observed climate variability and change. In *Climate Change 1995: The Science of Climate Change*, 132-192, (Eds J. T. Houghton, L. G. M. Filho, B. A. Callander, N. Harris, A. Kattenberg, and K. Maskell), Cambridge University Press, Cambridge, UK.
- Nicholls, R.J., Tol, R.S.J., 2006. Impacts and responses to sea-level rise: A global analysis of the SRES scenarios over the twenty-first century. *Philosophical Transaction of the Royal Society A*, 364(1841): 1073-1095.
- Partal, T., 2010. Wavelet transform-based analysis of periodicities and trends of Sakarya basin (Turkey) streamflow data. *River Research and Applications*, 26(6): 695-711.
- Partal, T., Kahya, E., 2006. Trend analysis in Turkish precipitation data. *Hydrological Processes*, 20: 2011-2026.
- Partal, T., Küçük, M., 2006. Long-term trend analysis using discrete wavelet components of annual precipitations measurements in Marmara region (Turkey). *Physics and Chemistry of the Earth*, 31(18): 1189-1200.
- Percival, D.B., 2008. Analysis of Geophysical Time Series Using Discrete Wavelet Transforms: An Overview, in *Nonlinear Time Series Analysis in the Geosciences - Applications in Climatology, Geodynamics, and Solar-Terrestrial Physics*, edited by R. V. Donner and S. M. Barbosa. Berlin/Heidelberg: Springer.

- Pišoft, P., Kalvová, J., Brázdil, R., 2004. Cycles and trends in the Czech temperature series using wavelet transforms. *International Journal of Climatology*, 24(13): 1661-1670.
- Polyakov, I.V. et al., 2003. Variability and trends of air temperature and pressure in the Maritime Arctic, 1875–2000. *Journal of Climate*, 16(12): 2067-2077.
- Popivanov, I., Miller, R.J., 2002. Similarity search over time-series data using wavelets, *Data Engineering, 2002. Proceedings. 18th International Conference on*, pp. 212-221.
- Prokoph, A., Patterson, R.T., 2004. Application of wavelet and regression analysis in assessing temporal and geographic climate variability: Eastern Ontario, Canada as a case study. *Atmosphere Ocean*, 43(2): 201-212.
- Rebetez, M., Reinhard, M., 2007. Monthly air temperature trends in Switzerland 1901-2000 and 1975-2004. *Theoretical and Applied Climatology*, 91(1-4): 27-34.
- Shrestha, A.B., Wake, C.P., Mayewski, P.A., Dibb, J.E., 1999. Maximum temperature trends in the Himalaya and its vicinity: An analysis based on temperature records from Nepal for the period 1971–94. *Journal of Climate*, 12(9): 2775-2786.
- Solheim, J-K., Stordahl, K., Humlum, O., 2011. Solar activity and Svalbard temperatures. *Advances in Meteorology*, 2011, Article ID 543146.
- Su, H., Liu, Q., Li, J., 2011. Alleviating border effects in wavelet transforms for nonlinear time-varying signal analysis. *Advances in Electrical and Computer Engineering*, 11(3): 6.
- Torrence, C., Compo, G.P., 1998. A practical guide to wavelet analysis. *Bulletin of the American Meteorological Society*, 79(1): 61-78.
- Vincent, L.A., Gullett, D.W., 1999. Canadian historical and homogeneous temperature datasets for climate change analyses. *International Journal of Climatology*, 19(12): 1375-1388.
- Vincent, L.A., Milewska, E.J., Hopkinson, R., Malone, L., 2009. Bias in minimum temperature introduced by a redefinition of the climatological day at the Canadian synoptic stations. *Journal of Applied Meteorology and Climatology*, 48(10): 2160-2168.

- Vincent, L.A., van Wijngaarden, W.A., Hopkinson, R., 2007. Surface temperature and humidity trends in Canada for 1953–2005. *Journal of Climate*, 20(20): 5100-5113.
- Vonesch, C., Blu, T., Unser, M., 2007. Generalized Daubechies wavelet families. *Signal Processing, IEEE Transactions on Signal Processing*, 55(9): 4415-4429.
- Wang, J.Z., Wiederhold, G., Firschein, O., Xin Wei, S., 1998. Content-based image indexing and searching using Daubechies' wavelets. *International Journal on Digital Libraries*, 1(4): 311-328.
- Wang, N., Lu, C., 2009. Two-dimensional continuous wavelet analysis and its application to meteorological data. *Journal of Atmospheric and Oceanic Technology*, 27(4): 652-666.
- Wettstein, J.J., Mearns, L.O., 2002. The influence of the North Atlantic–Arctic Oscillation on mean, variance, and extremes of temperature in the northeastern United States and Canada. *Journal of Climate*, 15(24): 3586-3600.
- Yue, S., Pilon, P., Phinney, B., Cavadias, G., 2002. The influence of autocorrelation on the ability to detect trend in hydrological series. *Hydrological Processes*, 16(9): 1807-1829.
- Zhang, X., Vincent, L.A., Hogg, W.D., Niitsoo, A., 2000. Temperature and precipitation trends in Canada during the 20th century. *Atmosphere-Ocean*, 38(3): 395-429.



## CONNECTING STATEMENT TO CHAPTER 4

As introduced in chapter 1 and reviewed in chapter 2, trend detection in hydrological time series associated with climate change is of significant importance. This is also true for Canada – trend detection is important not only at the national and regional level, but should also be looked at a more localized spatial coverage. This chapter focuses on the application of the discrete wavelet transform (DWT) and the Mann-Kendall trend test on streamflow and precipitation time series obtained from a total of 13 stations in the southern part of Ontario and Quebec. Using the DWT in conjunction with the MK test is a very new approach in studying hydroclimatic trends, especially in the context of Canadian studies. In this chapter, a new criterion proposed in chapter 3, which is based on the relative error of the MK Z-values to determine the number decomposition levels, mother Daubechies (db) wavelet, and the periodic extension to be used in the DWT, is used.

The results of this chapter have been accepted for publication in the *Journal of Hydrology* (DOI:10.1016/j.jhydrol.2012.09.049) and have been presented at the *2012 NABEC-CSBE/SCGAB Joint Meeting and Technical Conference, July 15-18, 2012, Orillia, Ontario, Canada*. The manuscript is co-authored by Deasy Nalley, Jan Adamowski, and Bahaa Khalil.

## **CHAPTER 4 – USING DISCRETE WAVELET TRANSFORMS TO ANALYZE TRENDS IN PRECIPITATION AND STREAMFLOW IN QUEBEC AND ONTARIO (1954 – 2008)**

Deasy Nalley, Jan Adamowski, and Bahaa Khalil

### **Abstract:**

This paper aims to detect trends in mean flow and total precipitation data over southern parts of Quebec and Ontario, Canada. The main purpose of the trend assessment is to find out what time scales are affecting the trends observed in the datasets used. In this study, a new trend detection method for hydrological studies is explored, which involves the use of wavelet transforms (WT) in order to separate the rapidly and slowly changing events contained in a time series. More specifically, this study co-utilizes the discrete wavelet transform (DWT) technique and the Mann-Kendall (MK) trend tests to analyze and detect trends in monthly, seasonally-based, and annual data from eight flow stations and seven meteorological stations in southern Ontario and Quebec during 1954-2008. The combination of the DWT and MK test in analyzing trends has not been extensively explored to date, especially in detecting trends in Canadian flow and precipitation time series. The mother wavelet type and the extension border used in the wavelet transform, as well as the number of decomposition levels, were determined based on two criteria. The first criterion is the mean relative error of the wavelet approximation series and the original time series. In addition, a new criterion is proposed and explored in this study, which is based on the relative error of the MK Z-values of the approximation component and the original time series. Sequential Mann-Kendall analysis on the different wavelet detail components (with their approximation component added) that result from the time series decomposition was also used and found to be helpful because it depicts how harmonious each of the detail components (plus approximation) is with respect to the original data. This study found that most of the trends are positive and started during the mid-1960s to early 1970s. The results from the wavelet analysis and Mann-Kendall tests on the different data types (using the 5% significance level) reveal that in general, intra- and inter-annual events (up to 4 years) are more influential in affecting the observed trends.

**Keywords:** trend detection, streamflow, precipitation, discrete wavelet transform, Mann-Kendall trend test

#### **4.1. Introduction**

The intensification of the hydrologic cycle is one of the most evident effects caused by climate warming (Ampitiyawatta and Guo, 2009; Zhang et al., 2009; Durdu, 2010). Changes in hydrological processes may in turn affect the overall availability and quality of water resources, and alter the spatiotemporal characteristics of hydrologic occurrences, such as the timing of flow events, and the frequency and severity of floods and droughts (Mishra and Singh, 2010; Burn et al., 2010). High-latitude areas have been projected to experience more severe impacts associated with climate change (Zhang et al., 2001). Labat et al. (2004) who studied the global and continental runoff associated with temperature increases found that North America is very vulnerable to recent climate change. One of the most significant consequences of temperature increases and changes in precipitation patterns is the dramatic modification of the hydrologic regimes of northern rivers (Boyer et al., 2010).

The impacts of changing climate in Canada vary from one area to another and have been studied by numerous authors, both at the national and regional scale. Studies on trends of various hydro-climatic indices reveal a variety of results; both positive and negative trends were found across different parts of Canada. According to Ehsanzadeh et al. (2011), who analyzed Canadian low flows, there is a positive trend in winter low flows (including in eastern Canada), but the trends are negative in western Canada. Summer low flows are found to exhibit positive trends in central Canada, but the trends are negative in regions such as eastern Ontario and Quebec (Ehsanzadeh et al., 2011). Similarly, Adamowski and Bocci (2001) found that there is a significant positive trend in the yearly low flow in western Quebec and southern Ontario; however, the opposite was observed for central and eastern Canada for the same variable. The latest assessment by the Intergovernmental Panel on Climate Change (IPCC) also stated that annual precipitation has increased over much of North America, especially in northern Canada,

but has decreased in the Canadian Prairies (IPCC, 2007). Recent changes in annual total precipitations in Canada were between -10% and +35% (Zhang et al., 2001).

One of the predicted effects of climate change in Quebec is the increase in the intensity and frequency of heavy floods, resulting from heavy precipitation (Assani et al., 2010). McBean and Motiee (2006) also found that there are significant upward trends at the 5%-level in flow and precipitation for the Great Lakes watershed over the period of 1930-1990. These findings are relatively consistent with the predictions of the General Circulation Models (GCMs) for the year 2050 (McBean and Motiee, 2006). The results of the Canadian General Circulation Model (CGCMI) and a coupled hydrologic-hydraulic model used by Roy et al. (2001) predicted that the magnitude of heavy precipitation occurrences will increase significantly in Quebec; and Burn and Hag Elnur (2002) observed that annual maximum flows were increasing in southern Quebec (the Great Lakes and St. Lawrence areas). Zhang et al. (2000) found that the annual precipitation has gone up by between 5% and 35% in southern Canada for the period of 1900-1998. Using a hydrological model on different future climatic scenarios (based on greenhouse gas emission scenarios), Boyer et al. (2010) also projected that in the next 100 years there will be changes in river discharges for both the north and south shores of the St. Lawrence River.

It is not surprising that many of the arguments made concerning both climate variability and climatic change are directly related to the detection of trends (or lack thereof) in hydroclimatic parameters such as temperature, precipitation, and streamflow (Birsan et al., 2005). Changes in the patterns and other characteristics of precipitation caused by the daily, seasonal, yearly, and decadal variations should be monitored because they have important ramifications (Ampitiyawatta and Guo, 2009). It is therefore essential to investigate trends associated with hydrological events in order to better assess the potential future impacts of climatic change on water resources (e.g. at the regional level). Hydrologic variables are also regarded as useful indicators of how the climate has changed and varied over time (Burn and Hag Elnur, 2002). It has been suggested that public policies tailored to consider the effects of regional climate change could be modified to cater for a specific eco-zone. This would take into account knowledge of

local climatic and hydrological trends, rather than general patterns of global climate change (Clark et al., 2000).

One way to accomplish trend assessments is through time-series analysis. Using observational data instead of the output of a model minimizes the uncertainties associated with the modelling process such as assumption concept simplifications (Svensson et al., 2005). Studies have applied several methods to detect and quantify trends in precipitation and streamflow data. Some of the more common methods found in the recent literature involve the use of the bootstrap methods (Adamowski and Bougadis, 2003; Cunderlik and Burn, 2004; Abdul Aziz and Burn, 2006; Burn et al., 2010); regression models (Svensson et al., 2005; Shao et al., 2010; Timofeev and Sterin, 2010); and non-parametric statistical tests (Birsan et al., 2005; Zhang et al., 2009; Durdu, 2010; Zhang et al., 2010; Liu et al., 2010). The Mann-Kendall (MK) trend test (Mann, 1945; Kendall, 1975) is probably the most widely used non-parametric test in detecting monotonic trends (Yue and Pilon, 2004; Hamed, 2008). The most attractive features of this test are that it is powerful even for skewed distributions (Önöz and Bayazit, 2003), simple to compute, and resilient to non-stationary data and missing values (Partal and Küçük, 2006; Adamowski et al., 2009). A noticeable weakness of the MK test is that it does not account for serial correlation, which is very often found in precipitation and streamflow data (Hamed and Rao, 1998; Partal and Küçük, 2006). McBean and Motiee (2006) also specified that the MK test may not necessarily detect non-linear trends. As a result, the MK test is often used in conjunction with other methods or models for trend-related studies in hydrology.

More recently, the wavelet transform – a relatively recent development in signal processing – has also emerged as a tool used in trend analysis (Wang et al., 2011). Wavelet transform has a major advantage over classical signal analysis techniques such as the Fourier Transform, which only uses a single-window analysis, resulting in time-averaged results that lose their temporal information (Torrence and Compo, 1998; Drago and Boxall, 2002). The main issue with the fixed window size used in the Windowed Fourier Transform is that it loses the time localization at high frequencies when the window is sliding along the time series because there are too many oscillations captured within the window. It also loses the frequency localization at low frequencies because

there is only a few low-frequency oscillations included in the window (Santos et al., 2001). The wavelet transform can handle these issues by decomposing a one-dimensional signal into two-dimensional time-frequency domains at the same time (Adamowski et al., 2009). Unlike sine waves, which are the main functions used in Fourier analysis, wavelets are usually irregular and asymmetric in shape. This property makes a wavelet ideal for analyzing signals that contain sharp changes and discontinuities – a localized signal analysis (Quiroz et al., 2011). Wavelet transforms use different window sizes, which are able to compress and stretch wavelets in different scales or widths; these are then used to decompose a time series (Santos et al., 2001). Narrow windows are used to track the high-frequency components or rapidly-changing events of the analyzed signals (which are represented by the lower detail levels), whereas wider window sizes are used to track the signals' low-frequency components including trends (which are represented by the higher detail levels and the approximation component) (Santos et al., 2001; Cannas et al., 2006). Additionally, wavelet analysis is able to show many properties of a time series or data that may not be revealed by other signal analysis techniques, such as trends, discontinuities, change points, and self-similarity. In summary, the wavelet transform is capable of analyzing a wider range of signals more accurately when compared to the Fourier analysis (Nolin and Hall-McKim, 2006; Goodwin, 2008). The results of wavelet analysis can be used to determine the main components or modes in the time series that may contribute to producing trends (Kim, 2004). These results can then be used to examine the temporal patterns of both a signal's frequency and time domains (Labat, 2005; Wang et al., 2011).

Several different studies conducted to analyze trends in streamflow and precipitation in different climate settings have employed the use of wavelet-based methods. Zume and Tarhule (2006) used the continuous wavelet transform and the MK test to analyze the variability of precipitation and streamflow in northwestern Oklahoma for a period of over 100 years. They found that both annual precipitation and streamflow experience interannual to decadal variability. Xu et al. (2009) studied the impact of climate change in the Tarim River basin in China for the period of 1959–2006, by approximating non-linear trends in annual temperature, precipitation, and relative humidity time series using a wavelet-based decomposition and reconstruction technique.

They found that all variables showed non-linear trends and/or fluctuating patterns, especially at the 4-and 8-year scales. Partal (2010) analyzed streamflow datasets from four stations with different climatic conditions in Turkey, three from the Sakarya basin and one from the Seyhan basin. The study found different scales were responsible for the different trends in different climatic areas. In the Sakarya basin, the real trends were associated with the 16-year periodic component, whereas in the Seyhan basin, the trends were associated with the 4-year and 8-year modes.

The main purpose of this study is to combine the use of the discrete wavelet transform (DWT) technique and the Mann-Kendall trend tests in order to investigate trends in streamflow and precipitation datasets in Ontario and Quebec by analyzing their monthly, seasonally-based, and annual time series. The analysis of monthly to yearly data should allow this study to investigate the rapidly and slowly changing events in the datasets used. The trend analysis is done by examining the behaviour and fluctuation of high-frequency and low-frequency components of the available time series, and whether they are contributing to the possible existence of trends in these series. This is important because although research on trend assessment of flow and precipitation has been conducted in different parts of Canada, they have rarely focused on the details of the time-scale fluctuations or cycles that affect the trends in flow and precipitation in Ontario and Quebec. There could be longer cycles than daily or seasonal fluctuations that exist to affect the trends in these variables, which will be explored in this present study. Using the DWT technique in conjunction with the MK test has not been extensively explored to date, in analyzing streamflow and/or precipitation data (especially in Canadian studies). Additionally, a new criterion of using the relative error of the trend values between the original data and the approximation component of the DWT is proposed and successfully applied in this study. The usefulness of this new criterion for the DWT procedure is discussed in detail in section 4.4.3.

In this study, the possible existence of significant autocorrelations and seasonality patterns in the data sets used is first checked. Following this, each time series is decomposed via the DWT approach into its appropriate number of decomposition levels (the explanation on how to determine the appropriate number of decomposition levels is provided in section 4.4.3). Finally, depending on the characteristics of the analyzed time

series (e.g. the presence or absence of significant autocorrelations or seasonality cycles), the most suitable MK test is applied to the original data and the series resulting from the DWT decomposition. Although this type of detailed information is very important to be explored and included in the methodology, it is often overlooked or missing in most published trend detection/estimation studies.

Water resource planners and managers can use the results obtained from this study to address issues in water resources that are associated with climate variability, by creating appropriate policies and strategies. Some potential applications include the implementation of useful adaptation and mitigation strategies as a response to climate change; the optimization of various hydrologic structural designs such as dams and reservoirs; and improvements in stormwater planning (Coats, 2010) and flood protection projects. In addition, in order to improve the forecasting precision of water resources for current and future management, an accurate understanding of the temporal variations of hydrologic variables is vital (Nolin and Hall-McKim, 2006). The authors of this paper believe that the findings from this study can serve as a baseline reference for future research and watershed planning/management, and will advance the understanding of precipitation and streamflow dynamics in Canada and at the smaller, watershed-scale in Quebec and Ontario.

## **4.2. Theoretical Background**

### **4.2.1. Wavelet Transforms (WT)**

A WT is used to mathematically decompose a signal into multiple lower resolution levels by controlling the scaling and shifting factors of a single wavelet – the mother wavelet  $\Psi$ . This is accomplished by using a high-pass filter and a low-pass filter. A wavelet function is a function having a wave shape and limited but flexible length with a mean value that is equal to zero, and is localized in both time and frequency domains. The term wavelet function generally refers to either orthogonal or non-orthogonal wavelets (Torrence and Compo, 1998).



One of the main reasons to utilize wavelet-based methods in hydrological studies is due to its robust property – it does not involve any possibly incorrect assumptions of distribution and parametric testing protocols (Kisi and Cimen, 2011). The WT also filters out the high-frequency components of a signal (de Artigas et al., 2006). Wavelet transforms involve shifting forward the wavelet in a number of steps along an entire time series, and generating a wavelet coefficient at each step. This measures the level of correlation of the wavelet to the signal in each section. The variation in the coefficients indicates the shifting of similarity of the wavelet with the original signal in time and frequency. This process is then repeated for each scaled version of the wavelet, in order to produce sets of wavelet coefficients at the different scales. The lower scales represent the compressed version of the mother wavelet, and correspond to the rapidly changing features or high-frequency components of the signal. The higher scales are the stretched version of a wavelet, and their wavelet coefficients are identified as slowly changing or low-frequency components of the signal. Therefore, wavelet transforms analyze trends in time series by separating its short, medium, and long-period components (Drago and Boxall, 2002).

WT can be performed using two approaches: Continuous Wavelet Transform (CWT) and Discrete Wavelet Transform (DWT). CWT operates on smooth continuous functions and can detect and decompose signals on all scales. Examples of mother wavelets used in CWT are the Morlet and Paul wavelets, among others. DWT may use mother functions such as the Mallat or à trous algorithms, which operate on scales that have discrete numbers. The scales and locations used in DWT are normally based on a dyadic arrangement (i.e. integer powers of two) (Chou, 2007). DWT is especially useful for time series containing sharp jumps or shifts (Partal and Küçük, 2006). One requirement of DWT is that the mother wavelet has to have an orthogonal basis, while a non-orthogonal wavelet can be used with either DWT or CWT.

#### 4.2.1.1. Continuous Wavelet Transform (CWT)

For a time series,  $x_t$ , that has a continuous scale but a discrete recording sequence and  $t = 0, \dots, t - I$ , then the wavelet function ( $\Psi$ ), which depends on a time variable ( $\eta$ ), is generally defined as (Partal and Küçük, 2006):

$$\Psi(\eta) = \Psi(s, \gamma) = \frac{1}{\sqrt{s}} \Psi\left(\frac{t - \gamma}{s}\right) \quad (4.1)$$

where  $t$  represents time; variable  $\gamma$  is the translation factor (time shift) of the wavelet over the time series; and variable  $s$  ranging from 0 to  $+\infty$  denotes the wavelet scale (scale factor). When  $\gamma = 0$  and  $s = 1$ ,  $\Psi(t)$  represents the mother wavelet – all wavelets following this computation are the rescaled (translated and dilated) versions of the mother wavelet. In order to be acceptable as a wavelet, the function  $\Psi(\eta)$  has to satisfy the condition of having zero mean (implying the existence of oscillations) and be localized in time-frequency space (Torrence and Compo, 1998). As can be seen in equation (4.1), when  $s$  is less than 1,  $\Psi(\eta)$  corresponds to a high-frequency function; when  $s$  is greater than 1,  $\Psi(\eta)$  corresponds to a low-frequency function.

The wavelet coefficients ( $W_\Psi$ ) of CWT for the time series  $x_t$  (with equal time interval,  $\delta t$ ), is calculated using the convolution of  $x_t$  with the scaled and translated versions of the wavelet,  $\Psi(\eta)$  (Partal and Küçük, 2006):

$$W_\Psi(s, \gamma) = \frac{1}{\sqrt{s}} \int_{-\infty}^{+\infty} x(t) \Psi^*\left(\frac{t - \gamma}{s}\right) \delta t \quad (4.2)$$

where the asterisk symbol represents the complex conjugate numbers. If the scale ( $s$ ) and translation ( $\gamma$ ) functions are smoothly changed according to time  $t$ , a scalogram can be produced from the calculation, revealing the amplitude of a specific scale and how it fluctuates over time (Torrence and Compo, 1998).

#### 4.2.1.2. Discrete Wavelet Transform (DWT)

Although CWT is able to locate specific events in a signal that may not be obvious, one of the main disadvantages of the CWT is that the construction of the CWT inverse is more complicated (Fugal, 2009). In practice this may not always be desirable because often, signal reconstructions are needed (Fugal, 2009). In addition, the use of the CWT can generate too many data (coefficients) and is more difficult to implement. It may also be more desirable to choose the DWT over CWT because CWT does not produce information in the form of a time series, but rather in a two-dimensional format (Percival, 2008). This causes a high amount of redundant information produced by CWT and the coefficients are correlated spatially and temporally (Percival, 2008). If the DWT is chosen, the process of transformation is simplified and the amount of work is reduced; yet, it still produces a very efficient and accurate analysis (Partal and Küçük, 2006). This is because the DWT is normally based on the dyadic calculation of position and scale of a signal (Chou, 2007). The DWT of a vector is the outcome of a linear transformation resulting in a new vector that has equal dimensions to those of the initial vector (Chou, 2011). This transformation is the decomposition process. The discretization of wavelet functions is accomplished using a logarithmic uniform spacing that has a coarser resolution at higher scales (Mallat, 1989; Daubechies 1990).

Some important features of DWT are: i) at each scale, the number of convolutions using orthogonal wavelets is proportional to the width of the wavelet function at that particular scale (Torrence and Compo, 1998; Kulkarni, 2000); ii) the wavelet spectra generated are in discrete steps and give a very compact representation of the signal (Kulkarni, 2000); iii) due to its orthogonal property, signal reconstruction is not complicated (Torrence and Compo, 1998); and iv) results of transformations using DWT do not contain the unwanted relation between the wavelet coefficients, which are observed in the CWT (i.e. DWT removes the redundant information within the wavelet coefficients in order to better identify processes contained in signals) (Daubechies, 1992). DWT adopts the following form (Partal and Küçük, 2006):

$$\Psi_{(a,b)}\left(\frac{t-\gamma}{s}\right) = \frac{1}{(s_0)^{a/2}} \Psi\left(\frac{t-b\gamma_0 s_0^a}{s_0^a}\right) \quad (4.3)$$

$\Psi$  denotes the mother wavelet;  $a$  and  $b$  are integers, which represents the amount of dilation (scale factor) and translation of the wavelet, respectively;  $s_0$  denotes a dilation step whose value is unchanged and is greater than 1; and  $\gamma_0$  symbolizes the location variable whose value is greater than zero. Generally, for practical reasons, the values for  $s_0$  and  $\gamma_0$  are chosen to be 2 and 1, respectively (Mallat, 1989; Daubechies, 1992). This is the DWT dyadic grid arrangement (i.e. integer powers of two; logarithmic scaling of the translations and dilations). If a time series exhibits discrete properties, with a value of  $x_t$ , occurring at a discrete time  $t$ , the wavelet coefficient ( $W_\Psi(a,b)$ ) for the DWT becomes (Partal and Küçük, 2006):

$$W_\Psi(a,b) = \frac{1}{(2)^{\frac{a}{2}}} \sum_{t=0}^{N-1} x_t \Psi\left(\frac{t}{2^a} - b\right) \quad (4.4)$$

The wavelet coefficient for the DWT is calculated at scale  $s = 2^a$  and location  $\gamma = 2^a b$ , revealing the variation of signals at different scales and locations (Partal and Küçük, 2006). Since most precipitation and streamflow data are sampled in discrete intervals, it makes sense to use the DWT.

#### 4.2.2. The Mann-Kendall (MK) Trend Test

The computation of the MK  $S$ -statistic value from the raw data can yield a large positive or negative value for  $S$ , indicating a positive or negative trend, respectively. The null hypothesis ( $H_0$ ) of the MK test assumes that the ranked data ( $X_c, c = 1, 2, 3, \dots, n-1$ ) and ( $X_d, d = c + 1, \dots, n$ ) belong to a sample of  $n$  independent and identically distributed random variables. The alternative hypothesis ( $H_1$ ) of the two-sided test assumes that the distributions of  $X_c$  and  $X_d$  are not identical for all  $c, d \leq n$  with  $c \neq d$  (Partal, 2010). The  $S$ -statistic of the MK test is computed as (Hirsch and Slack, 1984):

$$S_t = \sum_{c=1}^{n-1} \sum_{d=c+1}^n \text{sign}(X_d - X_c) \quad (4.5)$$

$$\text{Sign}(X_d - X_c) = \begin{cases} +1 & \text{when } X_d > X_c \\ 0 & \text{when } X_d = X_c \\ -1 & \text{when } X_d < X_c \end{cases} \quad (4.6)$$

$X_c$  and  $X_d$  denote the ranked values of the data, and  $n$  is the length of the data record. For data that are distributed identically and independently with a zero mean, the variance for the  $S_t$  statistics can be calculated as (Adamowski and Bougadis, 2003):

$$\text{Variance}(S_t) = \left\{ n(n-1)(2n+5) - \sum_{c=1}^n t_c(c-1)(2c+5) \right\} / 18 \quad (4.7)$$

$t_c$  represents the summation of  $t$ , which is the number of tied values to the extent of  $c$ . The statistics of the Mann-Kendall test,  $Z$ , is then given as (Xu et al., 2009):

$$Z = \begin{cases} \frac{S_t - 1}{\sqrt{\text{Variance}(S_t)}}, & (\text{if } S_t > 0) \\ 0, & (\text{if } S_t = 0) \\ \frac{S_t + 1}{\sqrt{\text{Variance}(S_t)}}, & (\text{if } S_t < 0) \end{cases} \quad (4.8)$$

The statistic of the MK test,  $Z$ , given in equation (4.8) can be used where the number of records,  $n$ , is larger than 10. The trend's significance is assessed by comparing the  $Z$  value with the standard normal variate at the pre-specified level of statistical significance (Hamed and Rao, 1998). In a two-sided trend test, with alpha ( $\alpha$ ) representing the significance level, the null hypothesis should not be accepted if  $|Z| > Z_{\alpha/2}$ ;

this suggests that the trend is significant. A positive Z-value at the significance level implies that there is a positive trend, whereas a negative value indicates a negative trend. The probability value (*p*-value) obtained from the MK Z-value can be used to verify the significance of a trend. If the *p*-value is less than the pre-determined significant level (e.g.  $\alpha = 5\%$ ) or greater than the confidence level (if  $\alpha = 5\%$ , confidence level = 95%), it means that the null hypothesis of no trend cannot be accepted.

#### **4.2.2.1. Modified Mann-Kendall (MK) Trend Tests that Account for Seasonality and Autocorrelation Structures in the Data**

It is well known that the original Mann-Kendall test does not consider the autocorrelation factor that may be present in the time series being analyzed. The presence of an autocorrelation in a dataset may lead to inaccurate interpretations of the MK test. A time series exhibiting positive autocorrelation causes the effective sample size to be less than the actual sample size, thereby increasing the variance and the possibility of detecting significant trends when in fact, there are no trends (Hamed and Rao, 1998; Ehsanzadeh et al., 2011). On the contrary, the existence of negative autocorrelation in a time series enhances the possibility of accepting the null hypothesis (absence of significant trends), when actually, there are significant trends (Ehsanzadeh et al., 2011).

There have been several approaches developed that deal with the effects of autocorrelation in a time series. Yue et al. (2002) developed the Trend-Free Pre-whitening method (TFPW) – the trend component is assumed to be linear, and is first removed before the pre-whitening procedure is applied. Kumar et al. (2009) found that for data that have significant autocorrelation coefficients extending beyond the first lag, the TFPW method was not the best method to account for all these significant autocorrelations. In the present study, significant autocorrelations may be present for more than just one lag in several time series. Therefore, the TFPW method is not considered in this study.

Hirsch and Slack (1984) proposed a modified MK test that accounts for seasonality and serial dependence factors. This method separates observations into different seasons, which eliminates the dependence problem between seasons (Hirsch et

al., 1982; Hirsch and Slack, 1984). This method, however, is not as powerful when there is long-term persistence (with autoregressive parameter  $> 0.6$ ) or when there are less than five years worth of monthly data (Hirsch and Slack, 1984).

Hamed and Rao (1998) proposed another modified version of the MK test in order to deal with the issue of autocorrelation structures for all lags in a dataset, because autocorrelations may still exist past the first lag (note: seasonality issues are not taken into consideration in this modified version of the MK test). Since the presence of autocorrelation underestimates the variance if calculated using the MK formula for uncorrelated data, the method by Hamed and Rao (1998) modifies the calculation for the variance of the MK test statistics when the data are serially correlated by using an empirical formula (see section 4.2.2.3.). When applied to autocorrelated data with a large sample size, this test was found to be practically as powerful as when the original MK test is applied to independent data (Hamed and Rao, 1998).

#### **4.2.2.2. Modified Mann-Kendall (MK) Test to Account for Seasonality and Autocorrelation by Hirsch and Slack (1984)**

Hirsch and Slack (1984) modified the original Mann-Kendall trend test to account for seasonality and autocorrelation factors present in a dataset. Let the matrix:

$$x = \begin{pmatrix} x_{11} & x_{12} & x_{13} & \dots & x_{1k} \\ x_{21} & x_{22} & x_{23} & \dots & x_{2k} \\ x_{31} & x_{32} & x_{33} & \dots & x_{3k} \\ \cdot & \cdot & \cdot & \dots & \cdot \\ \cdot & \cdot & \cdot & \dots & \cdot \\ \cdot & \cdot & \cdot & \dots & \cdot \\ x_{j1} & x_{j2} & x_{j3} & \dots & x_{jk} \end{pmatrix} \quad (4.9)$$

where the data in the matrix  $x$  represent a series of observations recorded over  $k$  seasons for  $j$  years (without any tied values) (Hirsch and Slack, 1984). The ranks of the data in matrix  $x$  are represented in the following matrix (Hirsch and Slack, 1984):

$$r = \begin{pmatrix} r_{11} & r_{12} & r_{13} & \dots & r_{1k} \\ r_{21} & r_{22} & r_{23} & \dots & r_{2k} \\ r_{31} & r_{32} & r_{33} & \dots & r_{3k} \\ \vdots & \vdots & \vdots & \ddots & \vdots \\ r_{j1} & r_{j2} & r_{j3} & \dots & r_{jk} \end{pmatrix} \quad (4.10)$$

Since the values within each season are ranked among themselves, the calculation of the rank ( $r_{dz}$ ) becomes (Hirsch and Slack, 1984) (for  $c$  and  $d$  notations, see equation (4.5)):

$$r_{dz} = \frac{[j + 1 + \sum_{c=1}^j \text{sgn}(x_{dz} - x_{cz})]}{2} \quad (4.11)$$

The test statistic  $S_z$  is calculated using (for each season):

$$S_z = \sum_{c < d} \text{sgn}(x_{dz} - x_{cz}); \text{ where } z = 1, 2, 3, \dots, k \quad (4.12)$$

The test statistics for the seasonal Kendall is calculated using:

$$S_s = \sum_{z=1}^k S_z \quad (4.13)$$

with variance of:

$$\text{Variance } S_s = \sum_z (\sigma_z)^2 + \sum_{z, w; z \neq w} \sigma_{zw} \quad (4.14)$$

$\sigma_z^2$  is the variance of ( $S_z$ ),  $\sigma_{zw}$  denotes the covariance of ( $S_z, S_w$ ). The estimator for the covariance  $\hat{\sigma}_{zw}$  was developed by Dietz and Killeen (1981), which is as follows:



$$\hat{\sigma}_{zw} = \frac{K_{zw}}{3} + (j^3 - j) \frac{r_{zw}^*}{9} \quad (4.15)$$

With no missing values, the estimator of the covariance becomes (Hirsch and Slack, 1984):

$$\hat{\sigma}_{zw} = \frac{(K_{zw} + 4 \sum_{c=1}^j r_{cz} r_{cw} - j(j+1)^2)}{3} \quad (4.16)$$

Where  $K_{zw}$  and  $r_{zw}^*$  are calculated using:

$$K_{zw} = \sum_{c < d} \text{sgn}((X_{dj} - X_{cj})(X_{dw} - X_{cw})) \quad (4.17)$$

$$r_{zw}^* = (3/(j^3 - j)) \sum_{c,d,p} \text{sgn}(X_{dj} - X_{cj})(X_{dw} - X_{pw}) \quad (4.18)$$

However, in the event that there are no ties and no missing data values,  $r_{zw}^*$  is simply the Spearman's correlation coefficient for seasons  $z$  and  $w$  (Hirsch and Slack, 1984). By adopting the estimates of  $\sigma_{zw}$  to calculate the variance  $S_s$ , the test no longer needs the assumption of independence (Hirsch and Slack, 1984).

#### 4.2.2.3. Modified Mann-Kendall Test for Autocorrelated Data by Hamed and Rao (1998)

Since using the original MK for autocorrelated data underestimates the variance of the data, the calculation of the variance of the test statistics  $S$  is altered and given by an empirical formula (Hamed and Rao, 1998):

$$\text{Variance}(S') = \left( n(n-1)(2n+5)/18 \right) \cdot \left( \frac{n}{n_e^*} \right) \quad (4.19)$$

where  $n^*$  is the effective number of sample size needed in order to account for the autocorrelation factor in the dataset. The notation  $n/n_e^*$  is the factor that represents the correction associated with the autocorrelation of the data. Empirically, the correction is expressed by (Hamed and Rao, 1998):

$$\frac{n}{n_e^*} = 1 + \left( \frac{2}{n^3 - 3n^2 + 2n} \right) \cdot \sum_{f=1}^{n-1} (n-f)(n-f-1)(n-f-2)\rho_e(f) \quad (4.20)$$

$\rho_e(f)$  symbolizes the autocorrelation function between the ranks of the observations, computed using the inverse of equation (4.19) (Kendall, 1975; Hamed and Rao, 1998). This transforms the rank autocorrelation into the normalized data autocorrelation, as the estimate of the normalized autocorrelation structure is needed to evaluate the variance of  $S$  for data  $X$  whose distribution may not be normal or rather arbitrary (Hamed and Rao, 1998).

$$\rho(f) = 2 \sin \left( \frac{\pi}{6} \rho_e(f) \right) \quad (4.21)$$

### 4.3. Study Sites and Datasets

The monthly, seasonally-based and annual flow and precipitation data from a total of eight Reference Hydrometric Basin Network (RHBN) stations and seven meteorological stations, respectively, were analyzed. These stations are located in Ontario and Quebec, Canada. Six of the RHBN stations used are located in Ontario, and two are in Quebec. The smallest drainage area of the flow stations is 181 km<sup>2</sup> and the largest one is 22,000 km<sup>2</sup>. As for the meteorological stations, there are three situated in Quebec, and one in Ontario. The two Quebec RHBN stations – Richelieu River and Eaton River – are located in the south western corner of the province, on the south shore portion of the St. Lawrence stream. Four RHBN stations in Ontario (the Neebing, North Magnetawan, Black, and Sydenham rivers) are located around the Great Lakes basin. The Missinaibi and Nagagami rivers (Ontario) are the most northerly stations. The locations

of the flow and precipitation stations are shown in figure 4.1 and the key features of the RHBN stations and the meteorological stations are summarized in tables 4.1 and 4.2, respectively.

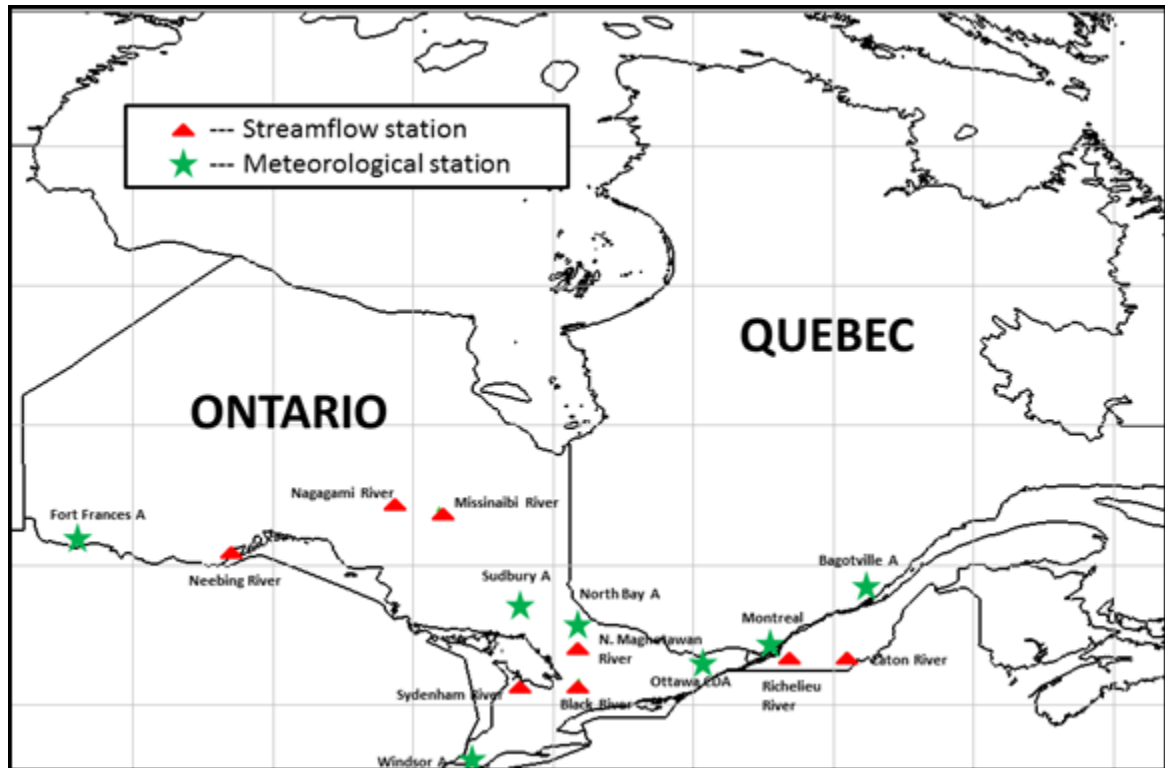


Figure 4.1. A map of the flow and precipitation stations used this study.

Monthly datasets were chosen because it includes the analysis of short-term monthly variations such as the intra-annual and inter-annual cycles. Seasonally-based values were examined to allow the analysis of seasonal cycles (it will be seen later that most time series – especially flow time series – exhibit strong annual cycles). Annual datasets were analyzed in order to study the long-term fluctuations (e.g. multi-year, decadal, and multi-decadal events) that are potentially present in the flow and precipitation time series.

One of the advantages in using monthly datasets compared to annual datasets in trend detection is that annual data values may not deal well with the presence of missing records (which causes the annual summary value to be biased), and the seasonality factor

(Hirsch and Slack, 1984). If both factors (missing data and seasonality) are present in a yearly time series, the trends detected may simply be caused by the yearly variation in the sampling schedule (Hirsch and Slack, 1984). Having said this, a monthly time series has more autocorrelation issues compared to a yearly time series (Hirsch and Slack, 1984). Therefore, this present study chose to incorporate monthly and annual data in order to thoroughly analyze the variations and trends of flow and precipitation within the study area.

Table 4.11. Unregulated RHBN gauging stations in Ontario and Quebec recording the streamflow data, which were used in this study.

Station Id.	Station Name	Province	Latitude (°)	Longitude (°)	Drainage Area (km <sup>2</sup> )
02AB008	Neebing River near Thunderbay	ON	48.38	-89.31	187
02EA005	North Magnetawan River Near Burk's Falls	ON	45.66	-79.37	321
02EC002	Black River Near Washago	ON	44.71	-79.28	1521
02FB007	Sydenham River Near Owen Sound	ON	44.52	-80.93	181
02OE027	Eaton (Riviere) Pres De La Riviere Saint-Francois-3	QC	45.46	-71.65	642
02OJ007	Richelieu (Riviere) Aux Rapides Fryers	QC	45.39	-73.25	22000
04JC002	Nagagami River At Highway No. 11	ON	49.77	-84.53	2410
04LJ001	Missinaibi River At Mattice	ON	49.61	-83.26	8940

Table 4.2. Meteorological stations in Ontario and Quebec recording the precipitation data, which were used in this study.

Station Id.	Station Name	Province	Latitude (°)	Longitude (°)	Joint Station	Elevation (m)
6022476	Fort Frances A	ON	48.7	-93.43	Yes	342
6068150	Sudbury A	ON	46.6	-80.8	Yes	348
6085700	North Bay A	ON	46.4	-79.4	Yes	370
6105976	Ottawa CDA	ON	45.4	-75.7	No	79
6139525	Windsor A	ON	42.3	-82.9	Yes	190
7025250	Montreal/Pierre Elliot Trudeau Intl. A	QC	45.5	-73.8	Yes	36
7060400	Bagotville A	QC	48.33	-71	No	159

#### 4.3.1. Selection Criteria for the RHBN Flow Stations and Meteorological Stations

The stations used in this study were chosen based on the regulation type (for flow stations), and the completeness and length of their available records for the period of 1954-2008. The three main criteria used for this selection are summarized as follows: (1) there must be an absence of hydrological structural controls upstream of a RHBN gauging station (for flow stations only). Upstream controls and regulation, such as reservoir storage or containment structures, hydropower activities, and water diversions may have considerable impacts on the quality of data (Yue and Pilon, 2005). As a consequence, less accurate frequency analysis and interpretation may be obtained. Therefore, this study only considered gauging stations, which are stated as “natural” according to Environment Canada. (2) Stations must have a record length of at least 55 years, starting from 1954 to 2008. In order to obtain a valid mean statistic in assessing trends in flow associated with climate change, Kahya and Kalayci (2004) and Burn and Hag Elnur (2002) consider at least 31 and 25 years worth of data, respectively, are required. Furthermore, Partal (2010) considered 40 years’ worth of data adequate for trend analysis studies. Therefore, we concluded that having 55 years worth of data would be sufficient for the purpose of trend detection in our study. The start and end years in this study were chosen because they would give the highest number of stations in Quebec and Ontario to be analyzed without any missing records. (3) Although up to three-percent

missing data is considered acceptable for meteorological studies (Mishra and Singh, 2010), this study chose to include only stations with fully complete records over the chosen time period. This was done in order to avoid possible uncertainties associated with the computation of extrapolation procedures. Criterion number 1 was applied only to the flow stations; criteria number 2 and 3 were applied to both flow and precipitation stations. In summary, there are a total of eight RHBN stations in Ontario and Quebec that meet the three selection criteria. As for the meteorological stations, there are a total of seven meteorological stations in Ontario and Quebec that have a record length of 55 years without missing values.

#### **4.3.2. Flow Data**

The monthly, seasonal, and annual average flow data were obtained from the Environment Canada HYDAT database. Only data from stations that are categorized as RHBN were chosen. First, the RHBN designation for a station indicates that its data accuracy is further evaluated qualitatively by local experts by taking into consideration the hydraulic condition of that particular station (Coulibaly and Burn, 2004). Secondly, the stage-discharge relationship and channel geometry were considered, and the reliability of data records influenced by ice conditions was checked (Zhang et al, 2001). Thirdly, the RHBN stations represent pristine or stable hydrological conditions, having at least 20 years of good-quality data (Zhang et al., 2001). In summary, only RHBN gauging stations were included in this study in order to ensure that good-quality data are used. In addition to this, many Canadian studies on flow trend and variability have also used data from selected RHBN stations because of their record length and reliability (e.g. Burn and Hag El Nur, 2002; Coulibaly and Burn, 2004; Ehsanzadeh and Adamowski 2007; Ehsanzadeh et al., 2011; etc).

The flow data used in this study cover the period from January 1954 to December 2008, except for Eaton River station that has records ending in September 2008. The data analysis therefore covers the years 1954-2008 (except for Eaton River which only covers up to 2007 due to the incomplete 2008 data).

### 4.3.3. Precipitation Data

The monthly, seasonally-based and annual total precipitation data were obtained from Environment Canada's second generation adjusted and homogenized precipitation database (with trace corrections to account for trace amounts of both rainfall and snowfall). The detailed explanation of the adjustment procedures can be found in Mekis and Vincent (2011). Daily rainfall and snowfall measurements were adjusted separately – the adjusted rainfall and snow-water equivalent make up the daily total precipitation (Mekis and Vincent, 2011). Mekis and Vincent (2011) also applied several statistical adjustments to the original daily data (which were taken from the National Climate Data Archive of Environment Canada). These procedures address issues regarding changes in location, modifications to recording instruments, faulty equipment, and alterations to recording procedures. These corrections were done to ensure that factors such as wind undercatch, evaporation losses, and gauge specific wetting losses for specific types of rain-measuring instruments, have been taken into account. Other improvements and revisions that were also implemented by Mekis and Vincent (2011) in these second generation datasets include: better rain-gauge adjustment procedures, improved snow-water equivalent maps, better adjustment procedures to trace records due to more accurate metadata information, and further tests on the combined stations. Since the datasets contained in the second generation adjusted precipitation data have been developed mainly for climate-related research, their quality is very suitable for the purpose of this study.

Many precipitation stations included in the second-generation datasets have long records as a result of data combinations among nearby stations (Mekis and Vincent, 2011). The procedures and adjustments involved in joining the data of nearby stations are given in detail in Mekis and Vincent (2011). The stations used in this study were combined stations, except for the Ottawa CDA and Bagotville A stations (table 4.2). All precipitation stations used have data that extend prior to 1954. Station Sudbury A has incomplete data for year 2008; therefore the data analysis for this station only covers up until 2007. To be consistent with the analysis of the flow trends, it was decided to use the common period of 1954-2008. Kumar et al. (2009) suggested that the same length of

records should be used when analyzing trends of different variables to avoid misleading conclusions.

#### **4.4. Methodology**

Three data types were used in the data analysis: monthly, seasonally-based, and annual. Monthly time series allowed for the investigation of the short-term fluctuations that affect the flow and precipitation. Since annual cycles were strongly apparent in most monthly data, the seasonal average flow and the seasonal total precipitation were used to assess if these annual cycles may have an influence on trends in flow and precipitation data – the second decomposition level in the seasonally-based data represented the yearly (12-month) cycle. Finally, annual data were used in order to assess the long-term fluctuations of streamflow and precipitation over the study area.

The procedures for data analysis are organized in the following order:

1. Autocorrelation tests or analysis were performed for each of the precipitation and streamflow series in order to check for the presence of a serial correlation and seasonality patterns.
2. Each time series was decomposed via the discrete wavelet transforms (DWT) using Daubechies wavelets, splitting the signal into its approximation and detail components.
3. The Mann-Kendall tests were computed on the original data, the detail time series, as well as on the combinations of each of the detail components plus their approximations.
4. The sequential Mann-Kendall analysis was applied to every time series, starting from the original series to the different detail components, approximations, and the combinations of the details with their approximations.
5. The periodic component(s) responsible for trends in each dataset were determined based upon the MK Z-values and the sequential MK graphs of each periodicity.
6. The sequential MK graphs of the original annual time series were analyzed and used to determine the starting point of a trend increase or decrease. This was done



in order to examine whether these starting times are similar among the different flow and precipitation stations.

The following sections describe each of these steps in detail.

#### 4.4.1. Autocorrelation Analysis

The presence of significant autocorrelation in a time series can compromise the interpretation of its trend analysis because it can alter the dispersion of the data distribution by changing the variance. This then increases the occurrence of type I error (Yue et al., 2002), in which a significant trend may be found when in fact the null hypothesis should be accepted (Hamed and Rao, 1998; Partal, 2010). It is expected that the monthly and seasonally-based data would have more autocorrelation issues compared to the annual data. An autocorrelation assessment in the monthly and seasonal datasets was accomplished by using the following equation (Yue et al., 2002; Mohsin and Gough, 2010):

$$R = \frac{(1/n - 1) \sum_{t=1}^{n-1} [x_t - \bar{x}_t] [x_{t+1} - \bar{x}_t]}{(1/n) \sum_{t=1}^n [x_t - \bar{x}_t]^2} \quad (4.22)$$

$$\frac{\{-1 - 1.645 \sqrt{n - 2}\}}{n - 1} \leq R \leq \frac{\{-1 + 1.645 \sqrt{n - 2}\}}{n - 1} \quad (4.23)$$

$R$  is the lag-1 autocorrelation coefficient of the sample data  $x_t$ ,  $\bar{x}_t$  is the sample mean, and  $n$  is the number of observations in the data. If the calculated lag-1 autocorrelation coefficient is within the interval defined by equation (23), it can be assumed that the monthly or seasonal dataset does not contain a significant autocorrelation. If, on the other hand, the calculated  $R$  is found to be outside of the range, the corresponding dataset is assumed to exhibit a significant autocorrelation at the 5% significance level. For the annual datasets, their correlograms showing the ACFs of each dataset for several lags were analyzed and used to determine whether the data are autocorrelated.

#### 4.4.2. Seasonality Factor

The monthly and seasonally-based flow and precipitation time series were checked for seasonality by examining their correlograms. These correlograms were used to visually determine the presence (or lack thereof) of seasonality patterns, or of any cyclical and oscillatory behavior. Looking at the original data, many time series display the patterns of significant autocorrelation and annual cycles. It is important to note that the detail components of signal decomposition in WT can be associated with factors such as seasonal cycles, and other influencing variables that may be external to the time series (Choi et al. 2011). Therefore, the correlograms of the detail components were used to check whether any cyclical patterns were still present post-decomposition.

#### 4.4.3. Time Series Decomposition via the Discrete Wavelet Transform (DWT)

The conventional discrete wavelet analysis of signals was performed on each flow and precipitation time series using the *multilevel 1-D wavelet decomposition* function in MATLAB (MATLAB Wavelet Toolbox). This produces the wavelet transform of the input data at all dyadic scales. Rather than relying on an upsampling procedure, the DWT relies more on downsampling, which is excellent for denoising (Fugal, 2009). The mean flow and total precipitation input signals (data) are all one-dimensional.

Decomposing the signals using specified filters (wavelet and scaling functions) produces two types of coefficients: the approximation or residual, and detail vectors (Chou, 2007). These coefficients resulted from the convolution of the original signal with a low-pass filter and a high-pass filter. The low-pass filter is the scaling function and the high-pass filter is the wavelet function. The convolutions of signals with the low-pass filter produced the approximation coefficients, which represent the large-scale or low-frequency components of the original signal. Convolutions with the high-pass filter produced the detail coefficients, which represent the low-scale or high-frequency components (Bruce et al., 2002). The process of signal decomposition was repeated multiple times, decomposing the original signal into several different lower-resolution components (Partal, 2010).

The detail and approximation coefficients produced from the signal decomposition were then reconstructed since they are merely intermediate coefficients. These have to be re-adjusted to the entire one-dimensional signal in order to enable the investigation of their contribution to the original signal (Dong et al., 2008). This contribution may be reflected in the different time scales such as intra-annual, inter-annual, decadal, and multi-decadal.

The Daubechies (db) wavelets were used in this study because they are commonly used mother wavelets for the DWT in hydro-meteorological wavelet-based studies. Daubechies wavelets provide compact support (Vonesch et al., 2007), indicating that the wavelets have non-zero basis functions over a finite interval, as well as full scaling and translational orthonormality properties (Popivanov and Miller, 2002; de Artigas et al., 2006). These features are very important for localizing events in the time-dependent signals (Popivanov and Miller, 2002).

Relatively large numbers of data points used in this study were from the monthly and seasonally-based datasets. For the period of 55 years, there were 657 or 660 data points for the monthly sets and 219 or 220 for the seasonally-based sets, depending on when the records ended in 2008. In order to avoid unnecessary levels of data decomposition in these larger datasets, the number of decomposition levels had to be determined first. This number is based upon the number of data points, as well as the mother wavelet used. The highest decomposition level should correspond to the data point at which the last subsampling becomes smaller than the filter length (de Artigas et al., 2006). According to de Artigas et al. (2006), who analyzed monthly geomagnetic activity indices, if  $v$  is the number of vanishing moments of a db wavelet and  $n$  is the number of data points in a monthly-based time series, the maximum decomposition level  $L$  is calculated using the following equation:

$$L = \frac{\text{Log} \left( \frac{n}{2^v - 1} \right)}{\text{Log} (2)} \quad (4.24)$$

In MATLAB, the number of vanishing moments for a db wavelet is half of its starting filter length. For example, db5 in MATLAB refers to the Daubechies5 wavelet,

which has a 10-point filter length. If one uses db5 to analyze the monthly data, for example, in equation (4.24), with  $v$  equal to 5, the resulting maximum level of decomposition for the monthly data is 6.20 (the DWT performed in MATLAB would consider the data up to the next dyadic arrangement, which is 1024 data points instead of 660).

Smoother db wavelets (db5-db10) were then tried for each monthly and seasonally-based dataset. Smoother wavelets are preferred here because the trends are supposed to be gradual and represent slowly-changing processes. Smoother wavelets should be better at detecting long-term time-varying behavior (good frequency-localization properties) (Adamowski et al., 2009). In addition to this, several trend studies used smoother db mother wavelets (e.g. Kallache et al., 2005 used *least asymmetric* LA (8); de Artigas et al., 2006 used db7). With the smoother db wavelets, the levels of decomposition resulting from the calculations using equation (24) were between 5.8 and 6.8 (for monthly-based data), and 3.8 and 4.8 (for seasonally-based data). Therefore, six and seven levels; and four and five levels were tried for the monthly and seasonally-based data, respectively.

The border conditions were also taken into consideration when performing the DWT. This is because for signals with a limited length, convolution processes cannot proceed at both ends of the signal since there is no information available outside these boundaries (Su et al., 2011). This is referred to as the border effect (Su et al., 2011). As a result, an extension at both edges is needed. Border extensions that are commonly used are zero-padding, periodic extension, and symmetrization – all of which have their drawbacks, due to the discontinuities introduced at both ends of the signals (de Artigas et al., 2006; Su et al., 2011). The default extension method used in MATLAB is symmetrization, which assumes that signals outside the original support can be recovered by symmetric boundary replication (de Artigas et al., 2006). Zero-padding pads the signal with zeros beyond the original support of the wavelet; periodic padding assumes that signals can be recovered outside of the original support by periodic extension (de Artigas et al., 2006). The inverse discrete wavelet transform (IDWT) was then computed to ensure perfect signal reconstruction.

For each monthly dataset, six and seven levels of decomposition were tried for each smooth db wavelet. In order to determine the smooth mother wavelet and the extension mode to be used in the data analysis for each data type and dataset, two criteria were used. The first criterion used was proposed by de Artigas et al. (2006): all three extension modes for each db wavelet were employed in order to determine the extension method, and the db type, that would produce the lowest mean relative error (*MRE*). The mean relative error (*MRE*) was calculated using the following equation (Popivanov and Miller, 2002; de Artigas et al., 2006):

$$MRE = 1/n \sum_{j=1}^n \frac{|a_j - x_j|}{|x_j|} \quad (4.25)$$

where  $x_j$  is the original data value of a signal whose number of records is  $n$ , and  $a_j$  is the approximation value of  $x_j$ . The second criterion is the one proposed in this study and is based on the relative error  $e_r$ . Each of the extension modes for each of the smooth db wavelets was examined in order to determine the combination (of border condition and the mother wavelet) that would produce the lowest approximation Mann-Kendall Z-value relative error  $e_r$ . The computation of the relative error was done using the following proposed equation:

$$e_r = \frac{|Z_a - Z_o|}{|Z_o|} \quad (4.26)$$

where  $Z_a$  is the MK Z-value of the last approximation for the decomposition level used, and  $Z_o$  is the MK Z-value of the original data.

For the monthly datasets, the calculated *MREs* did not differ significantly among the different border conditions and the different db wavelet types used, for the six and seven levels of decomposition. However, once the  $e_r$  calculations were completed, the lowest errors were generally obtained for six decomposition levels. Therefore, for the monthly data analysis, six decomposition levels were used in their DWT procedures (the db type and border extensions may vary from one station to another). The  $e_r$  was then used to determine the db type as well as the border extension to be used for the data

analysis. Using the monthly total precipitation for station Montreal/Pierre Elliot Trudeau as an example, the *MREs* for the different db types and border extensions were between 0.42 and 0.43 (this applied both for six and seven decomposition levels). The ranges of the  $e_r$  for six decomposition levels were: 97.35-341.05, 44.78-421.94, and 17.46-134.65 using zero-padding, periodic extension, and symmetrization borders, respectively. As can be seen, there were very noticeable differences in the relative errors among the different extensions. For this station, the lowest  $e_r$  produced was by using the symmetrization border with db9 ( $e_r$ : 17.46, *MRE*: 0.42).

For the seasonally-based data analysis, similar procedures to that of the monthly data analysis were used, in order to find the levels of decomposition, db type, and border extension that would produce the lowest *MRE* and  $e_r$ . Four and five levels of decomposition were tried with different border conditions for the different smooth db wavelets. The lowest *MRE* and  $e_r$  were obtained when four levels of decomposition were used. Therefore, four levels of decompositions were used for the seasonally-based data analysis, but the extensions and db types may vary for the different stations.

For the annual data, similar observations were seen where the *MREs* of the different border conditions did not show substantial differences. The differences in the relative errors were also more noticeable among the different border extensions and the different db wavelets. Since the annual datasets have 55 years worth of records, they could be decomposed up to five levels, which correspond to 32 years. Even so, four decomposition levels – which have a maximum of 16 years in fluctuation – were also explored. The  $e_r$  and *MRE* of four decomposition levels were then compared to those of five decomposition levels. So, four and five levels of decompositions were assessed for the annual data. The *MREs* between the two levels did not produce significant differences, but lower relative errors were observed for four decomposition levels. For example, for the North Magnetawan River station, the *MREs* for levels four and five were 0.17-0.22 and 0.17-0.25, respectively. The lowest relative errors for this station were observed when the periodic border extension was used at four decomposition levels with different db types ( $e_r$  = 0.98-4.97). Therefore, for this station, four decomposition levels were used in the DWTs, with the periodic extension border and db10 wavelet – this produced the lowest relative error (i.e. 0.98). The same procedures were applied to the

rest of the annual datasets – four decomposition levels were used, but the extension condition and db wavelet types may vary from one station to another.

#### **4.4.4. Applying the Mann-Kendall (MK) Trend Tests**

For each study location, the MK test  $S$ -statistic and its variance were calculated in order to obtain the test's  $Z$  standard normal value. The absolute value of this  $Z$ -value was then compared to the critical two-tailed  $Z$ -value (area under the normal curve) corresponding to the significant level of  $\alpha/2$  (this study used  $\alpha = 5\%$ ). The  $Z$  values in a two-tailed test for  $\alpha$  of 5% are  $\pm 1.96$ . If the  $Z$ -value obtained from the MK calculation is found outside the boundary of -1.96 and +1.96, then that indicates that the trends detected are significant.

For the monthly and seasonally-based datasets, the modified MK test by Hirsch and Slack (1984) was used because all of these time series showed seasonality patterns and most of them exhibited significant lag-1 autocorrelations. For the annual datasets, the original MK test was applied to datasets that did not exhibit significant autocorrelation. The modified MK test by Hamed and Rao (1998) was applied to two annual datasets (Richelieu River and Montreal/Pierre Elliot Trudeau) because they possessed significant autocorrelations. These corresponding MK tests for the different data types were computed on the original time series, the time series resulting from the wavelet decomposition (details and approximations), and on a set of combinations of the details plus their respective approximations.

#### **4.4.5. Sequential Mann-Kendall (MK) Analysis**

The progressive MK values were calculated for the data used ranging from the beginning of the study period to the end (e.g. Partal, 2010). These MK values were obtained using the different MK tests for the different data characteristics (mentioned in section 4.4). The MK values were portrayed as line graphs and when the line crosses the upper or lower confidence limits, it is an indication that there is a significant trend because the calculated MK value is greater than the absolute value of the normal standard

Z value (at the 5% significance level). By using this significance level, it is implied that the upper confidence limits in a sequential MK graph represent the Z-value of +1.96, whereas the lower confidence limits represent the Z-value of -1.96. The purpose of conducting the sequential MK tests and graphing the results is to see how the trends fluctuated over the study period. Sequential MK analysis also allowed the depiction of a combination of a set of significant upward and downward trends in a time series that may cancel each other, resulting in a non-significant final MK Z-value for that specific dataset.

It is important to note that the normal approximation may be used on the MK test to obtain the Z-value only when the number of data points is greater than 10. Additionally, the power of the modified MK test by Hirsch and Slack (1984) is considered acceptable when seasonal datasets have at least 10 years worth of monthly values. In light of this, the present study considered the MK values to be accurate starting from the 10<sup>th</sup> year since the beginning of the data record, which is 1963. Although all of the sequential MK graphs presented in this paper cover the entire study period from 1954-2008, the portions covering the first 10 years of the graphs may be overlooked. The sequential MK analysis/graphs on the original annual flow and precipitation series were also used to examine and determine the possible starting time point (years) in which the apparent trends started to appear. The results obtained from the different stations can be compared in order to see whether the starting times shared any similarity.

#### **4.4.6. Determining the Most Dominant Periodic Components for Trends**

The procedures for determining the periodic component(s) that are most dominant for trends in a time series consisted of two parts. Firstly, the sequential MK graphs of each detail components (with its approximation added) were examined with respect to their original data. These comparisons were done in order to find the detail components (with approximation added) whose progressive trend lines behave in the most similar manner with respect to their original data. Secondly, the MK Z-value for each of the detail components was compared to the MK Z-value of the original data to see if they are close (even if the values were not statistically significant). The periodic component(s)



that satisfied these two requirements were considered the most dominant periodicities affecting the production of trends.

In determining the most influential periodic component for trends, different combinations of detail components were also tried and tested. For example, if a time series was decomposed into four decomposition levels, we also tested several combinations of detail components (with the approximation added) such as  $D1 + D2 + A4$ , etc. We found that the results of using these combinations were not always conclusive. For example, the most dominant periodicity for station Richelieu River is the  $D4$  component (with approximation) (table 4.9; see section 4.5.4) but in a combination of  $D3 + D4$  (with approximation), the MK  $Z$ -value increased very significantly to +8.05. This is not close to the MK  $Z$ -value of the original data, and its sequential MK graph was not harmonious with the original data. Hence, we chose to only present the results using individual detail components (with its approximation added). This provides clearer information about the most dominant periodicities responsible for trends because of the closeness of the MK  $Z$ -values (between the individual most dominant periodic mode and the original data) and the sequential MK graph (which showed a harmonious trend line between the individual most dominant periodic mode and the original data). This was not always observed when the different detail components were combined.

## **4.5. Results and Discussions**

### **4.5.1. Preliminary Data Analysis**

Flow and total precipitation time series (from the beginning of 1954 to the end of 2008) from eight flow stations and seven meteorological stations in Quebec and Ontario were analyzed for trends. First, the autocorrelation analysis was applied to each of the monthly, seasonally-based, and annual data flow and precipitation series in order to determine the significance of the lag-1 autocorrelation and to assess seasonality patterns. The summaries of flow and precipitation ACF values for their monthly, seasonally-based, and annual data are presented in tables 4.3 and 4.4, respectively.

Table 4.3. Lag-1 Autocorrelation Functions (ACFs) of the original monthly, seasonally-based, and annual flow series.

Flow Station	Monthly data	Seasonally-based data	Annual data
Neebing River	0.34* (S)	-0.20* (S)	0.25
North Magnetawan River	0.27* (S)	-0.25* (S)	0.08
Black River	0.42* (S)	-0.13* (S)	0.09
Sydenham River	0.43* (S)	-0.07 (S)	0.21
Nagagami River	0.41* (S)	-0.07 (S)	0.05
Missinaibi River	0.32* (S)	-0.26* (S)	0.13
Eaton River	0.19* (S)	-0.31* (S)	0.07
Richelieu River	0.69* (S)	0.10* (S)	0.34*

\* indicates significant lag-1 serial correlations at  $\alpha = 5\%$ .

(S) indicates the presence of seasonality cycles

Table 4.4. Lag-1 Autocorrelation Functions (ACFs) of the original monthly, seasonally-based, and annual precipitation series.

Precipitation Station	Monthly data	Seasonally-based data	Annual data
Fort Frances A	0.30* (S)	-0.03 (S)	-0.02
Sudbury A	0.09* (S)	-0.02 (S)	0.03
North Bay A	0.12* (S)	0.02 (S)	0.21
Ottawa CDA	0.02 (S)	-0.02 (S)	0.19
Windsor A	0.06* (S)	0.03 (S)	-0.22
Montreal/Pierre Elliot Trudeau	0.08* (S)	-0.04 (S)	0.28*
Bagotville A	0.02 (S)	0.05 (S)	0.06

\* indicates significant lag-1 serial correlations at  $\alpha = 5\%$ .

(S) indicates the presence of seasonality cycles

As can be seen, the serial correlation in the flow series is more pronounced compared to that of the precipitation series. This is perhaps due to the nature of Nordic rivers, which have flows that may lag by many months (Anctil and Coulibaly, 2004). The seasonality patterns were then visually determined based also on these correlograms. All monthly and seasonally-based data for both streamflow and precipitation show patterns of seasonality; the cycles are much clearer in flow data. The presence of strong annual cycles – especially in the flow data – is seen and indicated by the high ACF values that repeat at about every 12<sup>th</sup> lag (for monthly data) and every 4<sup>th</sup> lag (for seasonally-based data) - see figures 4.2 and 4.3 for examples. The influence of this yearly cycle on trends is looked into in more detail in the seasonally-based data analysis, where the second level of decomposition represents the 12-month periodic mode.

Three MK tests were employed to examine the presence of trends in the original time series and those resulting from the wavelet decomposition. Ideally, the modified MK test by Hirsch and Slack (1984) should be used when a time series shows a seasonality pattern (with or without a significant autocorrelation). If a time series only exhibits a significant autocorrelation without the seasonality effect, the modified MK by Hamed and Rao (1998) should be used. The original MK test should be used when a time series exhibits neither a seasonality pattern nor significant lag-1 ACFs.

In order to examine how the trends have progressed over time, the sequential MK tests were applied to the original data and to the time series of the different periodic components obtained from the discrete wavelet decomposition. It is important to examine the sequential MK values because a mix of positive and negative trends may be present in the same time series. The sequential MK analysis can also help to determine how the trend of a detail component may explain the trends found in the original data. Indeed, in this study, the behavior of the trend lines of the detail components (plus approximation) is important. Therefore, not only the MK Z-values of these details are considered when determining the most influential periodic component(s) on the trend, but also how similarly their trend lines fluctuate with respect to trend line of the original data.

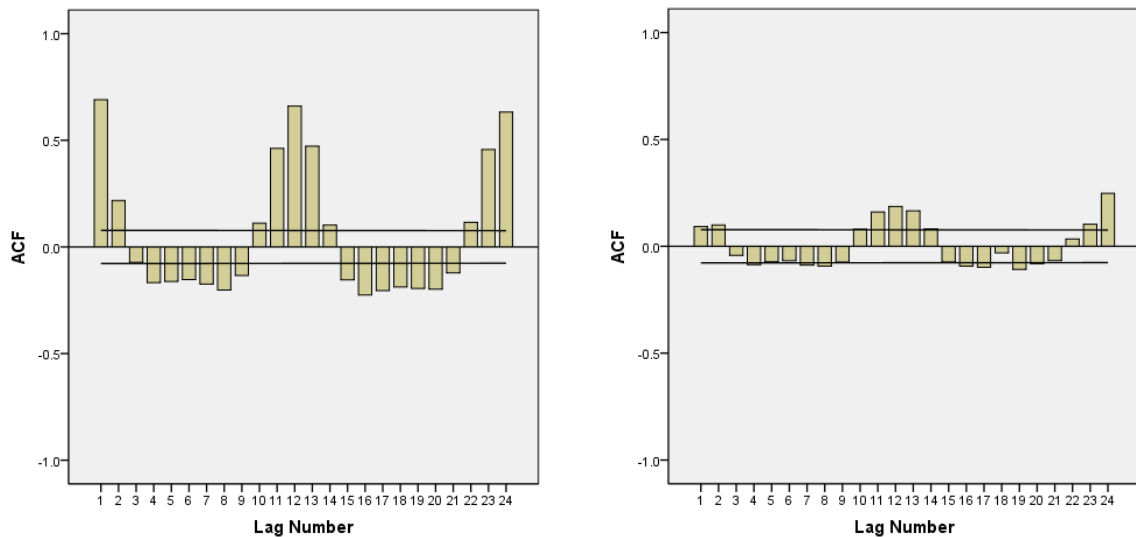


Figure 4.2. Examples of annual cycles in the monthly series (left: Richelieu River; right: Montreal/Pierre Elliot Trudeau) are seen in these correlograms as there are higher ACF values at every 12<sup>th</sup> lag. The upper and lower solid lines represent the confidence intervals.

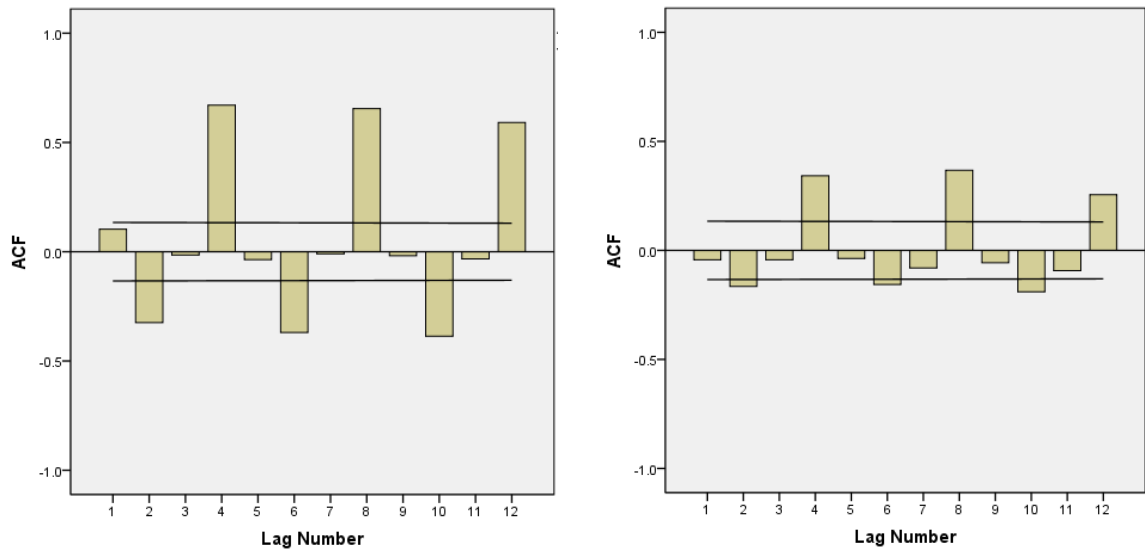


Figure 4.3. Annual cycles are also seen in the seasonally-based series (left: Richelieu River; right: Montreal/Pierre Elliot Trudeau), where the values of ACFs at every 4<sup>th</sup> lag are higher compared to the other lags. The upper and lower solid lines represent the confidence intervals.

#### 4.5.2. Monthly Data Analysis

Each monthly average flow and total precipitation dataset was decomposed into six lower resolution levels via the DWT approach. The detail components represent the 2-month periodicity (D1), 4-month periodicity (D2), 8-month periodicity (D3), 16-month periodicity (D4), 32-month periodicity (D5), and 64-month periodicity (D6). The A6 represents the approximation component at the sixth level of decomposition. Examples of the application of the discrete wavelet transform on monthly flow and precipitation series are shown in figures 4.4 and 4.5, respectively. These figures show the results when the DWT technique is used to decompose a time series. As can be seen, the lower detail levels have higher frequencies, which represent the rapidly changing component of the dataset, whereas the higher detail levels have lower frequencies, which represent the slowly changing component of the dataset. The approximation components (A6) in figures 4.4 and 4.5 represent the slowest changing component of the dataset (including the trend). It should be noted that due to space limitation, the results of every station are not presented graphically. The authors of this paper chose to only include the results of

several stations, which were chosen with the purpose of illustrating the application of the DWT technique in conjunction with the MK trend test.

#### **4.5.2.1. Monthly Average Flow Data**

The application of the MK test on the eight original flow series over the study period showed a mix of positive and negative trends. Increasing trends are seen as being more dominant since five out of the eight flow stations show positive trend values. Three stations experience significant trend values, two being positive (Sydenham River and Richelieu River) and one negative (Missinaibi River). Table 4.5 shows the MK values for the original series, their detail components (Ds), approximations (A6), and the combination of the Ds with the approximation added to them. It can be seen in table 4.5 that except for the D1 components of Black River ( $Z = 2.00$ ) and Eaton River ( $Z = 1.96$ ), none of the MK values of the different individual details (D1-D6) is statistically significant, even for stations whose original series showed significant MK values. For Sydenham River, Richelieu River, and Missinaibi River – whose original MK Z-values are significant, their approximation (A6) trend values are also significant.

A very interesting finding is that after the approximation components (A6) were added to the different details, many of the trend values became statistically significant. This is not only observed for stations with significant original trend values (i.e. Sydenham River, Missinaibi River, and Richelieu River), but also North Magnetawan River, which did not have a significant original trend value ( $Z = +1.09$ ). This is perhaps due to MK Z-value of the A6 component being relatively high ( $Z = 1.85$ ). Higher MK Z-values were also obtained in most cases, after the addition of the A6, compared to the MK values of the corresponding detail (D) alone (table 4.5). In addition, the trend directions after the addition of A6 are also always in agreement with those of the corresponding original data (except for the D1 component for station Eaton River). It is clear that the approximation components have an effect on the original data because these approximations should carry most of the trend component. Furthermore, as supported by the information in table 4.5, the results of the MK trend analysis on the detail components can be better interpreted after the addition of their respective approximation components.

In light of these observations, graphs presented in this study are of the detail components with their respective approximations added. Discussions concerning the detail components also refer to the details plus their approximations. This is also applied to the seasonally-based and the annual data analysis, for both flow and precipitation variables.

Table 4.5. Mann-Kendall values of the monthly flow series: original data, details components (D1-D6), approximations (A6), and a set of combination of the details and their respective approximations. The most effective periodic components for trends are indicated in bold format.

Data	Neebing River	N. Magnetawan River	Black River	Sydenham River	Nagagami River	Missinaibi River	Eaton River	Richelieu River
Original	-0.26	1.09	1.26	3.10*	1.19	-2.05*	-0.42	3.18*
D1	-0.64	0.68	2.00*	-0.95	0.52	-1.25	1.96*	-0.39
D2	-0.37	-0.20	0.38	-0.46	-1.09	0.85	-0.12	-0.38
D3	0.50	0.22	0.77	0.87	-0.32	-0.10	0.00	0.73
D4	0.00	-0.36	-0.10	0.06	0.06	-0.28	-0.21	0.12
D5	-0.06	-0.28	-0.20	-0.02	0.06	-0.06	0.03	-0.18
D6	-0.18	-0.30	0.23	0.15	0.22	0.01	0.50	0.35
A6	-1.17	1.85	1.17	3.08*	1.20	-3.69*	-0.38	3.37*
D1+A6	-1.01	2.47*	1.56	3.47*	1.26	-3.05*	0.14	3.54*
D2+A6	-0.81	2.50*	1.44	3.66*	0.51	<b>-2.53*</b>	-0.15	3.66*
D3+A6	-1.00	2.60*	1.11	<b>3.07*</b>	1.05	-2.73*	-0.10	3.44*
D4+A6	<b>-0.92</b>	2.34*	<b>1.17</b>	<b>2.95*</b>	<b>1.22</b>	-2.70*	-0.49	3.23*
D5+A6	<b>-0.76</b>	<b>1.90</b>	1.13	<b>2.61*</b>	<b>1.17</b>	<b>-2.68*</b>	<b>-0.37</b>	<b>2.91*</b>
D6+A6	-1.62	2.25*	0.99	3.69*	1.15	-2.94*	<b>-0.38</b>	3.64*

\* indicates significant trend values at  $\alpha = 5\%$ .

Since all of the monthly flow data exhibit significant lag-1 ACFs and clearly portray seasonality patterns, the MK values presented in table 4.5 were obtained by using the modified MK test by Hirsch and Slack (1984), which accounts for seasonality and autocorrelation factors. The detail components (with A6) that are considered to be the most representative of the trend in the original data are indicated in table 4.5. The dominant periodic components vary from one station to another, which could be due to their different locations and sizes of drainage area. Generally speaking, the most influential periodicities over the study area are between D3 and D5. This indicates that the events between 8 and 32 months are the main drivers behind the observed trends. An example of how sequential MK graphs of the different periodic components portray their trend lines with respect to those of the original data is shown in figure 4.6 (station used: Sydenham

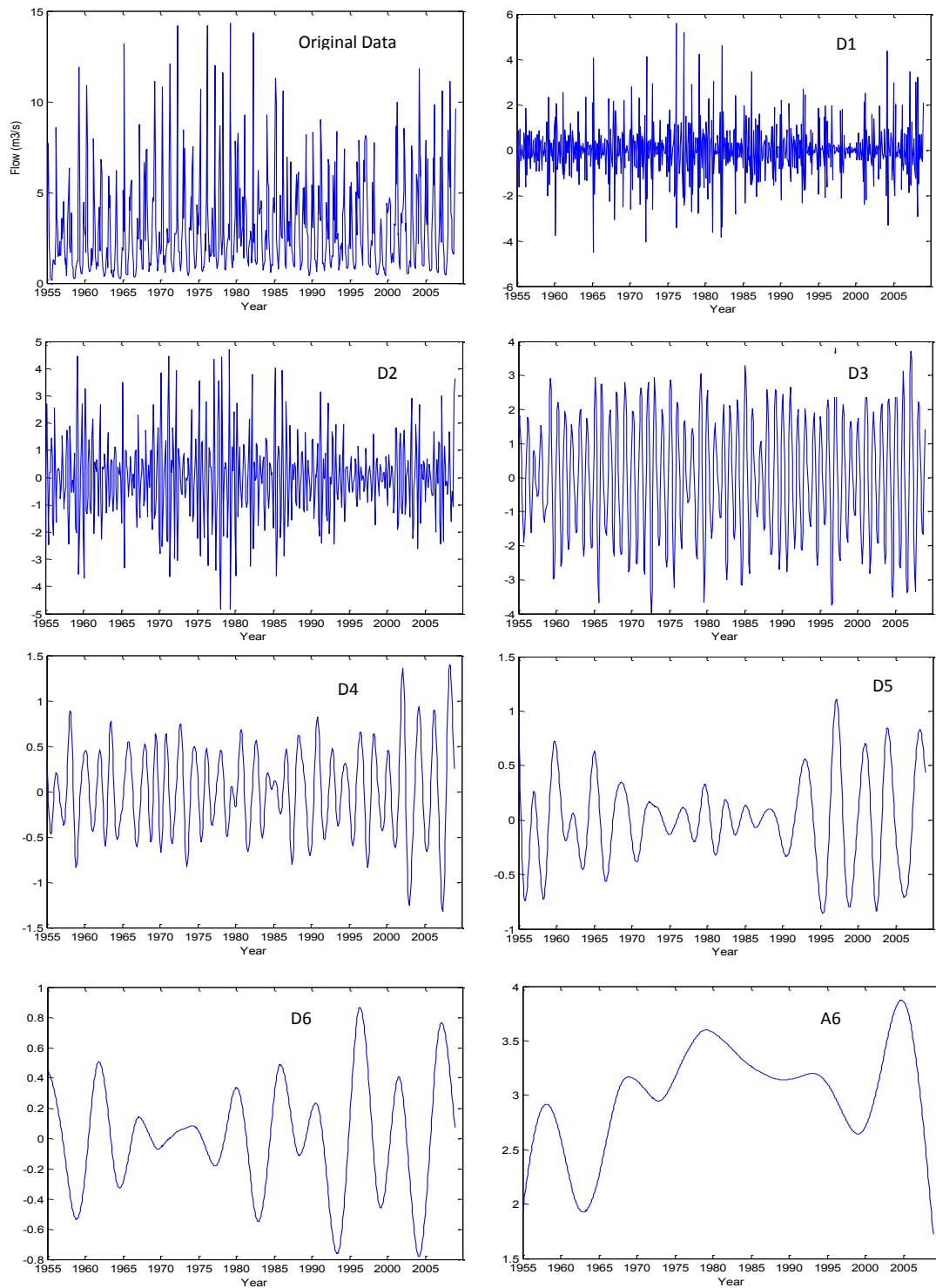


Figure 4.4. Sydenham River's original monthly flow series and its transforms via the DWT using db9 wavelet, into six decomposition levels (D1-D6) and one approximation (A6).

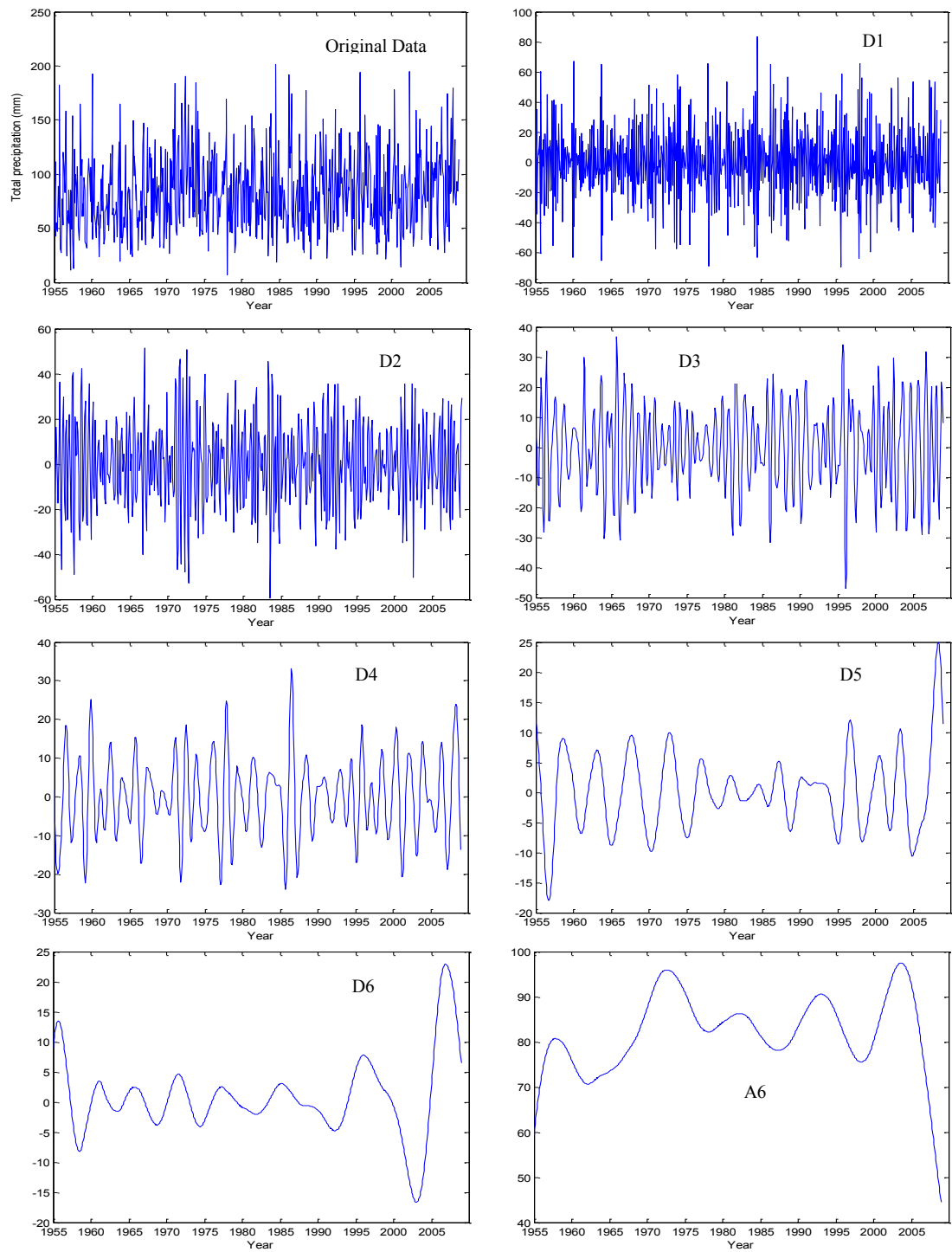


Figure 4.5. Montreal/Pierre Elliot Trudeau's original monthly flow series and its transforms via the DWT using db9 wavelet, into six decomposition levels (D1-D6) and one approximation (A6).



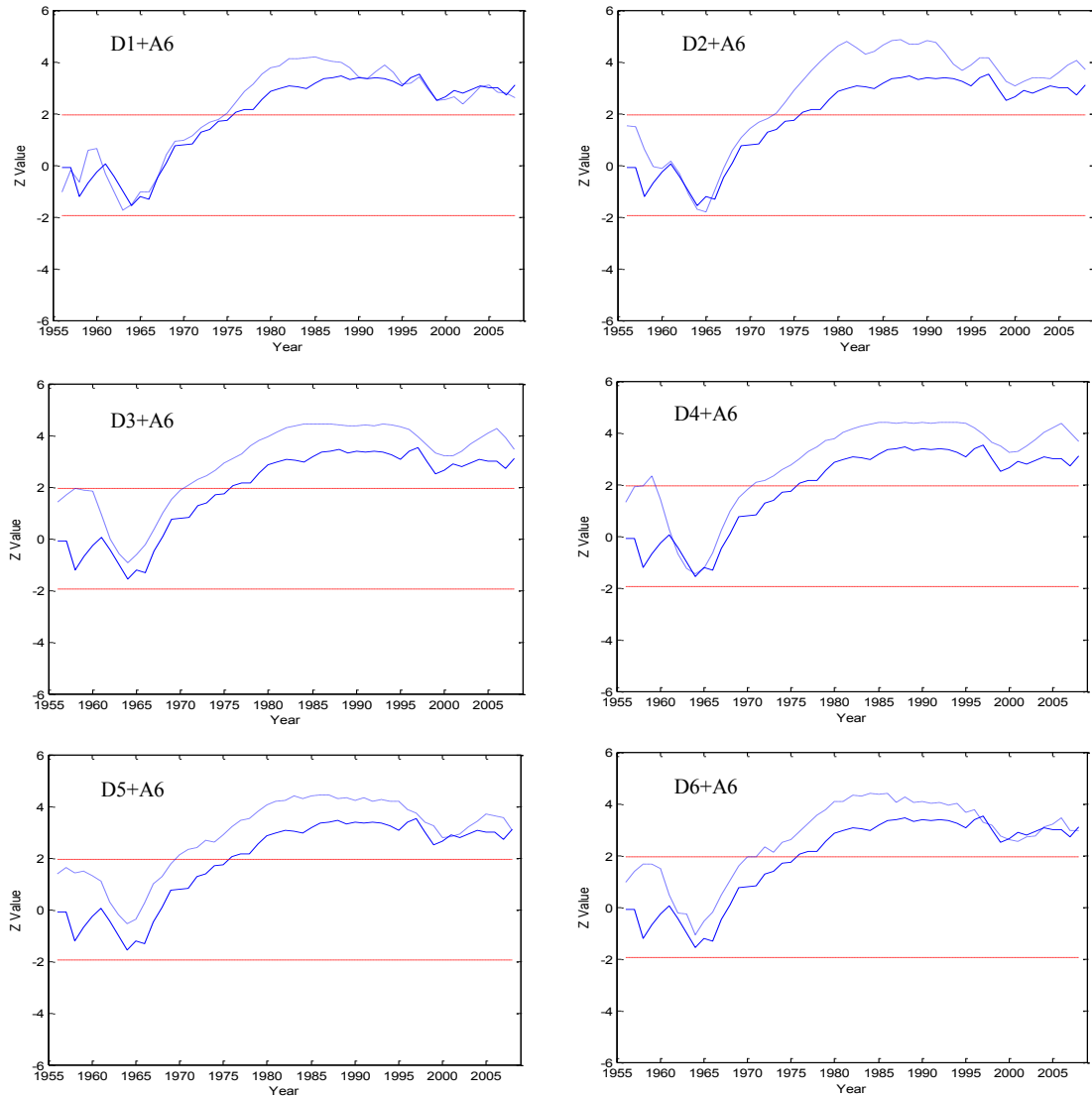


Figure 4.6. Sequential Mann-Kendall graphs of station Sydenham River monthly data displaying the progressive trend lines of each detail (with the approximation added). The upper and lower dashed lines represent the confidence limits ( $\alpha = 5\%$ ); the solid and dashed progressive lines are the original and detail sequential MK lines, respectively.

River). As for the D1 components of the Black River and Eaton River stations, it is seen that they are not the best representative periodic mode and after the addition of the A6 components, the MK Z-values became insignificant. This suggests that the 2-month periodicity is not contributing to the trend for the Black River and Eaton River stations. It also makes sense that the D1 periodicity for these stations is not the most dominant mode, because even though their MK Z-values are significant, the trend values of the original data are not significant.

#### 4.5.2.2. Monthly Total Precipitation Data

For the monthly precipitation data, all the MK values for the original data were positive, except for station Montreal/Pierre Elliot Trudeau, which has a very weak negative trend value ( $Z = -0.0049$ ). Three stations – North Bay A, Ottawa CDA, and Windsor A – had statistically significant upward trend directions with  $Z = +3.67$ ,  $+2.39$ , and  $+2.38$ , respectively. After applying the MK test separately to the detail (D1-D6) and approximation (A6) components of each of the precipitation series, relatively similar findings were encountered to those of the flow results. None of the individual detail components alone showed significant MK values, even for the precipitation stations whose original series exhibited significant trends (table 4.6). Only after the addition of the A6 component did several MK values become statistically significant.

Table 4.6. Mann-Kendall values of the monthly precipitation series: original data, details components (D1-D6), approximations (A6), and a set of combination of the details and their respective approximation. The most effective periodic components for trend are indicated in bold format.

Data	Fort Frances A	Sudbury A	North Bay A	Ottawa CDA	Windsor A	Montreal/Pierre Elliot Trudeau	Bagotville A
Original	0.71	1.85	3.67*	2.39*	2.38*	-0.0049	0.75
D1	-0.23	-0.68	-0.83	-1.09	0.01	0.01	-0.10
D2	0.34	-0.68	0.18	-0.03	-0.05	0.65	0.39
D3	-0.70	-0.32	-0.60	0.23	-0.30	-0.27	-0.93
D4	0.18	-0.13	-0.03	0.15	-0.04	-0.16	0.34
D5	0.02	0.27	0.14	-0.17	0.50	0.28	0.02
D6	-0.33	0.12	0.15	0.16	1.00	0.53	0.43
A6	0.63	2.04*	4.18*	2.41*	3.47*	0.08	0.77
D1+A6	1.20	2.59*	3.43*	1.98*	2.87*	0.07	1.58
D2+A6	1.79	2.72*	3.85*	2.01*	3.05*	0.73	1.03
D3+A6	1.28	2.62*	3.78*	2.12*	3.43*	-0.23	0.92
D4+A6	1.01	2.06*	3.45*	1.85	1.87	<b>-0.08</b>	1.08
D5+A6	<b>0.76</b>	<b>1.79</b>	<b>3.64*</b>	2.00*	<b>2.84*</b>	<b>0.22</b>	<b>0.73</b>
D6+A6	1.03	2.98*	4.15*	<b>2.68*</b>	2.93*	0.61	1.29

\* indicates significant trend values at  $\alpha = 5\%$ .

Due to the presence of seasonality cycles, and in some, autocorrelation, the MK test by Hirsch and Slack (1984) was used in the monthly total precipitation data analysis. The results of the monthly precipitation data analysis show how the approximation

components of the decomposition affect the detail components by increasing their trend values (in most cases) as reflected by the higher MK values (table 4.6). This shows that the trend component is indeed contained within the approximation part of the wavelet transform, implying that the trends are changing slowly and gradually (see the A6 graphs in figures 4.4 and 4.5); and are perhaps long-term. Some of the long-term trend values are statistically significant, as shown by the  $Z$  values of the approximation components in table 4.6. The abrupt fluctuations can be considered noise and are reflected in the lower details (Ds) – these alone are not significant. Table 4.6 also shows that for most of the stations higher periodic modes (especially D5) are more prominent in affecting the trend structures found in the monthly total precipitation data. As with the flow monthly data analysis, the trends are mostly affected by higher periodicities (low-frequency events). Here, the importance of decomposing a dataset prior to analyzing its trends using the wavelet transform is highlighted. Although the application of the MK test on the original data did not necessarily show the presence of significant trends, the results of the application of the MK test on the decomposed data may reveal some significant values.

#### **4.5.3. Seasonally-based Data Analysis**

The presence of annual cycles in the monthly-based time series analysis led us to incorporate the seasonally-based data in our trend analysis. Again, the seasonally-based data also confirms the presence of annual cycles in some datasets as the ACFs show high values at every 4<sup>th</sup> lag (examples are given in figure 4.3). Each seasonally-based time series was decomposed into four detail components (D1-D4) and one approximation (A4). D1, D2, D3, and D4 represent the 6-month, 12-month, 24-month, and 48-month fluctuations, respectively. The A4 component corresponds to the approximation of the fourth decomposition level. As can be seen, the D2 component in the seasonally-based data decomposition represents the annual (12-month) periodicity. This is very useful in determining whether or not the annual cycles can explain the trends found in the flow and precipitation data.

Most of the first level of decomposition (D1) of the seasonally-based series – and sometimes the D2 component as well – portray a strong yearly cycle because the

corresponding ACF values are high at every 4<sup>th</sup> lag (illustrated in figure 4.7). The repeating cycles do not dampen over time. Oscillating patterns may also be observed at higher decomposition levels, but they dampen as the number of lags increases (see figure 4.8 for example). Similar behavior was also seen in the components resulting from the addition of each detail to its approximation (D+A4). The oscillations observed in the correlograms of the lower decomposition levels are actually expected because they should capture the oscillating properties (such as the seasonality) of the time series, thus filtering the stochastic components of the time series (Popoola, 2007). On the other hand, the ACFs of the approximation component should not have any oscillating behavior or behave in the manner of seasonal fluctuations, even if the original time series shows seasonality patterns (Popoola, 2007). Figure 4.9 displays the ACFs of several approximation components (A4 in this case); as can be seen, there is an absence of oscillatory patterns.

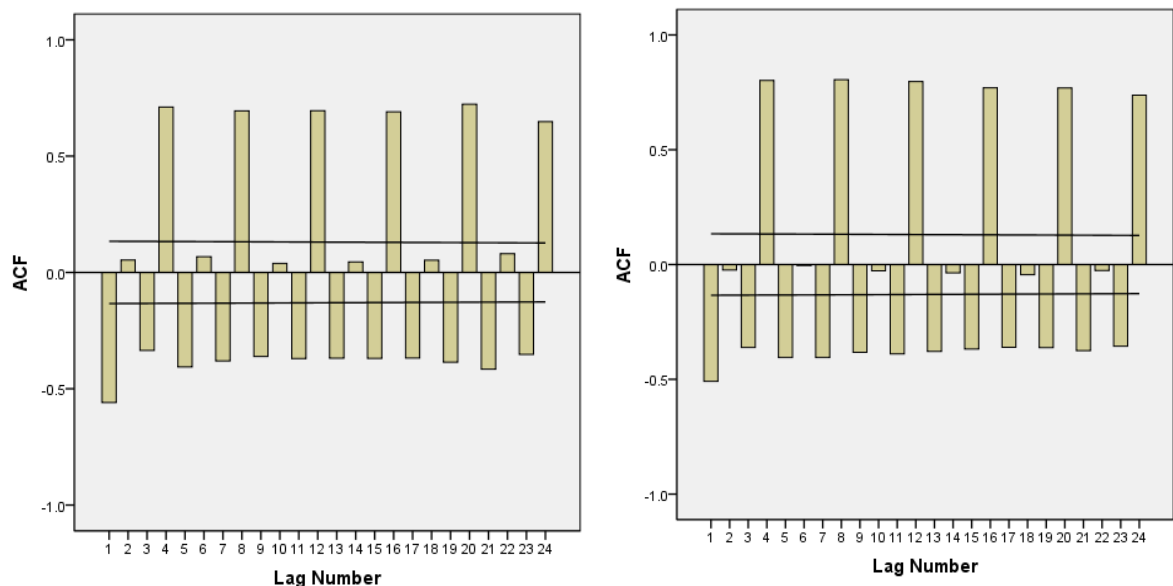


Figure 4.7. Examples of correlograms of the D1 periodic components (left: Neebing River; right: Missinaibi River) of the seasonally-based data, which display strong annual cycles as seen in their repeated high values at every 4<sup>th</sup> lag. Note that the cycles do not dampen over time.

#### 4.5.3.1. Seasonally-based Average Flow Data

As with the monthly flow data analysis, there is also a mix of positive and negative trends observed in the seasonally-based flow data. In fact, the directions of trend of the seasonally-based datasets are in agreement with the directions of their monthly data counterparts. For example, Neebing River, Missinaibi River and Eaton River stations experience negative trends in their monthly data, and also in their seasonally-based data. Only two out of the eight flow stations showed statistically significant trends: Sydenham River ( $Z = +3.13$ ) and Richelieu River ( $Z = +3.06$ ) (table 4.7).

Table 4.7 shows that none of the individual detail components alone (including D2) showed statistically significant MK Z-values. Again, after the addition of the A4s to their respective details, many of the MK Z-values became higher and statistically significant, emphasizing that the approximations carry most of the trend component. An example of the sequential MK analysis is shown in figure 4.10 (station used: Sydenham River).

As shown in table 4.7, none of the most dominant periodicities were represented by the D1 component, indicating that the 6-month fluctuation is not responsible for the observed trend. There are four stations for which the D2 components represent one of the most dominant periodicities affecting the observed trends. These stations are: Black River, Nagagami River, Missinaibi River, and Eaton River. Therefore, for these stations, their trends are affected by the annual periodicities (the MK sequential graphs for these D2 components are given in figure 4.11). The D3 and D4 components, which represent the 24- and 48-month time modes, are also seen to be important in affecting the trends.

It can be seen that the seasonally-based data are important variables to be included to assess the flow and precipitation trends in this study. This is because the monthly-based data analysis skipped the 12-month time scale as the third and fourth dyadic scales in the monthly data decomposition correspond to 8 and 16 months, respectively.

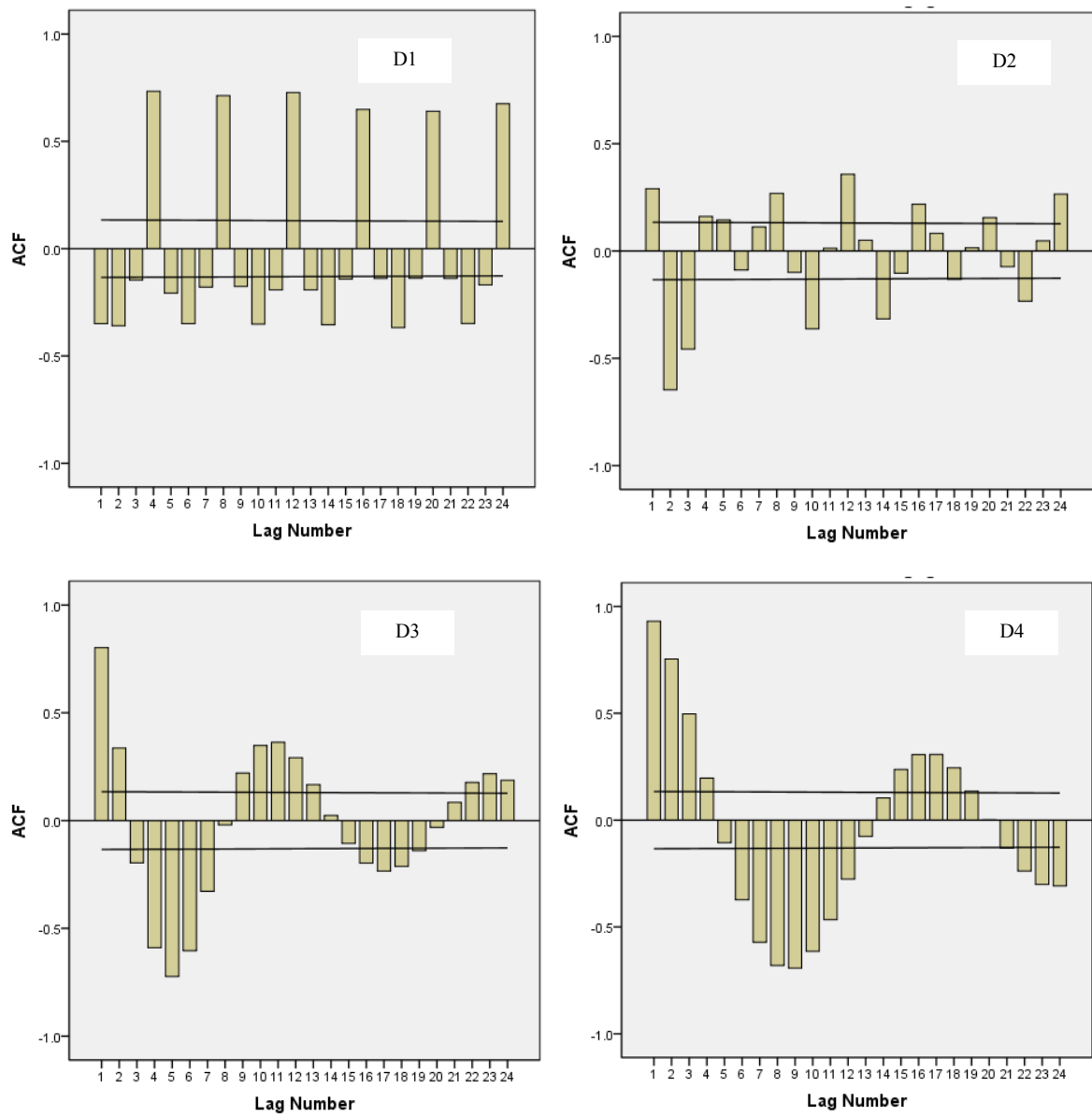


Figure 4.8. The correlograms of the D1-D4 components of Nagagami River's seasonally-based data. The D1 and D2 components have high ACF values at every 4<sup>th</sup> lag, which indicates the presence of 12-month cycles. D3 and D4 show some patterns of oscillations that may dampen over time, which are not considered annual cycles.

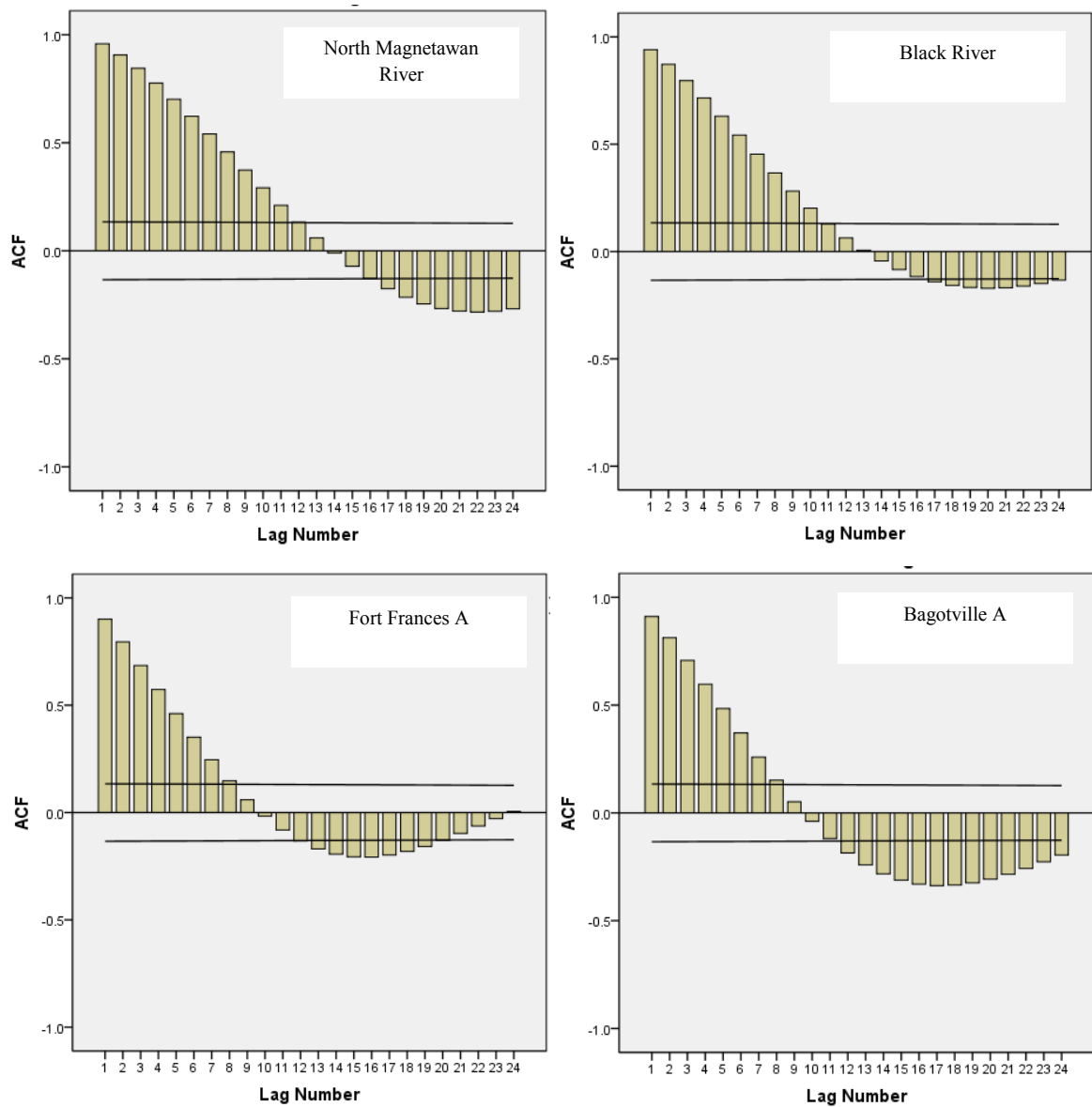


Figure 4.9. The correlograms of several approximation components (A4) of the seasonally-based data showing a lack of constant oscillations.

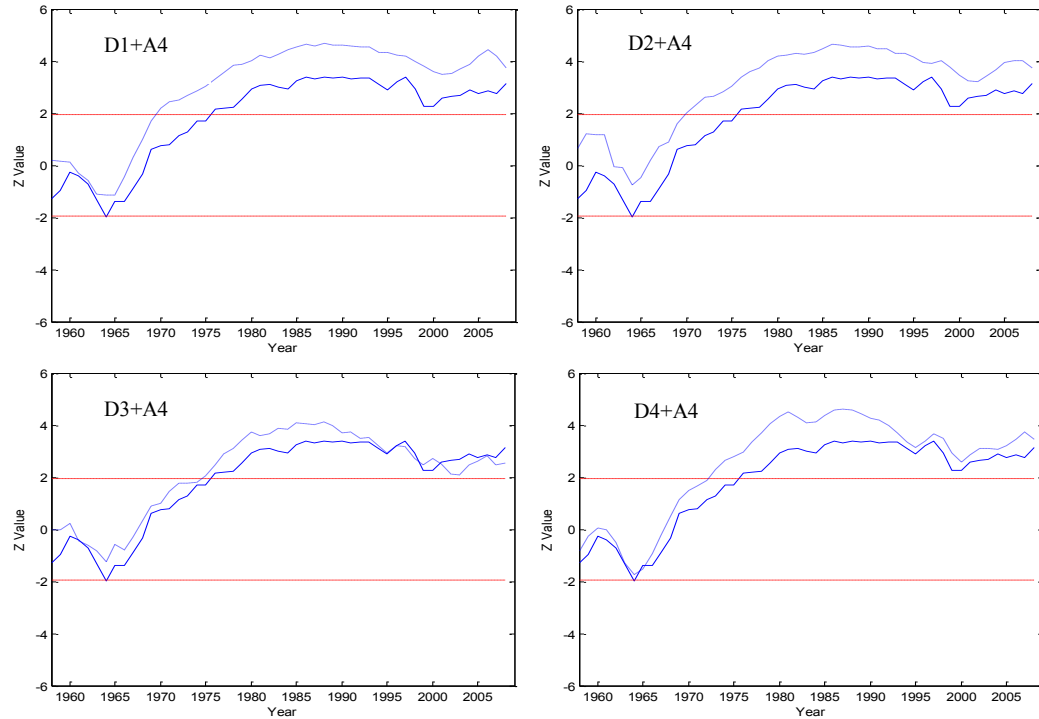


Figure 4.10. Illustration of the sequential Mann-Kendall graphs of the D1 – D4 components (with approximation) of the seasonally-based data in order to determine the most dominant periodic component for trend (Sydenham River's data were used in this example). The upper and lower dashed lines represent the confidence limits ( $\alpha = 5\%$ ); the solid and dashed progressive lines are the original and detail component sequential MK lines, respectively.

#### 4.5.3.2. Seasonally-based Total Precipitation Data

All the MK Z-values for the original seasonally-based total precipitation data showed positive trends (table 4.8); three stations experienced statistically significant trends: North Bay A ( $Z = 2.81$ ), Ottawa CDA ( $Z = 2.31$ ), and Windsor A ( $Z = 2.39$ ), which is in agreement with the results of the monthly total precipitation data. Again, it is seen that none of the individual detail components show significant trend values. Significant trends that were observed for A4 components belong to the three stations that have significant original trend values. The MK values of the detail components for the stations whose A4 components were not significant (Fort Frances, Sudbury A, Montreal/Pierre Elliot Trudeau, and Bagotville A) remain insignificant even after the addition of their respective approximations. This may indicate that the long-term trends



for these stations are not statistically significant as shown by their A4 components of the annual data, which were indeed insignificant and have the lowest absolute MK Z-values (see the following subsections).

Table 4.8 also shows the periodic components that are the most influential in affecting the trends in the seasonally-based total precipitation data. It is seen that the annual periodicity (D2) does not contribute to the trend production in the total precipitation data. This insignificant contribution can also be partly explained by the weaker annual cycles observed in the precipitation data, in comparison to the flow data. Most of the precipitation trends are affected by the D3 and D4 components, except for station North Bay A, where D1 is considered the most dominant periodic component. We can suggest that the periodic components that mainly affect trends in the seasonally-based total precipitation are the 24- to 48-month time scales (2-4 years). An example of the sequential MK graphs for the different periodic components portraying their trend lines with respect to their original data is given in figure 4.12 (station used: Ottawa CDA).

Table 4.7. Mann-Kendall values of the seasonally-based flow series: original data, details components (D1-D4), approximations (A4), and a set of combination of the details and their respective approximations. The most dominant periodic components for trend are indicated in bold format.

Data	Neebing River	N. Magnetawan River	Black River	Sydenham River	Nagagami River	Missinaibi River	Eaton River	Richelieu River
Original	-0.27	1.43	1.36	3.13*	1.31	-1.78	-0.22	3.06*
D1	-0.43	-0.20	0.89	-0.85	0.60	-0.43	-0.06	-0.45
D2	-0.05	0.44	-0.46	0.61	-0.07	0.14	0.01	0.00
D3	0.21	-0.59	0.16	-0.29	0.01	0.18	0.05	0.05
D4	0.10	0.52	0.38	-0.27	0.00	0.14	-0.11	-0.04
A4	-1.10	1.43	1.24	2.99*	1.53	-3.59*	-0.77	3.52*
D1+A4	-0.82	2.36*	0.91	3.75*	1.76	-3.19*	-0.72	3.70*
D2+A4	-0.99	2.09*	<b>1.52</b>	3.73*	<b>1.14</b>	<b>-2.32*</b>	<b>-0.53</b>	3.76*
D3+A4	<b>-0.45</b>	<b>1.64</b>	0.92	2.54*	1.80	<b>-2.48*</b>	<b>-0.54</b>	<b>2.97*</b>
D4+A4	-1.05	<b>1.83</b>	<b>0.81</b>	<b>3.47*</b>	<b>1.36</b>	-2.81*	-1.17	<b>3.51*</b>

\* indicates significant trend values at  $\alpha = 5\%$ .

Table 4.8. Mann-Kendall values of the seasonally-based precipitation series: original data, details components (D1-D4), approximations (A4), and a set of combination of the details and their respective approximation. The most dominant periodic components for trends are indicated in bold format.

Data	Fort Frances A	Sudbury A	North Bay A	Ottawa CDA	Windsor A	Montreal/Pierre Elliot Trudeau	Bagotville A
Original	0.72	1.32	2.81*	2.31*	2.39*	0.15	0.77
D1	0.29	-0.66	-0.51	0.47	-0.11	-1.70	-0.96
D2	0.00	0.04	-0.23	-0.45	0.31	0.43	0.22
D3	0.15	0.16	-0.02	0.41	-0.41	-0.25	0.06
D4	0.59	0.00	0.93	0.22	-0.20	-0.19	0.21
A4	0.81	1.76	5.09*	2.31*	2.41*	0.19	0.62
D1+A4	1.45	1.55	<b>3.39*</b>	2.94*	2.09*	-0.17	0.64
D2+A4	0.21	1.53	4.13*	2.17*	2.23*	0.03	0.63
D3+A4	<b>0.64</b>	1.55	4.01*	<b>2.35*</b>	1.21	-0.40	0.33
D4+A4	1.12	<b>1.17</b>	4.12*	<b>2.59*</b>	<b>2.36*</b>	<b>0.02</b>	<b>0.72</b>

\* indicates significant trend values at  $\alpha = 5\%$ .

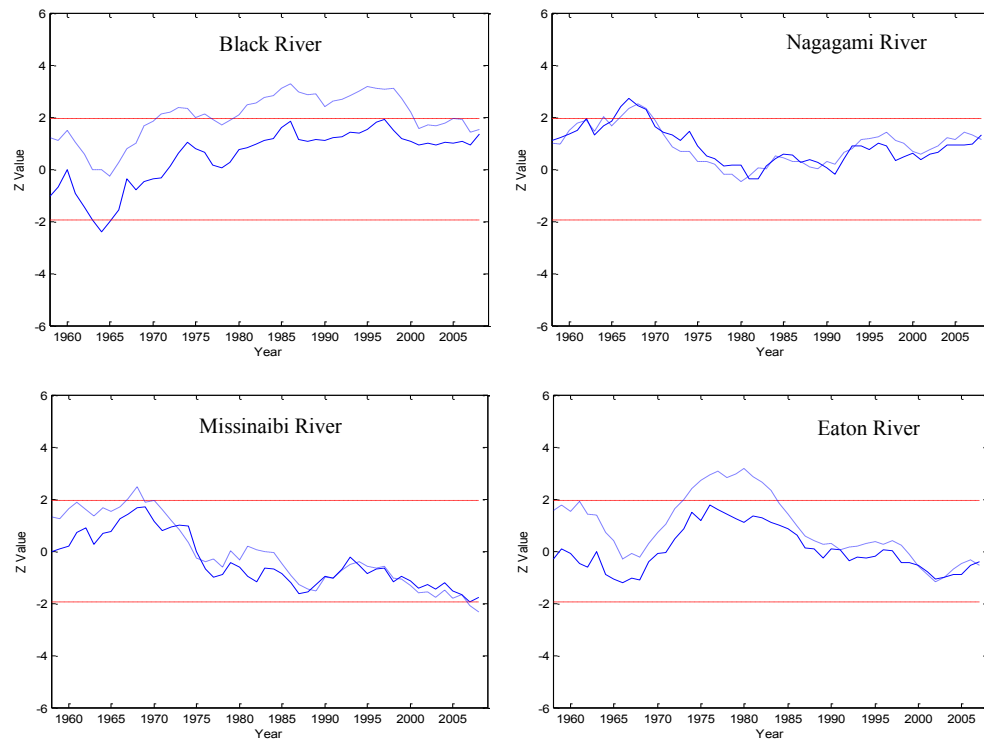


Figure 4.11. Sequential Mann-Kendall graphs of the D2 components, which represent the 12-month periodic components from several seasonally-based flow data. These trend lines show good matches with respect their original trend lines. The upper and lower dashed lines represent the confidence limits ( $\alpha = 5\%$ ); the solid and dashed progressive lines are the original and detail component sequential MK lines, respectively.

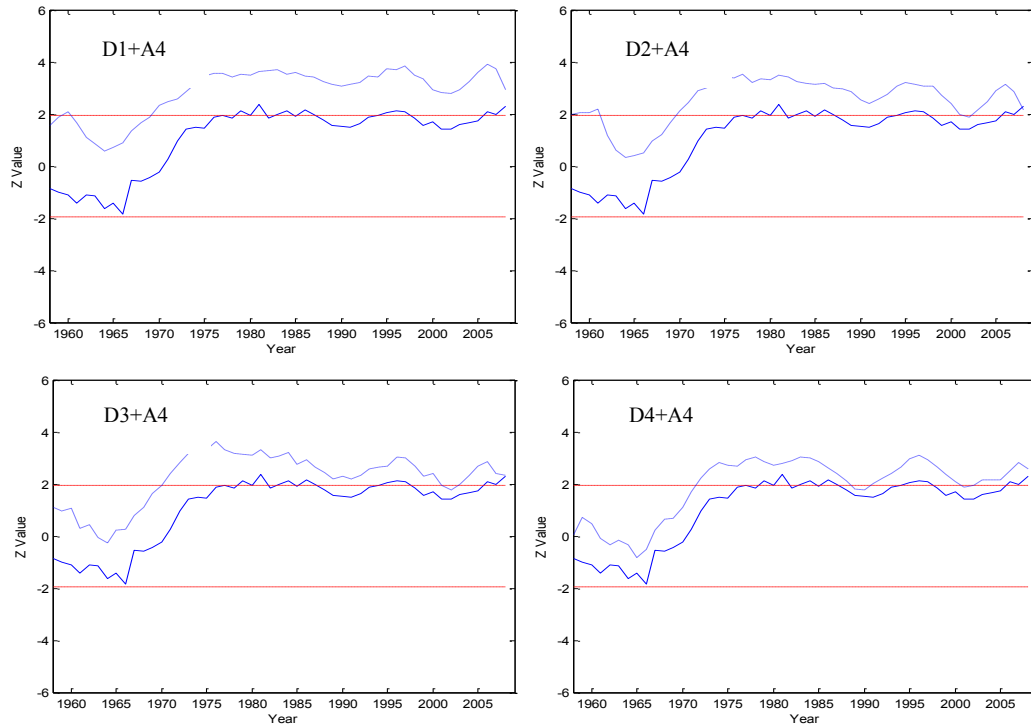


Figure 4.12. Progressive Mann-Kendall graphs of the components of the seasonally-based precipitation data from Ottawa CDA station. The upper and lower dashed lines represent the confidence limits ( $\alpha = 5\%$ ); the solid and dashed progressive lines are the original and detail sequential MK lines, respectively. Based on the MK values and the sequential MK graphs, D3 and D4 (with approximations) were determined to be the most effective periodic components contributing to the trend production.

#### 4.5.4. Annual Data Analysis

The trend analysis of the monthly and seasonally-based data suggests that there is a possibility of longer time-periodicity than just 48 and 64 months (which are the last periodic modes in the seasonally-based and monthly data decompositions, respectively). Many of the trends in the monthly and seasonally-based data are influenced by the higher time periodic components (i.e. lower-frequency events). The argument that there may be higher time periodicities affecting the trend in streamflow and precipitation is also reflected in the approximation components of the DWTs, which should carry the trend element (slowest-changing events) of the time series: (1) many approximation components in the data analysis showed significant MK Z-values; and (2) higher MK Z-

values of the detail components were observed after the addition of their respective approximations. Annual time series were then analyzed in order to obtain a more thorough trend analysis. Each annual time series was decomposed into four levels, which correspond to the 2-year, 4-year, 8-year and 16-year variations.

Although there is a mixture of positive and negative trends in the annual flow, most of the stations exhibit positive trends. Three streamflow stations have experienced significant trend: Sydenham River ( $Z = 2.37$ ), Missinaibi River ( $Z = -2.23$ ), and Richelieu River ( $Z = 2.92$ ) (table 4.9). Indeed, most studies focusing on streamflow trends in Canada have generally found that the flow trends in Canadian rivers are not uniform. There are areas that experience positive trends while others are experiencing negative trends (due to factors such as temperature, amount of precipitation, and evapotranspiration).

For the annual total precipitation, only stations North Bay A ( $Z = +3.57$ ) and Ottawa CDA ( $Z = +2.50$ ) experienced significant trend values (table 4.10). It is worth mentioning that all of the original annual precipitation data (as well as most of the monthly and seasonally-based precipitation data) show positive trend values – this prevalent increase in trends in the total precipitation seen in this study are in agreement with findings from several other precipitation studies. For example: Mekis and Hogg (1999) found that total annual precipitation in many parts of Canada is on the rise; Stone et al. (2000) reported that total annual precipitation in the south of Canada experienced an increase (from 1895-1996); Zhang et al. (2000) found that the total annual precipitation has increased across Canada by 5%-35%. Groleau et al. (2007) also found that 30% of the weather stations in southern Quebec and New Brunswick, Canada, experienced significant positive trends during winter rainfall.

The periodic component(s) considered the most influential in affecting trends in flow and precipitation data are indicated in tables 4.9 and 4.10, respectively. Examples of determining the most dominant periodic components that affect the production of trends in annual flow and precipitation series are given in figures 4.13 and 4.14, respectively. There are a few individual detail components (without approximation) that showed significant trend values (tables 4.9 and 4.10). However, these components do not end up being considered the most influential time periodicities to affect the trends. For example,

in table 4.9, the MK Z-value of the D4 component of Black River station is 2.38, but it is not found to be the most dominant periodic component for trend. It is also seen that the difference in MK Z-value between the D4 (with approximation) and the original data is high. It is therefore not expected that the D4 detail component in Black River station would be the most influential component to affect the trend. This illustrates that when analyzing trends in a dataset via the wavelet transform, not only should the final MK value for the different components be considered, but also their sequential MK values in comparison to the original data. Tables 4.9 and 4.10 show that the dominant periodic components playing major roles in affecting the trends in the annual data are not uniform. The most common dominant periodicities are D1 and D2 (both with approximations added). This is an indication that the trends in the annual data over the study area are mainly characterized by 2- to 4-year periodic events (interannual fluctuations).

Table 4.9. Mann-Kendall values of the annual flow series: original data, details components (D1-D4), approximations (A4), and a set of combination of the details and their respective approximation. The most influential periodic components for trends are indicated in bold format.

Data	Neebing River	N. Magnetawan River	Black River	Sydenham River	Nagagami River	Missinaibi River	Eaton River	Richelieu River
Original	-0.50	0.91	0.73	2.37*	1.12	-2.23*	-0.46	2.92*
D1	-0.13	0.00	-0.19	-0.01	0.15	-0.16	0.22	0.19
D2	-0.04	0.30	0.10	-0.15	0.17	-0.15	0.27	0.12
D3	0.57	-0.13	0.06	0.51	0.25	-0.30	-0.28	0.46
D4	-1.63	3.66*	2.38*	2.15*	1.22	-0.41	-0.55	0.15
A4	-0.48	1.80	1.15	2.66*	1.96*	-2.12*	-0.79	3.09*
D1+A4	<b>-0.57</b>	<b>1.39</b>	0.55	1.42	0.49	-1.73	<b>-0.60</b>	2.61*
D2+A4	<b>-0.73</b>	1.55	<b>0.68</b>	1.47	<b>0.96</b>	<b>-2.12*</b>	-0.87	2.98*
D3+A4	-0.19	<b>0.94</b>	0.80	<b>2.51*</b>	0.94	-2.47*	-0.97	1.99*
D4+A4	-3.03*	3.95*	4.33*	3.17*	3.44*	-4.57*	-1.16	<b>3.09*</b>

\* indicates significant trend values at  $\alpha = 5\%$ .

The progressive MK graphs of the annual data give indications that most of the trends – positive or negative – visibly started during the period from 1965 to early 1970s (figures 4.15 and 4.16). This timing is important as it has been noticed in several Canadian studies that 1970 serves as a point of change in streamflow and precipitation activities in relation to the atmospheric variability affecting Canadian climate, such as the Pacific/North America teleconnection (PNA) and the North Atlantic Oscillation (NAO).

Indeed, these periodic modes may also be associated with the North Atlantic Oscillation (NAO), which has one of its main peaks centered at 2 years (Cook et al., 1998; Anctil and Coulibaly, 2004). Fu et al. (2012), who studied the influence of solar activities and El Niño on streamflow in southern Canada, indicated that there is a correlation between streamflow activities and solar activities at 11 and 22 years. The correlation between streamflow activities in southern Canada and the El Niño cycles is at the 2-7 year periodicities (Fu et al., 2012). The combined effect of solar activities and El Niño is found at 18-32 years (Fu et al., 2012). Here, as can be observed in table 4.9, the most common dominant periodicities are 2-4 years, which could also be related to the El Niño effect. The Richelieu River's most dominant periodicity is the 16-year mode, which may be a result of the combined effect of solar activities and the El Niño cycle. Prokoph et al. (2012) also found that the maximum annual streamflow activities in southern Canada have strong 11-year cycles, which match the 11-year solar radiation activities. It is also suggested that the effects of ENSO and NAO on precipitation, which in turn affect the streamflow activities in southern Canada, are also evident (Prokoph et al., 2012). It is very likely that multiple factors are affecting the precipitation and streamflow trends over the study area.

Table 4.10. Mann-Kendall values of the annual precipitation series: original data, details components (D1-D4), approximations (A4), and a set of combination of the details and their respective approximation. The most influential periodic components for trends are indicated in bold format.

Data	Fort Frances A	Sudbury A	North Bay A	Ottawa CDA	Windsor A	Montreal/Pierre Elliot Trudeau	Bagotville A
Original	0.68	1.24	3.57*	2.50*	1.70	0.33	0.95
D1	0.54	-0.16	-0.13	-0.41	0.04	0.06	-0.33
D2	0.12	-0.28	0.39	0.19	0.33	0.25	-0.55
D3	0.00	-0.18	0.70	0.49	0.96	0.58	0.99
D4	1.32	2.51*	1.87	3.21*	2.31*	-0.70	1.09
A4	1.22	1.45	4.91*	2.45*	2.15*	-0.02	1.28
D1+A4	<b>0.68</b>	<b>1.34</b>	2.35*	0.00	<b>1.05</b>	<b>-0.31</b>	-0.29
D2+A4	1.06	<b>1.39</b>	<b>3.51*</b>	0.51	<b>1.93</b>	<b>0.00</b>	-0.12
D3+A4	0.65	2.45*	4.27*	<b>1.84</b>	3.27*	0.25	<b>0.90</b>
D4+A4	2.89*	3.82*	5.31*	3.14*	5.26*	-0.91	1.63

\* indicates significant trend values at  $\alpha = 5\%$ .

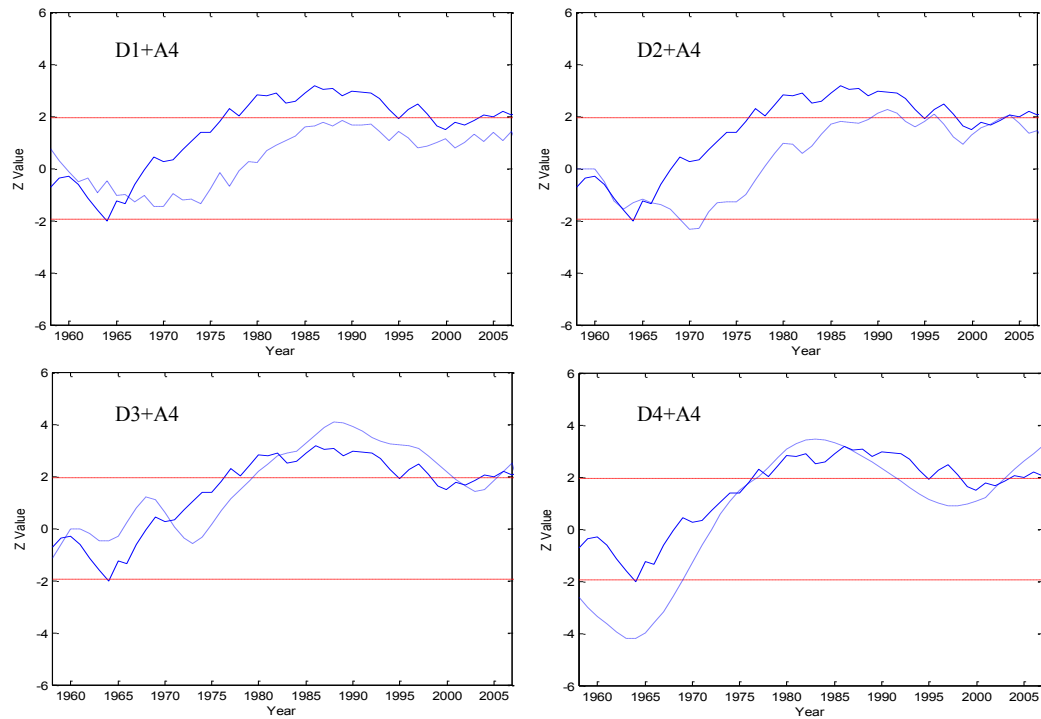


Figure 4.13. Examples of sequential Mann-Kendall graphs of the detail components of the annual flow data in order to determine the most dominant periodicity for trends (Sydenham River's data were used in this example). The upper and lower dashed lines represent the confidence limits ( $\alpha = 5\%$ ); the solid and dashed progressive lines are the original and detail sequential MK lines, respectively.

In Figure 4.15 it is observed that at six out of the eight flow stations, there were upward trends that started between 1965 and 1970. In four out of these six stations, the trends stopped between 1980 and 1985, followed by either downward trends or no trends. Figure 4.16 shows that positive trends started around 1965 at five out of the seven meteorological stations. Anctil and Coulibaly (2004), who analyzed the interannual variability of Quebec streamflow, also placed an importance on the year 1970 because there was a positive correlation between the streamflow activity (especially at the 2-3 year band) and the PNA index since around 1970. Similarly, Coulibaly and Burn (2004), who analyzed annual Canadian streamflow, also found 1970 as the change point in flow activity. They found that the PNA and the NAO are the main dominant teleconnection patterns for the period of 1950-1999 and after 1970, respectively (Coulibaly and Burn, 2004). Stone et al. (2000) studied the variability in Canadian precipitation and its

intensity and related them to the PNA and NAO. Different seasons and regions responded differently to the atmospheric variation, but both the NAO and the PNA were found to have a statistical significance in affecting precipitation intensity over Canada. For example, the NAO (positive phase) has a significant impact, which affected the precipitation intensity during a few three-month seasons in eastern Canada (Stone et al. 2000). The NAO has been in a positive phase since around 1970 (Anctil and Coulibaly, 2004). The PNA also significantly affected the precipitation increase during autumn and winter seasons in Ontario and southern Quebec, during the second half of the 20<sup>th</sup> century (Stone et al., 2000). Therefore, the trends observed in this study, both in flow and precipitation data, could be related to the activity of these influential hydroclimatic indices.

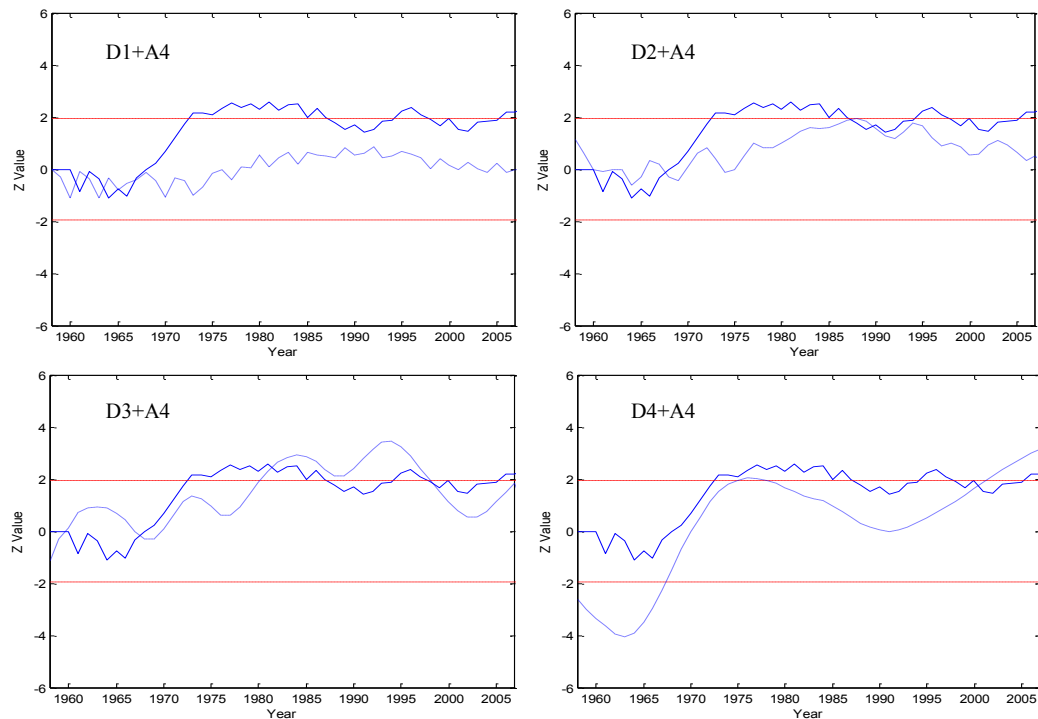


Figure 4.14. Examples of sequential Mann-Kendall graphs of the detail components of the annual precipitation data in order to determine the most dominant periodicity for trends (Ottawa CDA's data were used in this example). The upper and lower dashed lines represent the confidence limits ( $\alpha = 5\%$ ); the solid and dashed progressive lines are the original and detail sequential MK lines, respectively.



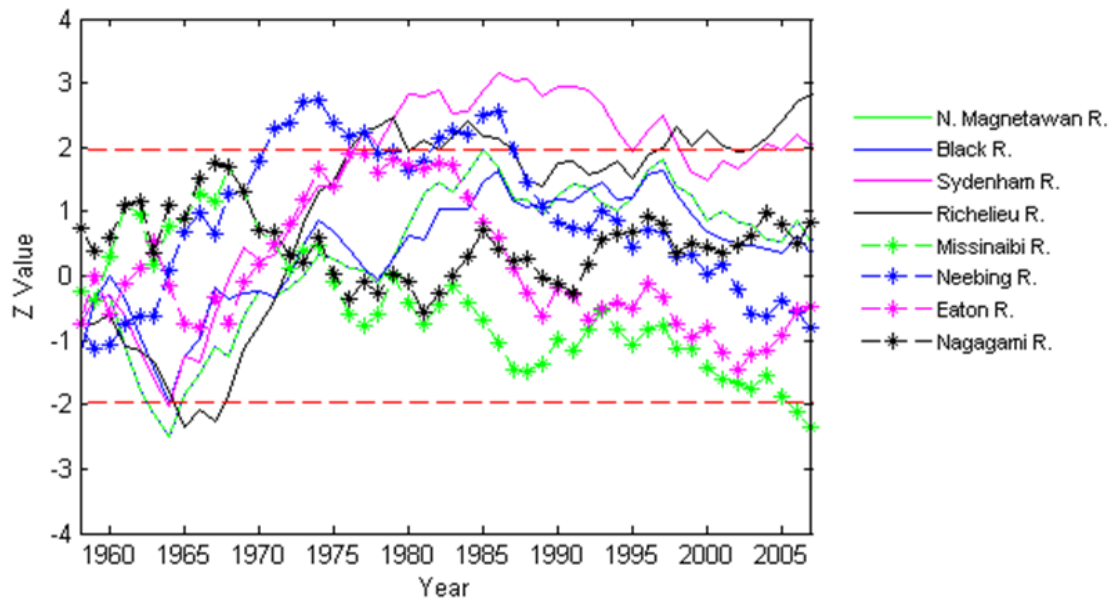


Figure 4.15. Progressive Mann-Kendall graphs of all the original annual flow data used in the study. The upper and lower dashed lines represent the confidence limits ( $\alpha = 5\%$ ). These graphs were used to determine the possible starting time of the observed trends for the different stations.

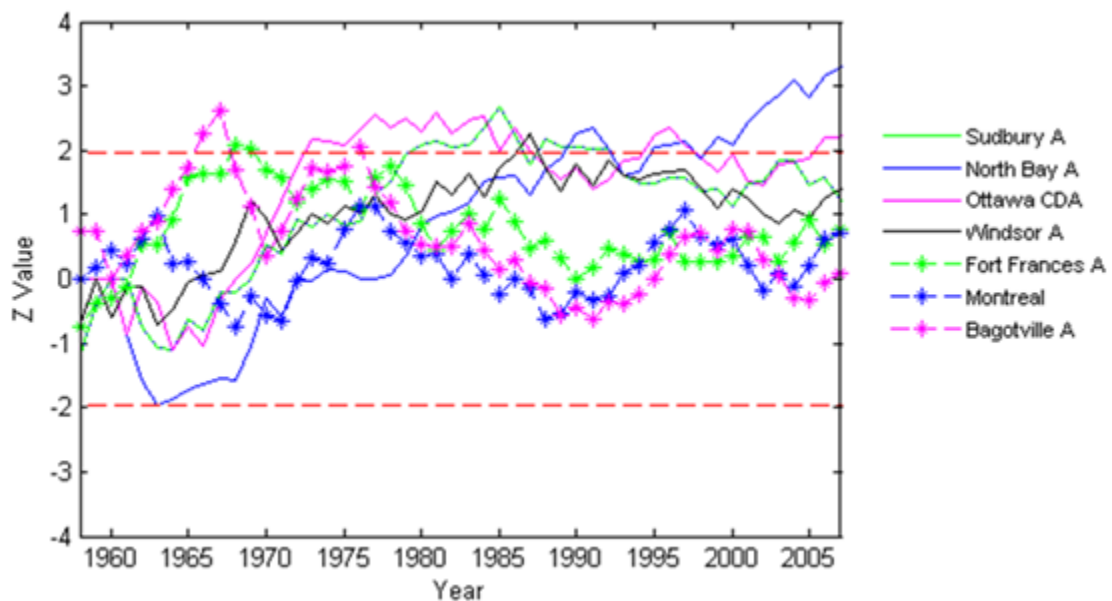


Figure 4.16. Progressive Mann-Kendall graphs of all the original precipitation data used in the study. The upper and lower dashed lines represent the confidence limits ( $\alpha = 5\%$ ). These graphs were used to determine the possible starting time of the observed trends for the different stations.

#### 4.6. Conclusions and Recommendations

The DWT and the MK tests were applied on the mean flow and total precipitation datasets, over southern parts of Quebec and Ontario, in order to analyze their trends. The results of the trend analysis showed that there are positive and negative trends; however, they were dominated mostly by positive trends. In order to determine the most appropriate Daubechies (db) wavelet type and border condition in the DWT procedure, not only were the *MREs* considered, but also the MK Z-value relative errors. This additional criterion proposed in this study was found to be very useful because the differences in the  $e_r e_r$  were much more noticeable compared to the differences in the *MREs*. In this study, the proposed relative error criterion served as a better indicator in determining the number of decomposition levels, the mother wavelet, as well as the extension border to be used in the data analysis – these issues have not been addressed properly or in any detail in the existing literature.

Although the periodic components that affect the trends are not all the same for all stations, a generalization can be made. For the monthly, seasonally-based, and annual flow data analysis, the most common periodic components that were found to be the most effective in producing the observed trends are 8-32 months, 12-48 months (1-4 years), and 2-4 years, respectively. For the monthly, seasonally-based, and annual precipitation analysis, the periodicities most commonly seen as the most important components are 32-months, 24-48 months (2-4 years), and 2-4 years, respectively. This may be correlated to the NAO cycle because one of the main peaks of the NAO cycles is centered around 2.1years (Cook et al., 1998; Anctil and Coulibaly, 2004), which seem to coincide with many of the main periodic components of the lower resolution data found in this study. As can be seen, the different data types produced relatively similar conclusions in terms of the most influential periodicities for trends. It may be concluded that for the mean flow and total precipitation over the study area, the trends are influenced by fluctuations of up to four years. Although there is a total of 13 stations used in this study, similar conclusions were obtained – this could be attributed by the fact that the stations are located in relatively close proximity to each other. Therefore, similar climatic factors are affecting the regions in which these stations are located.

The use of the DWT in this study clearly demonstrated how time-scale information can be extracted from a dataset – this information can then be applied to studying how the trends observed in the data were affected by certain time scales. Even for stations that did not exhibit significant trend values for their original data, the decomposition of these data via the DWT was able to identify the time scales that are considered important in affecting the trends. This was accomplished by applying the MK trend tests on the different time modes (detail components). With the sequential MK tests, we were also able to identify the possible starting time in which the trend in a dataset started to appear. In the datasets used in this study, an importance is placed at the time between 1965 and 1970 because most of the trends appeared to start around that time. Anctil and Coulibaly (2004) and Coulibaly and Burn (2004) showed the positive correlation between streamflow/precipitation activities with the PNA cycles since 1970. In this study, most of the flow and precipitation trends started between 1965 and 1970. Fu et al. (2012) also indicated the existence of positive correlations between streamflow in southern Canada and solar activities and El Niño cycles. As can be seen, a number of long-term changes in climate are also factors that may affect the streamflow and precipitation trends over the study area - there is no single factor that acts as the driver for the observed trends over the study area. This is reflected by the different large teleconnection patterns whose cycles seem to coincide with the dominant periodicities. Future studies could incorporate some quantitative linkages between the most dominant periodicities that affect trends (both in flow and precipitation) and the climatic descriptor cycles (or how the combined effects of these climatic descriptors influence the streamflow and precipitation over the study area). This may potentially explain the time-frequency characteristics that affect the trends in streamflow and precipitation over Quebec and Ontario. It would also be beneficial to include more stations from different hydrographic regions within Ontario and Quebec, as well as in other Canadian provinces in order to compare the periodic components that affect the trends in these other areas. Additionally, the implications of these time-frequency characteristics of trends on regional water resources can be looked at in more detail.

Finally, the results obtained from this present study presented some baseline information about the important periodicities that affect the flow and precipitation trends

over southern Ontario and Quebec. This information can be integrated into the methods/models aiming to investigate how natural fluctuations (e.g. changes in climate, fluctuations of climate indices, etc.) can affect flow and precipitation trends over southern Ontario and Quebec. Furthermore, the analysis obtained from this study can serve as grounds for basing the water resources design and planning within the watershed covered by the study area, as it involves making reasonable predictions or assumptions about future hydro-climatic conditions.

#### **4.7. Acknowledgement**

The authors of this paper would like to thank Dr. Eva Mekis from the Climate Research Division, Environment Canada for providing the second generation adjusted precipitation datasets used in this study. Funding provided by an NSERC Discovery Grant held by Jan Adamowski is also acknowledged.

#### **4.8. References**

- Abdul Aziz, O.I., Burn, D.H., 2006. Trends and variability in the hydrological regime of the Mackenzie River Basin. *Journal of Hydrology*, 319(1–4): 282-294.
- Adamowski, K., Bocci, C., 2001. Geostatistical regional trend detection in river flow data. *Hydrological Processes*, 15(18): 3331-3341.
- Adamowski, K., Bougadis, J., 2003. Detection of trends in annual extreme rainfall. *Hydrological Processes*, 17(18): 3547-3560.
- Adamowski, K., Prokoph, A., Adamowski, J., 2009. Development of a new method of wavelet aided trend detection and estimation. *Hydrological Processes*, 23(18): 2686-2696.
- Ampitiyawatta, A.D., Guo, S., 2010. Precipitation trends in the Kalu Ganga basin in Sri Lanka. *The Journal of Agricultural Science*, 4(1): 10-18.
- Anctil, F., Coulibaly, P., 2004. Wavelet analysis of the interannual variability in southern Québec streamflow. *Journal of Climate*, 17(1): 163-173.

- Assani, A.A., Charron, S., Matteau, M., Mesfioui, M., Quessy, J.-F., 2010. Temporal variability modes of floods for catchments in the St. Lawrence watershed (Quebec, Canada). *Journal of Hydrology*, 385(1–4): 292-299.
- Birsan, M.-V., Molnar, P., Burlando, P., Pfaundler, M., 2005. Streamflow trends in Switzerland. *Journal of Hydrology*, 314(1–4): 312-329.
- Boyer, C., Chaumont, D., Chartier, I., Roy, A.G., 2010. Impact of climate change on the hydrology of St. Lawrence tributaries. *Journal of Hydrology*, 384(1–2): 65-83.
- Bruce, L.M., Koger, C.H., Jiang, L., 2002. Dimensionality reduction of hyperspectral data using discrete wavelet transform feature extraction. *Geoscience and Remote Sensing, IEEE Transactions on Geoscience and Remote Sensing*, 40(10): 2331-2338.
- Burn, D.H., Hag Elnur, M.A., 2002. Detection of hydrologic trends and variability. *Journal of Hydrology*, 255(1–4): 107-122.
- Burn, D.H., Sharif, M., Zhang, K., 2010. Detection of trends in hydrological extremes for Canadian watersheds. *Hydrological Processes*, 24(13): 1781-1790.
- Cannas, B., Fanni, A., See, L., Sias, G., 2006. Data preprocessing for river flow forecasting using neural networks: Wavelet transforms and data partitioning. *Physics and Chemistry of the Earth*, 31(18): 1164-1171.
- Choi, T.-M., Yu, Y., Au, K.-F., 2011. A hybrid SARIMA wavelet transform method for sales forecasting. *Decision Support Systems*, 51(1): 130-140.
- Chou, C.-M., 2007. Applying multi-resolution analysis to differential hydrological grey models with dual series. *Journal of Hydrology*, 332(1–2): 174-186.
- Chou, C.-M., 2011. Wavelet-based multi-scale entropy analysis of complex rainfall time series. *Entropy*, 13(1): 241-253.
- Clark, J.S., Yiridoe, E.K., Burns, N.D., Astatkie, T., 2000. Regional climate change: trend analysis of temperature and precipitation series at selected Canadian sites. *Canadian Journal of Agricultural Economics*, 48(1): 27-38.
- Coats, R., 2010. Climate change in the Tahoe basin: Regional trends, impacts and drivers. *Climatic Change*, 102(3): 435-466.

- Cook, E. R., D'Arrigo, R.D., Briffa, K.F., 1998. A reconstruction of the North Atlantic Oscillation using tree-ring chronologies from North America and Europe. *Holocene*, 8: 1-9.
- Coulibaly, P., Burn, D.H., 2004. Wavelet analysis of variability in annual Canadian streamflows. *Water Resources Research*, 40(3): W03105.
- Cunderlik, J.M., Burn, D.H., 2004. Linkages between regional trends in monthly maximum flows and selected climatic variables. *Journal of Hydrologic Engineering*, 9(4): 246-256.
- Daubechies, I., 1990. The wavelet transform, time-frequency localization and signal analysis. *Information Theory, IEEE Transactions on Information Theory*, 36(5): 961-1005.
- Daubechies, I., 1992. Ten lectures on wavelets. Philadelphia: SIAM.
- de Artigas, M.Z., Elias, A.G., de Campra, P.F., 2006. Discrete wavelet analysis to assess long-term trends in geomagnetic activity. *Physics and Chemistry of the Earth*, 31(1-3): 77-80.
- Dietz, E.J., Killeen, T.J., 1981. A nonparametric multivariate test for monotone trend with pharmaceutical applications. *Journal of the American Statistical Association*, 76(373): 169-174.
- Dong, X., Nyren, P., Patton, B., Nyren, A., Richardson, J., Maresca, T., 2008. Wavelets for agriculture and biology: A tutorial with applications and outlook. *BioScience*, 58(5): 445-453.
- Drago, A.F., Boxall, S.R., 2002. Use of the wavelet transform on hydro-meteorological data. *Physics and Chemistry of the Earth*, 27(32-34): 1387-1399.
- Durdu, Ö.F., 2010. Effects of climate change on water resources of the Büyük Menderes River basin, western Turkey. *Turk. J. Agric. For.*, 34(4): 319-332.
- Ehsanzadeh, E., Adamowski, K., 2007. Detection of trends in low flows across Canada. *Canadian Water Resources Journal*, 32(4): 251-264.
- Ehsanzadeh, E., Ouarda, T.B.M.J., Saley, H.M., 2011. A simultaneous analysis of gradual and abrupt changes in Canadian low streamflows. *Hydrological Processes*, 25(5): 727-739.

- Fu, C., James, A.L., Wachowiak, M.P., 2012. Analyzing the combined influence of solar activity and El Niño on streamflow across southern Canada. *Water Resour. Res.*, 48(5): W05507.
- Fugal, D.L., 2009. Conceptual wavelets in digital signal processing: an in-depth, practical approach for the non-mathematician, 1st ed. Space & Signals Technologies LLC.
- Goodwin, D.A., 2008. Wavelet analysis of temporal data. Dissertation, Department of Statistics, The University of Leeds, Leeds, UK.
- Groleau, A., Mailhot, A., Talbot, G., 2007. Trend analysis of winter rainfall over southern Québec and New Brunswick (Canada). *Atmosphere-Ocean*, 45(3): 153-162.
- Hamed, K.H., 2008. Trend detection in hydrologic data: The Mann–Kendall trend test under the scaling hypothesis. *Journal of Hydrology*, 349(3–4): 350-363.
- Hamed, K.H., Rao, A.R., 1998. A modified Mann-Kendall trend test for autocorrelated data. *Journal of Hydrology*, 204(1–4): 182-196.
- Hirsch, R.M., Slack, J.R., 1984. A nonparametric trend test for seasonal data with serial dependence. *Water Resources Research*, 20(6): 727-732.
- Hirsch, R.M., Slack, J.R., Smith, R.A., 1982. Techniques of trend analysis for monthly water quality data. *Water Resources Research*, 18(1): 107-121.
- IPCC., 2007. Climate change 2007: the fourth IPCC scientific assessment. In: M.L. Parry, O.F. Canziani, J.P. Palutikof, P.J. van der Linden and C.E. Hanson (eds). Intergovernmental Panel on Climate Change. Cambridge University Press, Cambridge, United Kingdom and New York, NY, USA.
- Kallache, M., Rust, H.W., Kropp, J., 2005. Trend assessment: applications for hydrology and climate research. *Nonlinear Processes in Geophysics*, 12(2): 201-210.
- Kendall M.G., 1975. Rank Correlation Methods. Griffin: London, UK.
- Kim, S., 2004., Wavelet analysis of precipitation variability in northern California, U.S.A. *KSCE Journal of Civil Engineering*, 8(4): 471-477.
- Kisi, O., Cimen, M., 2011. A wavelet-support vector machine conjunction model for monthly streamflow forecasting. *Journal of Hydrology*, 399(1–2): 132-140.

- Kulkarni, J.R., 2000. Wavelet analysis of the association between the Southern Oscillation and the Indian summer monsoon. *International Journal of Climatology*, 20(1): 89-104.
- Kumar, S., Merwade, V., Kam, J., Thurner, K., 2009. Streamflow trends in Indiana: Effects of long term persistence, precipitation and subsurface drains. *Journal of Hydrology*, 374(1–2): 171-183.
- Labat, D., 2005. Recent advances in wavelet analyses: Part 1. A review of concepts. *Journal of Hydrology*, 314(1–4): 275-288.
- Labat, D., Godd  ris, Y., Probst, J.L., Guyot, J.L., 2004. Evidence for global runoff increase related to climate warming. *Advances in Water Resources*, 27(6): 631-642.
- Liu, D., Chen, X., Lian, Y., Lou, Z., 2010. Impacts of climate change and human activities on surface runoff in the Dongjiang River basin of China. *Hydrological Processes*, 24(11): 1487-1495.
- Mallat, S.G., 1989. A theory for multiresolution signal decomposition: The wavelet representation. *Pattern Analysis and Machine Intelligence, IEEE Transactions on Pattern Analysis and Machine Intelligence*, 11(7): 674-693.
- Mann, H.B., 1945. Nonparametric tests against trend. *Econometrica*, 13(3): 245-259.
- McBean, E., Motiee, H., 2006. Assessment of impacts of climate change on water resources – A case study of the Great Lakes of North America. *Hydrology and Earth System Sciences Discussions*, 3(5): 3183-3209.
- Mekis, E., Hogg, W.D., 1999. Rehabilitation and analysis of Canadian daily precipitation time series. *Atmosphere-Ocean*, 37(1): 53-85.
- Mekis,   ., Vincent, L.A., 2011. An overview of the second generation adjusted daily precipitation dataset for trend analysis in Canada. *Atmosphere-Ocean*, 49(2): 163-177.
- Mishra, A.K., Singh, V.P., 2010. Changes in extreme precipitation in Texas. *Journal of Geophysical Research*, 115(D14): D14106.



- Mohsin, T., Gough, W., 2010. Trend analysis of long-term temperature time series in the Greater Toronto Area (GTA). *Theoretical and Applied Climatology*, 101(3): 311-327.
- Nolin, A.W., Hall-McKim, E.A., 2006. Frequency modes of monsoon precipitation in Arizona and New Mexico. *Monthly Weather Review*, 134(12): 3774-3781.
- Önöz, B., Bayazit, M., 2003. The power of statistical tests for trend detection. *Turkish Journal of Engineering & Environmental Sciences*, 27(4): 247.
- Partal, T., 2010. Wavelet transform-based analysis of periodicities and trends of Sakarya basin (Turkey) streamflow data. *River Research and Applications*, 26(6): 695-711.
- Partal, T., Küçük, M., 2006. Long-term trend analysis using discrete wavelet components of annual precipitations measurements in Marmara region (Turkey). *Physics and Chemistry of the Earth*, 31(18): 1189-1200.
- Percival, D.B., 2008. Analysis of geophysical time series using discrete wavelet transforms: An overview, in *nonlinear time series analysis in the geosciences – Applications in climatology, geodynamics, and solar-terrestrial physics*, edited by R. V. Donner and S. M. Barbosa. Berlin/Heidelberg: Springer.
- Popivanov, I., Miller, R.J., 2002. Similarity search over time-series data using wavelets, *Data Engineering, 2002. Proceedings. 18th International Conference on*, pp. 212-221.
- Popoola, A.O., 2007. Fuzzy-wavelet method for time series analysis. Dissertation, Department of Computing, School of Electronics and Physical Sciences, University of Surrey, Guildford, UK.
- Prokoph, A., Adamowski, J., Adamowski, K., 2012. Influence of the 11 year solar cycle on annual streamflow maxima in Southern Canada. *Journal of Hydrology*, 442–443(0): 55-62.
- Quiroz, R., Yarlequé, C., Posadas, A., Mares, V., Immerzeel, W.W., 2011. Improving daily rainfall estimation from NDVI using a wavelet transform. *Environmental Modelling and Software*, 26(2): 201-209.
- Roy, L., Leconte, R., Brisette, F.P., Marche, C., 2001. The impact of climate change on seasonal floods of a southern Quebec river basin. *Hydrological Processes*, 15(16): 3167-3179.

- Santos, C.A.G., Galvão, C.d.O., Suzuki, K., Trigo, R.M., 2001. Matsuyama city rainfall data analysis using wavelet transform. *Annual Journal of Hydraulic Engineering, JSCE*, 45: 6.
- Shao, Q., Li, Z., Xu, Z., 2010. Trend detection in hydrological time series by segment regression with application to Shiyang River basin. *Stochastic Environmental Research and Risk Assessment*, 24(2): 221-233.
- Stone, D.A., Weaver, A.J., Zwiers, F.W., 2000. Trends in Canadian precipitation intensity. *Atmosphere-Ocean*, 38(2): 321-347.
- Su, H., Liu, Q., Li, J., 2011. Alleviating border effects in wavelet transforms for nonlinear time-varying signal analysis. *Advances in Electrical and Computer Engineering*, 11(3): 6.
- Svensson, C., Kundzewicz, W.Z., Maurer, T., 2005. Trend detection in river flow series: 2. Flood and low-flow index series. *Hydrological Sciences Journal*, 50(5): 824.
- Timofeev, A., Sterin, A., 2010. Using the quantile regression method to analyze changes in climate characteristics. *Russian Meteorology and Hydrology*, 35(5): 310-319.
- Torrence, C., Compo, G.P., 1998. A practical guide to wavelet analysis. *Bulletin of the American Meteorological Society*, 79(1): 61-78.
- Vonesch, C., Blu, T., Unser, M., 2007. Generalized Daubechies wavelet families. *Signal Processing, IEEE Transactions on Signal Processing*, 55(9): 4415-4429.
- Wang, W., Hu, S., Li, Y., 2011. Wavelet transform method for synthetic generation of daily streamflow. *Water Resources Management*, 25(1): 41-57.
- Xu, J., Chen, Y., Li, W., Ji, M., Dong, S., Hong, Y., 2009. Wavelet analysis and nonparametric test for climate change in Tarim River basin of Xinjiang during 1959-2006. *Chinese Geographical Science*, 19(4): 306-313.
- Yue, S., Pilon, P., 2004. A comparison of the power of the t test, Mann-Kendall and bootstrap tests for trend detection. *Hydrological Sciences Journal*, 49(1): 21-37.
- Yue, S., Pilon, P., 2005. Probability distribution type of Canadian annual minimum streamflow. *Hydrological Sciences Journal*, 50(3): 438.
- Yue, S., Pilon, P., Phinney, B., Cavadias, G., 2002. The influence of autocorrelation on the ability to detect trend in hydrological series. *Hydrological Processes*, 16(9): 1807-1829.

- Zhang, Q., Xu, C.Y., Zhang, Z., Chen, Y.D., Liu, C.L., 2009. Spatial and temporal variability of precipitation over China, 1951-2005. *Theoretical and Applied Climatology*, 95(1-2): 53-68.
- Zhang, X., Harvey, K.D., Hogg, W.D., Yuzyk, T.R., 2001. Trends in Canadian streamflow. *Water Resources Research*, 37(4): 987-998.
- Zhang, X., Vincent, L.A., Hogg, W.D., Niitsoo, A., 2000. Temperature and precipitation trends in Canada during the 20th century. *Atmosphere-Ocean*, 38(3): 395-429.
- Zhang, Z., Dehoff, A., Pody, R., Balay, J., 2010. Detection of streamflow change in the Susquehanna River basin. *Water Resources Management*, 24(10): 1947-1964.
- Zume, J., Tarhule, A., 2006. Precipitation and streamflow variability in Northwestern Oklahoma, 1894-2003. *Physical Geography*, 27(3): 189-205.

## CHAPTER 5 – SUMMARY AND CONCLUSIONS

### 5.1. General Summary

The use of both the discrete wavelet transform (DWT) and Mann-Kendall (MK) trend test to analyze and detect trends in hydroclimatic data has not been explored in much detail in the existing literature, especially in the context of Canadian studies. This study presents the results of the applications of the DWT and the MK trend test in analyzing trends in three hydroclimatic indices, namely temperature, precipitation and streamflow over parts of southern Ontario and Quebec, Canada. The data for the mean temperature (monthly, seasonally-based, seasonal, and annual) span from 1967 to 2006; the data for the mean streamflow and total precipitation (monthly, seasonally-based, and annual) span from 1954 to 2008.

DWT decomposes a time series in the dyadic scale, which implies that the first scale is  $2^1$  and the subsequent scales are arranged in higher integer powers of two. By doing so, the work is simplified but still produces accurate information because the redundancy in the wavelet coefficients is removed. Perfect signal reconstructions in DWT are also easily achieved. Each dataset used in this study was decomposed into several levels of decomposition. This study proposed a new criterion to be used in the DWT procedure, which is based on the relative error of the MK Z-values between the approximation component and the original data. The proposed criterion was successfully applied in this study in determining: (i) the type of Daubechies (db) mother wavelet to be used for time series decomposition; (ii) the type of border extension to deal with the effects of border distortion; and (iii) the number of decomposition levels for the analyzed data.

The MK test and sequential MK were applied to the time series resulting from the decomposition in order to determine the most dominant periodic mode that affects the trend in each dataset. However, prior to applying the MK test, each time series was checked for whether significant autocorrelations are present in the data because the presence of either significant positive or negative autocorrelations can lead to inaccurate result interpretations. Three types of MK tests were used: the original MK was used when

the analyzed time series had neither seasonality patterns nor a significant autocorrelation; the modified MK test by Hirsh and Slack (1984) was used when the time series showed seasonality cycles with or without a significant autocorrelation; and the modified MK by Hamed and Rao (1998) was used when the analyzed time series exhibited a significant autocorrelation. As expected, all of the monthly and seasonally-based temperature, precipitation and flow data exhibited seasonality patterns (some with significant lag-1 autocorrelation coefficient). For this reason, the modified MK test by Hirsch and Slack (1984) was used on these data. Significant autocorrelations in annual data were only observed for three stations in total – Vineland (temperature), Montreal/Pierre Elliot Trudeau (precipitation), and Richelieu River (flow). As such, these were the only three stations whose annual data were analyzed using the modified MK test by Hamed and Rao (1998). All the other annual data were analyzed using the original MK test.

Based on the findings observed in this study, we may conclude that the applications of the DWT to extract the low- and high-frequency components in a time series prior to testing them with the MK test is very useful in detecting and analyzing trends in hydroclimatic variables. To analyze these trends, it was also found that it was very useful to examine different types of data (in this case, monthly, seasonal, and annual) in order to obtain more thorough results.

## **5.2. Trends in Temperature, Precipitation and Streamflow**

All types of temperature data show warming trends as reflected by the MK Z-values being all positive. For high-resolution temperature data (i.e. monthly and seasonally-based data), the trends are more affected by high-frequency intra-annual fluctuations, which perhaps subdued the underlying trends. On the other hand, longer time-periodic components (multiyear and decadal variability) are more prominent in affecting the trends for the annual and seasonal data – 8- and 16-year periodic modes are the most commonly seen as the most influential periodicities. It was further concluded that the apparent warming in annual temperature was attributed to the increase in winter and summer temperatures, which also have similar most dominant periodicities to that of the annual data.

Data analysis using the DWT and the MK tests revealed that streamflow and precipitation trends are dominated by positive trends; and that the trends in the study area are mostly affected by similar periodicities: intra-annual and inter-annual events, up to four years. Since all of the flow and precipitation stations are situated relatively close to each other, it may be said that the similarity is caused by similar climatic factors influencing the study area. Furthermore, it is apparent that the trends in streamflow and precipitation started approximately during the mid-60s to early 70s, which could be related to climatic fluctuations such as the PNA and NAO (which are major climatic phenomenon in the northern hemisphere).

Although linking the trends in temperature with the trends in precipitation and streamflow was not done quantitatively in this work (as it was not part of the objectives of this study), we suggest that warming trends in temperature have affected the precipitation trends, and hence the streamflow. This is because all trends in the different temperature data types are positive and most trends in streamflow and precipitation are also positive.

In annual temperature data, 8- to 16-year periodicities seem to be the most dominant for trends, but in streamflow and precipitation, the main periodicities for trends are 2-4 years. We suggest that the common large-scale teleconnection variability that may be responsible for the apparent trends in temperature, precipitation and streamflow (in combination with other climatic factors and anthropogenic activities, such as the urban heat island effect, urbanization, humidity, dew point, evapotranspiration, etc.) is the NAO cycle. This is because some of the main peaks of the NAO cycles are centered at 2 and 8 years, which seem to coincide with most of the main periodic components of the lower resolution data found in this study. Although there were no quantitative analyses made between the NAO and any of the variables studied, we suggest that the NAO (which is a major teleconnection pattern in the northern hemisphere) may be one of the major drivers behind the observed trends. This hypothesis needs to be explored quantitatively in a future study. Apart from the NAO, PNA and El Niño cycles, solar activities may also act as important drivers for the streamflow and precipitation trends as past studies in Canada (e.g. Anctil and Coulibaly, 2004; Coulibaly and Burn, 2004; Fu et al., 2012) indicate the existence of positive correlations between streamflow/precipitation

and these large-scale teleconnection patterns that are important in the Northern Hemisphere. Anctil and Coulibaly (2004) and Coulibaly and Burn (2004) showed the positive correlation between streamflow/precipitation activities with the PNA cycles since 1970. In this study, most of the flow and precipitation trends started between 1965 and 1970.

Finally, some of the findings observed in this study were in accordance with other trend studies conducted in Canada while others were not in agreement with other trend studies conducted in Canada. Zhang et al. (2000) and Vincent et al. (2007) observed that the spring season showed significant temperature warming in southern Canada, but in our study we observed that the spring season does not show significant warming as most stations' trend values are not significant and are very low. We suspect that it may be caused by the different study period and/or length of data chosen. As well, stations' geographical areas may also make a difference; the areas covered in this study were rather more localized, concentrated around the southern parts of Ontario and Quebec. There are also results obtained in this study that are in accordance with the findings of other studies. For example, we found that autumn temperature seems to be the season with minimal warming in temperature, which is in agreement with the study conducted by Vincent et al. (2007). Our study also found that the winter season experiences the most significant warming, which is also in agreement with Canadian temperature trend analysis studies, such as those conducted by Vincent et al. (2007) and Mohsin and Gough (2010). General trends in the precipitation data that was explored in this study also showed positive trends, which are also commonly observed in many parts of Canada, as shown by studies such as Mekis and Hogg (1999), Stone et al. (2000), Zhang et al. (2000), and Groleau et al. (2007).

### **5.3. References**

- Anctil, F., Coulibaly, P., 2004. Wavelet analysis of the interannual variability in southern Québec streamflow. *Journal of Climate*, 17(1): 163-173.
- Coulibaly, P., Burn, D.H., 2004. Wavelet analysis of variability in annual Canadian streamflows. *Water Resources Research*, 40(3): W03105.

- Fu, C., James, A.L., Wachowiak, M.P., 2012. Analyzing the combined influence of solar activity and El Niño on streamflow across southern Canada. *Water Resour. Res.*, 48(5): W05507.
- Groleau, A., Mailhot, A., Talbot, G., 2007. Trend analysis of winter rainfall over southern Québec and New Brunswick (Canada). *Atmosphere-Ocean*, 45(3): 153-162.
- Mekis, E., Hogg, W.D., 1999. Rehabilitation and analysis of Canadian daily precipitation time series. *Atmosphere-Ocean*, 37(1): 53-85.
- Mohsin, T., Gough, W., 2010. Trend analysis of long-term temperature time series in the Greater Toronto Area (GTA). *Theoretical and Applied Climatology*, 101(3): 311-327.
- Stone, D.A., Weaver, A.J., Zwiers, F.W., 2000. Trends in Canadian precipitation intensity. *Atmosphere-Ocean*, 38(2): 321-347.
- Vincent, L.A., van Wijngaarden, W.A., Hopkinson, R., 2007. Surface temperature and humidity trends in Canada for 1953–2005. *Journal of Climate*, 20(20): 5100-5113.
- Zhang, X., Vincent, L.A., Hogg, W.D., Niitsoo, A., 2000. Temperature and precipitation trends in Canada during the 20th century. *Atmosphere-Ocean*, 38(3): 395-429.



## CHAPTER 6 – RECOMMENDATIONS FOR FUTURE STUDIES

Based on the findings and discussions provided by this study, it is recommended that future studies include the following in their work:

1. Apply the combination of the discrete wavelet transform (DWT) and the Mann-Kendall (MK) trend test to additional variables that seem to also directly affect the observed trends in this study (e.g. minimum/maximum temperatures, diurnal temperature range, evapotranspiration rate, infiltration, surface runoff, etc.), and compare the results to those obtained from this study in order to see if there are any similarities in terms of the most dominant periodic components for trends, and whether they may contribute to the periodicities of the observed trends.
2. Assessment of the relationship between the temperature, precipitation and streamflow data. Also, the correlation between the three variables and the teleconnection patterns that seem to be important in driving the trends observed in this study should be explored (i.e. the NAO, PNA, ENSO, and solar activities). The use of the cross wavelet transform – which is based on the continuous approach of the wavelet transform – can be explored by analyzing two variables (or time series) that show high common power within similar regions in terms of time-frequency space. If two time series have strong power at a certain waveband (during a certain period), their cross wavelet analysis can be used to confirm whether that specific waveband is actually significant. So, this method could be useful in examining the correlation of temperature and streamflow, for example, and relate the important wavebands resulting from the cross wavelet analysis to some major peaks of large-scale teleconnection patterns. In this way, the plausible teleconnection patterns that best explain the variability of temperature, precipitation and streamflow can be identified. The combined effects of more than one teleconnection pattern on temperature, streamflow, and precipitation could also be investigated.
3. Evaluate the performance of the newly proposed criterion (to be used in DWT procedures), which is based on the relative error of the MK Z-values (between the approximation at the last decomposition level and the original data) to determine

the appropriate number of decomposition levels, the type of Daubechies (db) mother wavelet, and the extension border type of the above mentioned and other climatic variables.

4. Explore the use of other types of mother wavelets (e.g. Least Asymmetric – LA) for the DWT decomposition and compare the results with those obtained in this study. Since different wavelet filters have different shapes, it is important to find wavelets that would capture the shape of a time series well.
5. Include more sites from Ontario and Quebec, and perhaps from other Canadian provinces, to compare the general trends and the main periodic modes responsible for trends. However, since the length of data ideally should be at least 40 years and many stations would have missing data records, suitable interpolation methods to fill these missing data values have to be carefully researched and assessed, in order to avoid errors associated with the interpolation.

## CHAPTER 7 – CONTRIBUTIONS TO KNOWLEDGE

This research was carried out to provide original contributions to knowledge in the area of trend detection and analysis in hydroclimatic variables, and more specifically in temperature, precipitation and streamflow in Canada (especially in southern Ontario and Quebec). The main contributions of the research presented in this thesis are:

1. Development and application of a new trend assessment method for hydroclimatic data that is based on coupling the discrete wavelet transform (DWT) and the different versions of the Mann-Kendall (MK) trend test, depending on the characteristics of the analyzed data. The DWT was used to separate the analyzed data into its high-frequency and low-frequency components/periodicities. The MK test is used to test for the trends of these different periodicities.
2. In this study, we determine the most influential periodicities affecting hydroclimatic trends in temperature, precipitation and streamflow over southern parts of Ontario and Quebec. This included a clear step by step methodology, which has not been addressed in detail in the existing literature:
  - Testing for autocorrelation prior to applying a trend test – this step is often ignored in many trend detection studies.
  - Decomposing the analyzed data via the DWT.
  - Choosing the appropriate MK test based on the characteristics of the data. Many trend detection studies do not indicate how they chose to use the MK test (for example the original MK test should not be used when there is a significant autocorrelation in the data). To date, there have not been any trend detection studies in the hydroclimatic field that employed the three different versions of the MK tests as used in this study. This research clearly defined the criteria for using the different MK tests in our study:
    - i. Original MK test was used on data that exhibited neither seasonality patterns nor significant autocorrelations.

- ii. Modified MK proposed by Hirsch and Slack (1984) was used on data that exhibited seasonality patterns (with or without significant autocorrelations).
    - iii. Modified MK test proposed by Hamed and Rao (1998) was used on data that exhibited only significant autocorrelations.
  - Applying sequential MK analysis on the original time series and on each detail component (with approximation added) to compare how harmonious the trend lines are. The appropriate MK test is run sequentially from the beginning to the end of the study period, which is important because sequential MK values (and graphs) show that positive and negative trends may be present in the same dataset at different times. In our studies, the sequential MK test is also applied to the time series that are produced from the DWT decomposition in order to obtain information on how similarly the trend line of each detail component progresses with respect to the trend line of the original data. Although sequential MK analysis has been used in many trend detection studies, to our knowledge, it has not been used in conjunction with the DWT.
  - Determining the most influential periodic mode(s) that affect trends based on the MK Z-values and the sequential MK analysis. Again, even though sequential MK analysis has been used to detect trends, using it together with the MK Z-values to determine important periodicities for trends has not been explored.
3. Proposal of a new criterion that is based on the relative error of the MK Z-values between the approximation component (of the last decomposition level) and the original data, which can be used to determine:
- The number of decomposition levels in the DWT.
  - The type of Daubechies (db) mother wavelet to be used in the DWT procedure.

- The type of extension border to be used in the DWT that would best deal with the issue of border distortion as convolution processes cannot proceed outside the ends of signals with finite length.

It is the first time that the relative error of the MK  $Z$ -values is used as a criterion in order to determine the above points to be used in the DWT procedure. Since the approximation component is assumed to contain the trend of the analyzed data, it makes sense to use an approximation MK  $Z$ -value that is close to the original value. The application of this criterion was found to be very useful in this study.